Interim Report For The Upper Mississippi River - Illinois Waterway System Navigation Study

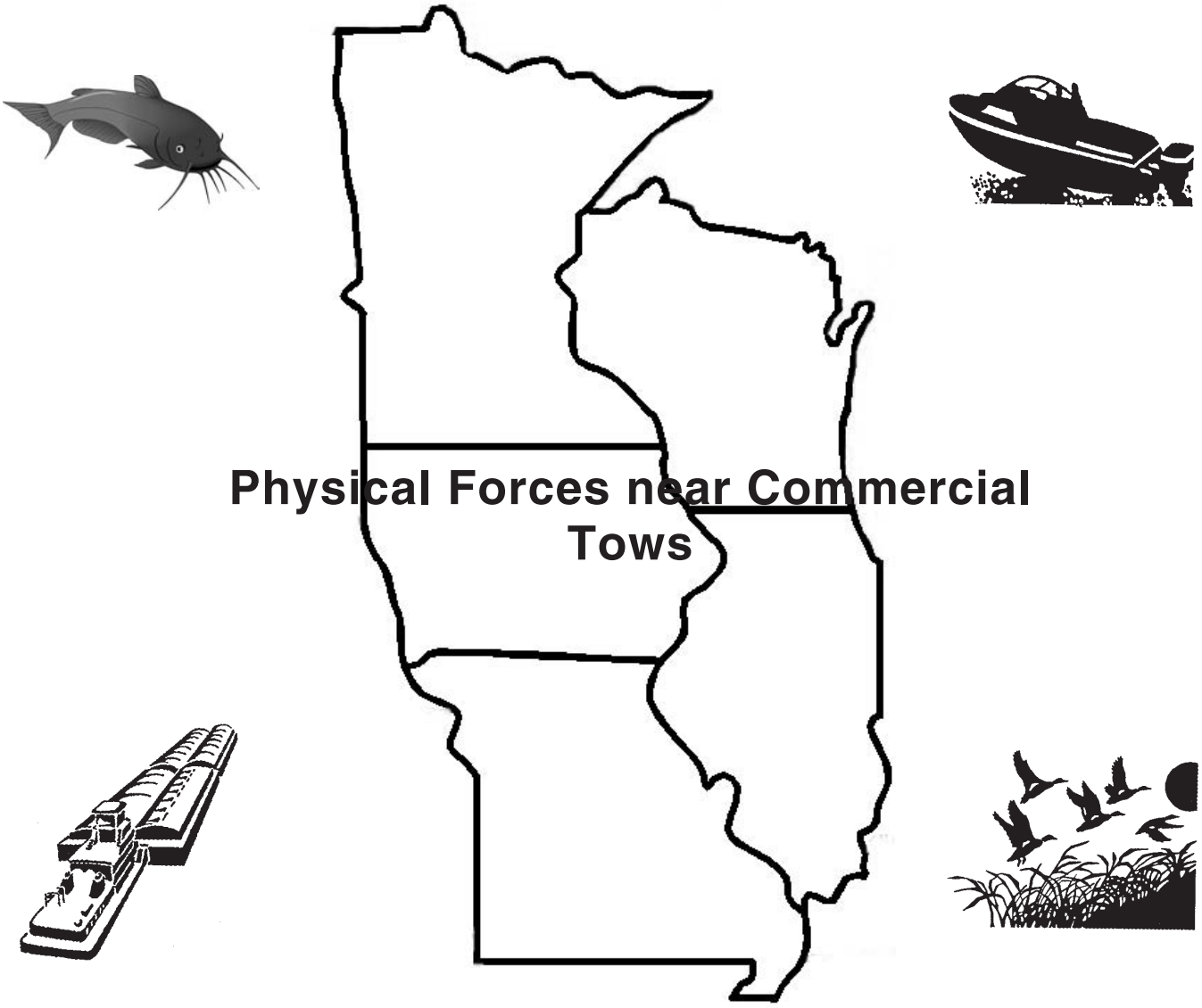

Physical Forces near Commercial Tows

March 2000

US Army Corps of Engineers

Rock Island District
St. Louis District
St. Paul District

Upper Mississippi River - Illinois Waterway System Navigation Study

ENV Report 19
March 2000

Physical Forces near Commercial Tows

by Stephen T. Maynord

U.S. Army Engineer Research and Development Center
3909 Halls Ferry Road
Vicksburg, MS 39180-6199

Interim report

Approved for public release; distribution is unlimited

Prepared for U.S. Army Engineer District, Rock Island
Rock Island, IL 61204-2004
U.S. Army Engineer District, St. Louis
St. Louis, MO 63103-2833
U.S. Army Engineer District, St. Paul
St. Paul, MN 55101-1638

1 Introduction

The Upper Mississippi River-Illinois Waterway System (UMR-IWWS) Navigation Study evaluates the justification of additional lockage capacity at sites on the UMR-IWWS while maintaining the social and environmental qualities of the river system. The system navigation study is implemented by the Initial Project Management Plan (IPMP) outlined in the "Upper Mississippi River-Illinois Waterway System Navigation Study," (U.S. Army Corps of Engineers (USACE) 1994). The IPMP outlines Engineering, Economic, Environmental, and Public Involvement Plans.

The Environmental Plan identifies the following: Significant environmental resources on the UMR-IWWS; the impacts to threatened and endangered species; water quality; recreational resources; fisheries; mussels and other macro invertebrates; waterfowl; aquatic and terrestrial macrophytes; and historic properties. In a preliminary way, the plan also considers the system-wide impacts of navigation capacity increases, while assessing potential construction effects of improvement projects. The physical forces studies are part of the Environmental Plan.

Physical forces in the region near and beneath commercial tows occur because of the propeller jet and the displacement of water by the hull of the vessel. Physical forces are quantified in terms of the changes in pressure, velocity, and shear stress and are used to determine substrate scour, sediment resuspension, and effects on aquatic organisms.

This study of forces near and beneath commercial tows is conducted in a physical model. The reason for this is that field measurements beneath a vessel are difficult to obtain because some of the primary tows of interest are operating in shallow water with as little as a 0.6-m clearance beneath the tow. In addition, propeller jet bottom velocities can exceed 4 m/sec. Operation of velocity meters or other measuring devices in such an environment is quite difficult. The difficulty of obtaining field data means that verification data for the physical model is lacking. The approach used herein is to use a large physical model to minimize scale effects. Propeller jets, a main emphasis of this study, are operated at speeds where the thrust coefficients are independent of Reynold's number, suggesting similarity with the prototype.

The objectives of this study are:

a. Measure channel bottom pressure under moving tow.

b. Measure near-bed velocity and bed shear stress changes under the barges of a moving tow.

c. Measure near-bed velocity and bed shear stress changes in the stern region from the propeller jet for a stationary tow and from the combined effects of the propeller jet and the wake flow for a moving tow.

d. Develop analytical/empirical methods to describe near-bed velocity and shear stress as a function of tow parameters.

2 Physical Model Description

General

Since all of the studies reported herein were conducted in the navigation effects flume with the same model towboat and barges, the flume is described in this section and differs only as described in the individual sections.

Navigation Effects Flume

Details of the navigation effects flume (Figure 1) are given by Maynord and Martin (1997). The flume is 125 m long, 21.3 m wide, and has a maximum depth of 1.22 m. Pumps recirculate flow through the flume. The center 61 m of the flume are molded out of plastic coated plywood to the cross section shown in Figure 2 at a length scale ratio of 1:25. The Figure 2 cross section represents the Mississippi River at Clark's Ferry, river mile 468.2. Cross-sectional area is shown versus thalweg depths in Figure 2.

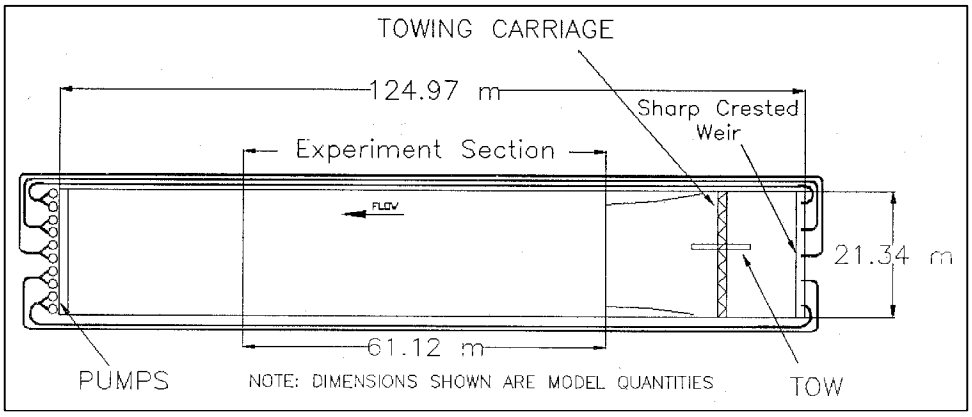

Figure 1. Navigation effects flume

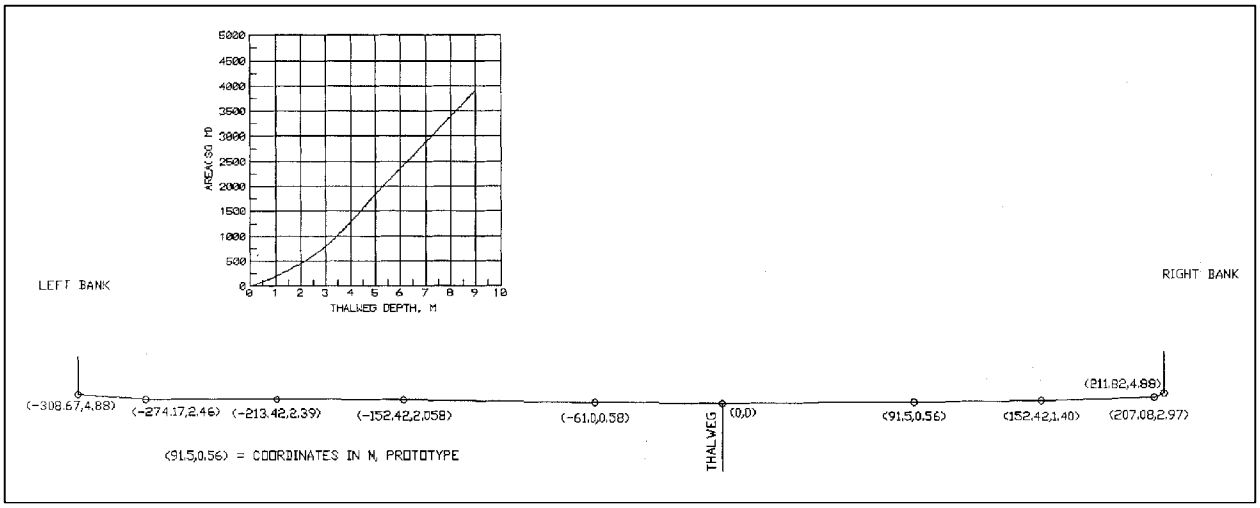

Figure 2. Cross section in experimental section, dimensions expressed as prototype equivalent of 1:25-scale model

Model Towboat and Barges

The 1:25-scale towboat (Figure 3) was modeled after the Corps' MV Benyaurd and is 52 m long by 12.4 m wide with a 2.74-m draft. The model towboat is equipped with two main rudders (3.6 m long) on the axis of the propeller shafts and four flanking rudders (1.8 m long), each 0.95 m on either side of the propeller shaft. Both the Kort nozzle and open-wheel propellers had 2.74-m diam, five blades, and were 6 m from shaft to shaft. As viewed from the towboat stern, the starboard propeller rotated counterclockwise and the port propeller rotated clockwise. The towboat had a tunnel stern. The Kort nozzle and open-wheel propellers had thrust coefficients at bollard pull conditions (zero vessel speed through water) of 0.475 and 0.51, respectively based on measurements of thrust in the model. The 1:25-scale model barges were Plexiglas and were 257 m long by 32 m wide with a 2.44-m draft. This is discussed in the following section on scale effects. The barges had a raked bow and the stern had a boxed end, as shown in Figure 4.

Scale effects

Maynord and Martin (1997) document the need to decrease the draft of the barges to provide agreement between return velocity and drawdown measured in the model and in the prototype. In the 1:25 scale used by Maynord and Martin (1997), a draft of 2.29 m in the physical model reproduced return velocity for a 2.74-m draft in the prototype. The decreased draft was required because the boundary layer growth on the barge hull and on the channel perimeter was exaggerated in the physical model due to the larger viscous forces in the model. The decreased draft worked well when studying changes away from the tow as in the Maynord and Martin (1997) study of return velocity and drawdown. The study reported herein addresses forces near and beneath the vessel. The exaggerated boundary layer growth is not present at the bow, where boundary layer growth

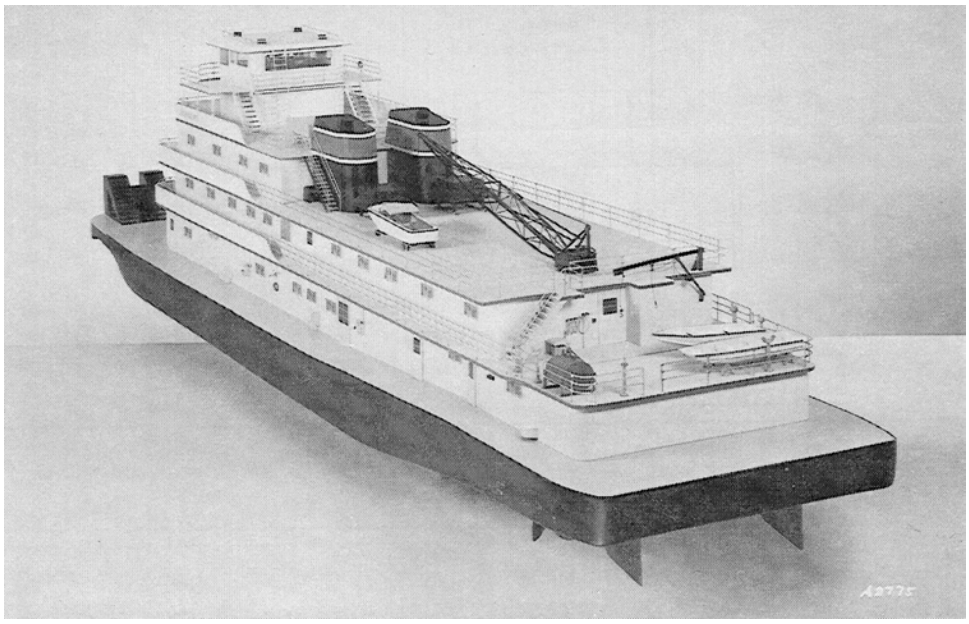

Figure 3. *MV Benyaurd,* 1:25-scale towboat

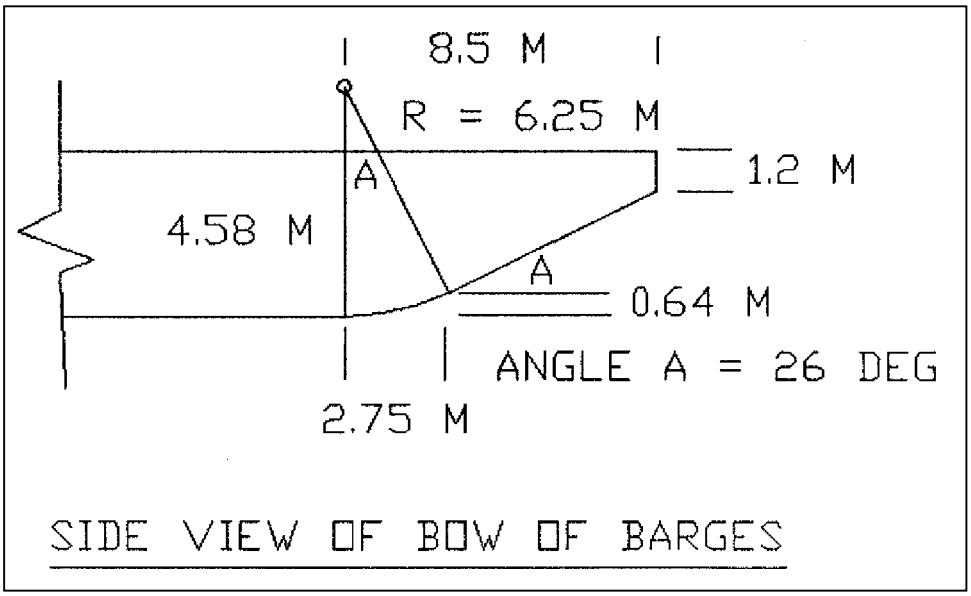

Figure 4. Shape of bow of experimental barges

begins, but is present at the stern where boundary layer growth ends. As will be shown in this study, two areas are of primary interest near and beneath the vessel. The first is the area beneath the bow of the barges where a rapid spike of velocity and bed shear occurs. Analyses of results in the barge bow region are assumed to be free of the boundary layer growth problems and the actual bow draft (2.44 m) was used in the analysis. The second area of interest is the area astern of the vessel in the wake and propeller jet of the tow. If the actual prototype draft (2.74 m) were simulated in the model, the exaggerated boundary layer growth at the stern of the barges would exaggerate the wake and affect flow into the propellers. Use

of the 2.29-m draft by Maynord and Martin (1997) likely overestimates the effect on the wake, because a portion of the dissimilarity of return velocity was a result of the boundary layer growth over the channel perimeter. For this study, a decreased draft of 2.44 m was selected to properly simulate the wake flow behind the tow. This value is equal to the 2.74-m draft minus the difference between displacement thickness in model and prototype for typical vessel speed and length for tows on the UMR-IWWS.

Thrust from the model propellers was measured for various speeds of rotation to ensure that the thrust coefficient was independent of Reynolds (R) number effects. Propeller speeds above about 120 RPM (prototype equivalent) provided a constant thrust coefficient which suggests similarity with prototype performance. The small-scale turbulence in model and prototype will not be similar, but large-scale features of the flow should be similar and are the goal of this study.

Instrumentation

Pressure transducers having an 0.8-cm-diam diaphragm were mounted flush with the floor of the navigation effects flume. The calibration of the transducers was checked each morning prior to running experiments.

Velocities were collected with two- and three-dimensional (2- and 3-D) acoustic doppler velocity (ADV) meters made by Sontek (Krauss, Lohrmann, and Cabrera 1994). Velocities beneath the moving tow were collected with 2-D ADVs having a flexible cable. The ADVs required seeding with hollow glass spheres which tended to settle out with slack-water conditions. Most tests were run with some ambient flow in the flume just to keep the seed in suspension. Velocities were also collected with a one-dimensional (1-D) miniature propeller meter manufactured by Nixon.

Shear stress was measured with Dantec flush mounted hot-film anemometer (HFA) sensors mounted in the bottom of the model in a 1.2- by 1.2-m acrylic sheet surrounded by the plywood channel. The hot-film sensors were calibrated in an acrylic closed channel having a rectangular cross section, 0.229 m wide, 0.0127 m high, and 4.57 m long. Pressure taps along the length of the calibration flume defined the pressure gradient from which the shear stress was computed. The shear stress measurements presented herein are applicable to hydraulically smooth bed conditions. A method is presented later in this report for converting smooth bed shear to a rough bed.

Model operation

One factor in studying jets has to do with the effects of the flume size and the setup of eddies in the flume that strongly affect the characteristics of the jet. This was not a significant problem when moving tows were being studied. For stationary tows, the eddies and jet interactions produced wide variations in observed velocities if the jet operated for a significant time period. Upon start-up of the jet for the stationary tow, there was a period of time where the jet exhibited stable characteristics before the eddies had a chance to dominate the jet characteristics; velocity data were only used from this stable period. The jet was

quickly shut off to keep the eddies weak and the time between tests to a minimum. This use of the initial velocity is believed to better represent the operation of a towboat. Stationary vessels in zones with no flow tend to operate their propellers for short durations compared to the setup time for eddies.

Data analysis

The objective of this study was to measure the rapid changes that occur near and beneath the tow. However, no attempt was made to measure turbulence quantities in the model with the ADV meters because high sampling frequencies would be required which dictates large amounts of seeding material present in the model. Obtaining high seeding concentrations is difficult because the model must be allowed to “settle out” between experiments and some of the seed drops out of suspension in the low ambient velocities.

After scaling model shear and velocity to prototype equivalents, a Fast Fourier Transform was used to filter out all fluctuations above 1 Hz. This approach retained the rapid changes beneath the tow but eliminated turbulent fluctuations greater than 1 Hz and noise resulting from less than optimum seeding concentration.

3 Pressure Changes Beneath Tow

General

Pressure measurements were made beneath the model tow to provide input to other elements of the UMR-IWWS study such as the effects of pressure drop on larval fish or the potential for low pressures on the bed increasing sediment resuspension. Low pressures at the bow observed herein may help explain why some vessels have experienced a diving of the bow when going from deep to shallow water.

Model Description

Pressures were measured on the channel bottom beneath the 1:25-scale moving tow in the navigation effects flume. Two pressure cells were mounted 34.2 and 35.2 m to the right (looking downstream) of the thalweg on the cross section in Figure 2. The pressure cells collected data at 25 Hz and were mounted in a 0.15-m-square piece of Plexiglas which was mounted flush with the plywood floor of the navigation effects flume. The tow configuration was the *MV Benyaurd* model towboat pushing 257-m-long by 32-m-wide by 2.44-m-draft barges. All experiments were conducted with the open-wheel propeller towboat drafting 2.74 m and having 2.74-m-diam propellers and zero rudder angle.

Description of Experiments

The thrust from both propellers at zero vessel speed was 382,500 N in these open-wheel experiments. All experiments were conducted with the tow heading upbound at a tow speed of 3.04 m/sec at depths and ambient velocities shown in Table 1, while measuring time-history of pressure on the channel bottom at different distances from the center line of the tow. Selected plots of pressure change are shown in Figures 5 and 6. Values in Table 1 and Figures 5 and 6 are in prototype equivalents as are all values in this report, unless noted.

Table 1
Prototype Depths, Ambient Velocity, and Pressure Drop from Pressure Tests

Depth, m	Ambient Velocity, m/sec[1]	Distance from Center Line of Tow, m	Pressure Drop at Bow, m	Pressure Drop at Stern of Barges, m	Pressure Drop at Stern of Towboat, m
3.35	0.5	0	1.1	0.8	0.5
		15.9	0.7	0.8	0.7
3.5	0.5	0	1.1	0.8	0.5
		15.9	1.5	0.7	0.3
		30.9	0.2	0.5	[2]
3.65	0.6	0	1.2	0.7	0.5
		1	1.3	0.8	0.6
	[3]	2	1.3	0.7	0.5
		3	1.4	0.7	0.5
		4	1.2	0.7	0.5
		5	1.2	0.7	0.5
	[3]	15.9	1.1	0.6	0.3
		16.9	1.1	0.6	0.3
		23.4	0.5	0.5	0.3
		24.4	0.5	0.5	0.4
		30.9	0.3	0.5	[2]
		31.9	0.4	0.5	[2]
		45.9	0.1	0.4	[2]
	[3]	46.9	0.1	0.5	[2]
4.7	0.7	0	0.8	0.5	0.4
		1	0.7	0.4	0.2

(Continued)

[1] Depth averaged velocity at 70 m left of thalweg.
[2] Not detected because far from towboat.
[3] Pressure shown on plots.

Table 1 (Concluded)

Depth, m	Ambient Velocity, m/sec[1]	Distance from Center Line of Tow, m	Pressure Drop at Bow, m	Pressure Drop at Stern of Barges, m	Pressure Drop at Stern of Towboat, m
	[3]	2	0.7	0.5	0.3
		3	0.7	0.4	0.3
		4	0.7	0.5	0.2
		5	0.7	0.5	0.3
5.87	0.8	0	0.5	0.4	0.3
		1	0.5	0.3	0.2
	[3]	2	0.5	0.4	0.3
		3	0.5	0.3	0.2
		4	0.5	0.3	0.3
		5	0.5	0.4	0.2
9.25	1.0	0	0.3	0.3	0.2
		1	0.3	0.2	0.2
	[3]	2	0.3	0.3	0.2
		3	0.3	0.2	0.1
		4	0.3	0.2	0.1
		5	0.3	0.2	0.1

[1] Depth averaged velocity at 70 m left of thalweg.
[2] Not detected because far from towboat
[3] Pressure shown on plots

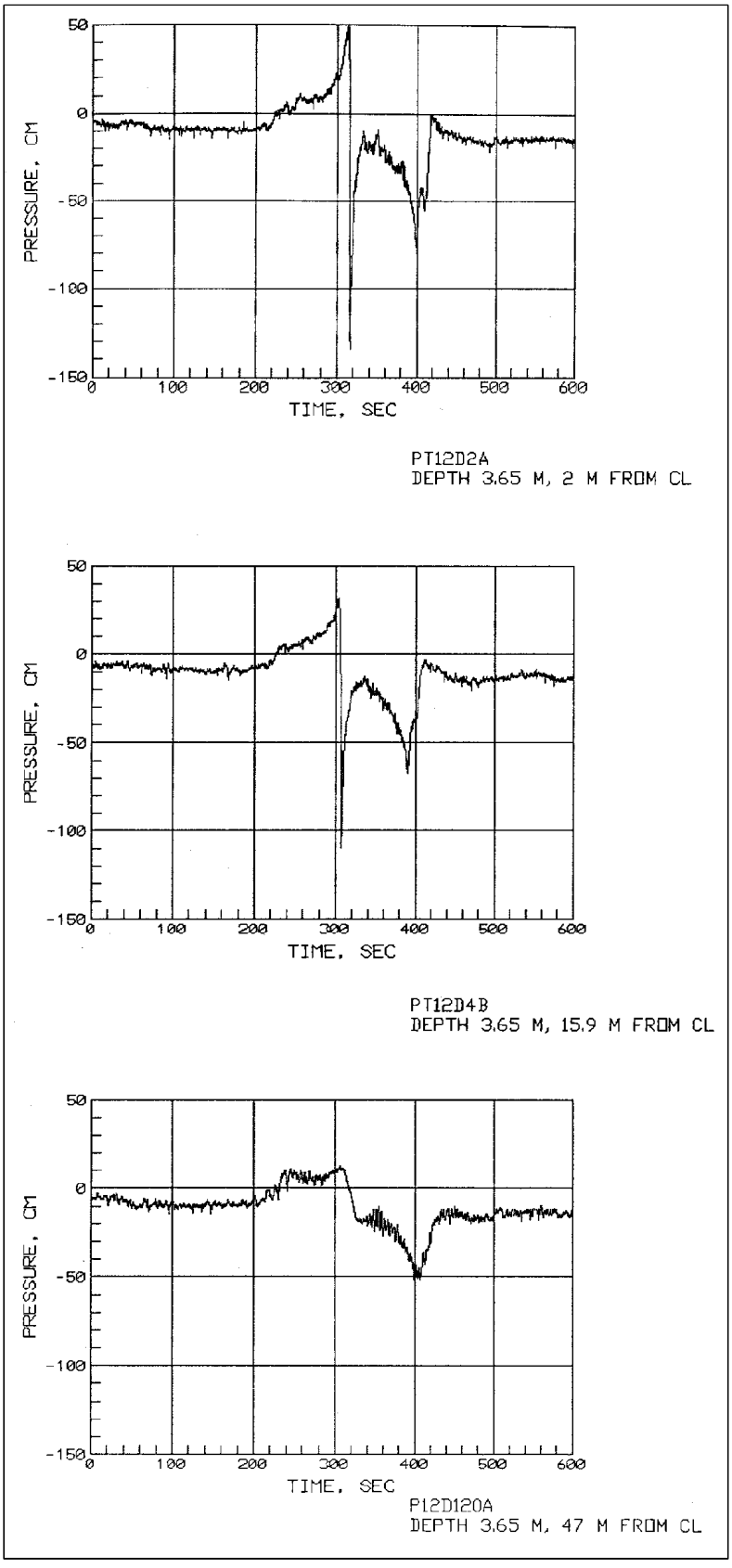

Figure 5. Bottom pressure during tow passage, 3.65-m depth

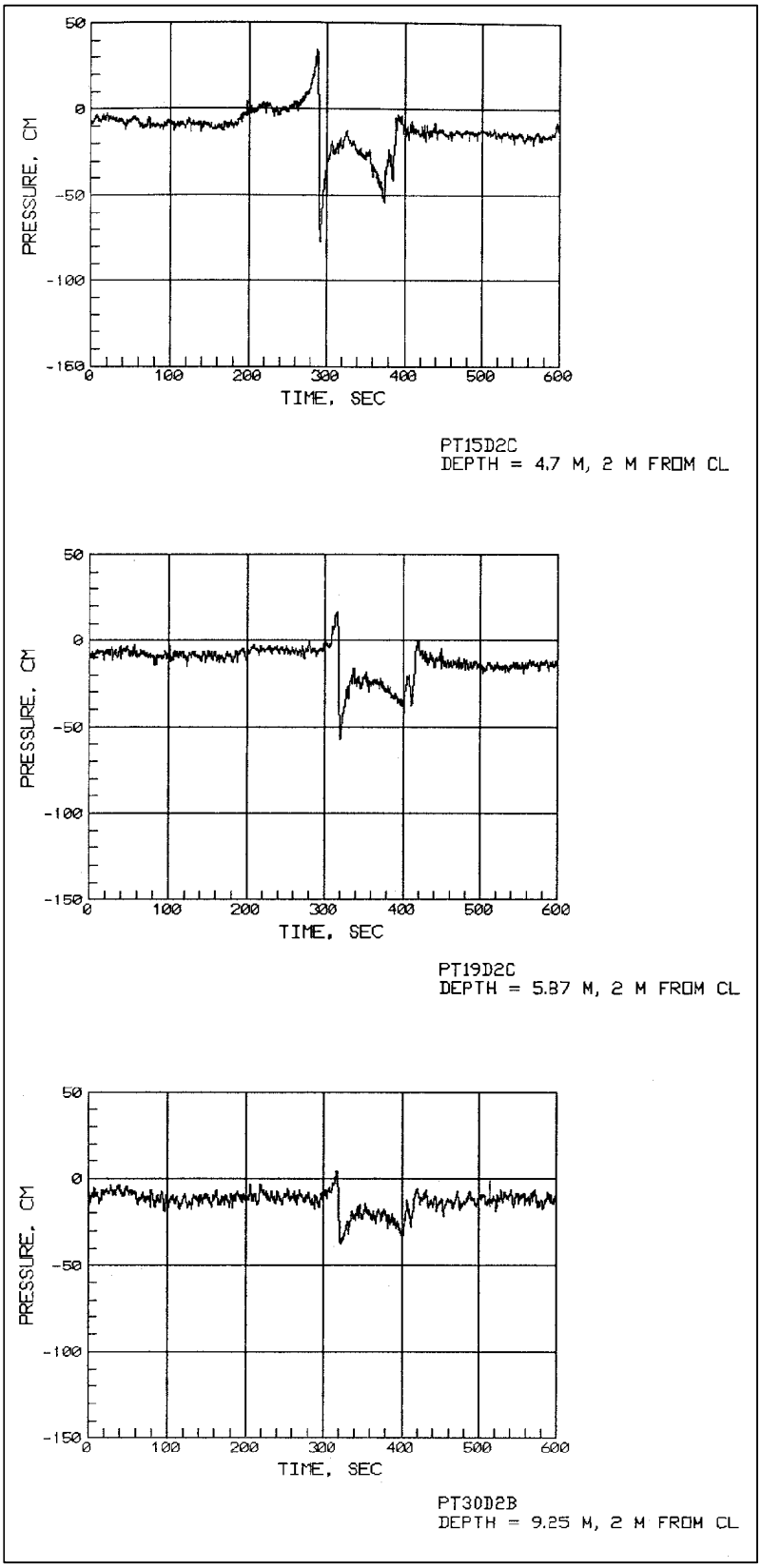

Figure 6. Bottom pressure during tow passage, 4.7-m, 5.87-m, and 9.25-m depths

4 Velocity Under Shallow-Draft Barges

Maximum Bottom Velocity Beneath Vessel (No Distribution)

Maximum bottom velocity near bow of barges

Near-bed velocity 0.6 m above the bed for depths of 4.0, 4.6, 5.5, and 7.3 m was measured beneath the hull of the moving tow without the propellers in operation. All tests were conducted with an upbound tow in an average channel velocity of 0.36 m/sec for a 4.0-m depth, 0.29 m/sec for a 4.6-m depth, 0.38 m/sec for a 5.5-m draft, and 0.29 m/sec for a 7.3-m draft. All tows were loaded to a draft of 2.44 m and were 32 m wide by 258 m long. The tow was centered on the velocity meter which was located 15 m left of the thalweg shown in Figure 2. Typical plots of the time-history of velocity are shown in Figure 7.

Several points should be noted on the time-history of velocity plots as follows:

a. **Bow wave velocity.** The first is the rapid decrease in velocity near the bow of the barges which is caused by the bow wave. The bow wave is somewhat exaggerated in the physical model because the acceleration in the model is larger than the prototype as a result of the relatively short model length. The prototype tows have far less power than the scaled power of the towing carriage. The typical acceleration used in the physical model was 0.06 m/sec/sec(in prototype quantities). Using a 1-Hz filter, the velocity data were used to determine the maximum change at the bow from ambient and plotted in Figure 8. The change at the bow for the upbound tow used herein is actually a decrease, whereas the change for a downbound tow would be an increase in velocity. The equation developed from these data is:

$$\frac{V_{bow}}{V_w} = 0.69\left(\frac{Depth}{Draft}\right)^{1.28} \quad (1)$$

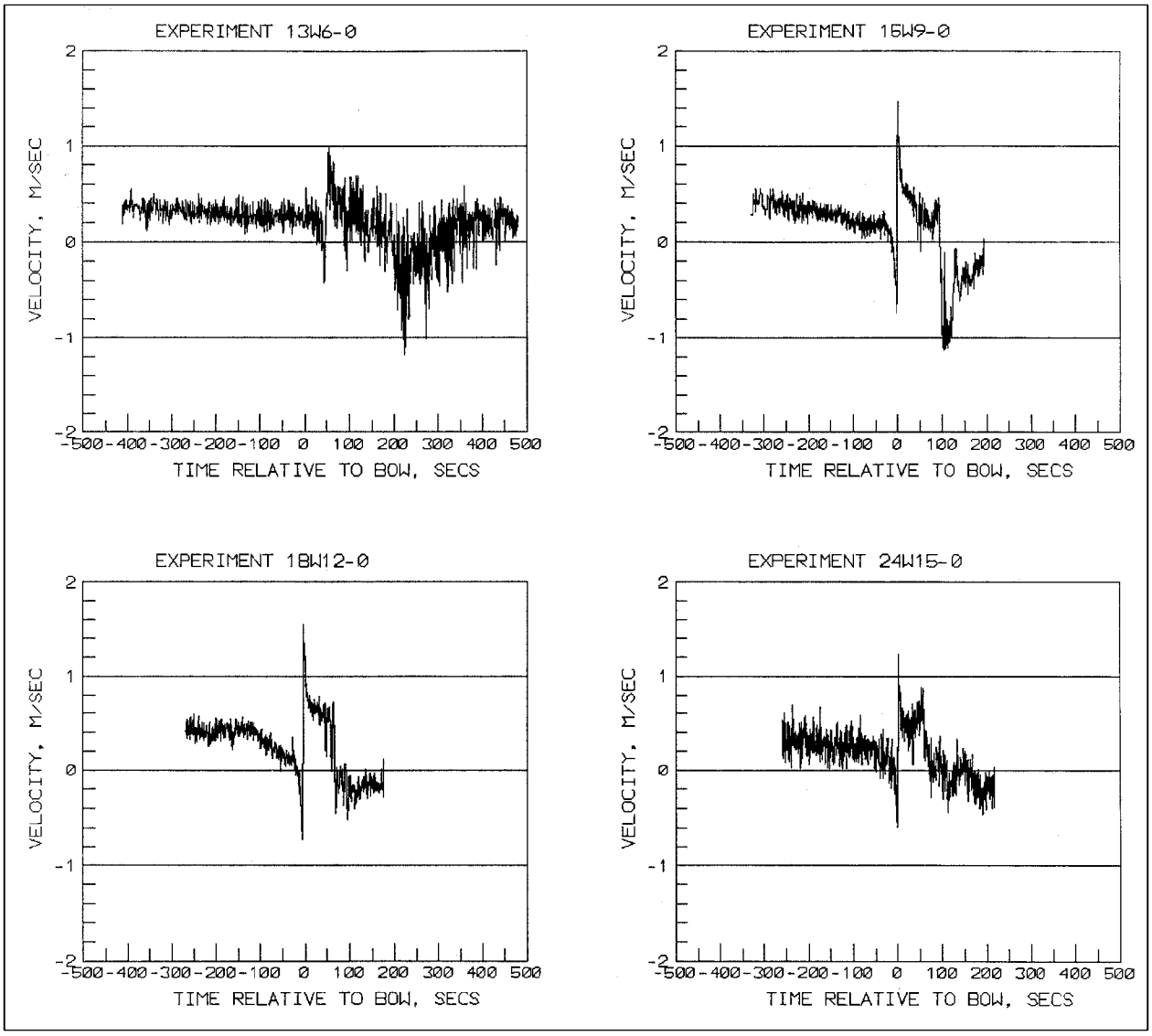

Figure 7. Near-bed velocity without propeller thrust

where

V_{bow}[1] = velocity change at the bow acting in the same direction as the vessel travels

V_w = vessel speed relative to the water

depth = local depth at the center line of the tow

draft = draft of the barges

A notation list is provided after the references.

[1] For convenience, symbols and abbreviations are listed in the Notation (Appendix D).

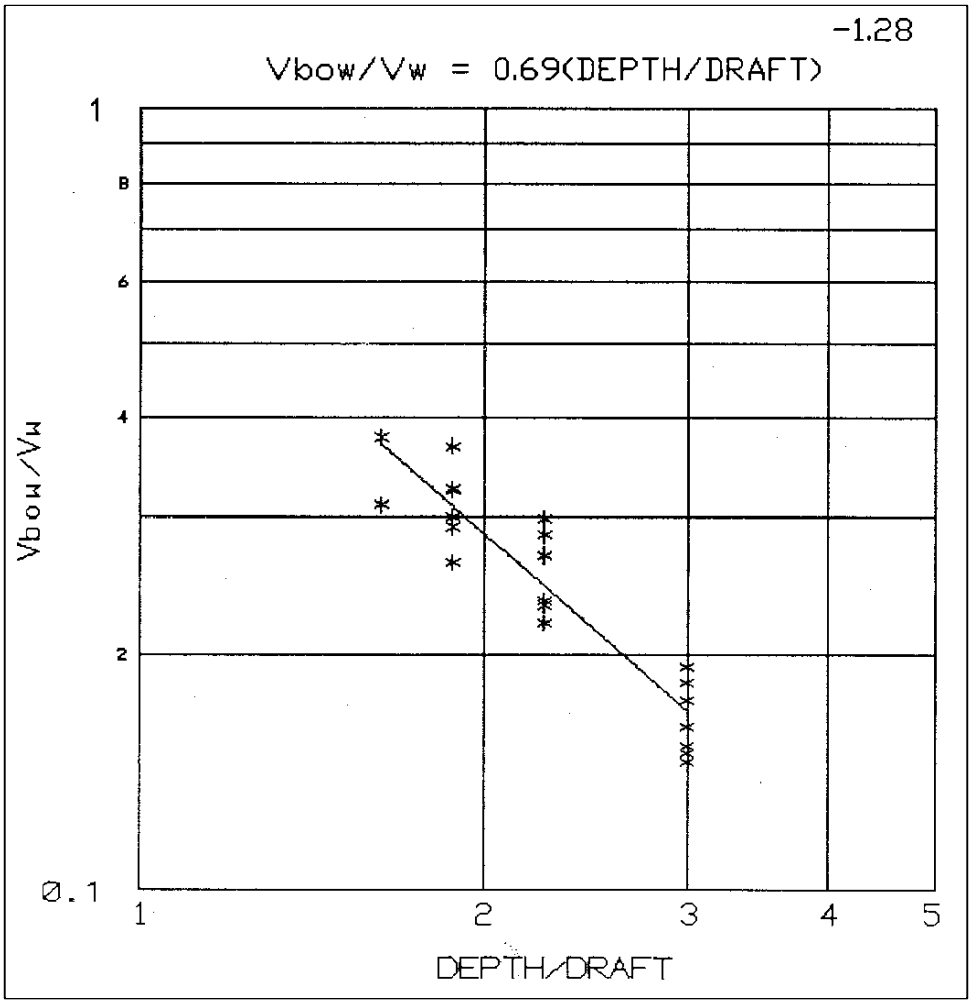

Figure 8. Near-bed maximum bow velocity

b. **Displacement velocity.** The second area of interest in Figure 7 is the rapid velocity increase following the bow wave. This velocity change V_{bd} was termed the "displacement velocity" by Maynord (1990) and was described by the equation:

$$\frac{V_{bd}}{V_w} = 0.16\left(\frac{Beam}{Depth}\right)^{0.54}\left(\frac{Depth}{Draft}\right)^{0.68} \tag{2}$$

where beam is the total width of the barges.

The velocity measurements herein resulted in a change to this equation as follows and is shown in Figure 9:

$$\frac{V_{bd}}{V_w} = 0.69\left(\frac{Depth}{Draft}\right)^{1.21} \tag{3}$$

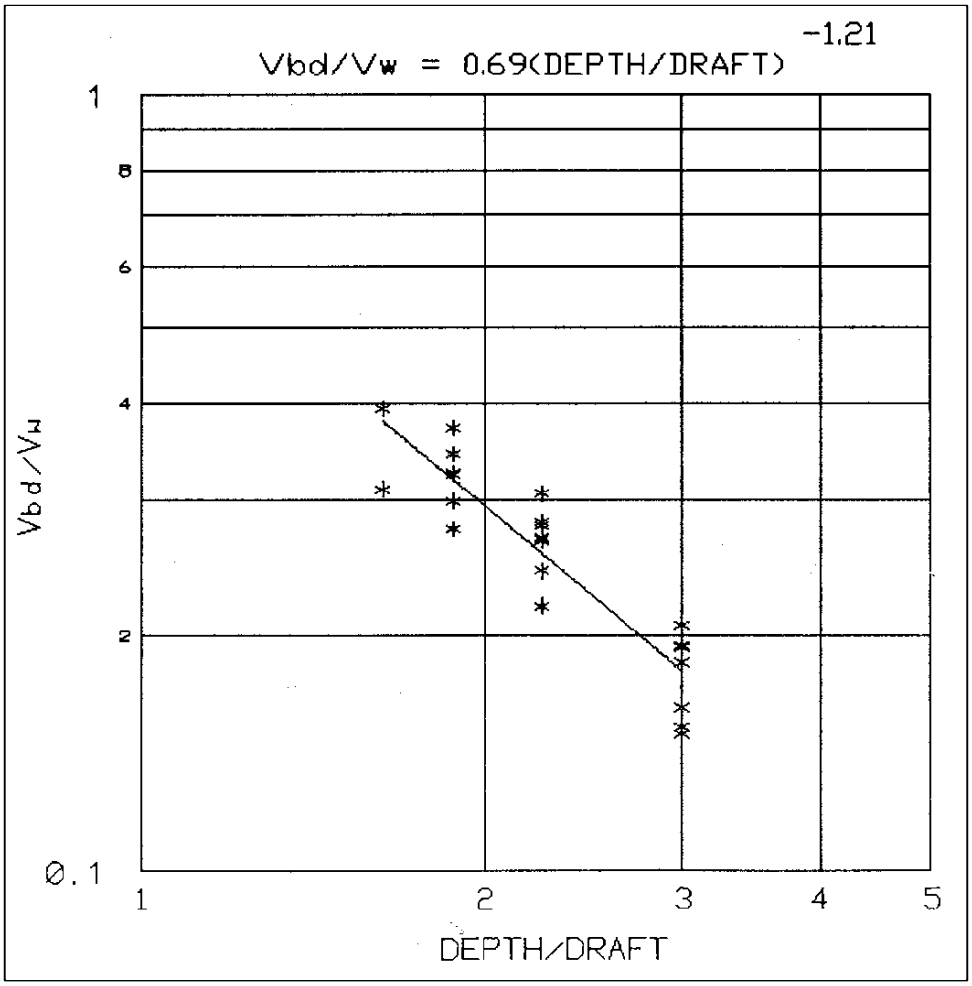

Figure 9. Near-bed maximum displacement velocity

After substituting the beam (32 m) used in these tests in Equation 2, Equation 3 results in a V_{bd} about 3 percent greater than given by Equation 2 at a 3.35-m depth and 30 percent greater at a 6-m depth. The difference between equations is partially due to the more rapid frequency response of the ADV's compared to the propeller meters used by Maynord (1990), allowing peak information to be captured that might have been otherwise missed at lower sampling frequencies.

c. **Return velocity.** The third area of interest on the velocity time-histories in Figure 7 is the return velocity that occurs after the displacement velocity and persists until passage of the stern of the barges. The navigation effects (NAVEFF) model (Maynord 1996) can be used to obtain return velocity magnitude after passage of the displacement velocity.

Maximum bottom propeller jet velocity

Fuehrer, Romisch, and Engelke (1981) determine maximum bottom velocity beneath and behind a moving tow as:

$$\frac{V_b \max}{V_2} = E\left(\frac{H_p}{D_p}\right)^{1}\left(1 \quad V_g / nD_p\right) \tag{4}$$

where

V_2 = velocity increase caused by the propeller

E = empirical coefficient

H_p = distance from center of propeller to channel bottom

D_p = propeller diameter

V_g = vessel speed relative to ground

n = propeller speed in rev/sec

Maynord (1998) documents that the stationary twin-screw towboat used in these experiments having twin screws with Kort nozzles and central rudders has an E = 0.58. Fuehrer, Romisch, and Engelke (1981) found the coefficient E to be 0.71 for fine stern shape (stern is streamlined rather than blocky like a barge) with central rudder, 0.42 for fine stern shape without central rudder, and 0.25 for inland ship, tunnel stern with twin rudder gear, all being single-propeller vessels. Based on diagrams accompanying the text and no mention of Kort nozzles, these E values are assumed applicable to open-wheel propellers. These E values demonstrate the significance of the central rudder used in these tests. The coefficient E for the model Benyaurd towboat used in these experiments was determined for the measured velocities as shown in Table 2 based on a stationary tow having twin open-wheel propellers. Values of E for both open-wheel and Kort nozzle propellers are based on the initial jet velocity as defined using the equation:

$$V_2 = \frac{1.13}{D_0}\sqrt{\frac{Thrust}{r}} \tag{5}$$

where

Thrust = propeller thrust per propeller

D_0 = jet diameter at the location of maximum contraction of the jet and is equal to D_p for a ducted (Kort nozzle) propeller and 0.71 D_p for an open-wheel propeller

= water density

The recommended E for twin open wheels with central rudders is 0.43 which is consistent with the values from Fuehrer, Romisch, and Engelke (1981).

Table 2
Coefficient E in Equation 4 for Stationary Twin-Screw Towboat, Open-Wheel, Central Rudder

Depth, m	H_p/D_p	Calculated V_2, m/sec	Measured V_b max, m/sec	E	Source
3.4	0.74	8.0	4.56	0.42	Figure 10[1]
5.5	1.50	8.0	1.91	0.36	Figure 10[1]
7.5	2.23	8.0	1.68	0.47	Figure 10[1]
3.6	0.80	5.5	3.15	0.46	Riprap tests (125 RPM)[2]
4.24	1.05	7.1	3.0	0.44	Riprap tests (162 RPM)[2]
4.9	1.29	8.5	2.2	0.33	Riprap tests (194 RPM)[2]

[1] The Figure 10 experiments were conducted with a smooth bed, ADV meter 0.6 m above bottom, 155-RPM propeller speed, stationary tow, thrust coefficient $K_t = 0.51$.
[2] Riprap bed, ADV meter 0.46 m above bed, stationary tow, these are only experiments with thrust coefficient $K_t = 0.36$.

For the same propeller thrust and a stationary tow, the larger V_2 from the twin-screw open-wheel propellers (because of the difference in D_0) combined with the lower E value (0.43 for open versus 0.58 for Kort) results in about the same maximum bottom velocity as the twin-screw Kort nozzle propellers.

The relationship between thrust (in pounds) and applied power and speed relative to water (in miles per hour) is given by the Toutant (1982) equations for open wheels as:

$$EP_o = 23.57\ HP^{0.974} \quad 2.3(S)^2\ (HP)^{0.5} \tag{6}$$

and Kort nozzles as:

$$EP_k = 31.82\ HP^{0.974} \quad 5.4(S)^2\ (HP)^{0.5} \tag{7}$$

The disadvantage of the Toutant equations is their empirical and dimensionally incorrect nature that limits their use to the system from which they were developed. Their advantage is they are based on UMRS tows and incorporate the effects of vessel speed. Equations 5, 6, and 7 are used herein for both stationary and underway vessels. Equations 6 and 7 will be used subsequently to compute thrust (or effective push (EP)) for an underway (moving) tow.

To determine the maximum bottom propeller jet velocity, the flow field behind the barges where the towboat operates must be defined. This flow field, referred to as the wake, varies depending on whether the towboat is traveling behind a single unloaded barge or behind three-wide loaded barges. Wake velocity acts in the

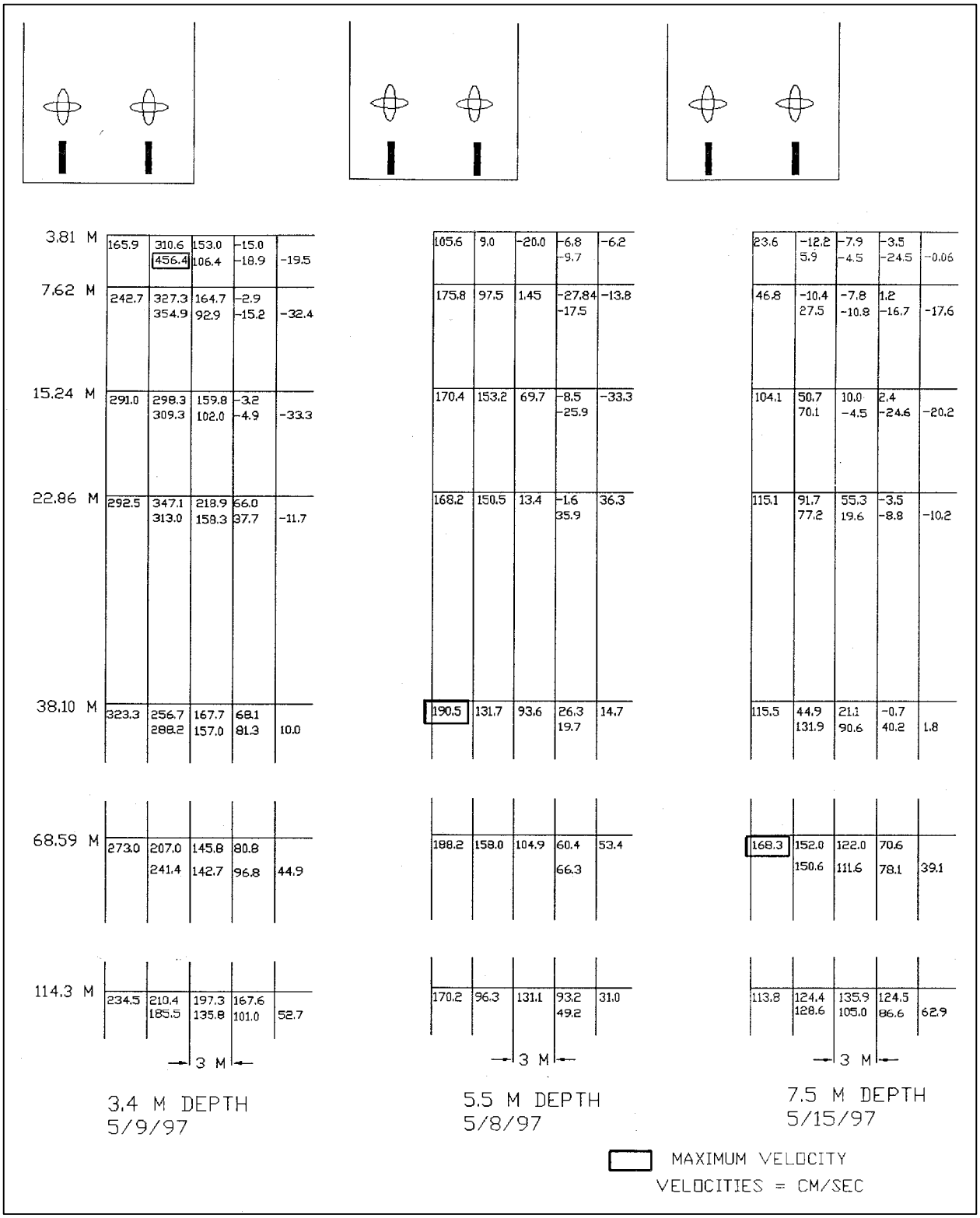

Figure 10. Near-bed propeller jet velocities, open-wheel propellers stationary tow

same direction as the vessel travels, so an upbound tow has wake velocity in an upstream direction and a downbound tow has wake velocity in a downstream direction. Verhey (1983) uses a superposition approach and defines the bottom velocity distribution behind the moving tow as the resultant of the propeller jet velocity relative to the vessel, the wake velocity relative to the vessel, and the vessel speed. The approach used herein combines the Fuehrer, Romisch, and Engelke (1981) approach for maximum bottom velocity with the superposition approach used by Verhey (1983) which incorporates the wake effect on the flow field. In the following analysis for velocities relative to ground, upstream water or vessel velocities are negative, and downstream water or vessel velocities are positive. Therefore, an upbound tow will have a negative vessel speed relative to ground. Ambient velocity V_a is always positive. Vessel speed through the water V_w is always positive, regardless of the direction of the tow and equal to abs(V_a - V_g). The resultant bottom velocity relative to the vessel is:

$$V_{res,v} = V_{prop,v} + V_{wake,v} \tag{8}$$

where

$V_{res,v}$ = resultant bottom velocity

V_{prop} = propeller jet bottom velocity

V_{wake} = wake bottom velocity.

The *v* indicates that the velocity is relative to the vessel. The effects of variations in ambient velocity are reflected in the $V_{wake,v}$ term. The resultant velocity relative to ground is:

$$V_{res,g} = V_{prop,v} + V_{wake,v} + V_g \tag{9}$$

The wake velocity relative to the vessel is:

$$V_{wake,v} = V_{wake,g} - V_g \tag{10}$$

The maximum bottom velocity from the propeller relative to the vessel is defined as:

$$V_{prop,v} = E\left(\frac{D_p}{H_p}\right) V_2 \, fn\left(\frac{V_a \quad V_g}{V_2}, \frac{D_p}{H_p}\right) \tag{11}$$

where V_a is the average channel velocity.

The function in Equation 11 will be defined subsequently.

Table 3 shows the maximum wake velocity data from experiments conducted with the towboat attached to the tow but without the propellers in operation.

Table 3
Maximum Wake Velocity behind Barges without Propeller Jet

Experiment	V_g, m/sec[1]	V_a, m/sec[1]	$V_{a(bott)}$, m/sec[1]	Depth, m	$V_{wake,a}(max)$, m/sec[1]
A13W6-0	-1.83	0.43	0.35	3.96	-0.95
A13w9-0	-2.74	0.43	0.3	3.96	-1.5
13W6-0	-1.83	0.43	0.3	3.96	-0.8
13W9-0	-2.74	0.43	0.2	3.96	-1.2
A15W6-0	-1.83	0.35	0.25	4.57	-0.75
A15W9-0	-2.74	0.35	0.3	4.57	-1.0
A15W12-0	-3.66	0.35	0.3	4.57	-1.2
15W6-0	-1.83	0.35	0.25	4.57	-0.75
15W9-0	-2.74	0.35	0.3	4.57	-1.3
15W12-0	-3.66	0.35	0.3	4.57	-0.9
A18W6-0	-1.83	0.46	0.3	5.49	-0.4
A18W9-0	-2.74	0.46	0.3	5.49	-0.8
A18W12-0	-3.66	0.46	0.3	5.49	-1.1
A18W15-0	-4.57	0.46	0.35	5.49	-1.15
18W6-0	-1.83	0.46	0.35	5.49	-0.45
18W9-0	-2.74	0.46	0.35	5.49	-0.6
18W12-0	-3.66	0.46	0.4	5.49	-0.8
18W15-0	-4.57	0.46	0.3	5.49	-1.0
A24W9-0	-2.74	0.34	0.2	7.32	-0.4
A24W12-0	-3.66	0.34	0.25	7.32	-0.65
A24W15-0	-4.57	0.34	0.3	7.32	-0.7
24W15-0	-4.57	0.34	0.3	7.32	-0.6

[1] All experiments were conducted with upbound tows, the reason that V_g and $V_{wake,a}(max)$ are negative.

The actual draft in the wake experiments was 2.44 m, but the effective draft used in the analysis was 2.74 m as discussed in the section under scale effects. Figure 11 provides a plot of the maximum wake velocity data and the resulting

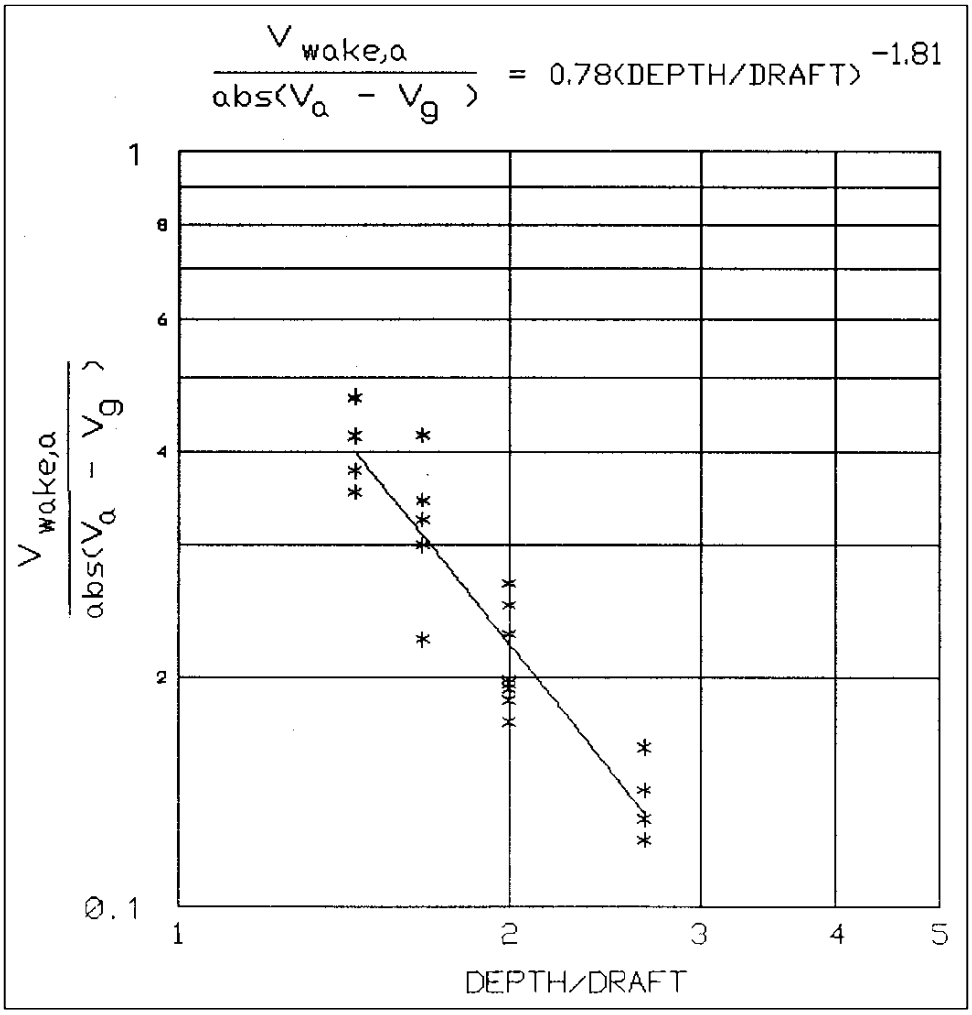

Figure 11. Maximum wake velocity without propeller thrust

best fit equation of the maximum wake velocity from the experiments relative to ambient conditions is:

$$V_{wake,a}(\max) = 0.78\left(\frac{Draft}{Depth}\right)^{1.81}\left(V_a \quad V_g\right) \tag{12}$$

The negative sign is added to the equation to result in negative wake velocity for upbound tows and positive wake velocity for downbound tows. Relative to ground, the maximum wake velocity is defined as:

$$V_{wake,g}(\max) = V_{wake,a}(\max) + V_{a(bott)} \tag{13}$$

However, the maximum wake velocity does not occur at the position of the maximum propeller jet velocity. This means that the distribution of wake velocity is required, the same approach used by Verhey (1983). Time-histories of velocity and shear stress are shown in the figures Appendix A. The location of the peak resultant velocity behind the moving vessel occurs at about

$H_p/(x - LBARGES-TBL) = 0.1$, where TBL is the towboat length, LBARGES is the total length of barges, and x is measured from the bow of the barges. $V_{wake,g}(x)$ is the distribution of the wake velocity that begins at the stern of the barges and reaches the peak $V_{wake,g}(max)$ at about the stern of the towboat. Knowing the distribution of wake velocity will allow computation of the wake velocity at the position where the peak resultant velocity occurs, $H_p/(x-LBARGES-TBL) = 0.1$. Based on the observed wake velocity data, the rise of the wake velocity between x = LBARGES and x = LBARGES + TBL is linear and is defined as:

$$V_{wake,g}(x) = V_{wake,a}(\max)\frac{x \quad LBARGES}{TBL} + V_{a(bott)} \tag{14}$$

For x greater than (TBL + LBARGES), the wake velocity decays at a linear rate according to:

$$V_{wake,g}(x) = V_{wake,a}(\max)\left(1 + 0.0075\frac{TBL}{draft} \quad 0.0075\frac{x \quad LBARGES}{draft}\right) + V_{a(bott)} \tag{15}$$

Equation 15 shows that the wake velocity decays to 0 at a distance of about 133 times the draft of the barges.

Substituting Equations 10 and 11 into Equation 9 results in:

$$V_{res,g} = V_{prop,v} + V_{wake,g}(x) = E\left(\frac{D_p}{H_p}\right)V_2 fn\left(\frac{V_a \quad V_g}{V_2}, \frac{D_p}{H_p}\right) + V_{wake,g}(x) \tag{16}$$

To solve for the maximum resultant velocity, $V_{wake,g}(x)$ is determined at x = [(towboat length) + barge length + $H_p/0.1$]. The function used to decrease the propeller jet velocity for an underway tow must go to a value of unity for a stationary tow as in the Fuehrer, Romisch, and Engelke (1981) Equation 4 and must be based on parameters that are known or can be easily calculated. The function must also reflect that the wake has a significant effect on the propeller jet which increases with decreasing depth. The propeller speed n used in Fuehrer, Romisch, and Engelke (1981) is not often known and is not used herein. Equation 16 was solved for the magnitude of the function using the maximum bottom velocity data for the underway tows. The magnitude of the function was described by:

$$fn\left(\frac{V_a \quad V_g}{V_2}, \frac{D_p}{H_p}\right) = 1 \quad cfunc\ abs\left(\frac{V_a \quad V_g}{V_2}\right)\left(\frac{H_p}{D_p}\right)^{1.5} \tag{17}$$

where cfunc = 0.25 for Kort nozzles and 0.50 for open wheels.

Using this function in Equation 16, V_2 must be negative for downbound tows and positive for upbound tows since upstream velocities are negative and downstream velocities are positive. Computed bottom velocity for underway tows is shown in Table 4 for Kort nozzles and Table 5 for open wheel propellers. Also shown in Tables 4 and 5 are the figure numbers for the observed data. The computed

Table 4
Computed Maximum Bottom Velocity from Combined Effects of Propeller, Wake, and Ambient Velocities, Upbound Tows, Kort Nozzles

Experiment	Depth, m	V_g, m/sec	V_a, m/sec	$V_{a,(bott)}$, m/sec	Computed Thrust, newtons	Computed V_2, m/sec	Computed $V_{res,g}$, m/sec Equations 16 and 17	Figure Number for Observed Data
KV1522AT	4.6	-2	0.29	0.20	393,000	5.8	2.0	A5
KV1524AT	4.6	-3	0.29	0.20	351,500	5.5	1.5	A9
KV1822AT	5.5	-2	0.38	0.30	390,000	5.8	1.6	A14
KV1824AT	5.5	-3	0.38	0.30	347,000	5.4	1.1	A17
KV1826AT	5.5	-4	0.38	0.30	429,000	6.0	1.0	A22
KV2323AT	7.1	-2.5	0.29	0.20	374,000	5.6	0.9	A23
KV2324AT	7.1	-3.0	0.29	0.20	351,500	5.5	0.6	A26
KV2325BT	7.1	-3.5	0.29	0.20	470,000	6.3	0.7	A29
KV2326AT	7.1	-4.0	0.29	0.20	435,500	6.1	0.5	A30

Table 5
Computed Maximum Bottom Velocity from Combined Effects of Propeller, Wake, and Ambient Velocities. Based on Tows with Open-Wheel Towboat

Experiment	Depth, m (up or dn)	V_g, m/sec	V_a, m/sec	$V_{a,(bott)}$, m/sec	Computed Thrust, newtons	Computed V_2, m/sec	Computed $V_{res,g}$, m/sec Equations 16 and 17	Figure Number for Observed Data
0304-2DX	4.3(up)	-1.5	0.55	0.45	368,000	7.9	2.5	A66
0304D2FX	4.3(dn)	3.1	0.55	0.45	360,000	-7.8	-1.3	A67
3718U2AX	5.6(up)	-2.1	0.55	0.45	358,500	7.8	1.4	A68
3618D2AX	5.6(dn)	3.6	0.55	0.45	350,500	-7.7	-0.3	A69
0306-2DX	7.0(up)	-2.1	0.60	0.50	357,500	7.8	1.0	A70
0306D2CX	7.0(dn)	3.6	0.60	0.50	351,500	-7.7	0.2	A71

velocity exiting the propeller jet V_2 is determined using the thrust for the moving tow. Thrust for the moving tows in Tables 4 and 5 is computed by determining the power for a stationary tow using the Toutant equations and a stationary thrust of 382,500 N for the open-wheel tow and 431,500 N for the Kort nozzle tow. (Both stationary thrust values were measured in the physical model.) The resulting power was 4,540 Hp for open wheels and 3,780 Hp for Kort nozzles. This same power was assumed to be exerted by the towboat while underway and used in the Toutant equations for the moving tows to determine the thrust for various speeds through the water. For example, experiment KV1522AT has a vessel speed through the water = $abs(V_a - V_g) = abs(0.29-(-2.0)) = 2.29$ m/sec = 5.1 MPH. Using a power of 3,780 Hp and 5.1 MPH results in EP_k from Equation 7 of 393,000 N. Time-histories for velocity and shear referenced in Tables 4 and 5 are shown in Appendix A.

Distribution of Velocity Near Path of Tow

The previous section defined only the maximum bottom velocity from the propeller jet without regard to location. This section presents a method for determining the lateral and longitudinal distribution of the bottom velocity from the propeller jet. As in the previous section, these empirical relations will provide a bottom velocity magnitude only, assumed to act parallel to the tow axis and opposite to the direction of tow travel, and at 0.6 m above the bed. Numerous previous studies have used the free jet equations developed by Albertson et al. (1950) to define the velocity distribution near the bed from a propeller jet. Note that propeller jets from shallow-draft navigation on the inland waterways of the United States differ from the assumptions used for the free jet as follows:

a. The close proximity of the channel bottom and the water surface inhibit spreading and cause the jet to deflect toward one or the other.

b. The jet is discharging into the highly disturbed flow field in the wake of the moving vessel.

c. The propeller has a radial component of velocity.

d. A central rudder splits the jet into two jets, one toward the surface, the other toward the bottom.

e. The tunnel stern affects the flow leaving the propeller.

f. The Kort nozzle and open wheel are different from an orifice.

g. The two propeller jets act independently near the towboat and merge some distance astern.

The complexity of the flow field behind a tow, particularly an underway tow, can not be overstated. In a previous report by the author (Maynord 1990), the Verhey (1983) method, which uses the free jet equations, was adopted and modified to predict propeller velocity distribution behind a moving tow. The

framework of the Verhey method is adopted herein primarily because it incorporates the effects of the wake as discussed previously.

The comment above about the central rudder effects is based on Fuehrer, Romisch, and Engelke (1981) who report that a central rudder splits the propeller jet into a surface jet and a bottom jet. As viewed from the stern, the clockwise rotation of the port propeller and the counterclockwise rotation of the starboard propeller results in the downward deflected jet to be between the center line of the tow and each rudder. Dye injections in the physical model, which were injected near the water surface, suggest that the surface jet may also have a component toward the outside of the vessel. Prosser (1986) reports that the central rudder jets are deflected 'sideways and upwards' and 'sideways and downwards.' The significance of the bottom jet on scour of the bed was demonstrated in recent riprap stability tests with the 1:25-scale towboat. All failures were located just inside the rudder for both propellers. Fuehrer, Romisch, and Engelke (1981) report that the bottom and surface jets are directed at 0.2 radians (12 degrees) (up or down) relative to the axis of the propeller. They also report that tunneling (the hull shape in the vicinity of the propellers where the lowest point around the perimeter of the hull in the stern region is below the upper tip of the propeller by up to 0.5 m) tends to divert the jet upward because of 'jet suction.' Results from Bergh and Magnusson (1987) also show a downward deflection of 0.2 radians (12 degrees) and show a sideways deflection of 0.1 radians (6 degrees), which is the average of the surface and bottom jet. Bottom velocities from Bergh and Magnusson (1987) with a central rudder were twice as high on the side with the bottom jet as compared with the side with the surface jet. Prosser (1986) reports that "This behavior cannot be explained using a simple description of the propeller jet which does not take tangential velocity components into account. In such a simple model where only axial velocities are considered, the rudder (in its zero position) would only act as a splitter with the flow dividing and recombining behind the rudder. With the tangential flow superimposed on the axial flow the rudder will act as a lifting surface and deflect part of the jet sideways. The effect will be most significant at zero advance ratio and will depend on the size of the rudder relative to the propeller and its distance behind the propeller."

Based on the numerous factors that violate the free jet equation assumptions, an empirical approach, rather than the free jet equation, is adopted herein.

Empirical method for bottom velocity distribution, stationary tow

The approach adopted herein for the lateral and longitudinal distribution of bottom velocity is to break the area behind the tow into two zones as shown in Figure 12 and described as follows:

a. **Zone 1**. The first zone is where the propeller jet velocity is dominated by the central rudder effects and the two jets have not merged. The confining effects of the water surface and bed are not dominant, and a circular jet equation can be justified if modified for the effects of the central rudder. For Zone 1, determine velocity as follows:

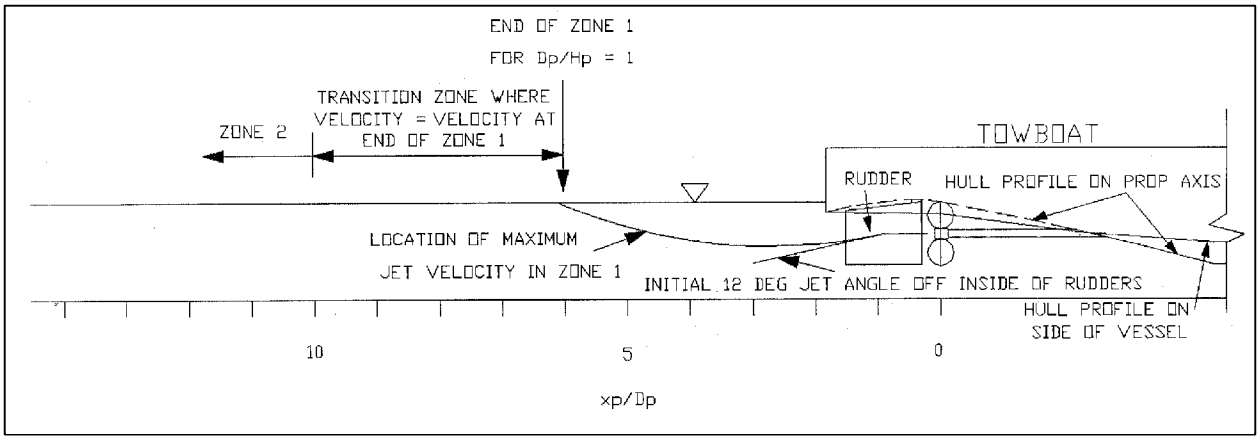

Figure 12. Zone locations for velocity distribution and tunnel stern configuration

(1) Define maximum jet velocity $V(xp)_{max}$ for a single propeller in Zone 1, where xp is the distance from the propeller. Jet theory as defined by Albertson et al. (1950) defines a zone of flow establishment where the velocity in the core of the jet does not decay and a zone of established flow where the maximum velocity decays with distance. This same approach is used in Verhey (1983). Hamill, Johnston, and Stewart (1995) conducted velocity measurements downstream of four stationary propellers and found velocity to immediately decay downstream of the propeller; there was no zone where the core velocity remained constant. Velocity measurements were taken downstream of the 1:25-scale towboat with the open-wheel propellers and a stationary vessel. Measurements were taken with the miniature propeller meter behind each propeller with a stationary tow in 3.35-, 5.5-, and 7.5-m depths. Only one propeller was operating during these tests and the velocity probe was positioned 1/2 D_p below the water surface. The probe was positioned initially on the axis of the propeller and moved laterally until the maximum velocity was found. This procedure corrects for the fact that the highest velocity in the propeller jet is generally not exactly on the propeller axis. Results are given in prototype values and are shown in Table 6.

The results shown in Table 6 and Figure 13 show that the velocity decays rapidly downstream of the propeller, similar to the findings of Hamill, Johnston, and Stewart (1995). A regression of the dimensionless distance from the propeller versus the dimensionless velocity for all depths resulted in:

$$\frac{V(xp)_{\max}}{V_2} = 1.21\left(xp/D_p\right)^{0.524} \tag{18}$$

Table 6
Maximum Propeller Jet Velocities for Single Propeller Operation, ½ D_p below Water Surface, Open-Wheel Propellers, Stationary Tow

Distance from Stern, m	xp, Distance from Props, m	xp/D_p	Right prop V(xp)max, m/sec	Left prop V(xp)max, m/sec	Average V(xp)max, m/sec	$V(xp)max/V_2$
3.35-m Depth:						
0.0	5.0	1.82	7.8	7.25	7.53	1.01
3.8	8.8	3.21	5.15	4.85	5.00	0.67
7.6	12.6	4.61	4.5	4.20	4.35	0.58
15.2	20.2	7.38	3.40	2.60	3.0	0.40
22.9	27.9	10.18	2.70	2.35	2.53	0.34
38.1	43.1	15.75	2.45	1.95	2.20	0.30
68.6	73.6	26.90	2.30	1.55	1.93	0.26
114.3	119.3	43.60	1.60	1.15	1.38	0.18
5.5-m Depth:						
0.0	5.0	1.82	7.5	7.2	7.35	0.94[1]
3.8	8.8	3.21	4.7	5.6	5.15	0.66[1]
7.6	12.6	4.60	4.1	3.7	3.9	0.52
11.4	16.4	6.00	3.1	3.1	3.1	0.42
15.2	20.2	7.38	2.9	2.5	2.7	0.36
22.9	27.9	10.18	2.8	2.2	2.5	0.34
30.5	35.5	12.96	2.2	2.2	2.2	0.30
7.5-m Depth:						
0.0	5.0	1.82	7.20	7.0	7.1	0.95
3.8	8.8	3.21	4.30	3.65	3.98	0.53
7.6	12.6	4.61	4.00	3.85	3.93	0.53
15.2	20.2	7.38	3.25	3.25	3.25	0.44
22.9	27.9	10.18	2.75	2.65	2.70	0.36
38.1	43.1	15.75	2.00	2.40	2.20	0.30
68.6	73.6	26.9	1.60	1.60	1.60	0.22
114.3	119.3	43.6	1.25	1.05	1.15	0.16

[1] V_2 = 7.8 m/sec, all others V_2 = 7.45 m/sec.

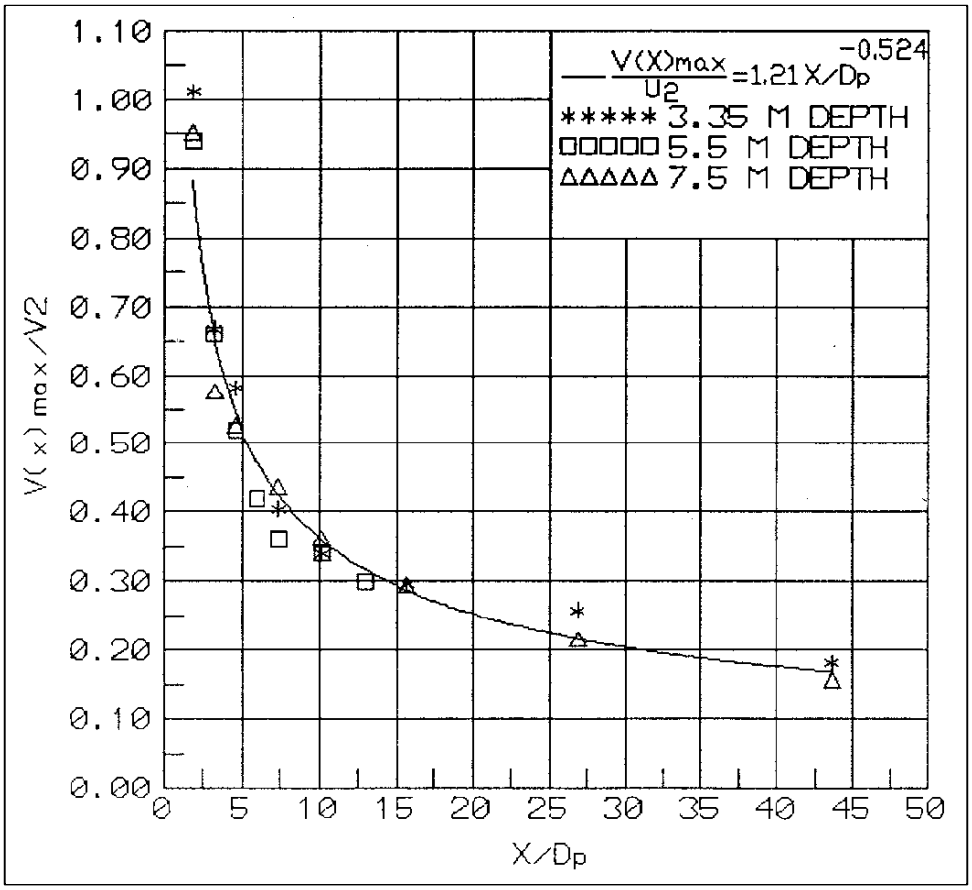

Figure 13. Maximum propeller jet velocity for single propeller

and is plotted in Figure 13 along with the observed data. No significant variation of velocity decay with depth was found. Subsequent tests showed that the maximum velocity at 0.6 m below the surface is greater than the velocity at ½ D_p below the water surface. Adopting the slope of Equation 18 because it was based on extensive measurements, the coefficient applicable to velocities 0.6 m below the surface was based on measurements given in Table 7 and the equation was:

$$\frac{V(xp)_{\max}}{V_2} = 1.45\left(xp/D_p\right)^{0.524} \tag{19}$$

Table 7
Maximum Propeller Velocities for Single-Propeller Operation 0.6 m Below Surface, Stationary Tow

Distance from stern, m	xp, Distance from props, m	xp/D_p	Left Prop V(xp)max, m/sec	$V(xp)max/ V_2$
3.66-m Depth:				
38.1	43.1	15.7	2.95	0.396
68.6	73.6	26.9	2.00	0.268
5.5-m Depth:				
22.9	27.9	10.2	3.5	0.470
38.1	43.1	15.7	2.6	0.349
68.6	73.6	26.9	2.08	0.279
114.3	119.3	43.5	1.35	0.182
7.4-m Depth:				
22.9	27.9	10.2	3.28	0.443
38.1	43.1	15.7	2.04	0.275
68.6	73.6	26.9	1.73	0.234

Equations 18 and 19 are similar to the Oebius (1984) equation for a stationary vessel and also similar to the Fuehrer, Romisch, and Engelke (1981) equation for a tunnel stern where no significant variation with depth was found. This bottom velocity distribution approach uses the same equation developed from surface jet measurements for the bottom jet. While the data used in developing Equation 19 were from Zone 2, Equation 19 is only used herein in Zone 1.

(2) Jet deflection by rudder. The vertical position of the maximum velocity is on the propeller axis from the propeller out to about half the distance between the propeller and the towboat stern based on observations of dye in the model. At this point, the central rudder deflects the maximum jet velocity down at an angle of 12 deg based on measurements by Fuehrer, Romisch, and Engelke (1981). The dye observations showed the jet coming off the inside of the rudder toward the bed. The profiles of velocity in Figures 14 to 20 show that the maximum jet velocity is at the surface at about $x/D_p = 10$. Two possible explanations for the jet behavior were considered herein. First, the downward deflected bottom jet decays at a more

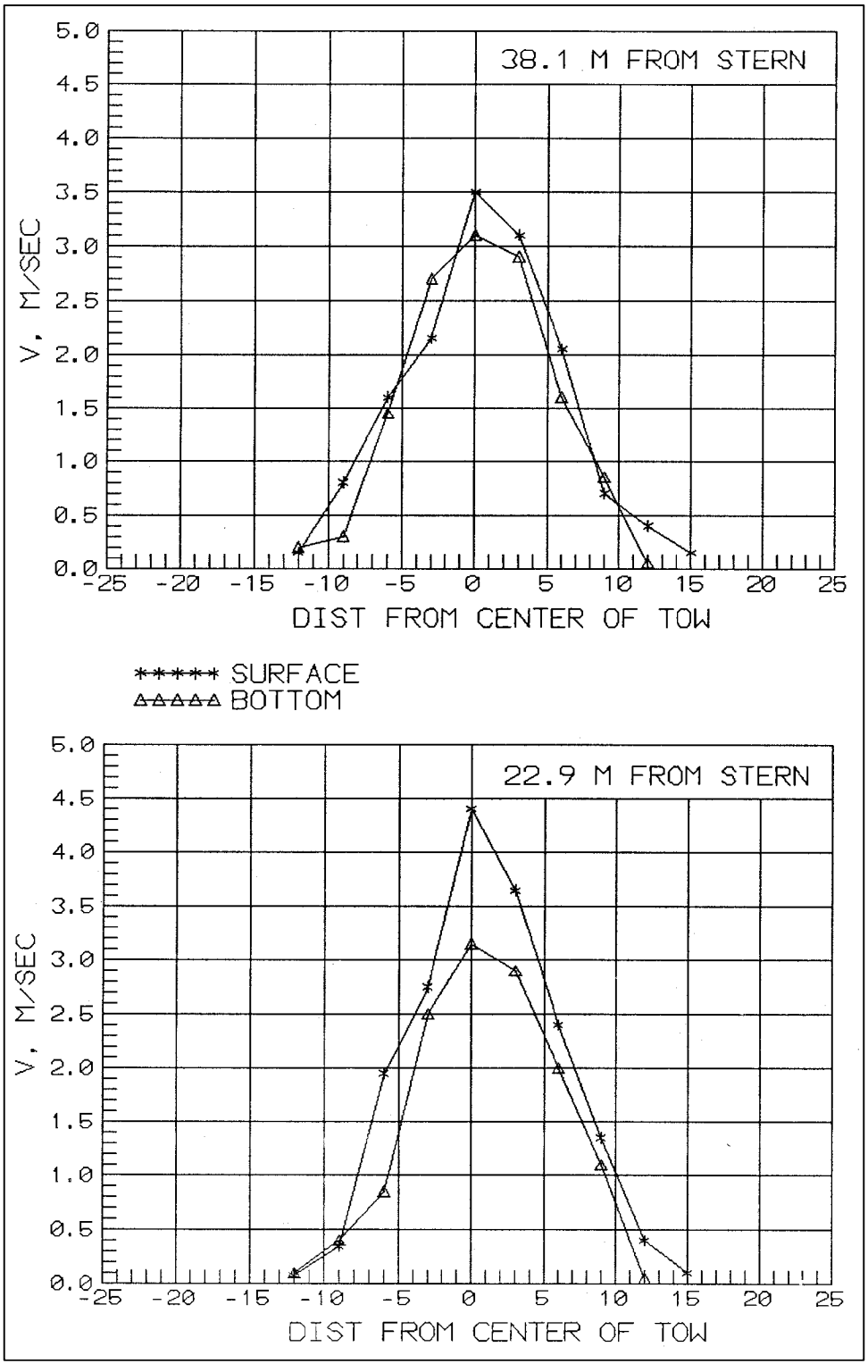

Figure 14. Lateral velocity distribution, 3.65-m depth, open-wheel propellers, 22.9 and 38.1 m from stern

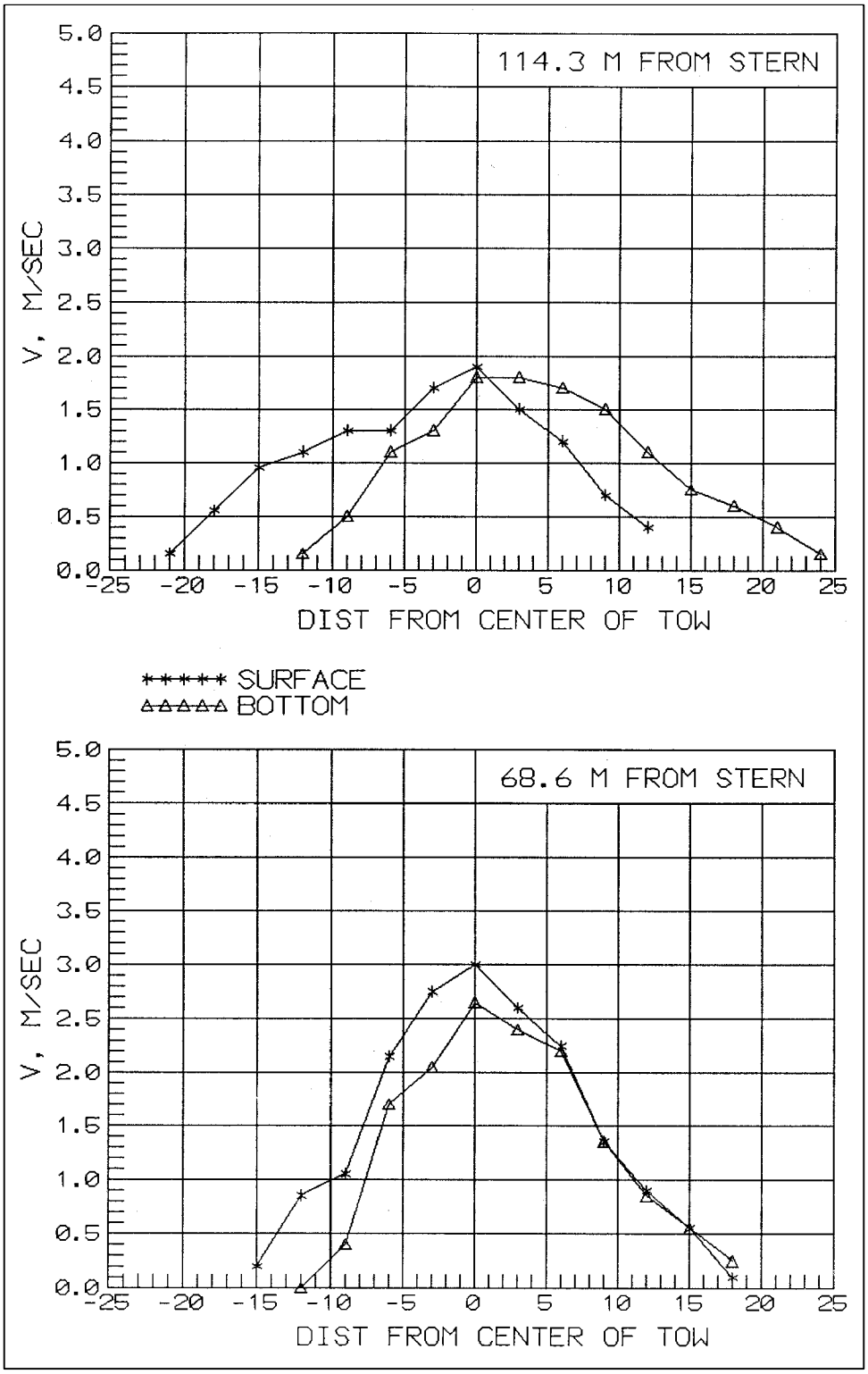

Figure 15. Lateral velocity distribution, 3.65-m depth, open-wheel propellers, 68.6 and 114.3 m from stern

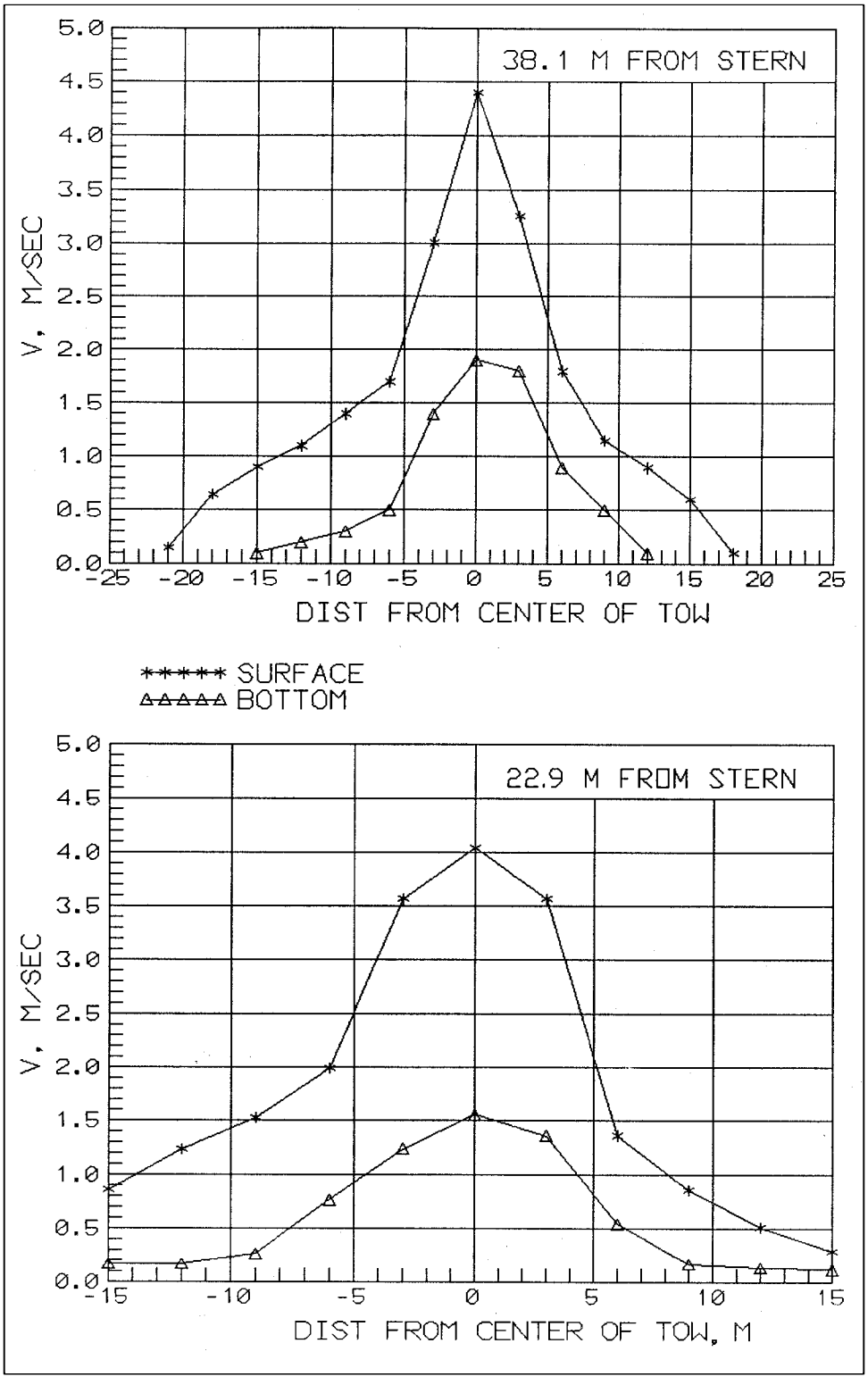

Figure 16. Lateral velocity distribution, 5.5-m depth, open-wheel propellers, 22.9 and 38.1 m from stern

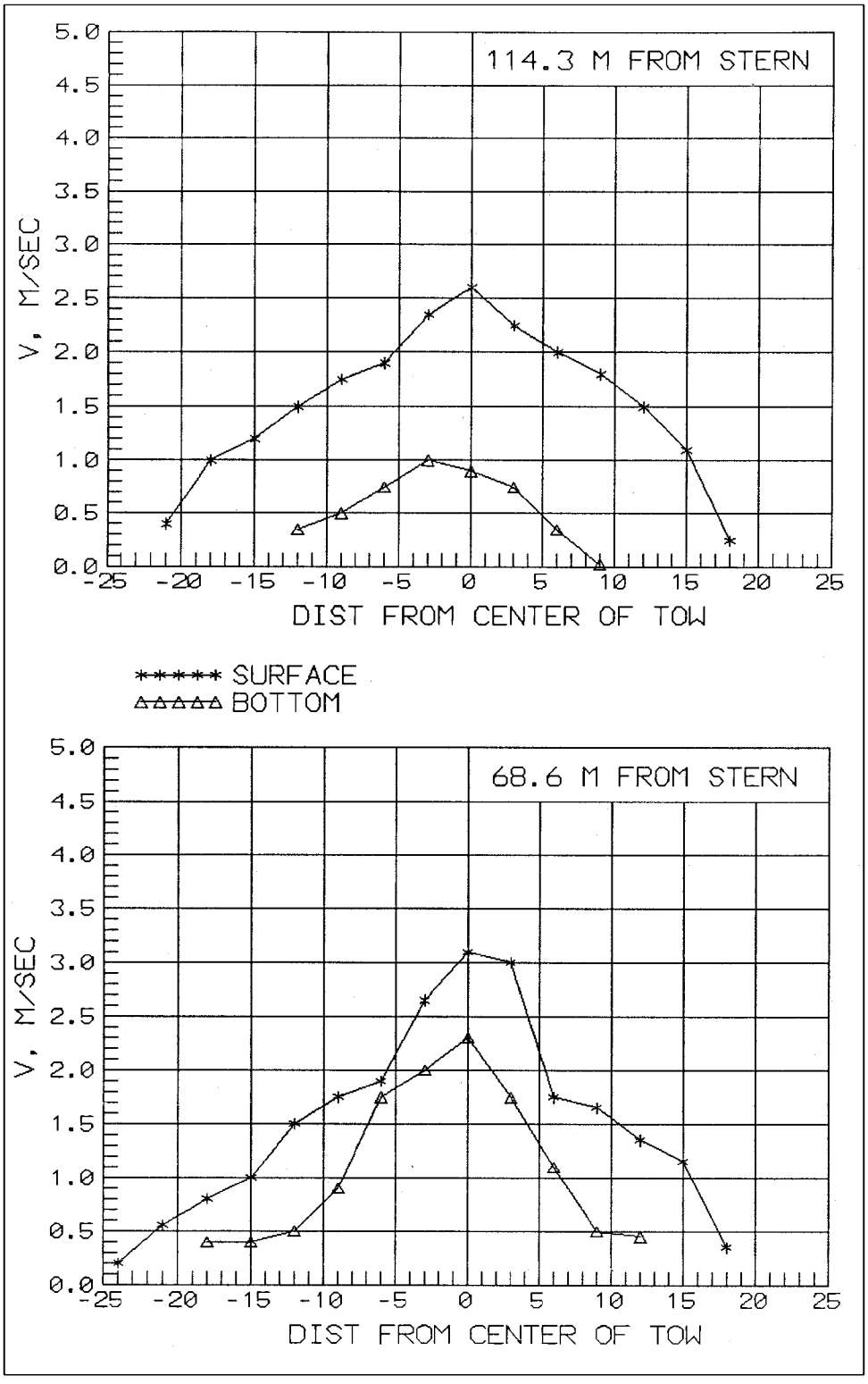

Figure 17. Lateral velocity distribution, 5.5-m depth, open-wheel propellers, 68.6 and 114.3 m from stern

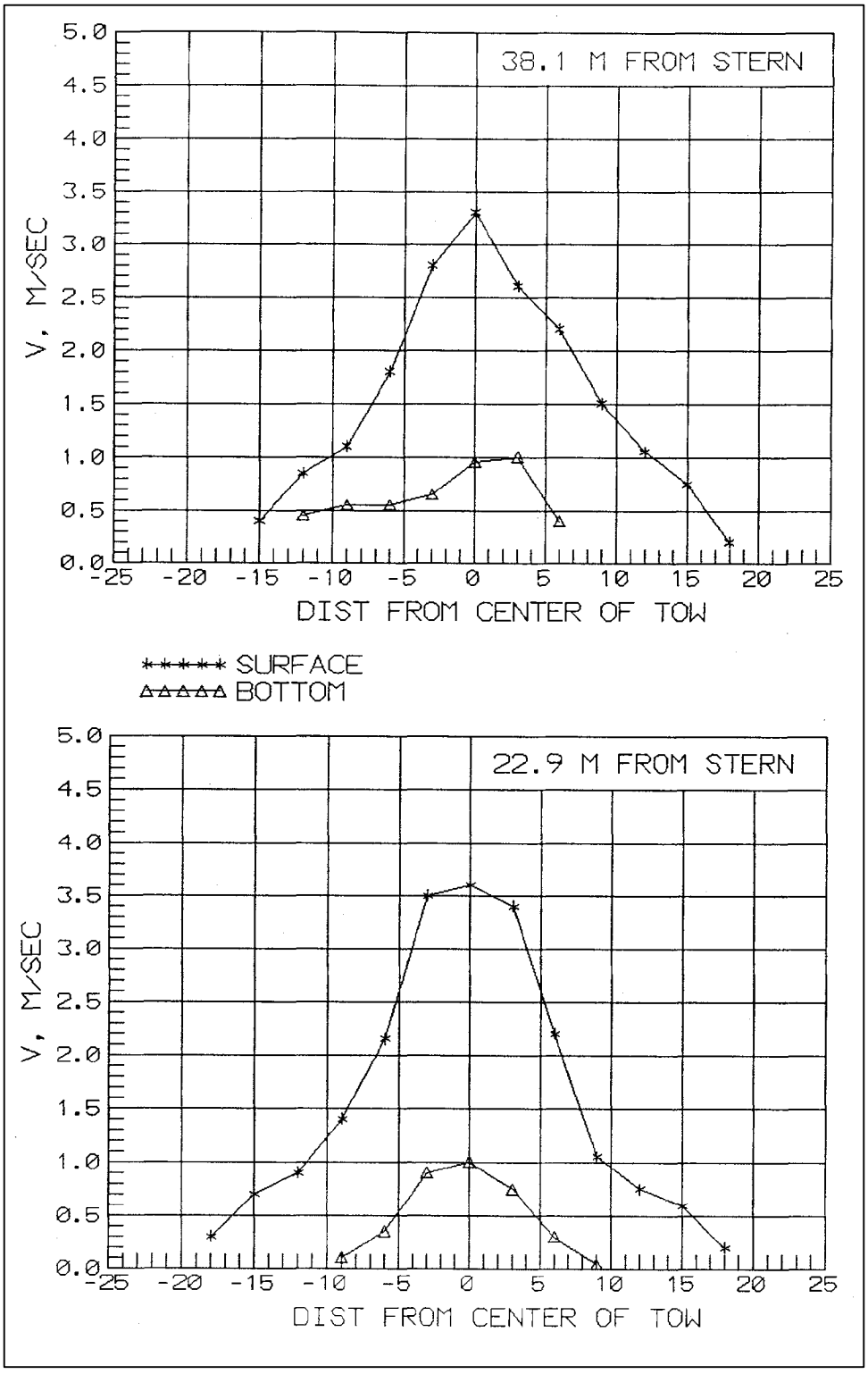

Figure 18. Lateral velocity distribution, depth = 7.4 m, open-wheel propellers, 22.9 and 38.1 m from stern

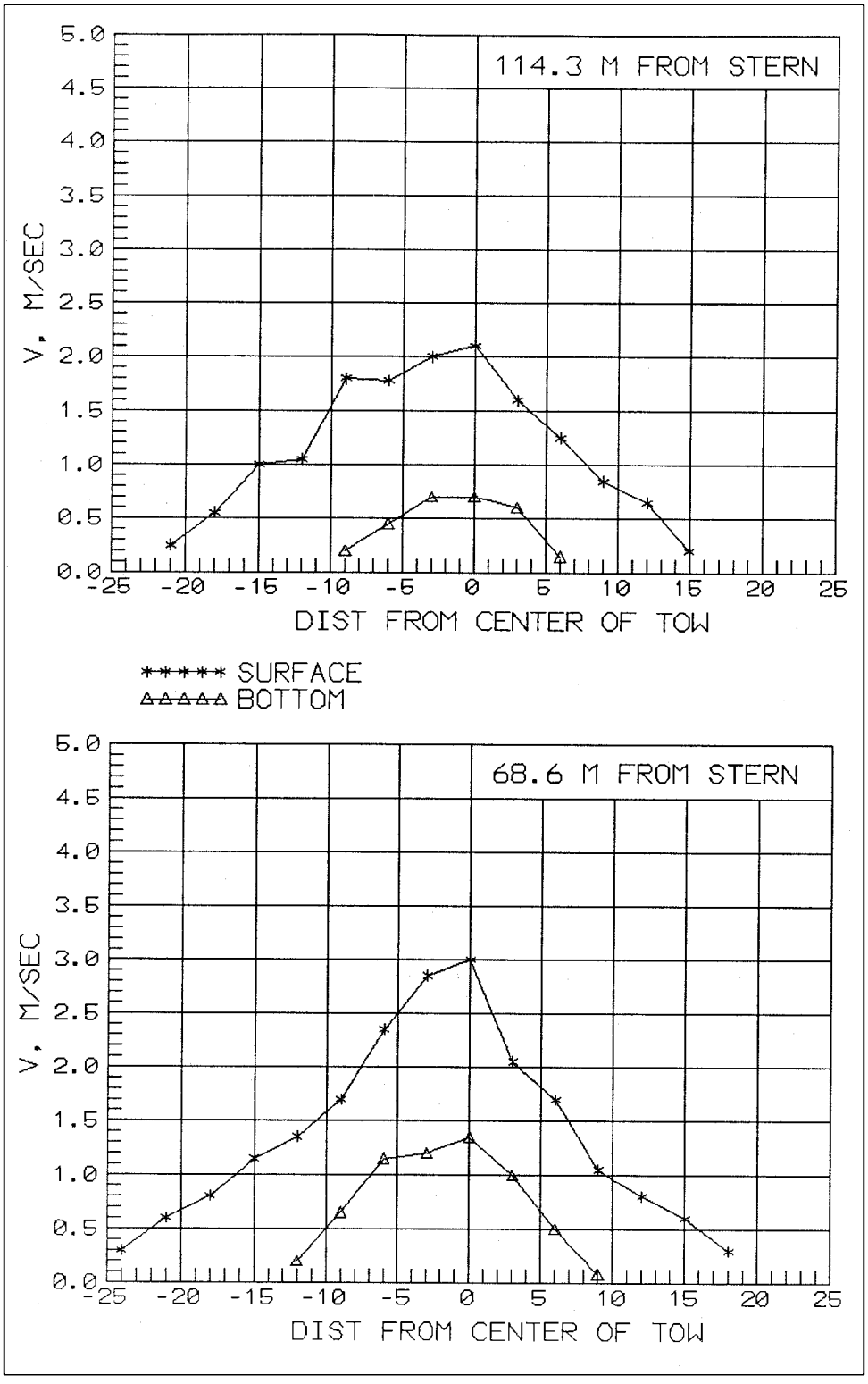

Figure 19. Lateral velocity distribution, 7.4-m depth, open-wheel propellers, 68.6 and 114.3 m from stern

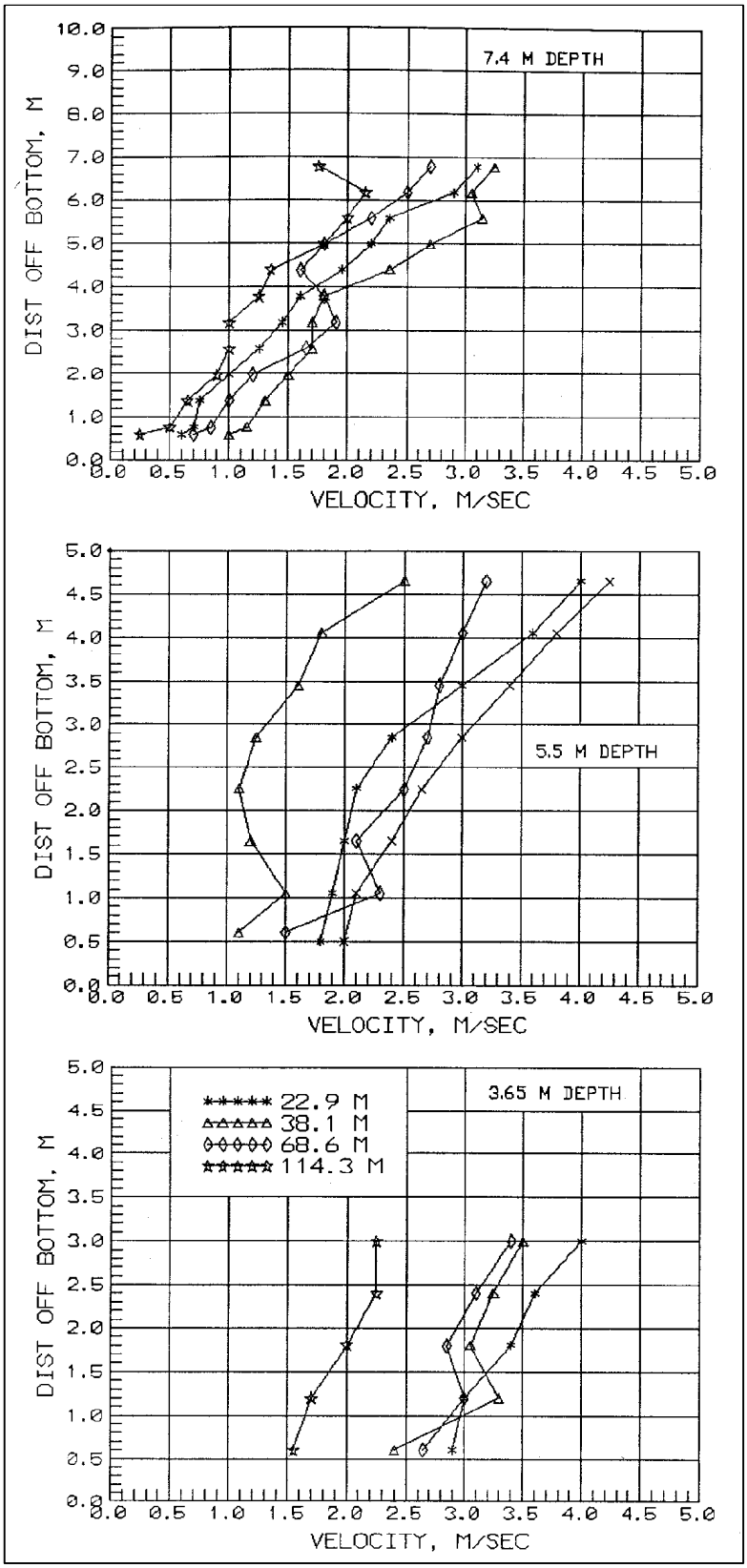

Figure 20. Vertical velocity distribution, center line of tow, open-wheel propellers

rapid rate than the surface jet measurements in the preceding paragraph. The second explanation is that the jet leaves the rudder at a downward angle and then begins to deflect back toward the water surface because of tunnel stern effects or effects of the bottom. The second approach resulted in a reasonable fit of the data when a parabolic shape was adopted for the position relative to the propeller shaft of the maximum jet velocity from the beginning of the 12-degree downward angle out to the point where the maximum velocity reaches the surface. The equation adopted is:

$$CJ = -\left[\tan(12°)(xp - SETBACK/2) - \frac{C_{para}\, g\,(xp - SETBACK/2)^2}{V_2^2 \cos^2(12°)} \right] \qquad (20)$$

where

CJ = vertical distance from the propeller shaft to the location of maximum velocity within the jet

SETBACK = horizontal distance from the propeller to the stern of the towboat

C_{para} = an empirical coefficient that will be determined subsequently

(3) Decay $V(xp)_{max}$ radially from each propeller using the jet equation for fully developed flow from Verhey (1983):

$$V_{x,r} = V(xp) \max \exp\left(-\frac{r^2}{2C^2 xp^2} \right) \qquad (21)$$

with C = 0.18 from Verhey (1983) and r measured from the position of the jet maximum as defined by CJ.

(4) Superposition is used to combine the lateral distribution of jet velocity from each propeller. Verhey (1983) recommends the addition of velocity from the single propeller equations using superposition of the determined velocity for each propeller.

(5) Using observed bottom velocity in Zone 1 shown in Figure 10, various values of C_{para} were used to test the computed bottom velocity against the observed bottom velocity. The best agreement for open-wheel propellers was found with $C_{para} = 0.12(Dp/Hp)^{2/3}$. For Kort nozzle propeller data given by Maynord (1998), $C_{para} = 0.04$ provided the best fit of the data.

(6) Zone 1 ends where the maximum jet velocity location is at the water surface according to Equation 20.

b. **Zone 2.** The second zone is represented by a single jet whose maximum velocity is at the surface and has a different lateral and vertical decay of velocity because of the effects of the bed and water surface. Zone 2

begins at xp/Dp = 10.0. Observations of the flow and measurements behind the vessel show that a twin-screw towboat has two distinct jets close to the vessel and a combined jet away from the vessel. In Zone 2, determine propeller jet velocity as follows:

(1) Treat the jet as one jet and define the vertical position of the maximum jet velocity as being at the surface as shown in the vertical velocity profiles in Figure 20.

(2) Decay the maximum near surface velocity from the combined jet. Lateral profiles of velocity were taken 0.6 m above the bottom and 0.6 m below the surface for depths of 3.4, 5.5, and 7.4 m for distances behind the stern of 22.9, 38.1, 68.6, and 114.3 m (Figures 14 to 19). Vertical profiles of velocity parallel to the tow axis along the center line of the tow are shown in Figure 20. The vertical profiles show the same trend as found by Fuehrer, Romisch, and Engelke (1981) showing the maximum jet velocity to be at the surface away from the vessel. Dye injections showed the two jets have formed into one jet at a distance of about 22.9 m, which is $xp/D_p = 10.2$. The maximum velocity at 0.6 m below the surface from lateral and vertical profiles was used to develop an equation for the decay of velocity of the combined jets and resulted in:

$$\frac{V(xp)_{\max}}{V_2} = C_{\exp} \exp\left(-0.0178\, xp/D_p\right) \tag{22}$$

where C_{exp} is 0.66 for open wheel propellers and 0.85 for Kort nozzle propellers.

Equation 22 is valid for Zone 2 only.

(3) Decay the maximum surface velocity laterally (in the horizontal plane) using Equation 21 with r = Y and $C = C_{z2}$. Determine C_{z2} using the surface velocity distributions given in Figures 14 to 19. Analysis of these figures shows that C_{z2} varies with distance from the tow according to:

$$C_{z2} = 0.84\left(xp / D_p\right)^{-0.62} \tag{23}$$

The lack of a constant C_{z2} likely results from the confining effects of the bed and water surface. Note that Equation 23 is based on data having xp/D_p less than 43.6 and is used for both open-wheel and Kort nozzle propellers.

(4) The next step is to define the decay of velocity in the vertical direction. The first approach tried was the application of Equation 21 treating the jet as a circular jet. This approach worked well for the 3.4-m depth. Bottom velocities were too high for the larger depths, because the circular jet equation shows a nearly uniform vertical velocity distribution at the larger distance from the propeller at the

larger depths. The vertical velocity profiles show a large difference between surface and bottom velocities for the larger depths. The adopted approach was to determine the ratio of bottom velocity to surface velocity as a function of x/D_p and D_p/H_p using the lateral and vertical profiles of velocity. The resulting equation is:

$$\frac{V_{bot}}{V_{surf}} = 0.34\left(\frac{D_p}{H_p}\right)^{0.93}\left(\frac{xp}{D_p}\right)^{0.24} \tag{24}$$

where the V_{surf} is the velocity from Equation 21 using $C = C_{z2}$.

Since the bottom velocity will likely not exceed the surface velocity in Zone 2, the ratio from Equation 25 is limited to 0.95. Data used in developing Equation 24 were limited to xp/D_p less than 43.6 and D_p/H_p from 1.35 to 0.448. Equation 24 is used for both open-wheel and Kort nozzle propellers.

c. Between Zone 1 and Zone 2, a transition region exists where the velocity is set equal to the velocity at the end of Zone 1.

d. Near-bed velocities computed using the adopted method for the stationary vessel are shown in Figure 21 for the same depths and vessel characteristics used for the observed data shown in Figure 10. The discontinuity between Zones 1 and 2 is present but not severe.

Many components of this approach are empirical. The author believes that application of only the free jet equations without considerable empiricism will never be successful because too many of the free jet equation assumptions have been grossly violated.

Empirical method for bottom velocity distribution, moving tow

The same procedures from the maximum bottom velocity for a moving tow are used to define the bottom velocity distribution for a moving tow. Wake flows are defined using Equations 12 through 15. The empirical bottom velocity equations are used in Equation 16 in lieu of the Fuehrer, Romisch, and Engelke (1981) equation for maximum bottom velocity, but bottom velocity from the empirical method is not allowed to exceed the maximum bottom velocity calculated using Equations 16 and 17. V_2 is calculated using Equation 5. The bottom velocity distribution equations are coded in QuickBASIC as shown in Appendix B. Bow velocity V_{bow} is set equal to 0.7 times V_{bd} from Equation 3, because the equation for V_{bow} from the model (Eq 1) is conservative as a result of the larger acceleration used in the model. The distribution of bottom velocity for the bow and displacement velocity is based on a linear change from zero bow velocity at 10 times the barge draft ahead of the bow to V_{bow} at the bow of the tow. The velocity then has a linear change V_{bow} at the bow of the vessel to V_{bd} at five times the vessel draft astern of the bow. The velocity then has a linear change from V_{bd} at five times the vessel draft astern of the bow to zero at 15 times the vessel draft astern of the bow. At that point, the return velocity defines the magnitude of the velocity beneath the

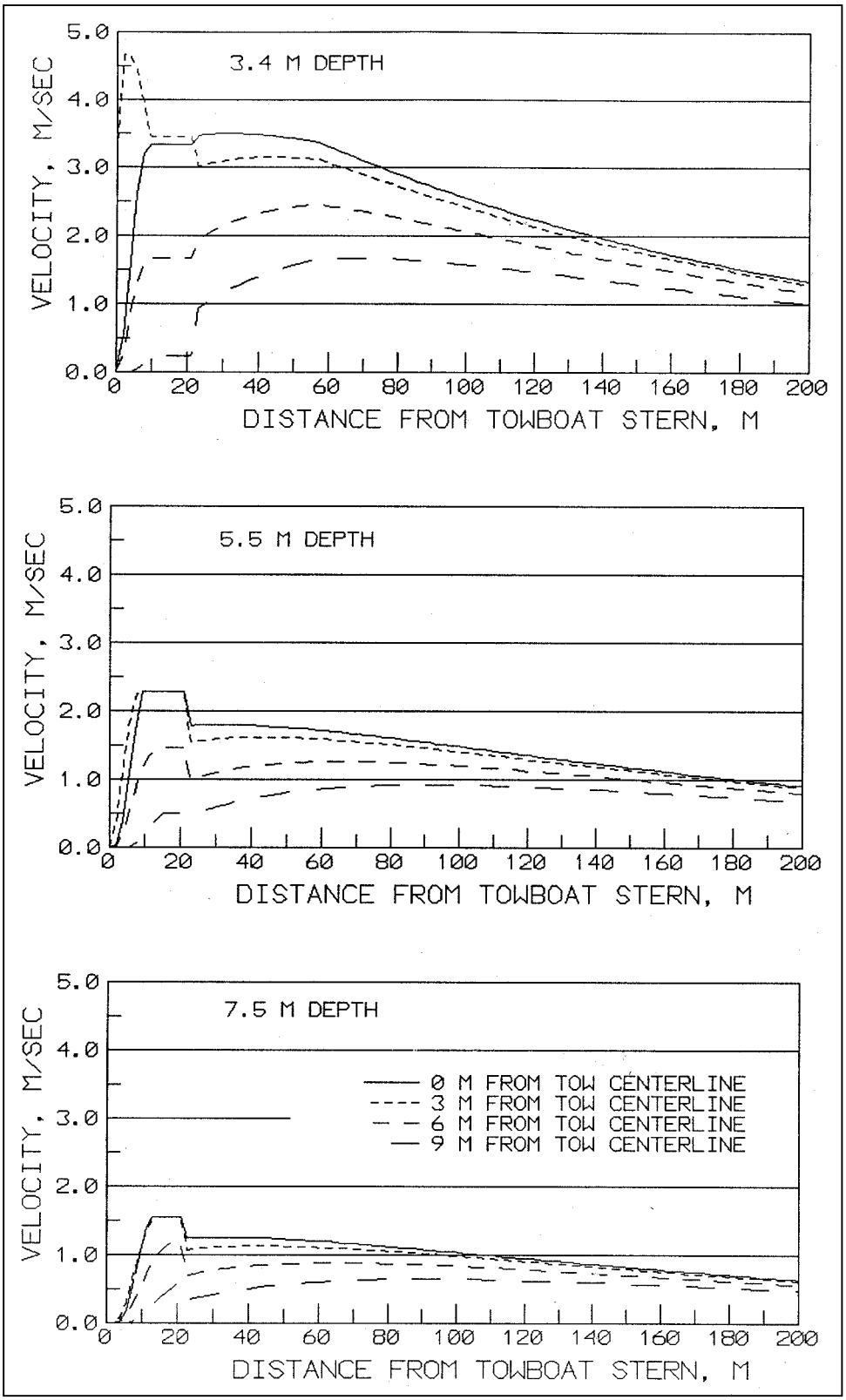

Figure 21. Computed near-bed velocity for open-wheel towboat stationary, thrust = 382,500 newtons

tow until the wake and propeller jet arrive. Computed bottom velocity distributions are also shown in Appendix B.

The equations to use for the maximum bottom velocity are as follows:

Velocity	Equations for Maximum Bottom Velocity	
Displacement velocity V_{bd}	$\frac{V_{bd}}{V_w} = 0.69\left(\frac{Depth}{Draft}\right)^{-1.21}$	(3 bis)
Bow velocity V_{bow}	$V_{bow} = 0.7\ V_{bd}$	
Resultant velocity	$V_{res,g} = E\left(\frac{D_p}{H_p}\right)V_2\, fn\left(\frac{V_a - V_g}{V_2}, \frac{D_p}{H_p}\right) + V_{wake,g}(x)$	(16 bis)
Velocity exiting propeller	$V_2 = \frac{1.13}{D_o}\sqrt{\frac{Thrust}{\rho}}$	(5 bis)
Propeller velocity at bottom	$V_{prop,v} = E\left(\frac{D_p}{H_p}\right)V_2\, fn\left(\frac{V_a - V_g}{V_2}, \frac{D_p}{H_p}\right)$	(11 bis)
	$fn\left(\frac{V_a - V_g}{V_2}, \frac{D_p}{H_p}\right) = 1 - cfunc\ abs\left(\frac{V_a - V_g}{V_2}\right)\left(\frac{H_p}{D_p}\right)^{1.5}$	(17 bis)
Wake velocity	$V_{wake,g}(x) = V_{wake,a}(\max)\left(1 + 0.0075\frac{TBL}{draft} - 0.0075\frac{x - LBARGES}{draft}\right) + V_{a(bott)}$	(15 bis)

The equations to use for the bottom velocity distribution are as follows:

Velocity	Equations for Bottom Velocity Distribution	
Displacement velocity V_{bd}	$\frac{V_{bd}}{V_w} = 0.69\left(\frac{Depth}{Draft}\right)^{-1.21}$	(3 bis)
and see text above for decay fore and aft.		
Bow velocity V_{bow}	$V_{bow} = 0.7\ V_{bd}$	
and see text above for decay fore and aft.		
Resultant velocity	$V_{res,g} = E\left(\frac{D_p}{H_p}\right)V_2\, fn\left(\frac{V_a - V_g}{V_2}, \frac{D_p}{H_p}\right) + V_{wake,g}(x)$	(16 bis)
Velocity exiting propeller	$V_2 = \frac{1.13}{D_o}\sqrt{\frac{Thrust}{\rho}}$	(5 bis)
Propeller velocity at bottom	$fn\left(\frac{V_a - V_g}{V_2}, \frac{D_p}{H_p}\right) = 1 - cfunc\ abs\left(\frac{V_a - V_g}{V_2}\right)\left(\frac{H_p}{D_p}\right)^{1.5}$	(17 bis)

For Zone 1:

$$V_{x,r} = V(xp)\max\exp\left(-\frac{r^2}{2C^2\, xp^2}\right) \qquad \text{(21 bis)}$$

Use superposition of the two propeller jets to determine combined velocity.

For Zone 2:

$$V_{surf} = V(xp)\max\exp\left(-\frac{\gamma^2}{2C_{x2}^2\, xp^2}\right) \qquad \text{(21 modified)}$$

$$\frac{V_{bot}}{V_{surf}} = 0.34\left(\frac{D_p}{H_p}\right)^{0.93}\left(\frac{xp}{D_p}\right)^{0.24} \qquad \text{(24 bis)}$$

Wake velocity

$$V_{wake,g}(x) = V_{wake,a}(\max 1)\left(+0.0075\frac{TBL}{draft} - 0.0075\frac{x - LBARGES}{draft}\right) + V_{a(bott)} \qquad \text{(15 bis)}$$

5 Propeller Jet Bed Shear Stress

General

The model for propeller jet bed shear stress distribution is based on the following approach:

a. Use previously described model for maximum (not distribution) propeller jet bed velocity.

b. Use maximum propeller jet bed velocity to determine the global peak shear stress from the propeller jet using a local skin friction coefficient. Global in this context means the maximum shear stress beneath the tow in the propeller jet region.

c. Define lateral variation of peak shear stress as a function of the global peak shear stress.

d. Define longitudinal variation of shear stress as a function of the lateral peak shear stress.

This section includes shear induced by the wake flow alone in addition to shear in areas where the wake and propeller jet are interacting. Details are presented in the following paragraphs.

Measurements of Shear Stress Time-History

The measured shear in Appendix A is based on either the average of three experiments or a single experiment as indicated on the figures. The shear measurements are scaled to prototype values of bed shear for a hydraulically smooth surface. A later section in this report provides a method for converting smooth bed shear to a rough bed.

Determine Local Skin Friction Coefficient

Table 8 shows the measured global peak shear stress from the moving Kort nozzle tests. Global peak shear stress occurs during peak near-bed velocity gradient rather than peak near-bed velocity. Velocity gradient is beyond the scope

Table 8
Observed and Computed Global Peak Shear and Computed Velocity Used in Shear Calculation Propeller Jet, Kort Nozzles

Experiment	# of runs	Depth, m	V_g, m/sec	V_a, m/sec	Thrust, newtons	Comp $V_{shear\ calc}$, m/sec	Obs peak shear, dynes/sq cm	Comp peak shear, dynes/sq cm
KU1222T4 KU1212T5	3,3	3.66	-2	0.38	389,500	4.04	1,030 850	978
TU1534T5	3	4.6	-3	0.29	351,500	2.53	265	272
TU1814T8	3	5.5	-3	0.38	347,000	1.67	95	93
KU2314T5	3	7.1	-3	0.29	351,500	0.92	65	20
KD1232T4 KD1242T5	3,3	3.66	2	0.38	412,000	4.39	1,380 1,060	1,155
TD1534T8 TD1534T5 TD1514T5	3,3,3	4.6	3	0.29	377,000	2.84	145 140 140	341
TD1814T8	3	5.5	3	0.38	380,500	2.13	100	150
KD2314T5	3	7.1	3	0.29	377,000	1.26	40	38

of the velocity model presented above. Maximum velocity is used to characterize shear stress in Verhey (1983). The maximum velocity gradient occurs during the change from the wake flow to the propeller jet flow as shown in velocity experiment KV1524AT which corresponds to shear experiment TU1514T5 (Appendix A, p A10). The change occurs at about 10 H_p astern of the propellers. Both experiments were conducted at a 4.6-m depth, upbound, 351,500-N thrust, a vessel speed of 3 m/sec relative to ground, and both were measured 3 m from the tow center line which is directly beneath the center of the propeller. The rapid rise in velocity from the upstream moving wake velocity (since this is an upbound tow) to the downstream moving propeller velocity corresponds to the zone of peak shear stress. The magnitude of the total velocity change or some portion of the change is believed to be the best indicator of the velocity gradient. Various combinations were evaluated to see which gave a good prediction of the shear along with a predictable friction coefficient C_{fs}. The velocity used to compute the shear stress $V_{shear\ calc}$ was selected as the absolute value of the propeller velocity from Equations 16 and 17 plus one-half of the absolute value of the wake velocity. The relationship between peak measured bottom velocity and global peak shear stress is:

$$\tau_{peak} = 1/2\ \rho\ C_{fs} \left(V_{shear\ calc}\right)^2 \qquad (25)$$

The measured shear data of Tables 8 and 9 resulted in a C_{fs} of $0.01(D_p/H_p)$. The region behind the barges but not behind the towboat experiences only the

Table 9
Observed and Computed Global Peak Shear and Computed Peak Velocity, Propeller Jet, Open-Wheel Propellers, Observed Data from Garcia et al. (1998)

Data Set	Velocity Experiment	Depth, m	V_g, m/sec	V_a, m/sec	Thrust, newtons	Comp $V_{shear\ calc}$, m/sec	Obs peak shear, dynes/ sq cm	Comp peak shear, dynes/ sq cm
UP B	none	3.4	1.5	0.45	368,000	4.51	1,282	1,376
DN B	none	3.4	2.3	0.45	370,000	4.89	1,485	1,616
UP A	0304-2DX	4.3	1.5	0.55	368,000	2.81	338	370
DN A	0304D2FX	4.3	3.1	0.55	360,000	3.20	378	478
UP D	3718U2AX	5.6	2.1	0.55	358,500	1.48	83	71
DN D	3618D2AX	5.6	3.6	0.55	350,500	1.84	93	110
UP C	0306-2DX	7.0	2.1	0.60	357,500	0.88	58	19
DN C	0306D2CX	7.0	3.6	0.60	351,500	1.12	37	30

inrush of the wake flow behind the vessel which also subjects the bed-to-shear stress. The magnitude and longitudinal distribution of wake velocity are given by Equations 12 through 15. The lateral distribution of the wake velocity across the width of the barges is assumed constant. Inserting $V_{wake,g}$ into Equation 25 provides the shear stress. The appropriate C_{fs} for the wake flow is determined by analysis of the data in which the characteristic spike of the propeller jet is not present behind the towboat. Experiment KV1524BT (wake flow only), Appendix A, p A11, shows a measured wake velocity approaching 1.0 m/sec, and experiments TU1524T8 (Appendix A, p A12) and TU1524T5 (Appendix A, p A13) have measured shear stresses of about 100 dynes/sq cm, resulting in a wake C_{fs} of 0.02. Experiments TD1524T8 and TD1524T5 (Appendix A, p A34) have shear stresses of about 50 dynes/sq cm and a computed wake velocity of 1.0 m/sec, resulting in a wake C_{fs} of 0.01. The larger C_{fs} of 0.02 is adopted herein because both velocity and shear were measured.

The computed peak $V_{shear\ calc}$ and observed global peak shear and computed shear for Kort nozzles are shown in Table 8. Table 9 shows the same values from the open-wheel tests reported in Garcia et al. (1998).

Normalization of Shear Stress Beneath and Behind Tow

The first requirement in defining the shear stress distribution is to define the variation of the peak shear stress as a function of lateral distance away from the tow center line. Figure 22 shows the variation of peak propeller shear at lateral

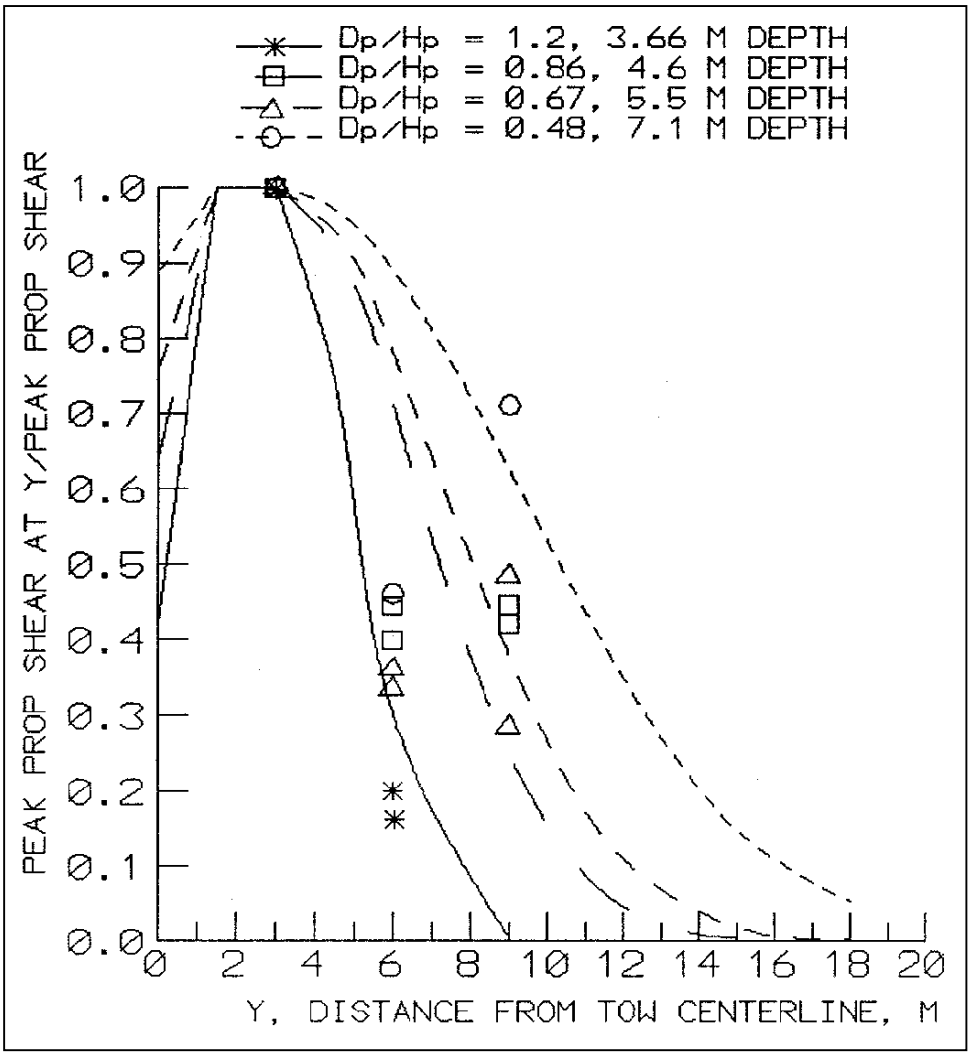

Figure 22. Lateral distribution of peak shear Kort nozzle propellers

distance Y away from the tow center line. The propeller shaft and the rudder axis are at 3 m from the tow center line. The distributions reflect the significance of the central rudder in splitting the jet into a surface and bottom jet. As viewed from the stern, the starboard propeller rotates counterclockwise and the port propeller rotates clockwise. The bottom directed jets come off the inside face of the rudder. With one or two exceptions, the shear measurements were made at 0, 3, 6, and 9 m away from the tow center line. The peak almost always occurred at 3 m which was directly under the propeller. In one test conducted at a 4.6-m depth, the shear was measured at 1.5 m from the tow center line and was slightly greater than at 3 m. Because of the results of that one test and the fact that the bottom directed jet is coming off the inside of the rudders, the peak was assumed to occur between 1.5 and 3 m from the tow center line. All values measured along the center line of the tow were plotted, and an envelope curve was drawn to represent the shear at the center line of the vessel. Values from the envelope curve are shown on the vertical axis on Figure 22 at Y = 0. A linear change was used from the value from the envelope curve at Y = 0 to the peak at 1.5 m. Shear values from 3, 6, and 9 m

from the tow center line were used to define an exponential decay of shear stress outside 3 m according to:

$$\frac{\tau(peak@Y)}{\tau_{peak}} = \exp\left[-C_s\left(\frac{Y - Pspace/2}{D_p}\right)^2\right] \quad (26)$$

where

$Pspace$ = spacing between the propellers

C_s =1.0 for 3.66-m depth

= 0.285 for 4.6-m depth

= 0.203 for 5.5-m depth

= 0.098 for 7.1-m depth

The equation for C_s is:

$$C_s = 0.022 \exp\left(3.14\frac{D_p}{H_p}\right) \quad (27)$$

The problems caused by extrapolation of these exponential relations beyond Y = 9 m are not significant because the shear stress outside 9 m is low at all depths. The peak distributions reflect a decreasing width of the propeller jet footprint with decreasing depth. This decrease is caused by the increasing strength of the wake which prevents lateral spreading of the jet. At larger depths, the jet spreads more because the wake effect is less and because of the increased vertical distance over which spreading can occur. Equations 26 and 27 are plotted in Figures 23 to 26 versus the lateral distribution of peak shear from the Garcia et al. (1998) experiments with open-wheel propellers.

The remaining requirement for the dimensionless description of the shear stress distribution is the longitudinal variation of the peak shear stress (Figures 27 through 33). Table 10 shows the ensemble plots used to develop the dimensionless description of the shear stress, the applicable shear stress, and the figure number showing the dimensionless plot.

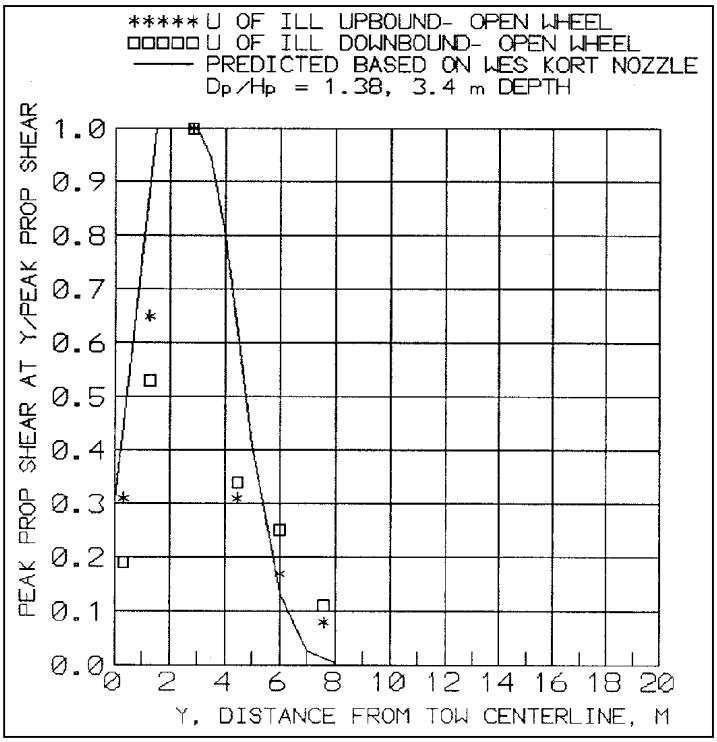

Figure 23. Lateral distribution of peak shear, open-wheel propellers, 3.4-m depth

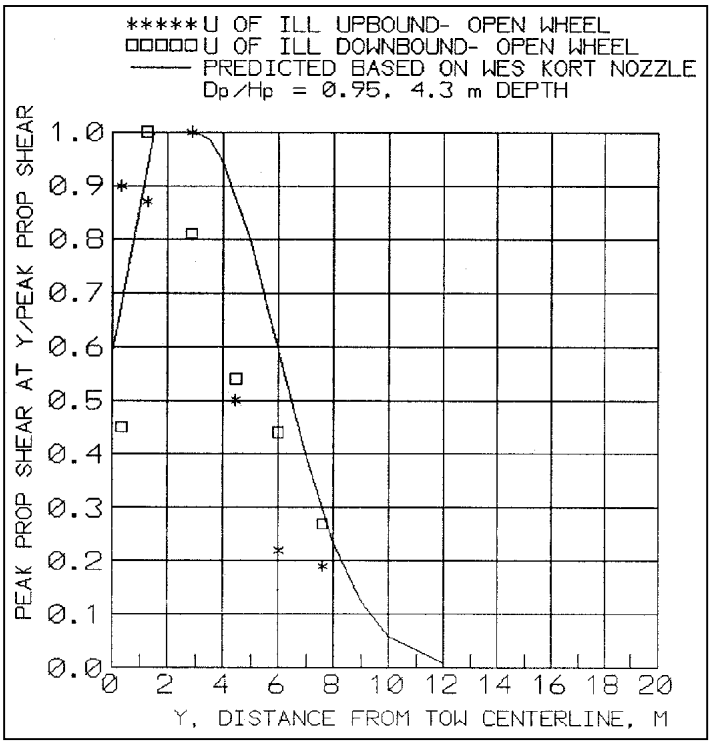

Figure 24. Lateral distribution of peak shear, open-wheel propellers, 4.3-m depth

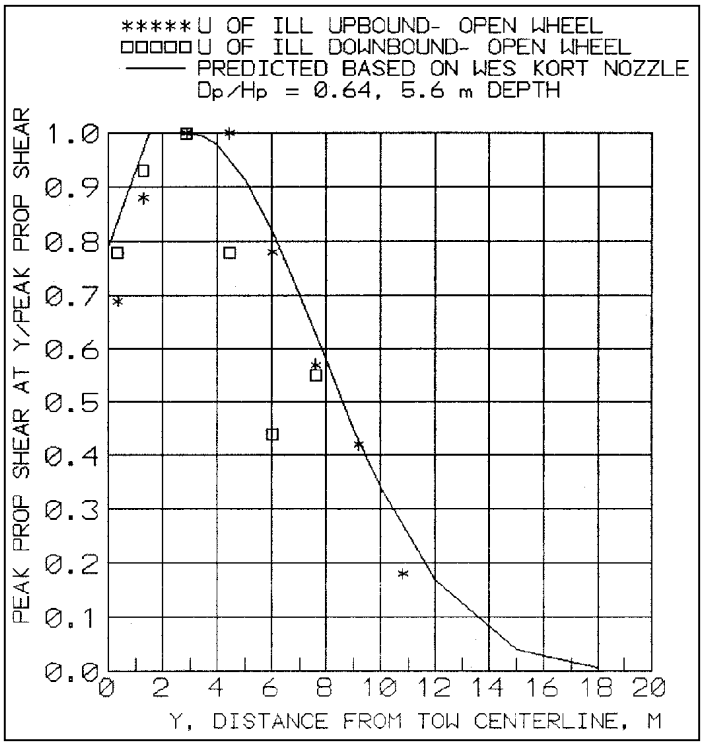

Figure 25. Lateral distribution of peak shear, open-wheel propellers, 5.6-m depth

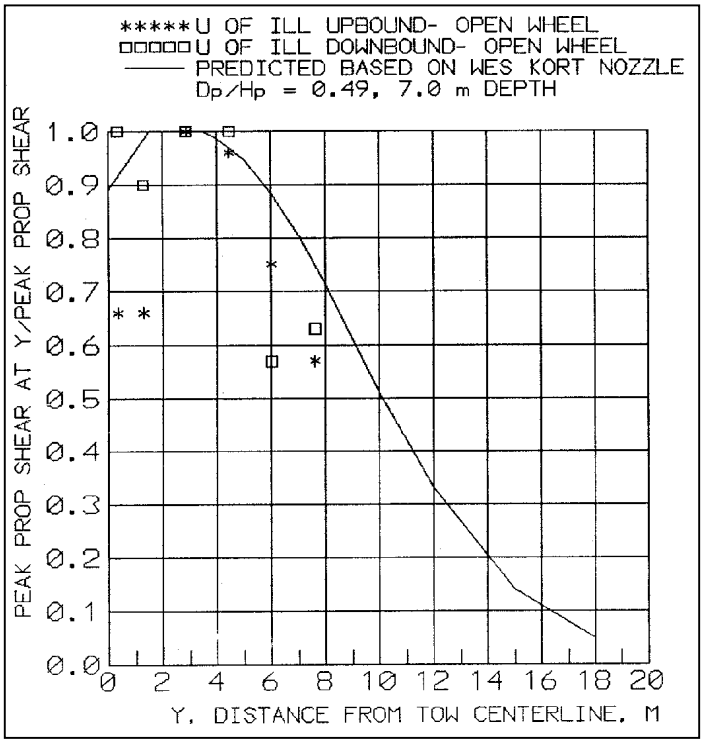

Figure 26. Lateral distribution of peak shear, open-wheel propellers, 7.8-m depth

Table 10
Ensemble Plots Used for Longitudinal Distribution of Shear Stress

Ensemble Plots Used	Y, dist from tow CL, m	Applicable Shear Stress, dynes/sq cm	Figure Number
KU1212T5 KU1222T4 KD1242T5 KD1232T4	3	1,000	27
TU1534T5 TU1514T5	3	235	28
TU1814T8 TD1814T8	3	100	29
KU2314T5 KD2314T5	3	50	30
KU1212T4 KD1242T4	0	340	31
KU1222T5 KD1232T5	6	190	32
TU1524T8 TD1524T8	6	78	33

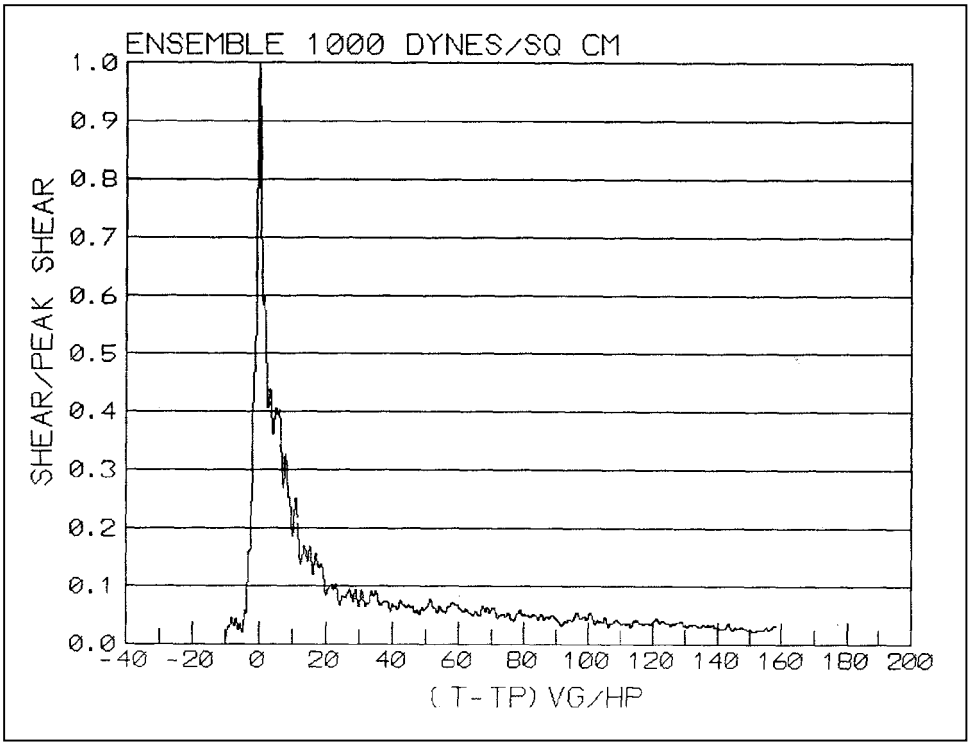

Figure 27. Longitudinal shear distribution, Kort nozzles, 1,000 dynes/sq cm

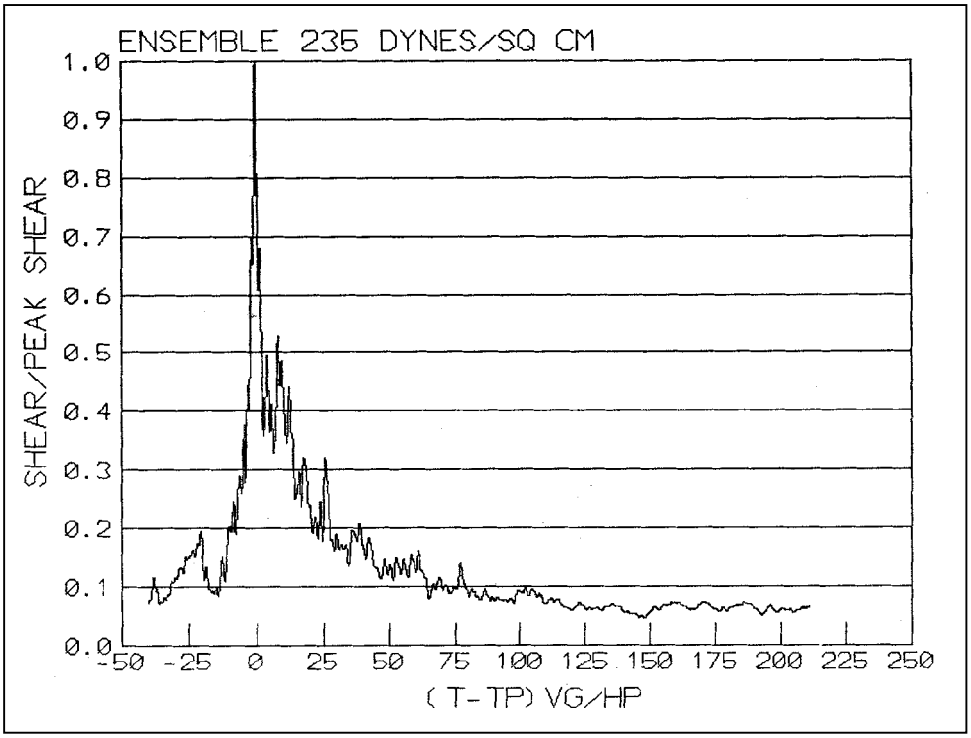

Figure 28. Longitudinal shear distribution, Kort nozzles, 235 dynes/sq cm

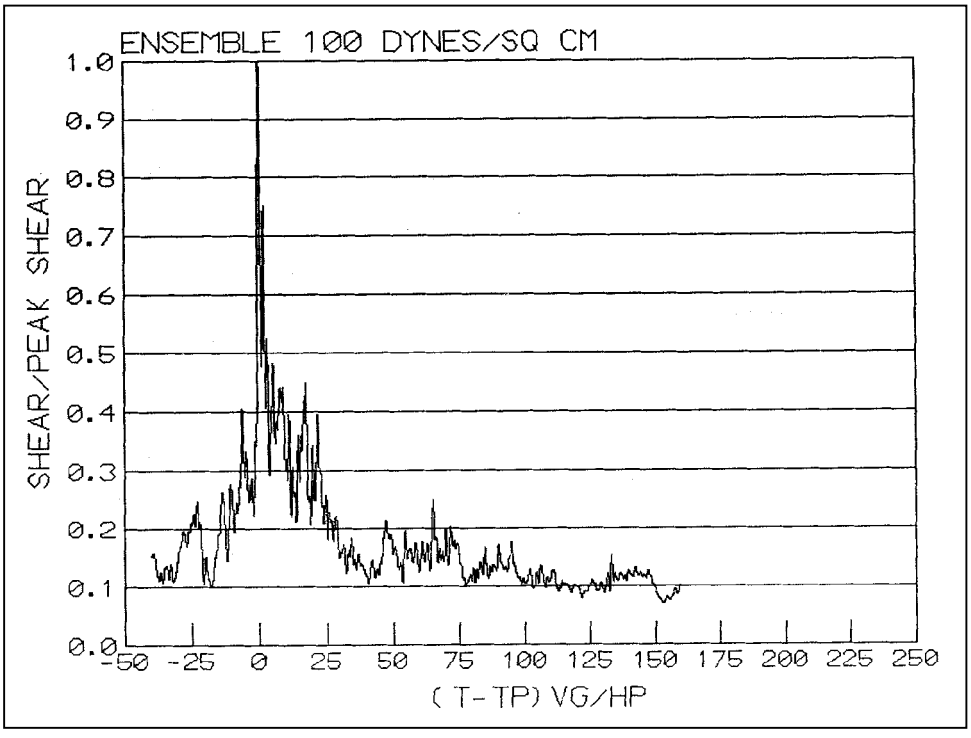

Figure 29. Longitudinal shear distribution, Kort nozzles, 100 dynes/sq cm

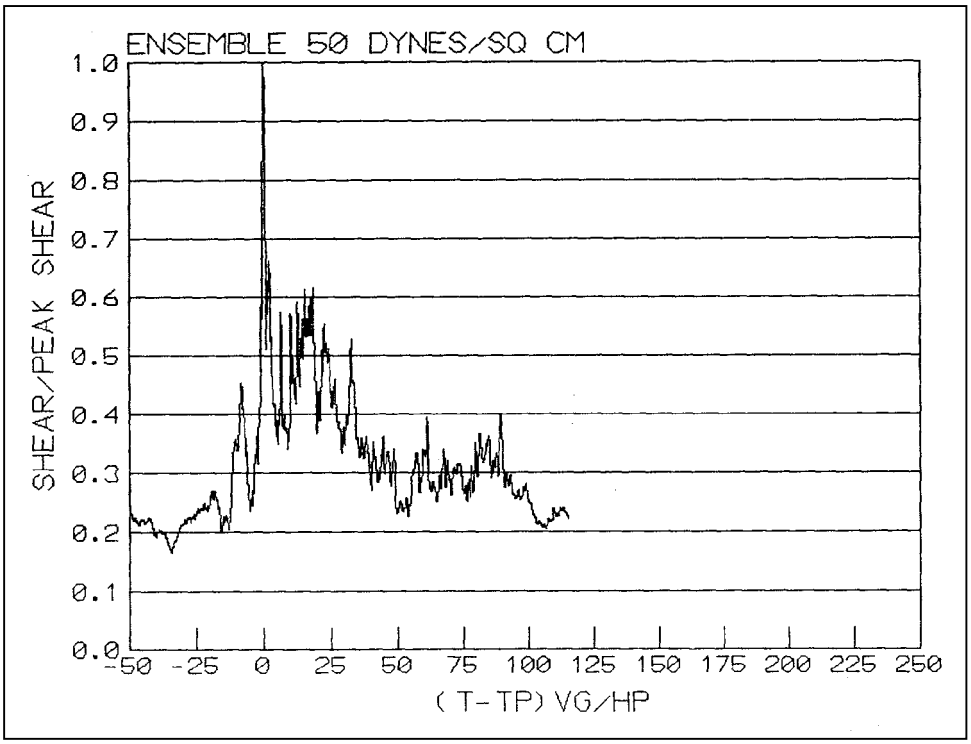

Figure 30. Longitudinal shear distribution, Kort nozzles, 50 dynes/sq cm

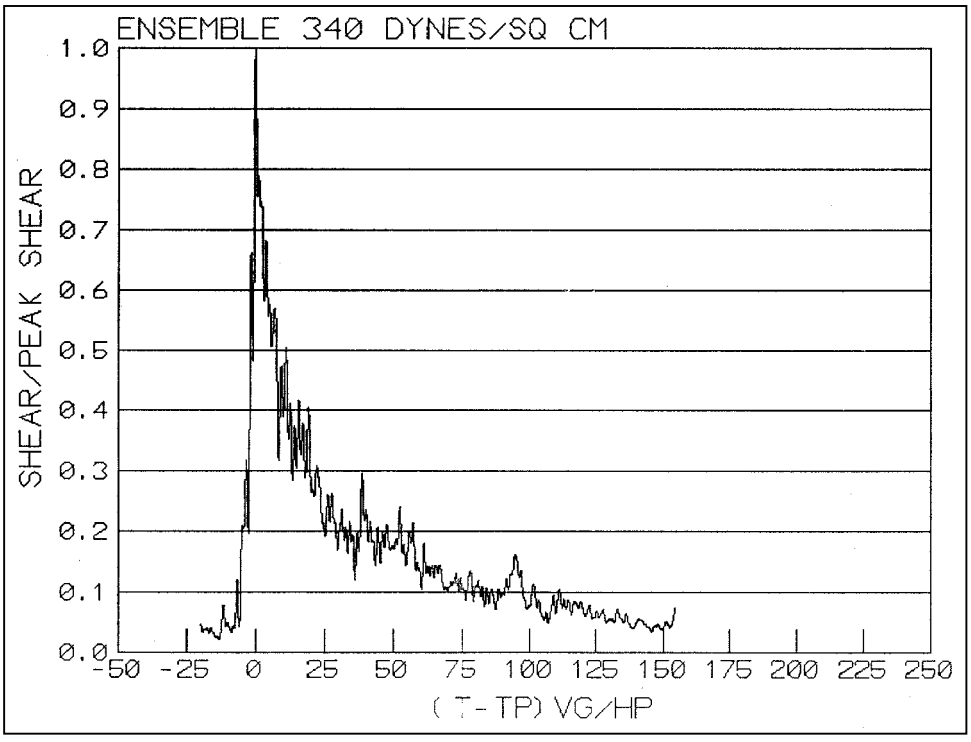

Figure 31. Longitudinal shear distribution, Kort nozzles, 340 dynes/sq cm

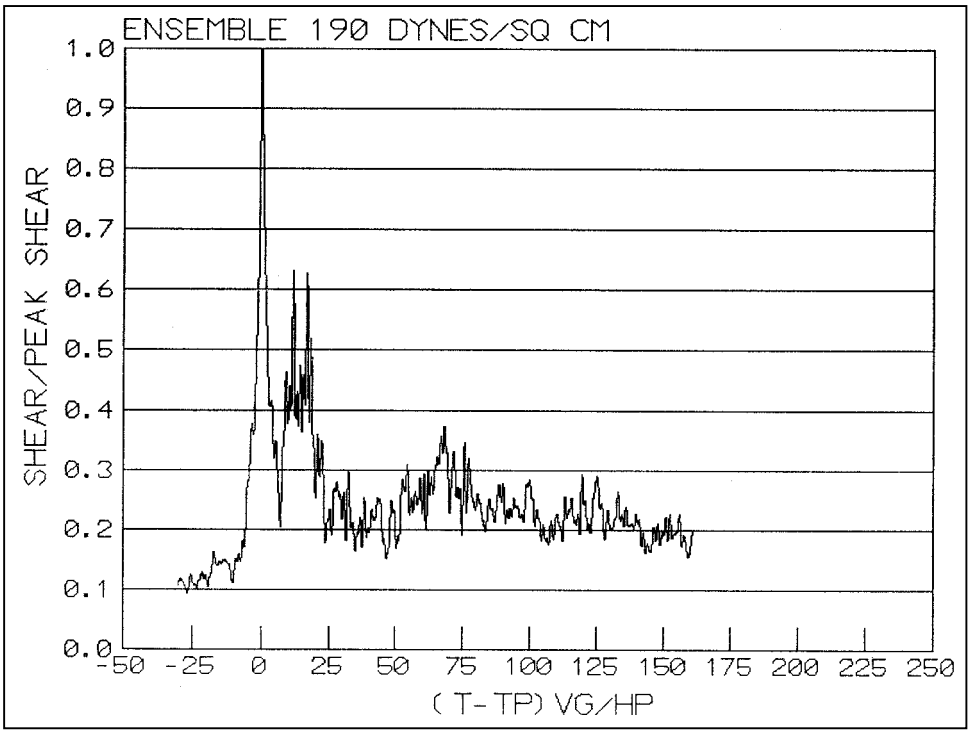

Figure 32. Longitudinal shear distribution, Kort nozzles, 190 dynes/sq cm

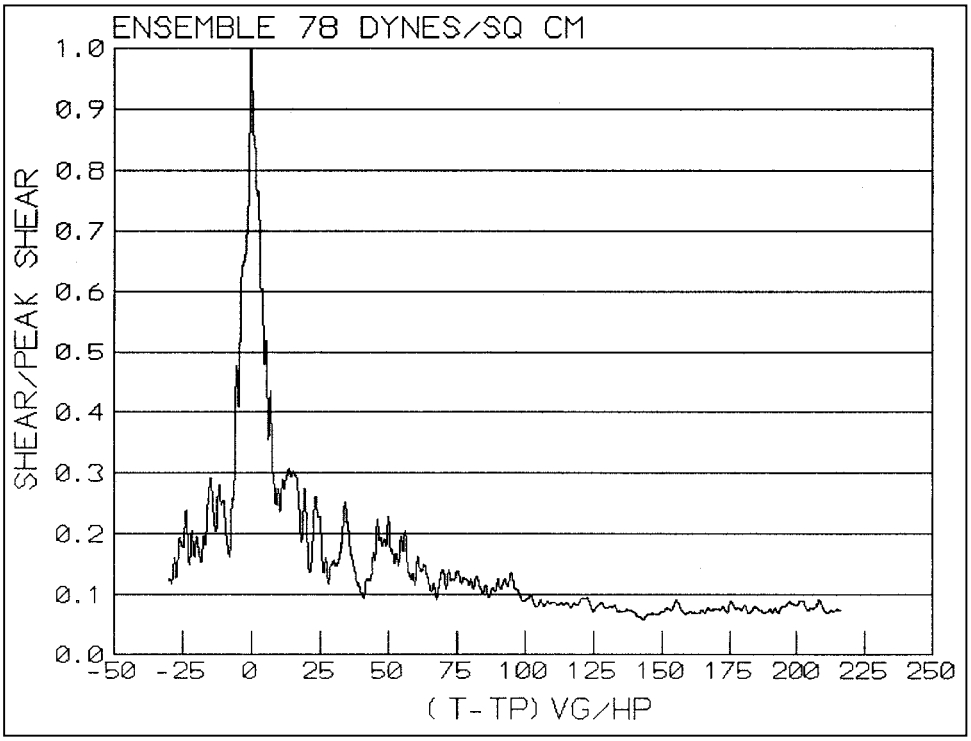

Figure 33. Longitudinal shear distribution, Kort nozzles, 78 dynes/sq cm

The dimensionless plots were based on the dimensionless time parameter $V_g (T-T_p)/H_p$ versus shear/peak shear. Table 11 shows the dimensionless values in tabular form at common values of shear/peak shear.

Table 11
Dimensionless Distribution of Longitudinal Shear

	$V_g (T-T_p)/H_p$						
	Applicable Shear, dynes/sq cm						
Shear/Peak Shear	1,000	235	100	50	340	190	78
0.1	-3.3	-13.5	-20	-30	-6.9	-20	?
0.25	-2.1	-6.7	-10	-15	-3.8	-5.2	-6.9
0.50	-1.0	-1.3	-1.0	-1.2	-1.9	-1.7	-4.1
0.75	-0.54	-0.57	-0.45	-0.38	-0.46	-0.72	-1.0
1.0	0	0	0	0	0	0	0
0.75	0.59	0.52	1.7	0.60	2.3	0.81	2.7
0.50	2.2	8.2	3.0	24	7.7	18	5.6
0.25	11	26	26	100	24	70	20
0.10	23	70	120	150	90	?	100
0.05	75	150	170	170	140	?	180
0.02	150	210	210	210	180	?	200
0.0	200	230	230	230	200	?	230

The ultimate goal of these distributions is to present them in a manner that can be used in the numerical models of sediment entrainment or substrate scour. The Table 11 shear/peak shear is plotted versus Vg(T-Tp)/Hp in Figure 34. A relatively consistent trend in the shape of the distributions can be observed with the magnitude of the peak shear stress. The curve for a peak shear of 1,000 dynes/sq cm stands alone in the data. The curve for 50 and 78 dynes/sq cm are averaged to represent a curve for 69 dynes/sq cm or below. The curves for 340, 235, 100, and 190 are similar both before the peak shear and after and are averaged to represent a curve for 215 dynes/sq cm. The dimensionless parameter Vg(T-Tp)/Hp versus shear stress/peak shear stress for peak shear stress of 1,000 dynes/sq cm or greater, 215 dynes/sq cm, and 69 dynes/sq cm or less are shown in Table 12.

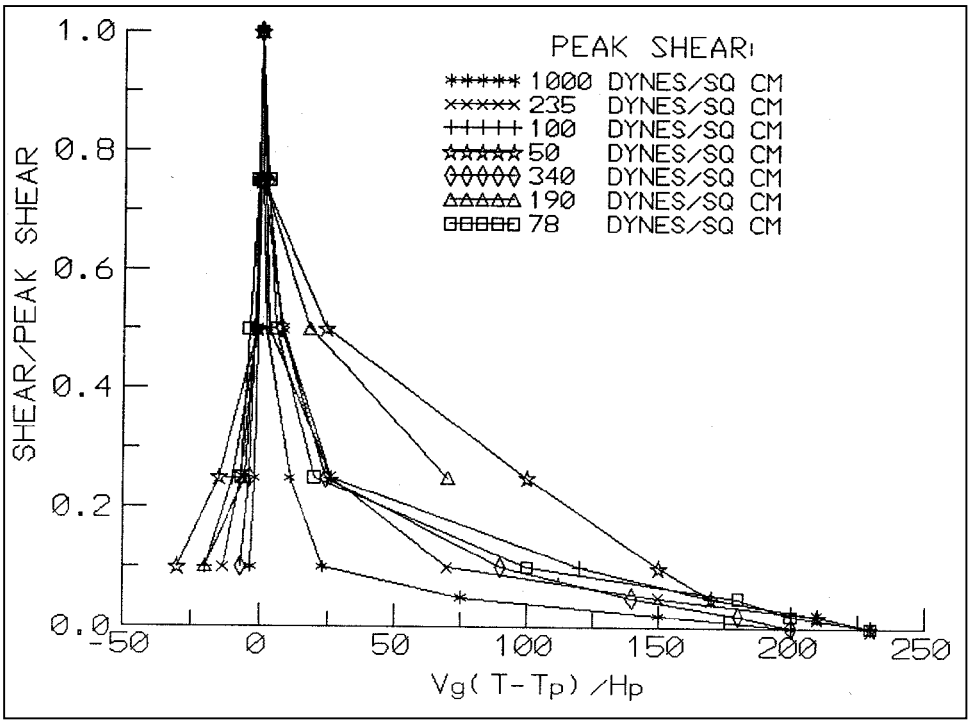

Figure 34. Longitudinal shear distribution, Kort nozzles, 50-1,000 dynes/sq cm

Table 12
Dimensionless Distribution of Longitudinal Shear, Recommended Values for Modeling

	$V_g(T-T_p)/H_p$		
	Shear, dynes/sq cm[1]		
Shear/Peak Shear	**> = 1,000**	**215**	**< = 69**
0.0	-6	-25	-50
0.1	-3.3	-15	-30
0.25	-2.1	-6.4	-11
0.50	-1.4	-1.5	-2.7
0.75	-0.54	-0.6	-0.7
1.0	0	0	0
0.75	0.6	1.3	1.7
0.50	2.2	9.2	15
0.25	11	37	60
0.10	23	93	125
0.05	75	153	175
0.0	230	230	230

[1] Linear interpolation should be used between 1,000 and 215 and between 215 and 69.

The time between the peak at the stern of the towboat and the passage of the bow of the barges must be estimated based on the distance from the propellers which, in these experiments, is 5 m ahead of the stern of the vessel. The peak shear stress occurs at 5 to 10 Hp measured from the propellers which is ahead of the peak velocity. The location of peak shear stress is calculated using the equation:

$$T_p = \frac{\left(LBARGES + TBL + H_p/0.1 - SETBACK\right)}{V_g} \tag{28}$$

A SETBACK of 5.0 m is the typical distance from the stern of the towboat to the propellers.

Extent of Increased Shear from Propeller/Wake behind Vessel

The time-history plots of shear from the plots in Appendix A and from Garcia et al. (1998) were examined to determine the distance behind the towboat where the shear is elevated above ambient shear levels. The ambient shear on the UMR-IWWS is on the order of 25 to 50 dynes/sq cm. It was expected that the limit of shear above ambient levels would depend on depth, but no dependence was found. Almost every run resulted in shear levels that decayed down to ambient shear levels at about 400 m behind the stern of the towboat.

Comparison with Open-Wheel Shear Distributions

The Table 12 distributions developed from the WES Kort nozzle tests were compared with the distributions measured from the open-wheel experiments conducted by Garcia et al. (1998) which were conducted in the model facility at WES. Figures 35 through 37 show the ensemble plots from the Garcia measurements and the WES Kort nozzle distribution for the same peak lateral shear. The agreement is best on the rising limb of the shear distribution where most substrate scour and resuspension would be expected to occur. The WES distribution is used for both Kort nozzle and open-wheel propellers.

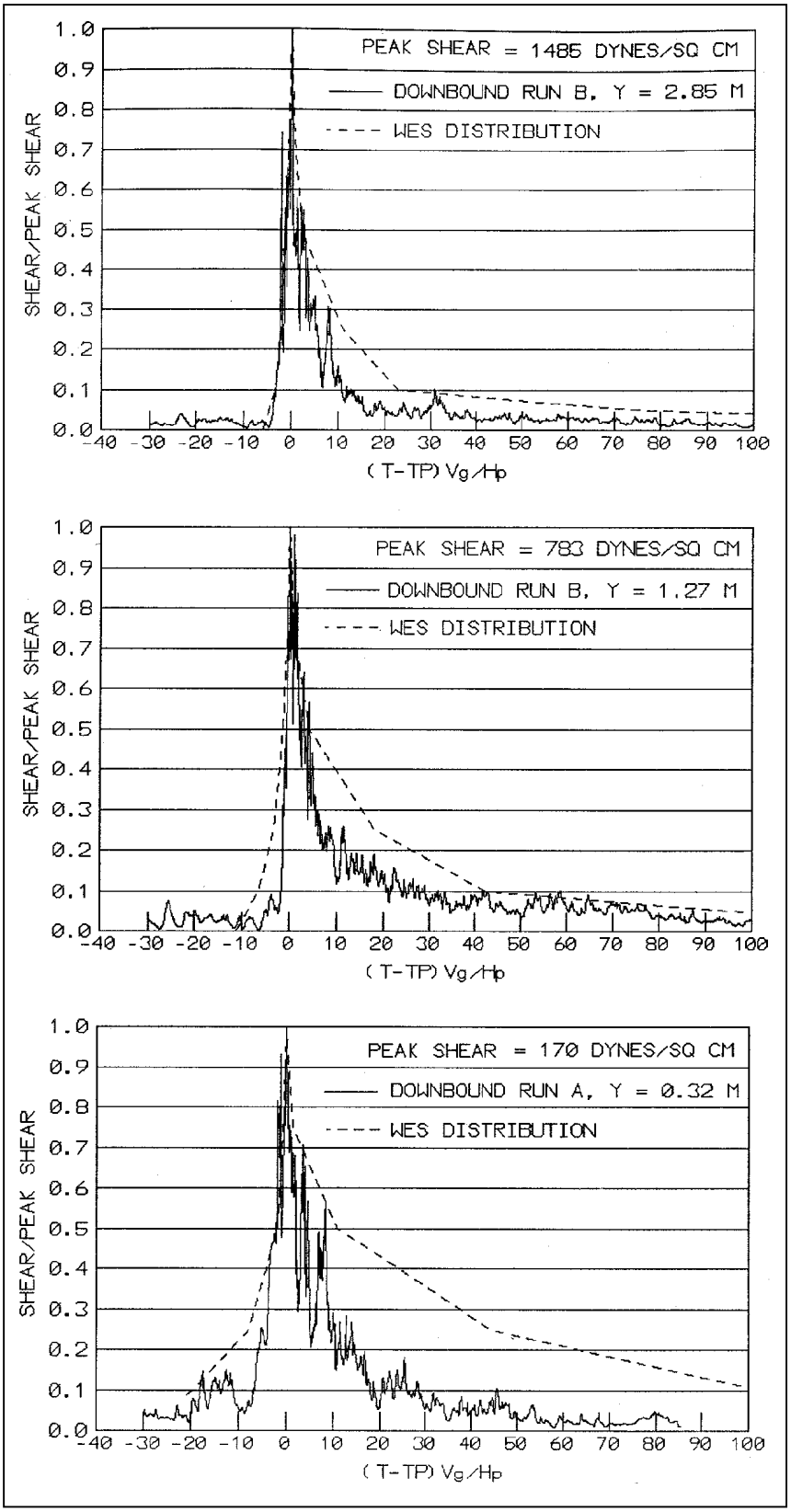

Figure 35. WES Kort nozzle distribution versus Garcia et al. (1998) open-wheel measurements

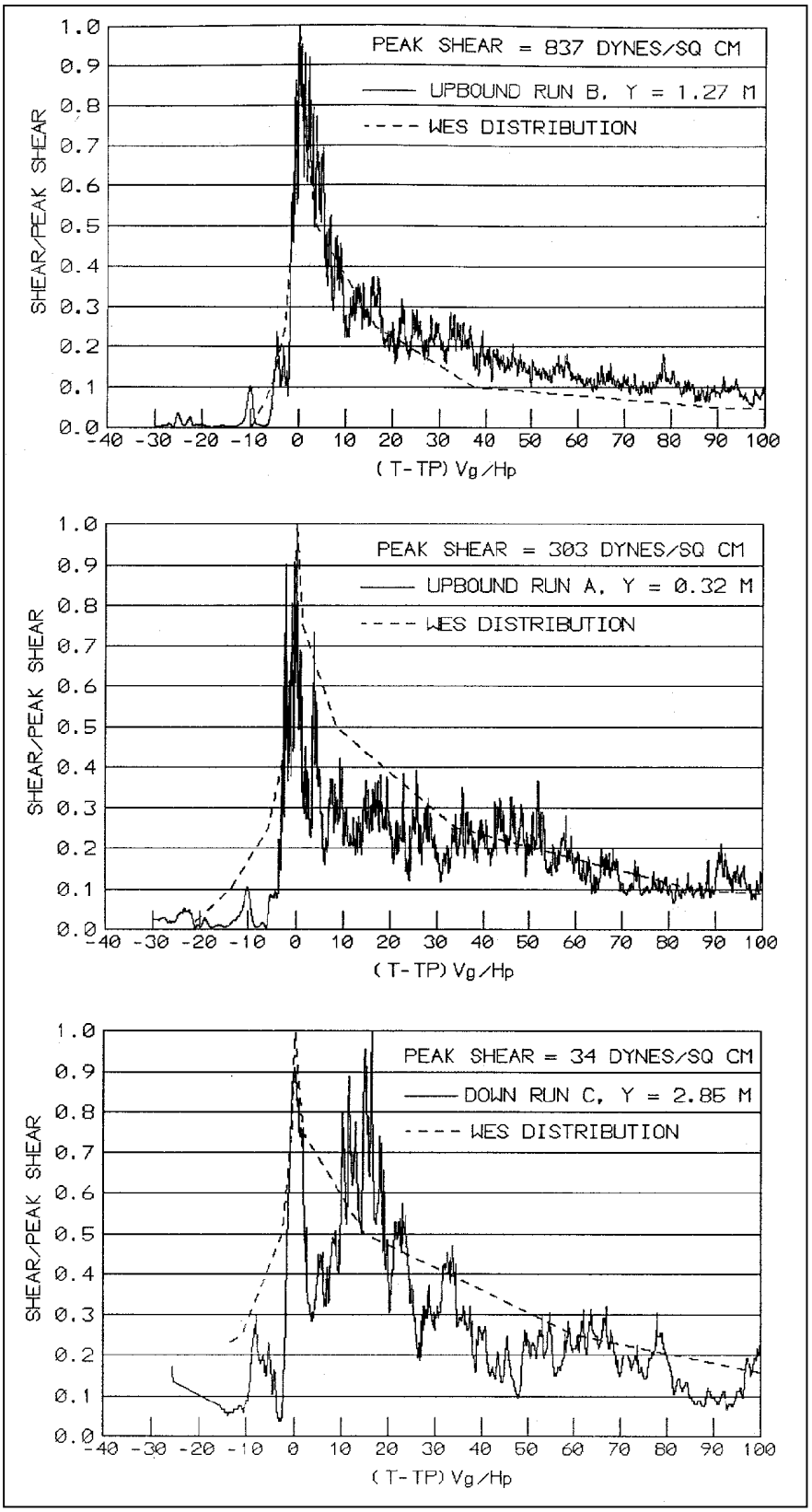

Figure 36. WES Kort nozzle distribution versus Garcia et al. (1998) open-wheel measurements

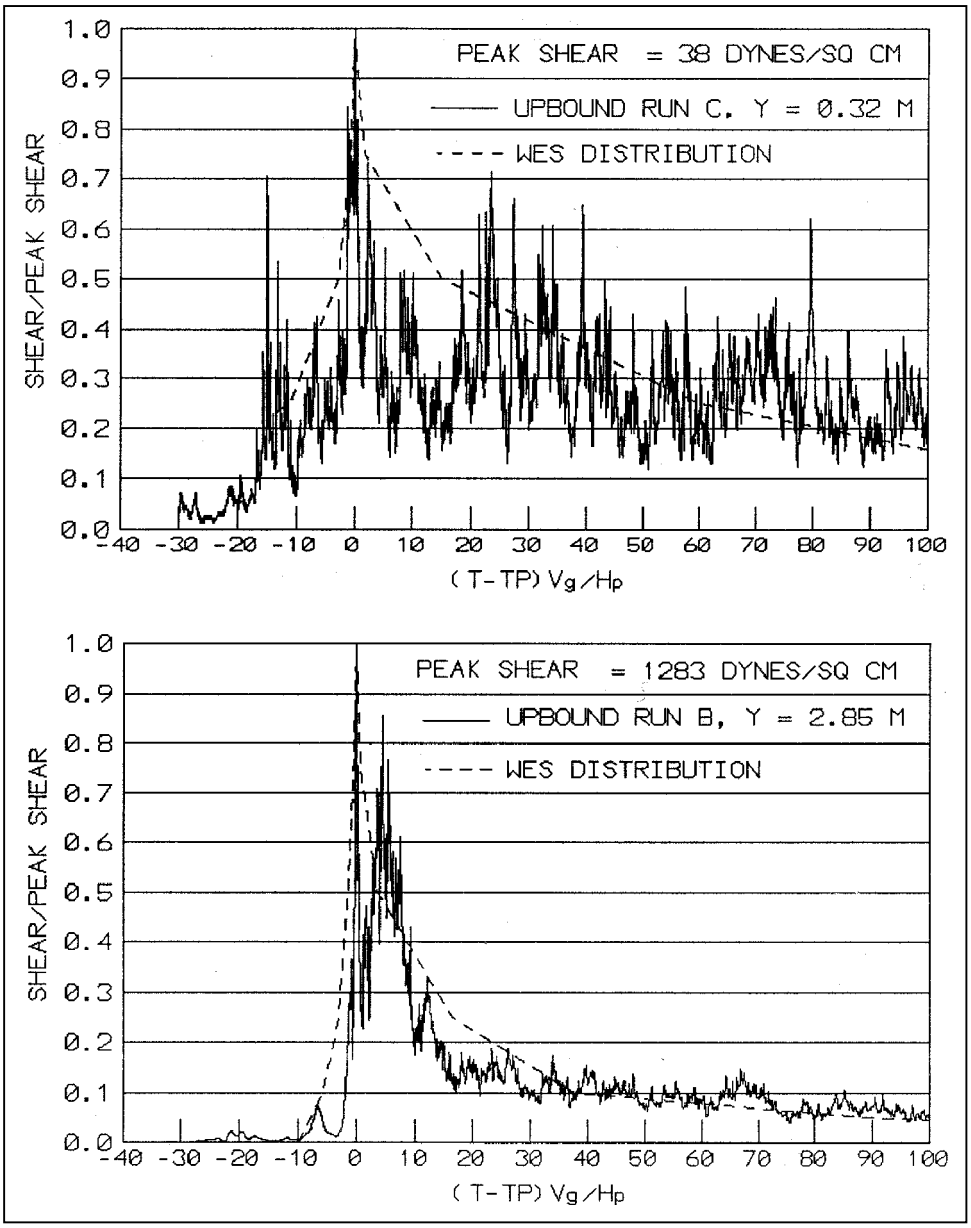

Figure 37. WES Kort nozzle distribution versus Garcia et al. (1998) open-wheel measurements

6 Bed Shear Stress from Return Velocity

Return Velocity Induced Shear Stress

Return velocity occurs all across the channel while the vessel passes. The NAVEFF model (Maynord 1996) provides the maximum return velocity during vessel passage and the HIVEL (Stockstill and Berger technical report in preparation) model provides the distribution of return velocity during vessel passage. About one vessel width away from the center line of the vessel, both HIVEL and NAVEFF are not valid. This analysis will assume that the return velocity in the invalid zone beside and under the barges is equal to the value of the return velocity at the edge of the valid zone. Behind the barges, the previously presented wake/propeller relations are used in the invalid region.

Shear Stress Calculation

In the absence of ambient currents, the shear stress over this entire region will be calculated with the equation for flow in a developing boundary layer:

$$\tau = 1/2\, C_{fr}\, \rho\, U_r^2 \tag{29}$$

where

τ = bed shear stress

U_r = return velocity

ρ = water density

$$C_{fr} = \left(2.87 + 1.58\, Log\, \frac{xbl}{K_s} \right)^{-2.5} \tag{30}$$

where

xbl = distance from the beginning of the boundary layer development

K_s = sand grain roughness equal to $3D_{50}$

In the presence of ambient currents, the bed shear must be determined according to Blaauw et al. (1984) according to:

$$\tau = 1/2\ \rho\ C_{fc} \left(U_c + \sqrt{\frac{C_{fr}}{C_{fc}}}\ U_r \right)^2 \qquad (31)$$

where U_c is the depth averaged velocity

Note that Equation 31 collapses to Equation 29 in the absence of ambient currents. C_{fc} is defined as:

$$C_{fc} = 0.06 \left(Log \frac{12h}{K_s} \right)^{-2} \qquad (32)$$

where h is the local water depth

The value of xbl controls the amount the return velocity is increased to make it equivalent to a depth-averaged velocity. Data are not available to define the proper value of xbl. A conservative xbl of 1 m is used herein which results in the square root term of about 1.4 for medium sand bed material (Eq. 31). The equations presented in this section are applicable to rough bed conditions and require no adjustment as do the smooth bed measurements.

7 Bed Shear from Bow Effects

The peak shear occurs at about 10 m astern of the bow and is computed using the equation:

$$\tau_{bow}(peak) = C_{bow}\ \rho V_w^2 \tag{33}$$

where

τ = pascals (1 pa = 10 dynes/sq cm) when velocity is in m/sec

ρ = 1,000 g/cm^3

The coefficient C_{bow} for smooth bed conditions is shown in Figure 38 which for upbound tows is described by:

$$C_{bow} = 0.0148\,(depth/draft)^{-2.85} \tag{34}$$

and for downbound tows by:

$$C_{bow} = 0.0118\,(depth/draft)^{-2.85} \tag{35}$$

Garcia et al. (1998) found the following equation for peak bow shear for upbound tows:

$$\tau_{bow}(peak) = 4.8\,V_w^2\ \exp\left(4.46\frac{draft}{depth}\right) \tag{36}$$

and described for downbound tows by:

$$\tau_{bow}(peak) = 0.95\,V_w^2\ \exp\left(5.40\frac{draft}{depth}\right) \tag{37}$$

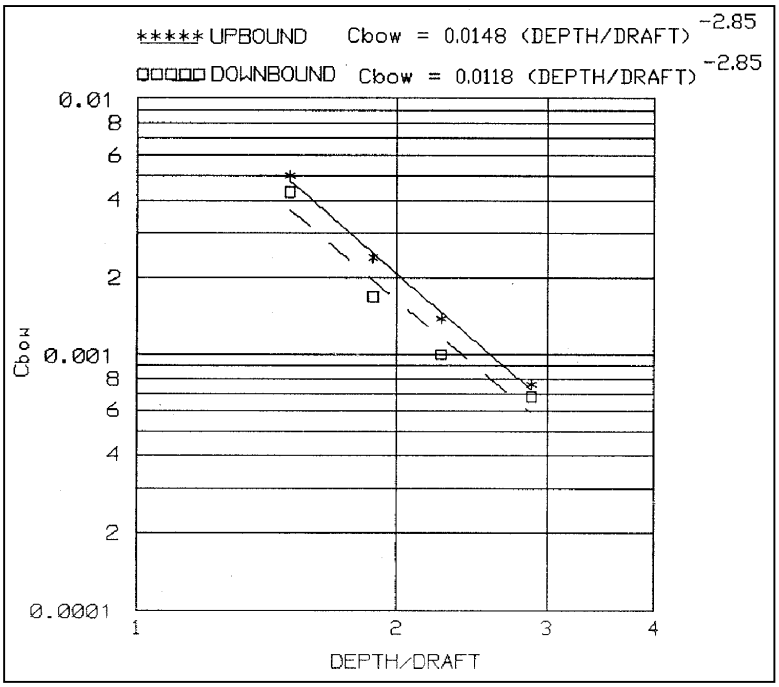

Figure 38. Skin friction coefficient for peak bow shear

Comparison of observed versus computed peak bow shear is shown in Figure 39 for upbound tows for both the WES equation and the Garcia et al. (1998) equation. Good agreement exists for the equations for upbound tows. Comparison of observed versus computed peak bow shear is shown in Figure 40 for downbound tows for both the WES equation and the Garcia et al. (1998) equation. The Garcia et al. equation results in peak bow shear stress considerably lower than the WES equation.

The distribution as a function of the peak is given in Figure 41 along with the distribution developed by Garcia et al. (1998). Good agreement exists for the distributions from WES and Garcia et al. (1998).

The equations for bed shear stress are coded in QuickBASIC as shown in Appendix C. Computed bed shear distributions are also shown in Appendix C and can be compared to the measured shear distributions in Appendix A.

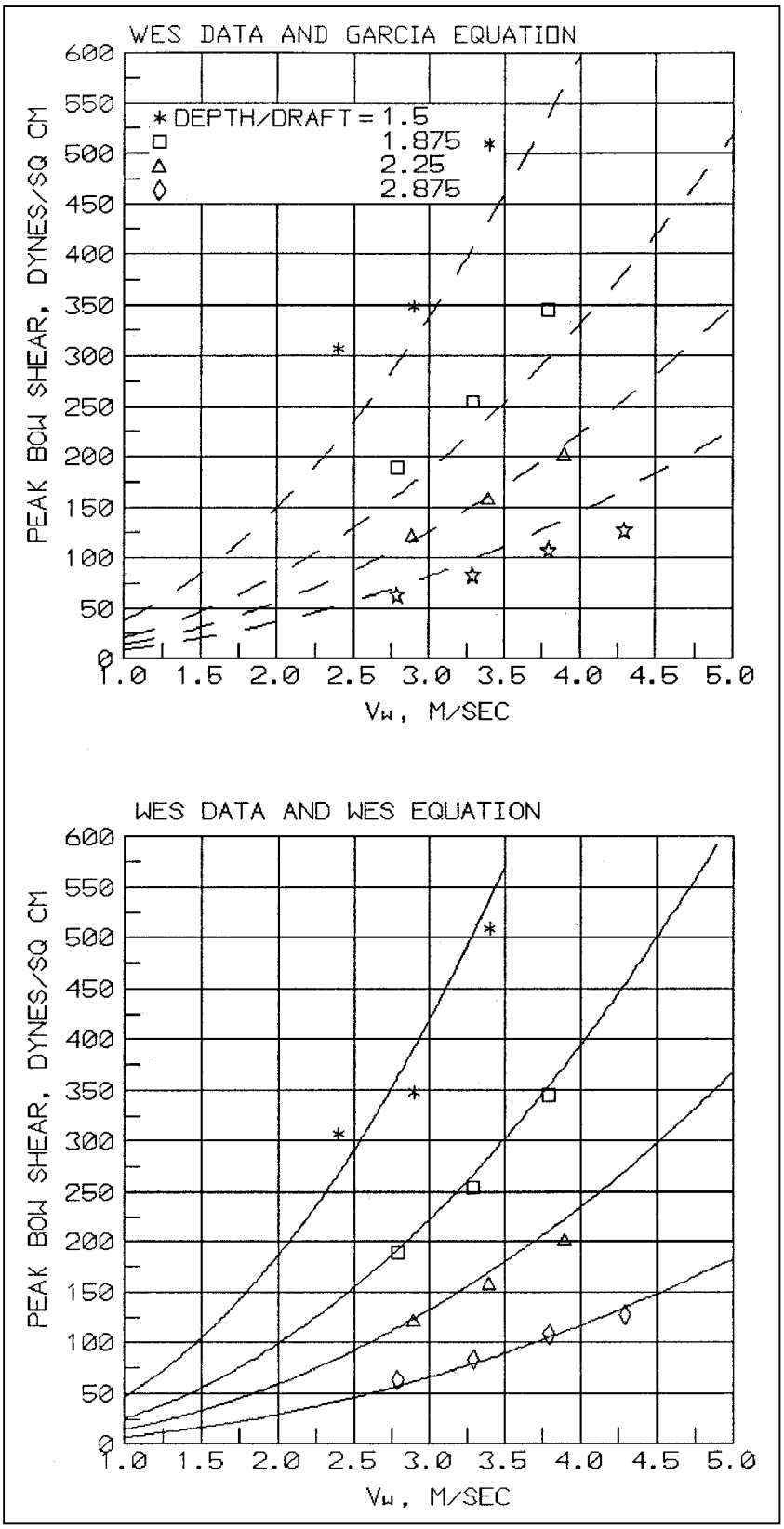

Figure 39. Observed and computed peak bow shear, upbound tow

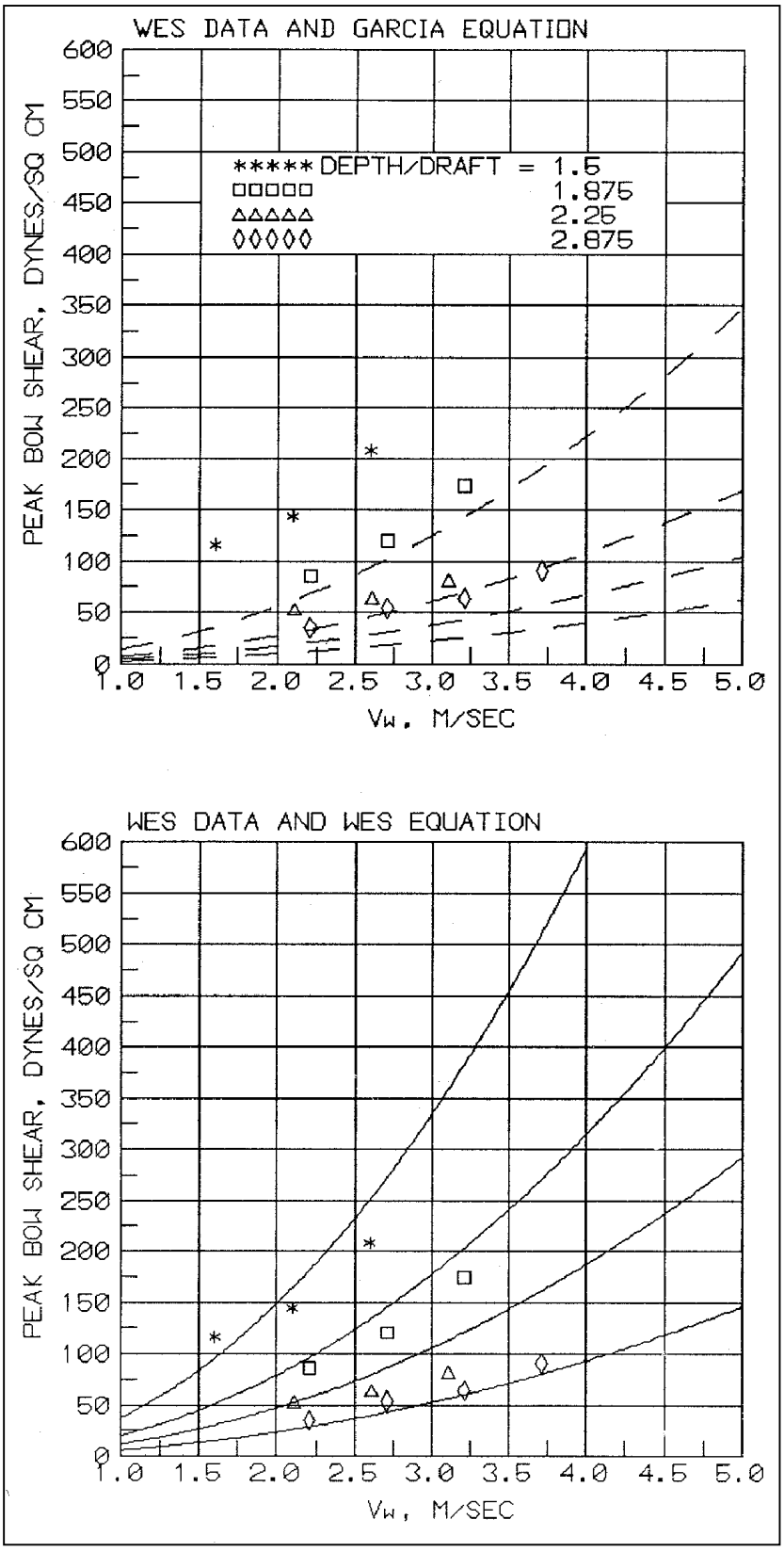

Figure 40. Observed and computed peak bow shear, downbound tow

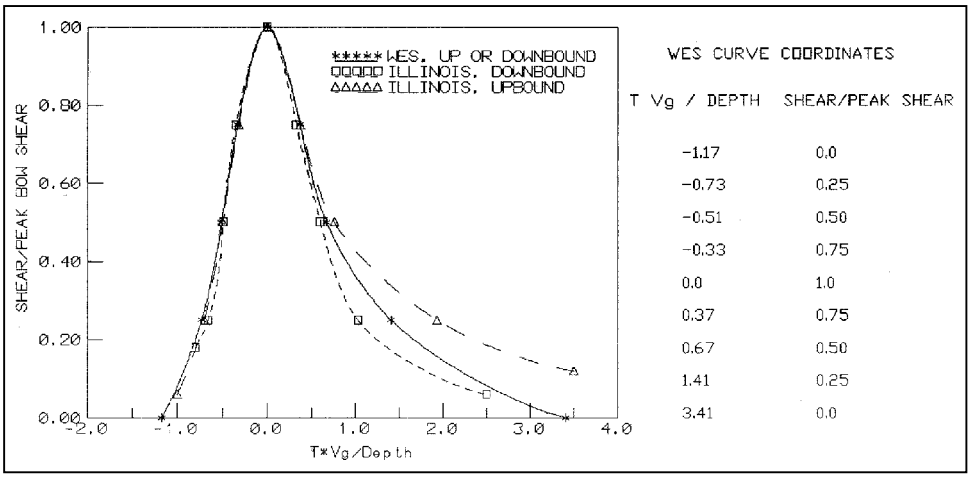

Figure 41. Bow shear distribution

8 Conversion of Smooth Bed Shear Stress to Rough Bed

All shear stress measurements conducted in this study and by Garcia et al. (1998) were conducted on a hydraulically smooth boundary and some adjustment is required to apply these results to hydraulically rough beds found in the prototype. A procedure is presented by Maynord (1998) that is adopted herein. The equations for developing boundary layers on smooth and rough surfaces by Schlichting (1968) provide an approximate means of increasing the shear stress from smooth to rough bed conditions. Required input was distance from beginning of boundary layer development xbl, velocity in propeller jet or at bow of barges, sand grain roughness $K_s = 2\ D_{50}$, and kinematic viscosity ν. The equation for local friction coefficient on a smooth developing boundary is Equation 21.18 from Schlichting (1968) and is shown here as:

$$C_{fs} = 0.37 \left(\log R_x\right)^{-2.584} \tag{38}$$

where R_x = Velocity xbl/ν

The equation for rough boundaries is Equation 30. Maynord (1998) evaluated propeller jet velocities and used a velocity in defining R_x that was about the average of the data of 2.8 m/sec. With xbl appearing in both smooth and rough boundary equations, the ratio is not sensitive to xbl and a value of 8 m was used in the Maynord (1998) analysis. The ratio of C_{fr}/C_{fs} which is equivalent to rough shear/smooth shear is plotted in Figure 42. The equation of the line can be approximated by:

$$\frac{C_{fr}}{C_{fs}} = 7.87\ D_{50}^{0.18} \tag{39}$$

Equation 39 is used to convert the smooth bed shear measurement to rough bed conditions with D_{50} given in millimeters. Equations 30, 38, and 39 should be limited to D_{50} = 10 mm based on the relative roughness limitations given by Schlichting (1968).

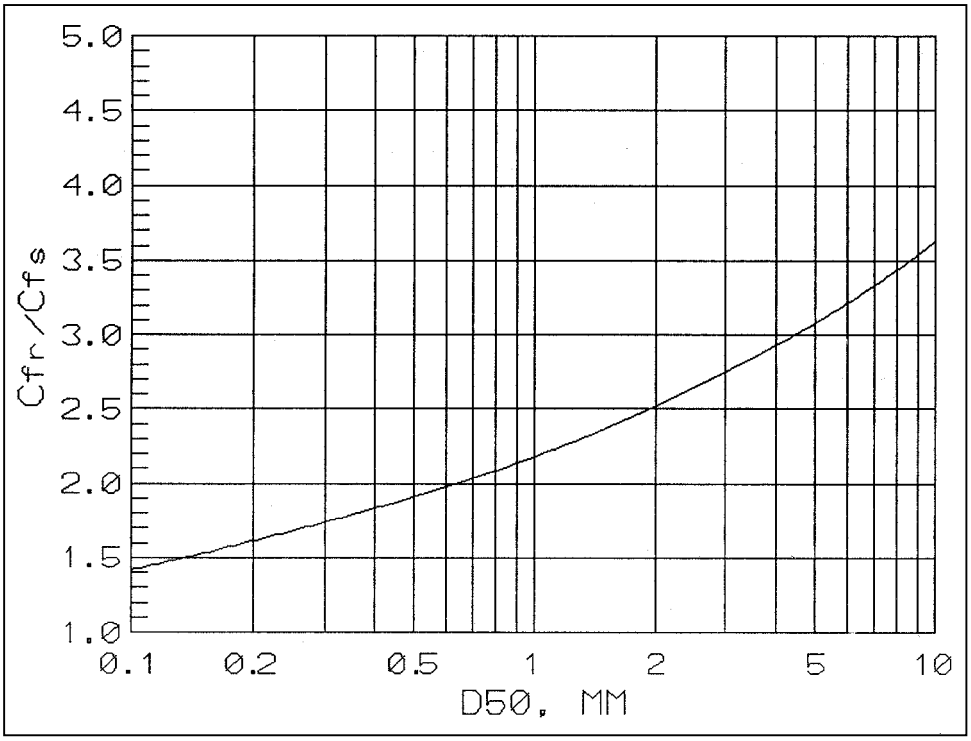

Figure 42. Local friction coefficient ratio versus D50

9 Summary and Discussion of Results

The results presented herein for the physical forces near commercial tows focus on the design tow using the UMR-IWWS. The design tow is a three-wide by five-long barge tow, loaded to about 2.74 m and pushed by a twin-screw towboat with open-wheel or Kort nozzle propellers, typically about 2.74 m in diameter. These data are from experiments in a 1:25-scale model channel, barges, and towboat that has operating propellers, rudders, and open-wheel or Kort nozzle propellers. Measurements included pressure changes, velocity, and bed shear stress.

Pressure on the channel bottom drops during passage of commercial navigation, particularly at the bow, with a maximum drop of 1.5 m in a 3.5-m water depth with a tow having a 2.44-m draft. Pressure drop was less significant at the stern of the barges and near the propeller jet and less significant with increasing water depth.

Equations were developed based on model data to define the peak value and distribution of velocity and bed shear stress in the bow region of the tow.

Two techniques were developed for estimating near-bed velocity from the propeller jet. The first technique provides the peak near-bed propeller velocity for moving and stationary tows without concern for the location or distribution. The second technique provides the lateral and longitudinal distribution of near-bed velocity for moving and stationary tows. Both techniques incorporate the effects of the wake flow behind the barges as well as ambient velocity.

Skin friction coefficients were determined from bed shear stress measurements to determine the peak bed shear stress using the velocity from the peak near-bed propeller velocity model. The peak bed shear stress was decayed laterally and longitudinally to provide the distribution of bed shear stress using dimensionless distributions.

Equations are presented for determining the bed shear stress from return currents.

Equations are developed for converting the shear stress measured herein on a smooth surface to the rough bed conditions found in the prototype.

The various bed shear stresses occur at different locations along the tow and are treated independently.

References

Albertson, M. L., Dai, Y. B., Jensen, R. A., and Rouse, H. (1950). "Diffusion of submerged jets," *Transactions, American Society of Civil Engineers* 115 (2409), New York.

Bergh, H., and Magnusson, N. (1987). "Propeller erosion and protection methods used in ferry terminals in the port of Stockholm," *58th PIANC Bulletin*, Edinburgh, Scotland.

Blauuw, H. G., van der Knaap, F. C. M., de Groot, M. T., and Pilarczyk, K. W. (1984). "Design of bank protection of inland navigation fairways," No. 320, Delft Hydraulics Laboratory, Delft, The Netherlands.

Fuehrer, M., Romisch, K., and Engelke, G. (1981). "Criteria for dimensioning the bottom and slope protections and for applying the new methods of protecting navigation canals," *25th PIANC Bulletin*, Edinburgh, Scotland.

Garcia, M. H., Admiraal. D. M., Rodriquez, J., and Lopez, F. (1998). "Navigation-induced bed shear stresses: Laboratory measurements, data analysis, and field application," Civil Engineering Studies, Hydraulic Engineering Series No. 56, Univ of Illinois at Urbana-Champaign.

Hamill, G. A., Johnston, H. T., and Stewart, D. P. J. (1995). "Estimating the velocities in a ship's propeller wash," *89th PIANC Bulletin*, Edinburgh, Scotland.

Krauss, N., Lohrmann, A., and Cabrera, R. (1994). "New acoustic meter for measuring 3D laboratory flows," *J of Hydraulic Engineering, ASCE* 120(3), 406-412.

Maynord, S. T. (1990). "Velocities induced by commercial navigation," Technical Report HL-90-15, U.S. Army Engineer Waterways Experiment Station, Vicksburg, MS.

_____ . (1996). "Return velocity and drawdown in navigable waterways," Technical Report HL-96-7, U.S. Army Engineer Waterways Experiment Station, Vicksburg, MS.

_____ . (1998). "Bottom shear stress from propeller jets," *Ports '98*, sponsored by ASCE and U.S. Section of the Permanent International Association of Navigation Congresses, Long Beach, Ca.

Maynord, S. T., and Martin, S. K. (1997). “Interim report for the Upper Mississippi River-Illinois Waterway System Navigation Study, physical forces study, Kampsville, Illinois Waterway,” ENV Report 3, U.S. Army Engineer Waterways Experiment Station, Vicksburg, MS.

Oebius, H. U. (1984). “Loads on bed and banks caused by ship propulsion systems,” *International conference on flexible armoured revetments incorporating geotextiles,* London, 29-30 March, 13-23.

Prosser, M. J. (1986). “Propeller induced scour,” prepared for British Ports Assoc. by BHRA, RR2570, Cranfield.

Schlichting, H. (1968). *Boundary layer theory.* McGraw-Hill, New York.

Stockstill, R. L., and Berger, R. C. “A two-dimensional model for vessel-generated currents,” (Technical Report in preparation), U.S. Army Engineer Research and Development Center, Vicksburg, MS.

Toutant, W. T. (1982). “Mathematical performance models for river tows,” Winter meeting, Great Lakes and Great Rivers Section, Society of Naval Architects and Marine Engineers, Clarksville, IN.

U.S. Army Corps of Engineers. (1994). “Upper Mississippi River- Illinois Waterway System Navigation Study,” Baseline Initial Project Management Plan, St Paul, Rock Island, and St Louis Districts.

Verhey, H. J. (1983). “The stability of bottom and banks subjected to the velocities in the propeller jet behind ships,” No. 303, Delft Hydraulics Laboratory, Delft, The Netherlands.

Appendix A
Time-Histories of Measured Velocity and Shear Stress

Table A1
Experimental Details for Shear and Velocity Measurements, Kort Nozzle Towboat

Experiment	Depth, m	Up or Down	V_g, m/sec	Y, m	Thrust, n	# of Runs[1]
KU1212T4	3.66	UP	2.0	0.0	389,500	3
KU1222T4	3.66	UP	2.0	3.0	"	3
KU1212T5	3.66	UP	2.0	3.0	"	3
KU1222T5	3.66	UP	2.0	6.0	"	3
KV1522AT	4.57	UP	2.0	3.0	393,000	1
TU1513T5	4.57	UP	2.5	3.0	372,000	1
KV1514AT	4.57	UP	3.0	0.0	351,500	1
TU1514T8	4.57	UP	3.0	0.0	"	3
TU1534T5	4.57	UP	3.0	1.5	"	3
KV1524AT	4.57	UP	3.0	3.0	"	1
TU1514T5	4.57	UP	3.0	3.0	"	3
KV1524BT	4.57	UP	3.0	3.0	0.0	1
KV1534AT	4.57	UP	3.0	3.0	351,500	1
TU1524T8	4.57	UP	3.0	6.0	"	2
TU1524T5	4.57	UP	3.0	9.0	"	2
TU1515T5	4.57	UP	3.5	3.0	470,000	1
KV1822AT	5.49	UP	2.0	3.0	390,000	1
TU1813T8	5.49	UP	2.5	3.0	369,000	1
KV1814AT	5.49	UP	3.0	0.0	347,000	1
TU1814T4	5.49	UP	3.0	0.0	"	3
KV1824AT	5.49	UP	3.0	3.0	"	1
TU1814T8	5.49	UP	3.0	3.0	"	3
KV1824BT	5.49	UP	3.0	3.0	"	1
KV1834AT	5.49	UP	3.0	6.0	"	1
TU1824T4	5.49	UP	3.0	6.0	"	3
TU1824T8	5.49	UP	3.0	9.0	347,000	3
TU1815T8	5.49	UP	3.5	3.0	463,000	1
KV1826AT	5.49	UP	4.0	3.0	429,000	1
KV2323AT	7.09	UP	2.5	3.0	374,000	1
KU2313T5	7.09	UP	2.5	3.0	374,000	1
KV2314AT	7.09	UP	3.0	0.0	351,500	1
KU2314T4	7.09	UP	3.0	0.0	"	3

(Continued)

[1] The plots were based on either one experiment or the average of two or three experiments.

Table A1 (Concluded)

Experiment	Depth, m	Up or Down	V_g, m/sec	Y, m	Thrust, n	# of Runs[1]
KV2314BT	7.09	UP	3.0	0.0	0.0	1
KV2324AT	7.09	UP	3.0	3.0	351,500	1
KU2314T5	7.09	UP	3.0	3.0	"	3
KV2334AT	7.09	UP	3.0	6.0	"	1
KU2334T4	7.09	UP	3.0	6.0	"	3
KU2334T5	7.09	UP	3.0	9.0	"	1
KV2325BT	7.09	UP	3.5	3.0	470,000	1
KU2315T5	7.09	UP	3.5	3.0	"	1
KV2326AT	7.09	UP	4.0	3.0	435,500	1
KU2316T5	7.09	UP	4.0	3.0	"	1
KD1242T4	3.66	DOWN	2.0	0.0	412,000	3
TD1232T5	3.66	DOWN	2.0	1.5	"	1
KD1232T4	3.66	DOWN	2.0	3.0	"	3
KD1242T5	3.66	DOWN	2.0	3.0	"	3
KD1232T5	3.66	DOWN	2.0	6.0	"	3
TD1513T5	4.57	DOWN	2.5	3.0	397,000	1
TD1534T8	4.57	DOWN	3.0	1.5	377,000	3
TD1514T8	4.57	DOWN	3.0	0.0	"	3
TD1534T5	4.57	DOWN	3.0	1.5	377,000	3
TD1514T5	4.57	DOWN	3.0	3.0	"	3
TD1524T8	4.57	DOWN	3.0	6.0	"	3
TD1524T5	4.57	DOWN	3.0	9.0	"	3
TD1515T5	4.57	DOWN	3.5	3.0	495,000	1
TD1813T8	5.49	DOWN	2.5	3.0	402,000	1
TD1814T4	5.49	DOWN	3.0	0.0	380,500	3
TD1814T8	5.49	DOWN	3.0	3.0	"	3
TD1824T4	5.49	DOWN	3.0	6.0	"	3
TD1824T8	5.49	DOWN	3.0	9.0	"	3
TD1815T8	5.49	DOWN	3.5	3.0	498,000	1
KD2313T5	7.09	DOWN	2.5	3.0	397,000	1
KD2314T4	7.09	DOWN	3.0	0.0	377,000	3
KD2314T5	7.09	DOWN	3.0	3.0	"	3
KD2334T4	7.09	DOWN	3.0	6.0	"	3
KD2334T5	7.09	DOWN	3.0	9.0	"	3
KD2315T5	7.09	DOWN	3.5	3.0	495,000	1
KD2316T5	7.09	DOWN	4.0	3.0	460,000	1

Table A2
Experimental Details for Velocity Measurements, Open-Wheel Towboat

Experiment	Depth, m	Up or Down	V_g, m/sec	Y, m	Thrust, n	# of Runs[1]
0304-2DX	4.3	UP	1.5	1.3	368,000	1
0304D2FX	4.3	DOWN	3.1	1.3	360,000	1
3718U2AX	5.64	UP	2.1	1.3	358,500	1
3618D2AX	5.64	DOWN	3.6	1.3	350,500	1
0306-2DX	7.0	UP	2.1	1.3	357,500	1
0306D2CX	7.0	DOWN	3.6	1.3	351,500	1

[1] The plots were based on a single experiment.

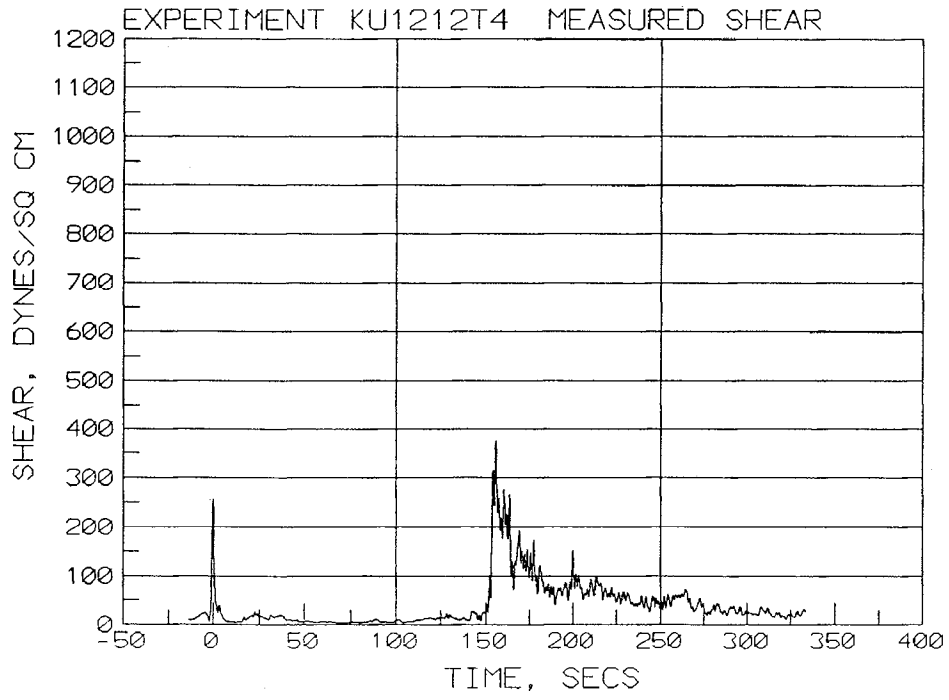
EXPERIMENT KU1212T4 MEASURED SHEAR
SHEAR, DYNES/SQ CM
1200
1100
1000
900
800
700
600
500
400
300
200
100
0
-50
0
50
100
150
200
250
300
350
400
TIME, SECS

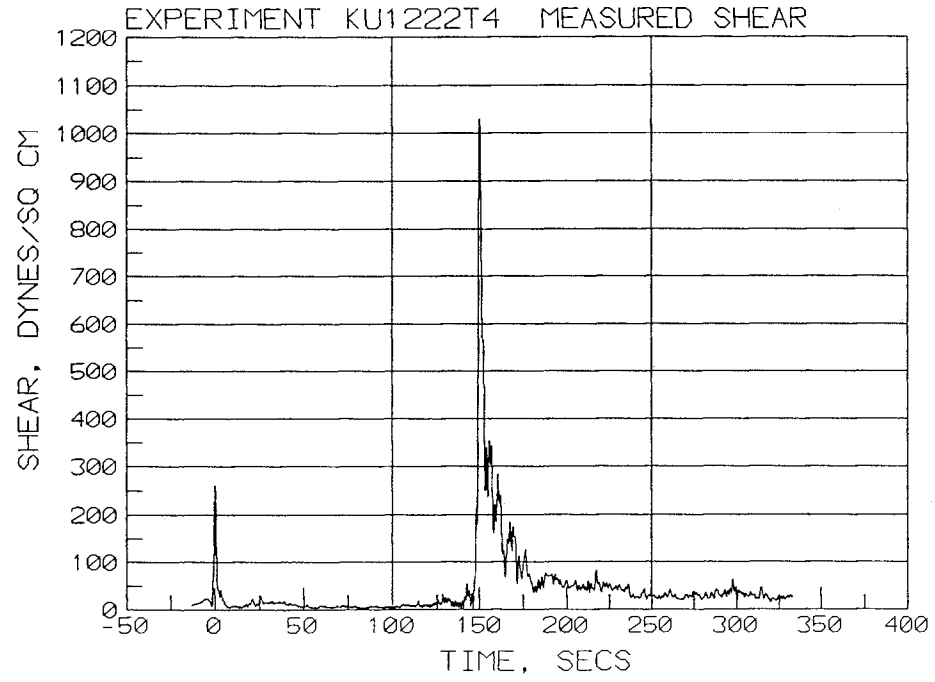
EXPERIMENT KU1222T4 MEASURED SHEAR
SHEAR, DYNES/SQ CM
1200
1100
1000
900
800
700
600
500
400
300
200
100
0
-50
0
50
100
150
200
250
300
350
400
TIME, SECS

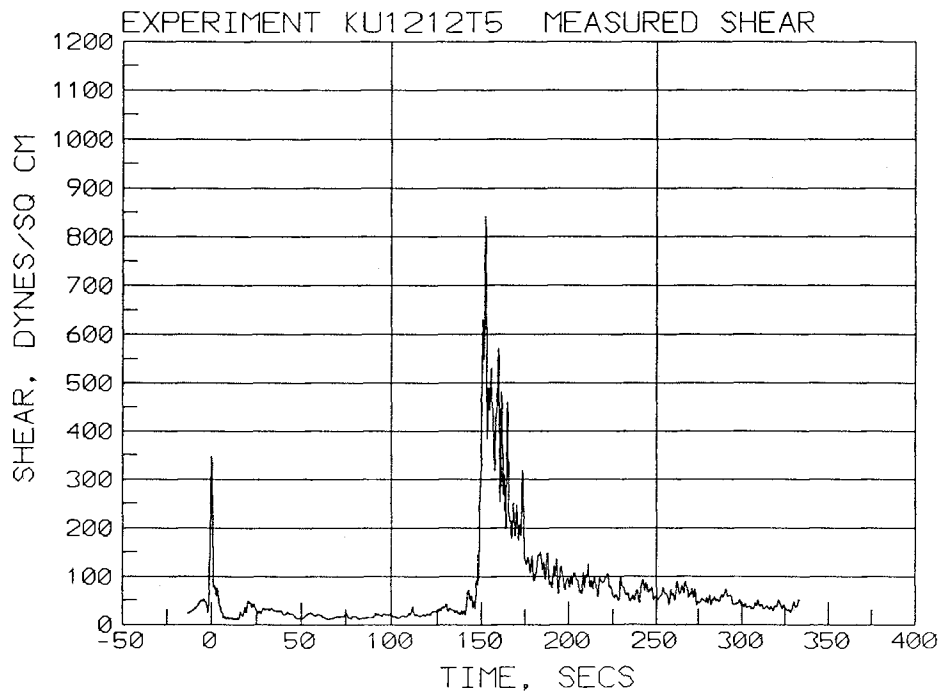
EXPERIMENT KU1212T5 MEASURED SHEAR
SHEAR, DYNES/SQ CM
1200
1100
1000
900
800
700
600
500
400
300
200
100
0
-50
0
50
100
150
200
250
300
350
400
TIME, SECS

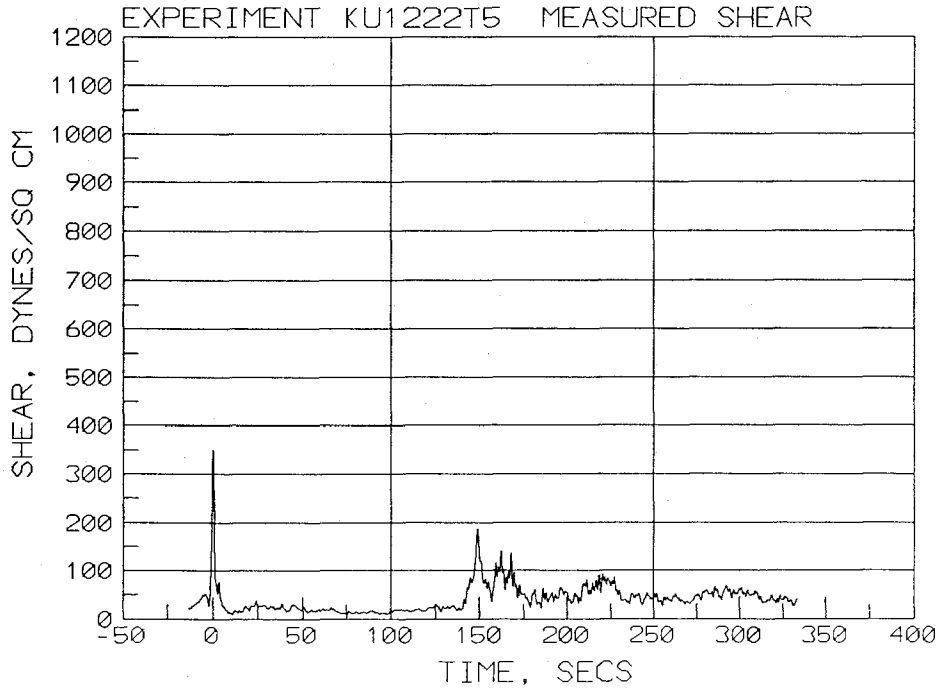
EXPERIMENT KU1222T5 MEASURED SHEAR
SHEAR, DYNES/SQ CM
1200
1100
1000
900
800
700
600
500
400
300
200
100
0
-50
0
50
100
150
200
250
300
350
400
TIME, SECS

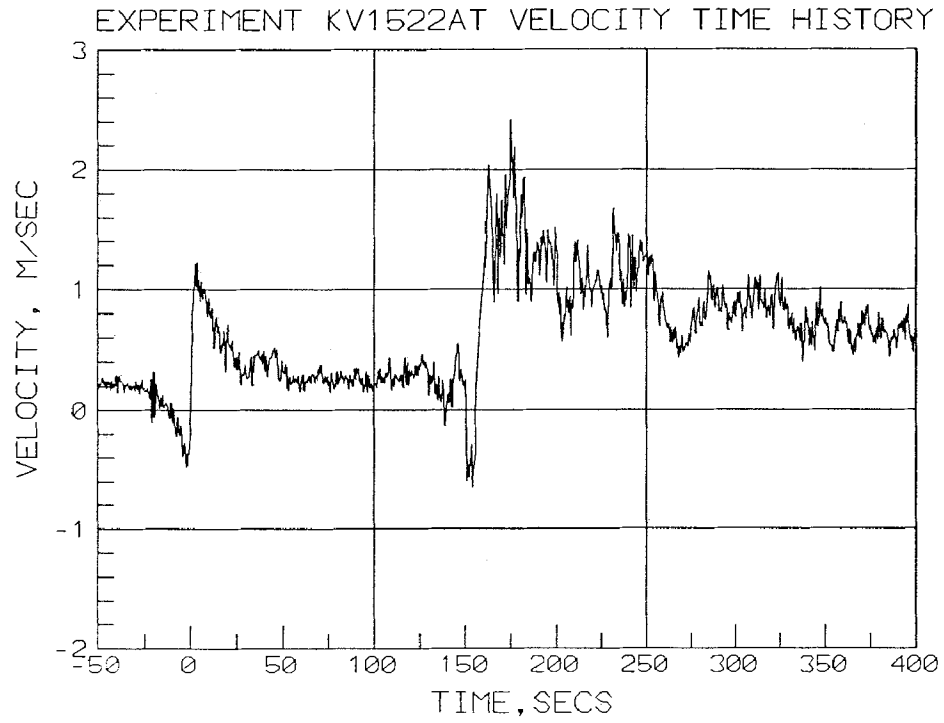
EXPERIMENT KV1522AT VELOCITY TIME HISTORY
VELOCITY, M/SEC
3
2
1
0
-1
-2
-50
0
50
100
150
200
250
300
350
400
TIME, SECS

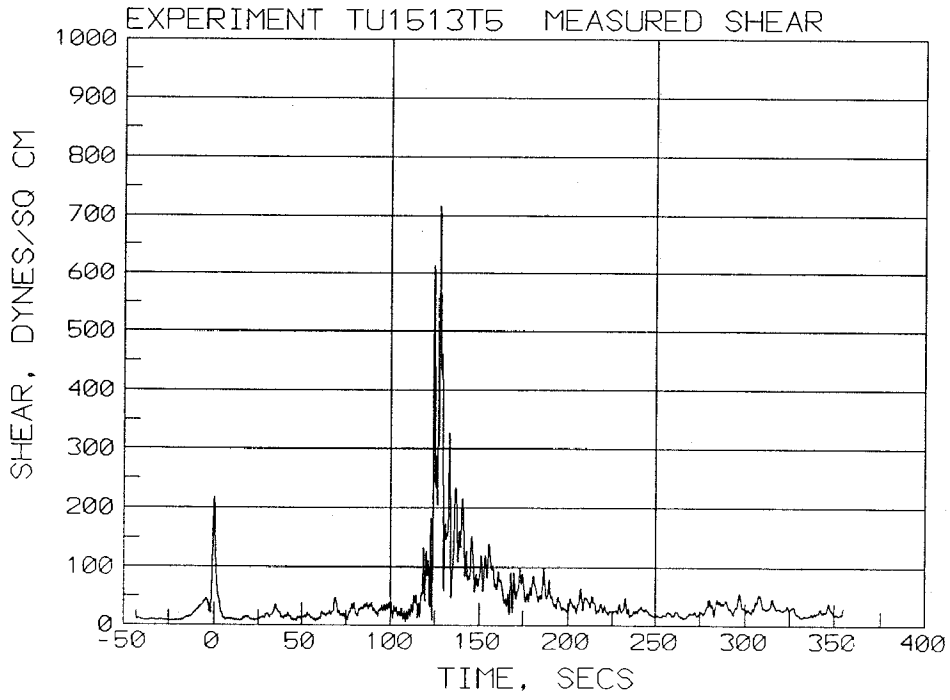
EXPERIMENT TU1513T5 MEASURED SHEAR
SHEAR, DYNES/SQ CM
1000
900
800
700
600
500
400
300
200
100
0
-50
0
50
100
150
200
250
300
350
400
TIME, SECS

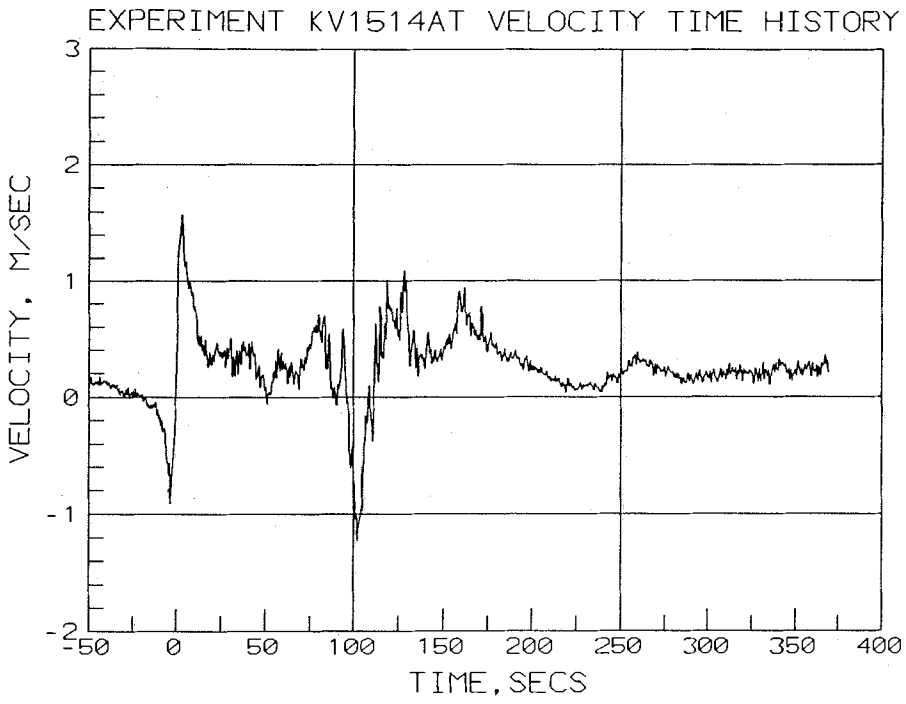
EXPERIMENT KV1514AT VELOCITY TIME HISTORY
VELOCITY, M/SEC
3
2
1
0
-1
-2
-50
0
50
100
150
200
250
300
350
400
TIME, SECS

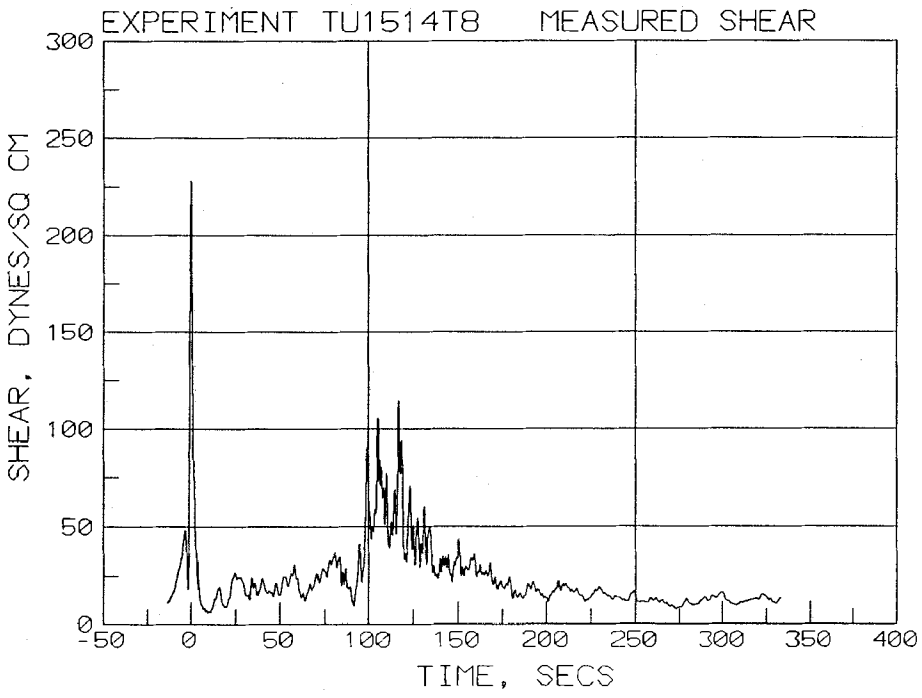
EXPERIMENT TU1514T8 MEASURED SHEAR
SHEAR, DYNES/SQ CM
300
250
200
150
100
50
0
-50
0
50
100
150
200
250
300
350
400
TIME, SECS

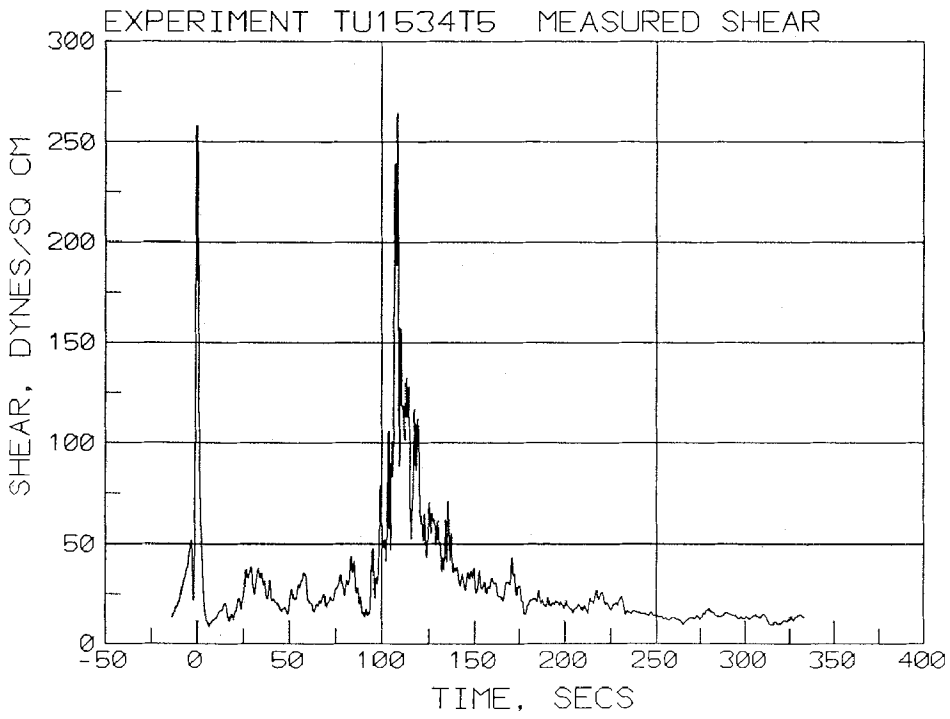
EXPERIMENT TU1534T5 MEASURED SHEAR
SHEAR, DYNES/SQ CM
300
250
200
150
100
50
0
-50
0
50
100
150
200
250
300
350
400
TIME, SECS

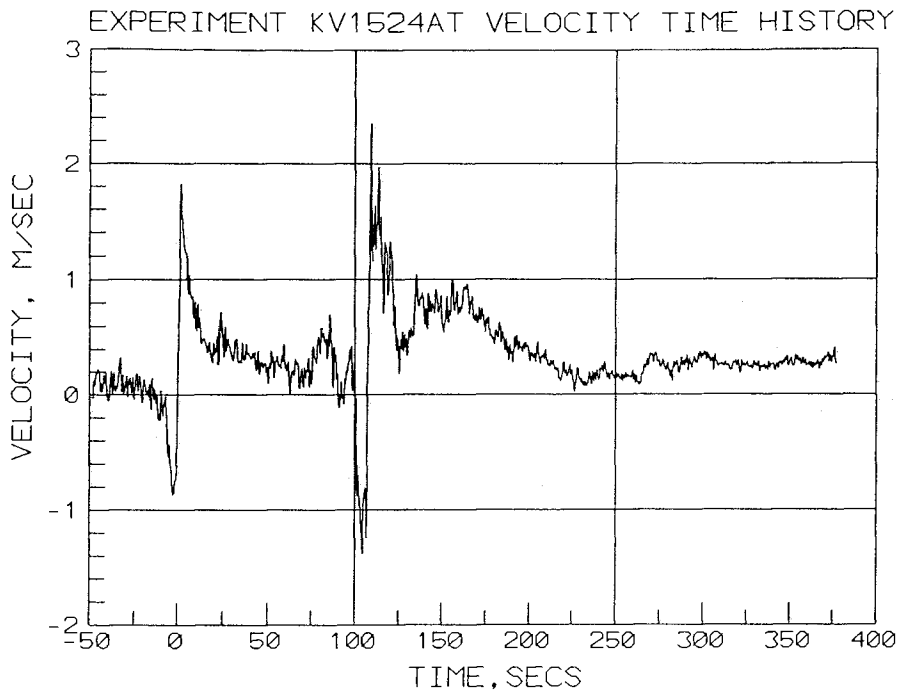
EXPERIMENT KV1524AT VELOCITY TIME HISTORY
VELOCITY, M/SEC
3
2
1
0
-1
-2
-50
0
50
100
150
200
250
300
350
400
TIME, SECS

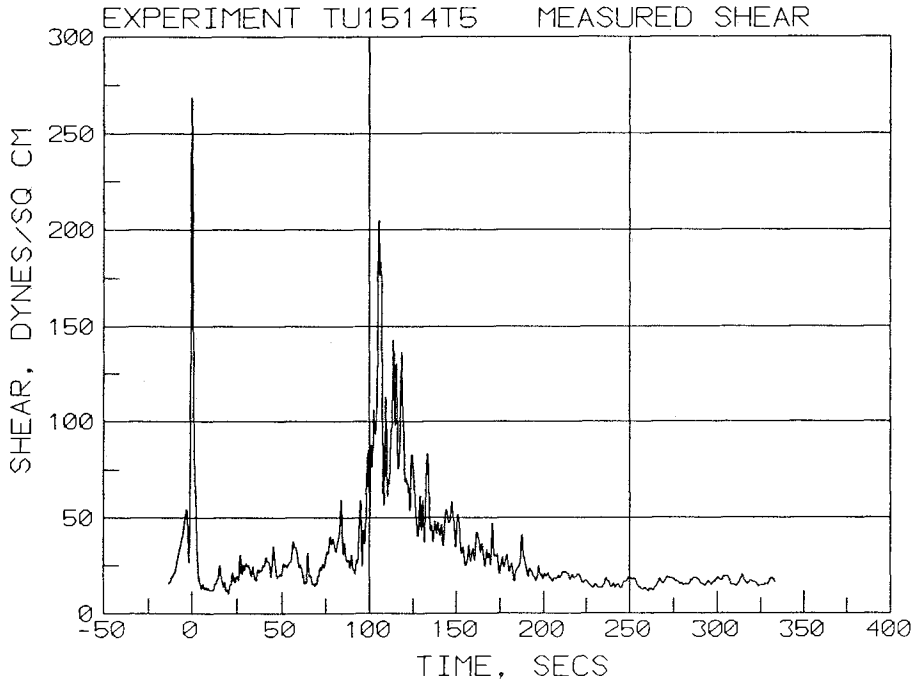
EXPERIMENT TU1514T5 MEASURED SHEAR
SHEAR, DYNES/SQ CM
300
250
200
150
100
50
0
-50
0
50
100
150
200
250
300
350
400
TIME, SECS

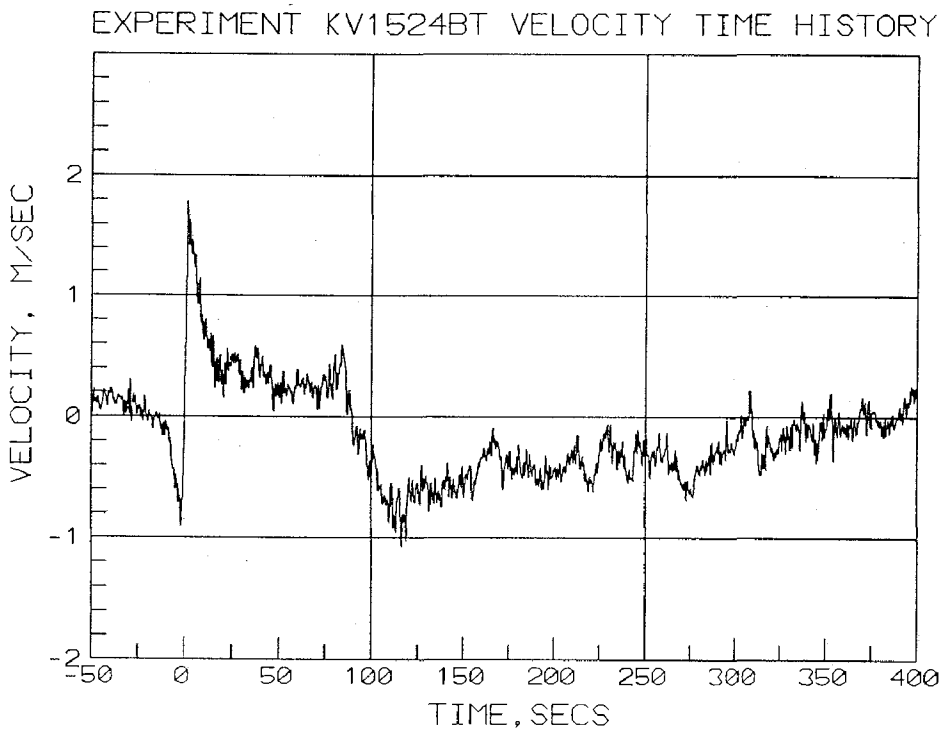
EXPERIMENT KV1524BT VELOCITY TIME HISTORY
VELOCITY, M/SEC
2
1
0
-1
-2
-50
0
50
100
150
200
250
300
350
400
TIME, SECS

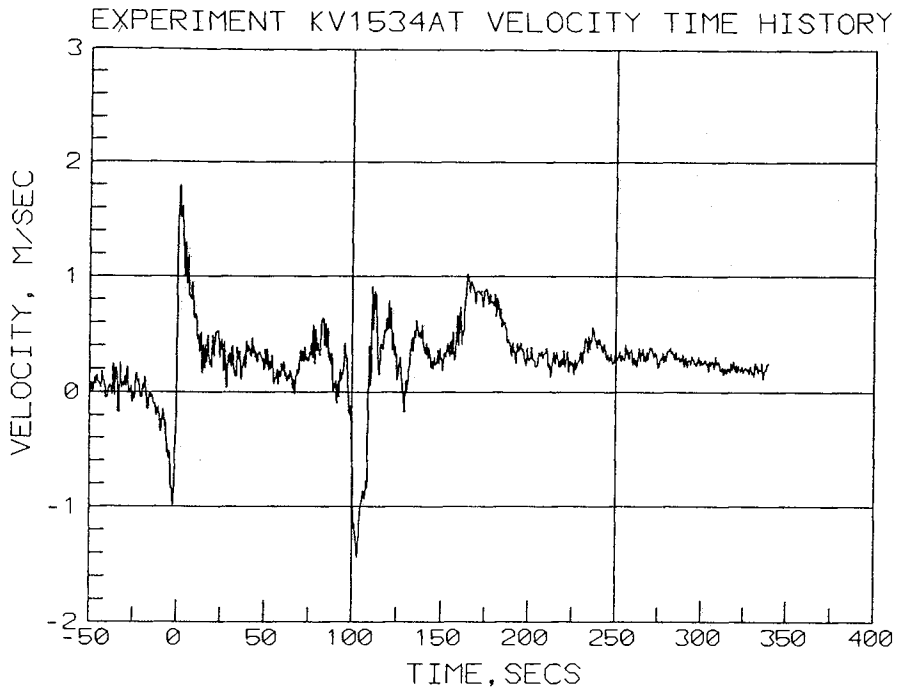
EXPERIMENT KV1534AT VELOCITY TIME HISTORY
VELOCITY, M/SEC
3
2
1
0
-1
-2
-50
0
50
100
150
200
250
300
350
400
TIME, SECS

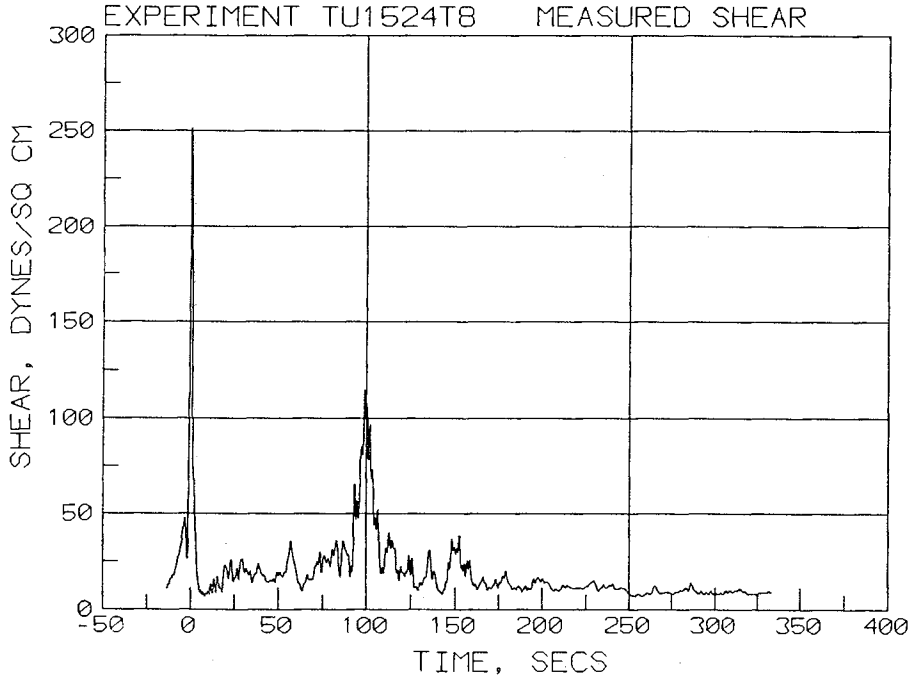
EXPERIMENT TU1524T8 MEASURED SHEAR
SHEAR, DYNES/SQ CM
300
250
200
150
100
50
0
-50
0
50
100
150
200
250
300
350
400
TIME, SECS

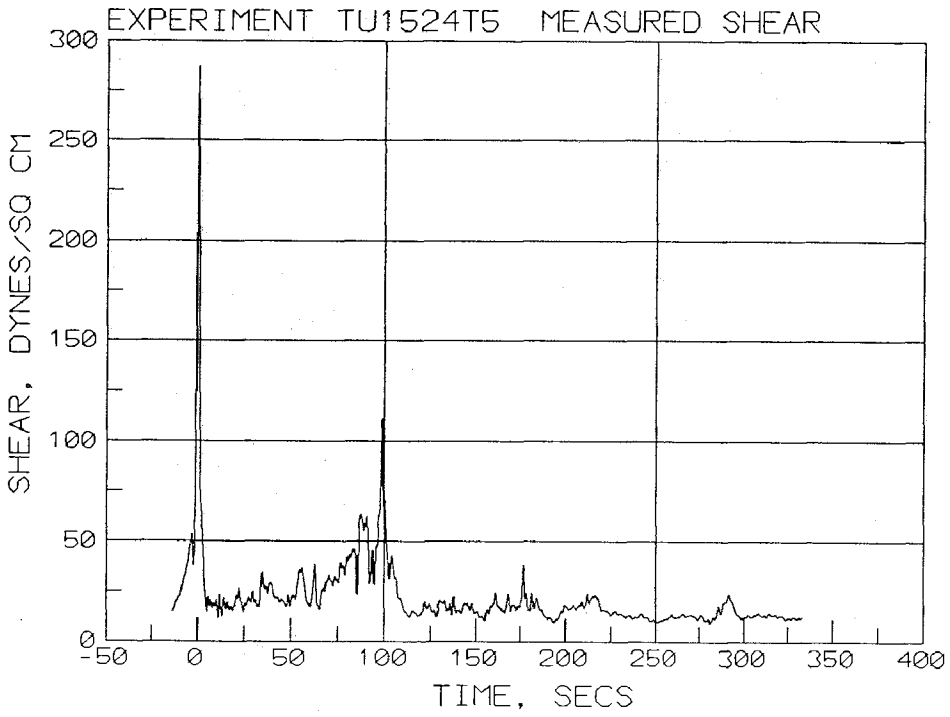
EXPERIMENT TU1524T5 MEASURED SHEAR
SHEAR, DYNES/SQ CM
300
250
200
150
100
50
0
-50
0
50
100
150
200
250
300
350
400
TIME, SECS

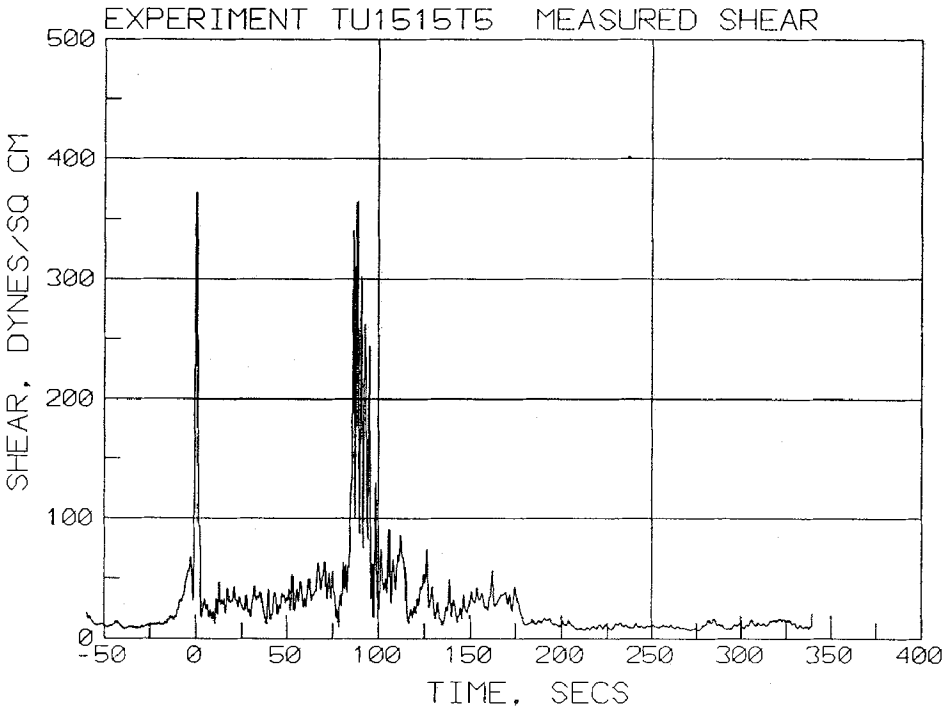
EXPERIMENT TU1515T5 MEASURED SHEAR
SHEAR, DYNES/SQ CM
500
400
300
200
100
0
-50
0
50
100
150
200
250
300
350
400
TIME, SECS

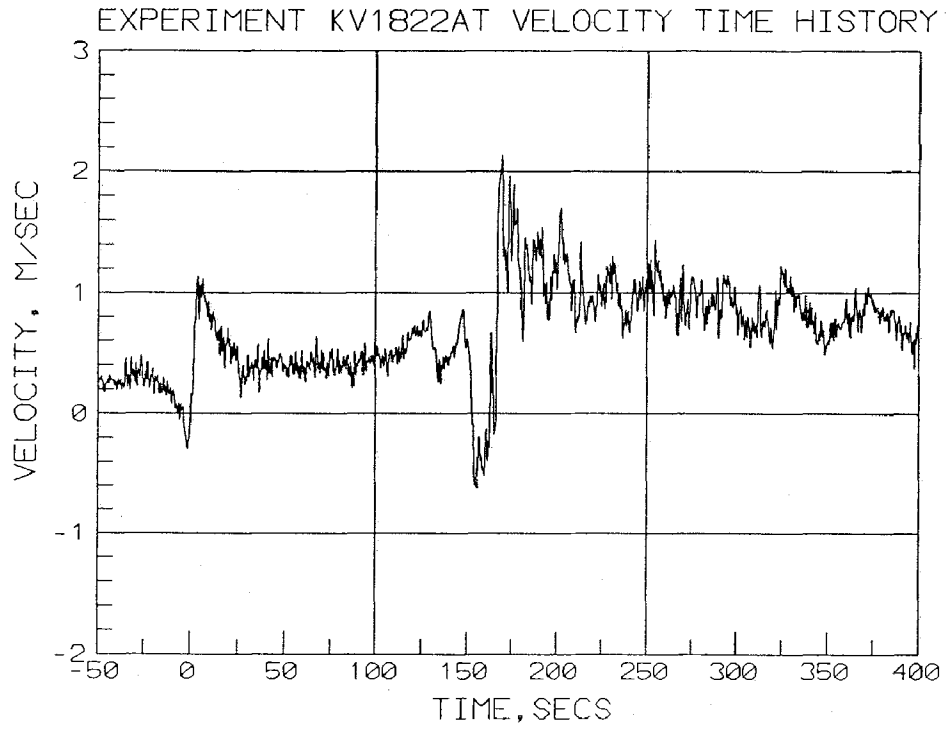
EXPERIMENT KV1822AT VELOCITY TIME HISTORY
VELOCITY, M/SEC
3
2
1
0
-1
-2
-50
0
50
100
150
200
250
300
350
400
TIME, SECS

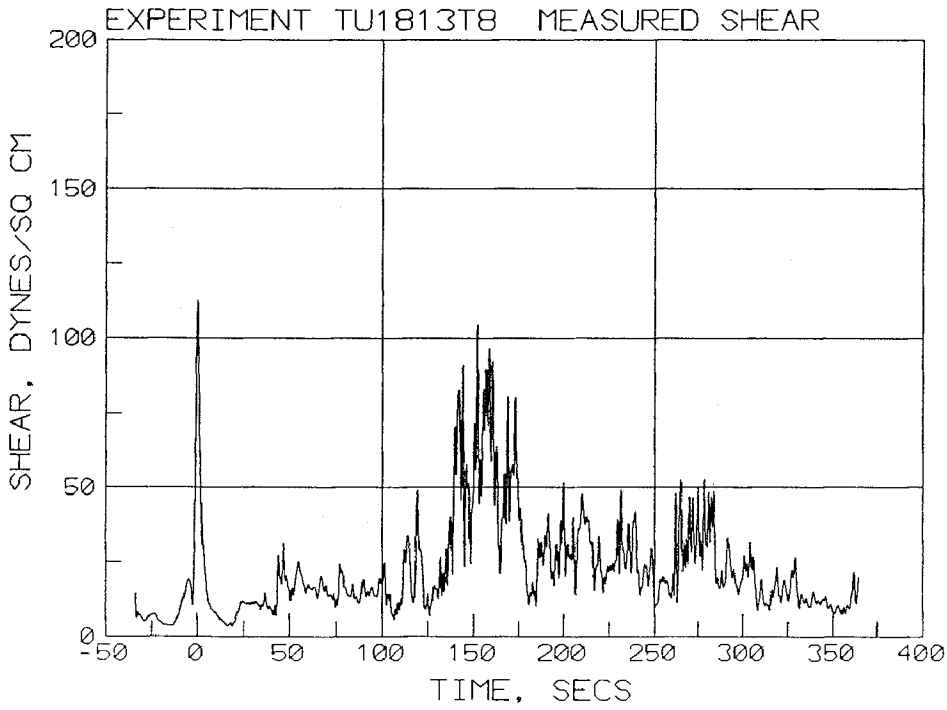
EXPERIMENT TU1813T8 MEASURED SHEAR
SHEAR, DYNES/SQ CM
200
150
100
50
0
-50
0
50
100
150
200
250
300
350
400
TIME, SECS

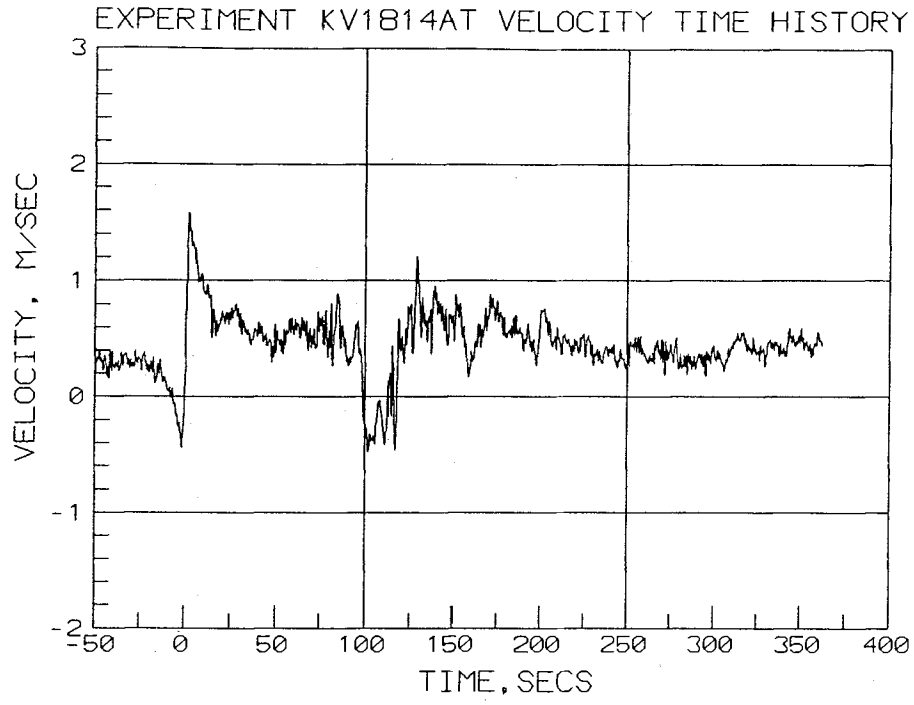
EXPERIMENT KV1814AT VELOCITY TIME HISTORY
VELOCITY, M/SEC
3
2
1
0
-1
-2
-50
0
50
100
150
200
250
300
350
400
TIME, SECS

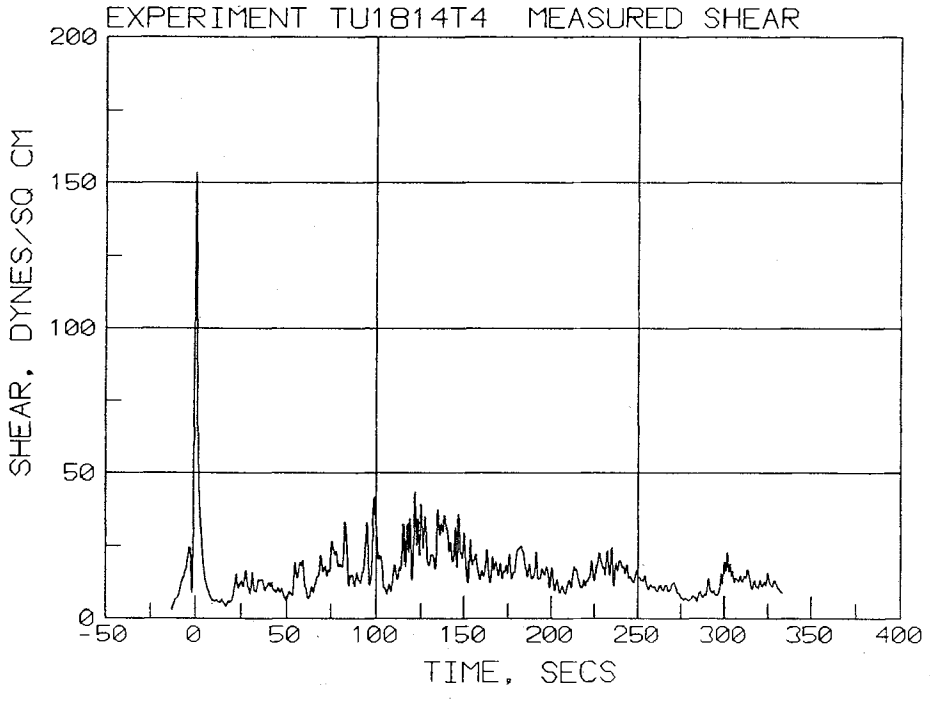
EXPERIMENT TU1814T4 MEASURED SHEAR
SHEAR, DYNES/SQ CM
200
150
100
50
0
-50
0
50
100
150
200
250
300
350
400
TIME, SECS

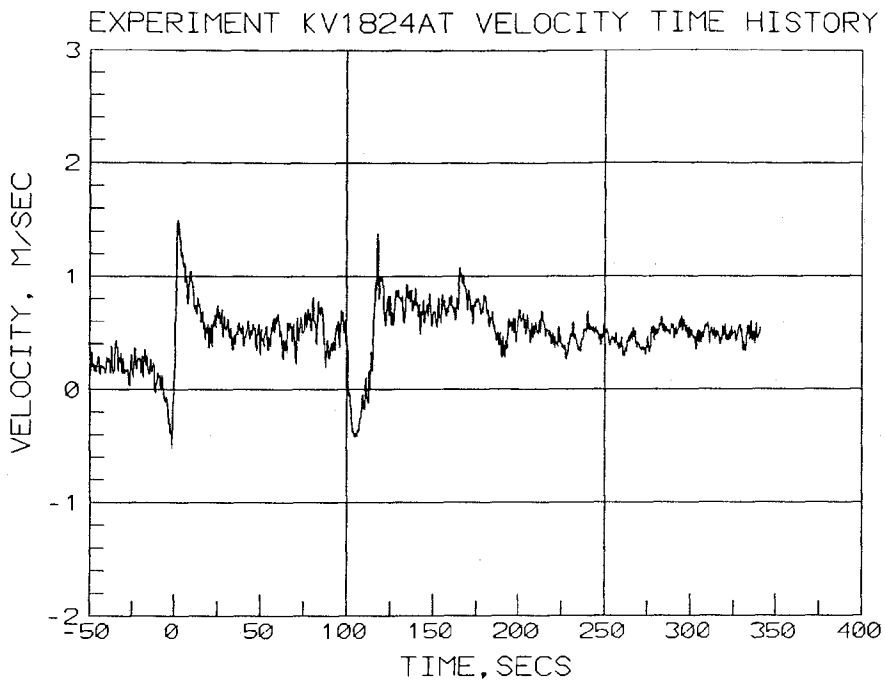
EXPERIMENT KV1824AT VELOCITY TIME HISTORY
VELOCITY, M/SEC
3
2
1
0
-1
-2
-50
0
50
100
150
200
250
300
350
400
TIME, SECS

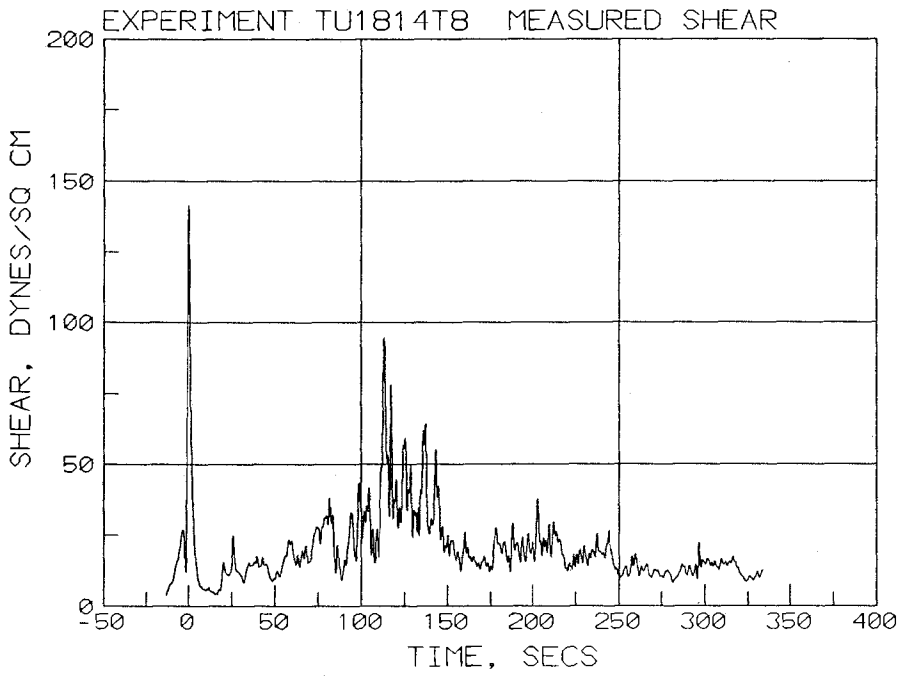
EXPERIMENT TU1814T8 MEASURED SHEAR
SHEAR, DYNES/SQ CM
200
150
100
50
0
-50
0
50
100
150
200
250
300
350
400
TIME, SECS

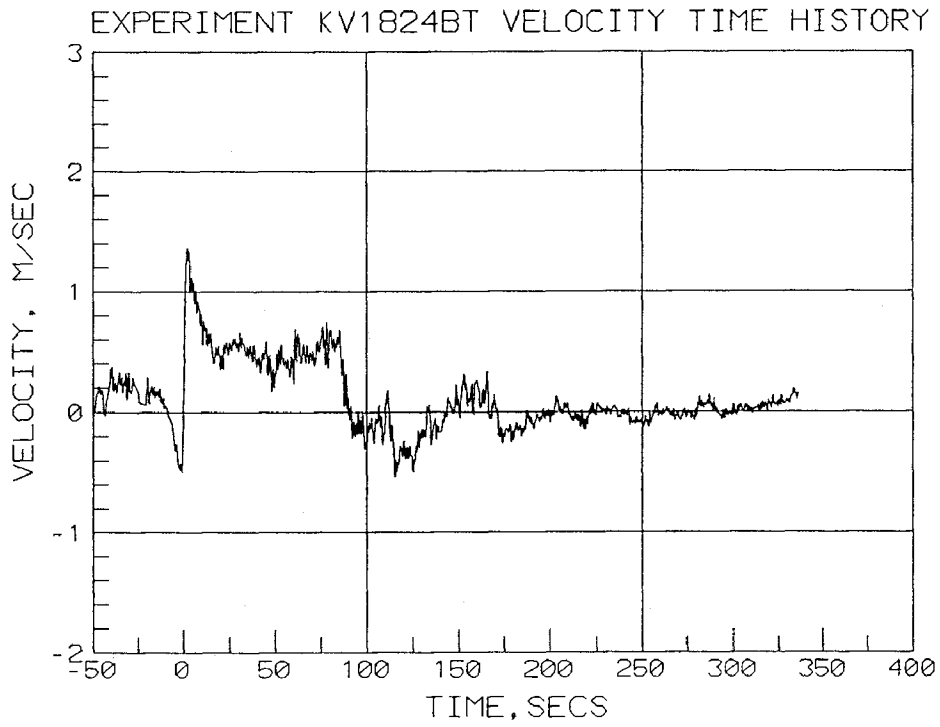
EXPERIMENT KV1824BT VELOCITY TIME HISTORY
VELOCITY, M/SEC
3
2
1
0
-1
-2
-50
0
50
100
150
200
250
300
350
400
TIME, SECS

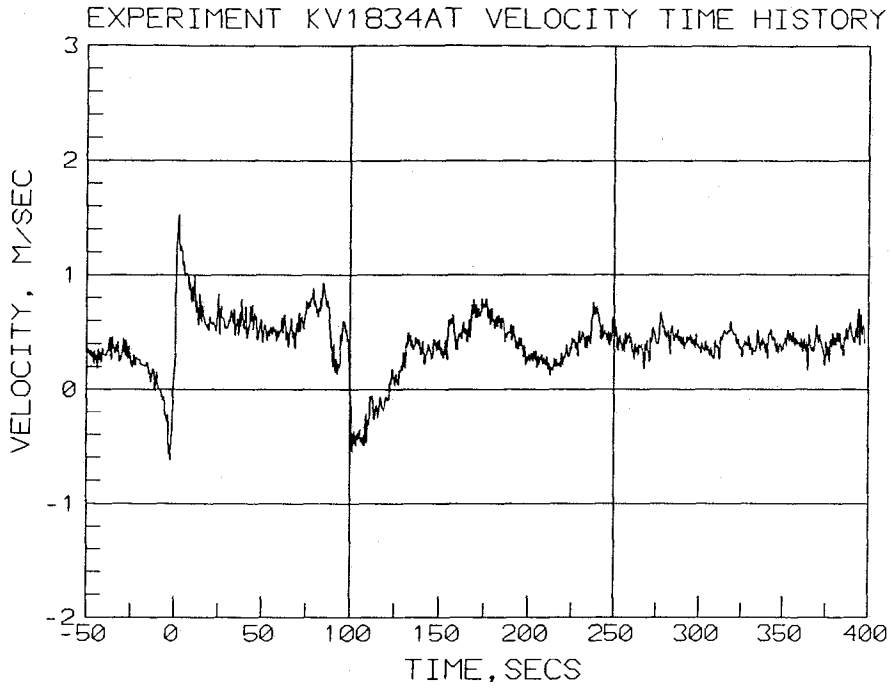
EXPERIMENT KV1834AT VELOCITY TIME HISTORY
VELOCITY, M/SEC
3
2
1
0
-1
-2
-50
0
50
100
150
200
250
300
350
400
TIME, SECS

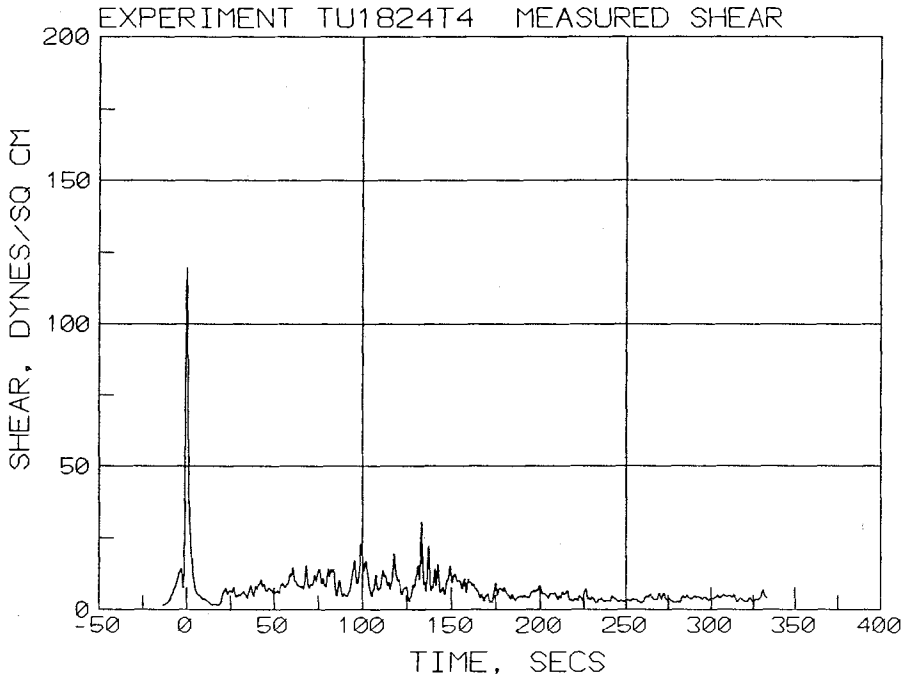
EXPERIMENT TU1824T4 MEASURED SHEAR
SHEAR, DYNES/SQ CM
200
150
100
50
0
-50
0
50
100
150
200
250
300
350
400
TIME, SECS

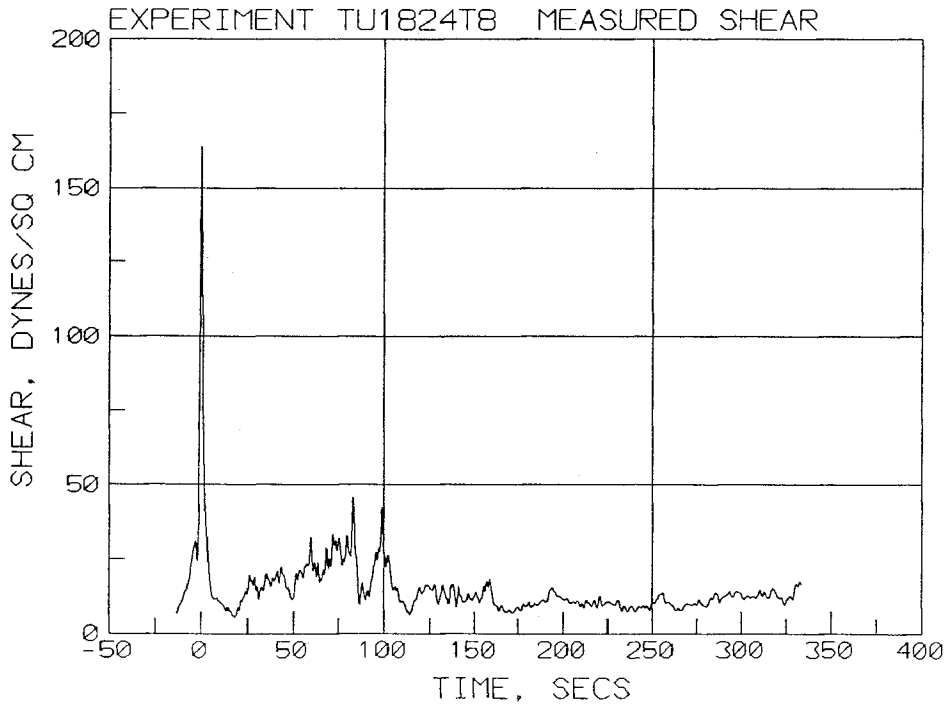
EXPERIMENT TU1824T8 MEASURED SHEAR
SHEAR, DYNES/SQ CM
200
150
100
50
0
-50
0
50
100
150
200
250
300
350
400
TIME, SECS

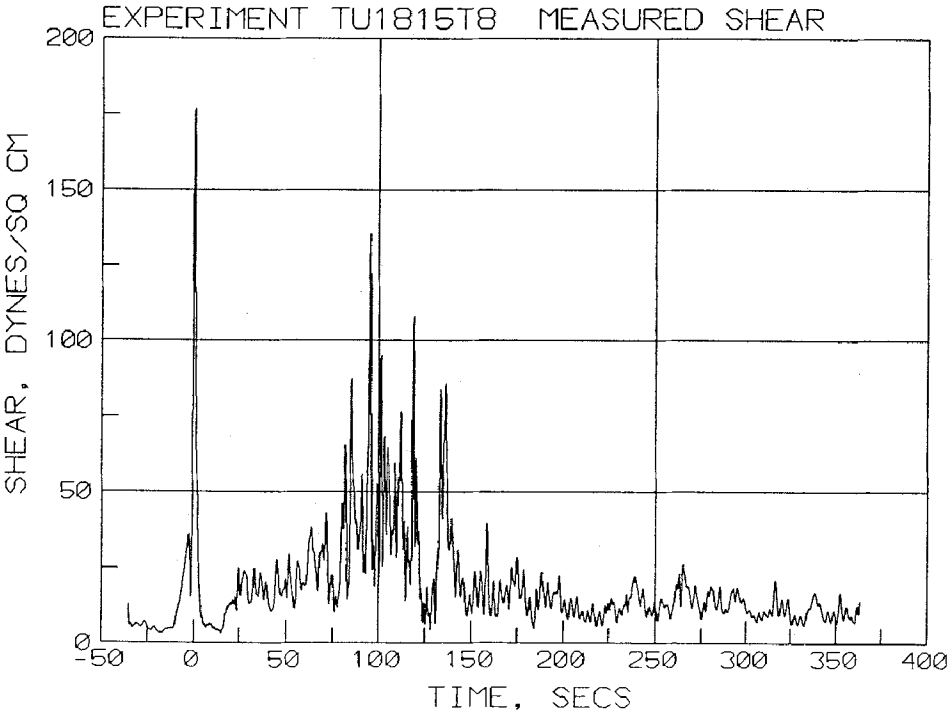
EXPERIMENT TU1815T8 MEASURED SHEAR
SHEAR, DYNES/SQ CM
200
150
100
50
0
-50
0
50
100
150
200
250
300
350
400
TIME, SECS

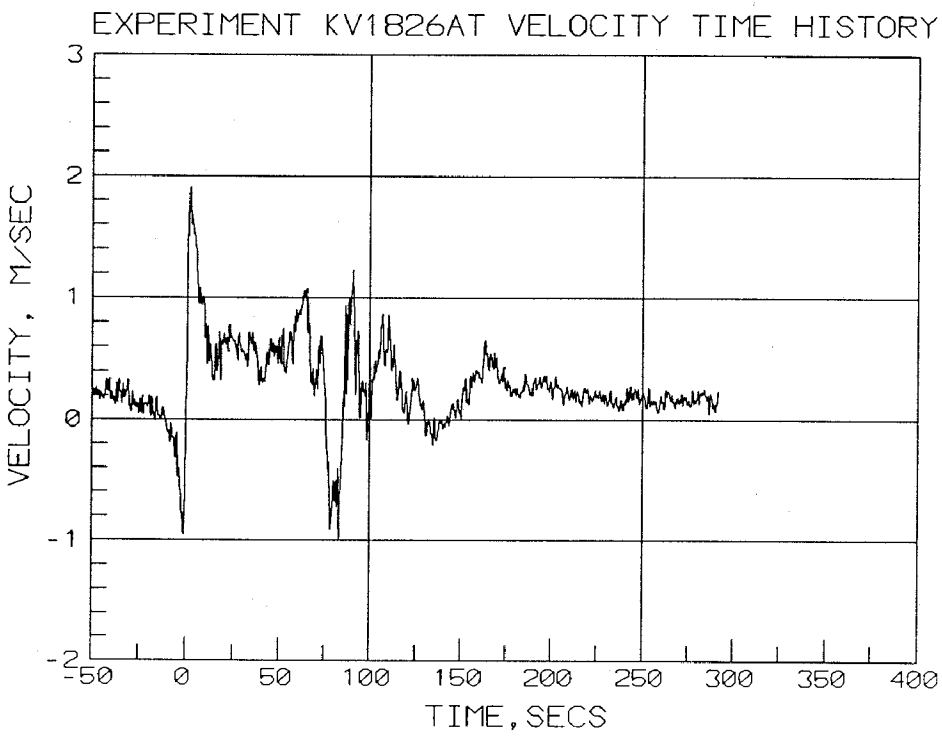
EXPERIMENT KV1826AT VELOCITY TIME HISTORY
VELOCITY, M/SEC
3
2
1
0
-1
-2
-50
0
50
100
150
200
250
300
350
400
TIME, SECS

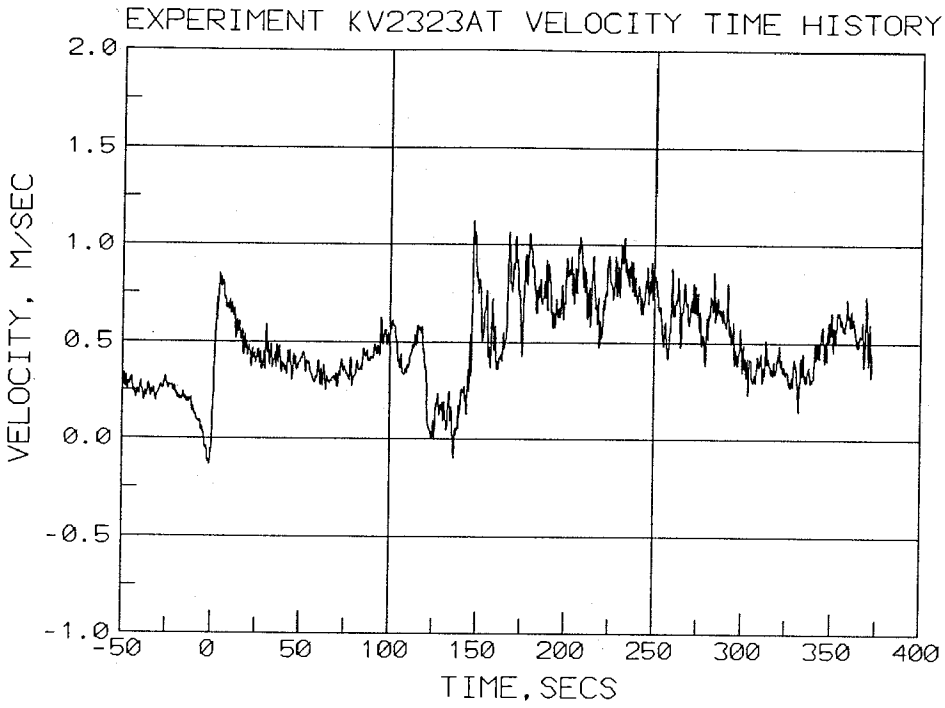
EXPERIMENT KV2323AT VELOCITY TIME HISTORY
VELOCITY, M/SEC
2.0
1.5
1.0
0.5
0.0
-0.5
-1.0
-50
0
50
100
150
200
250
300
350
400
TIME, SECS

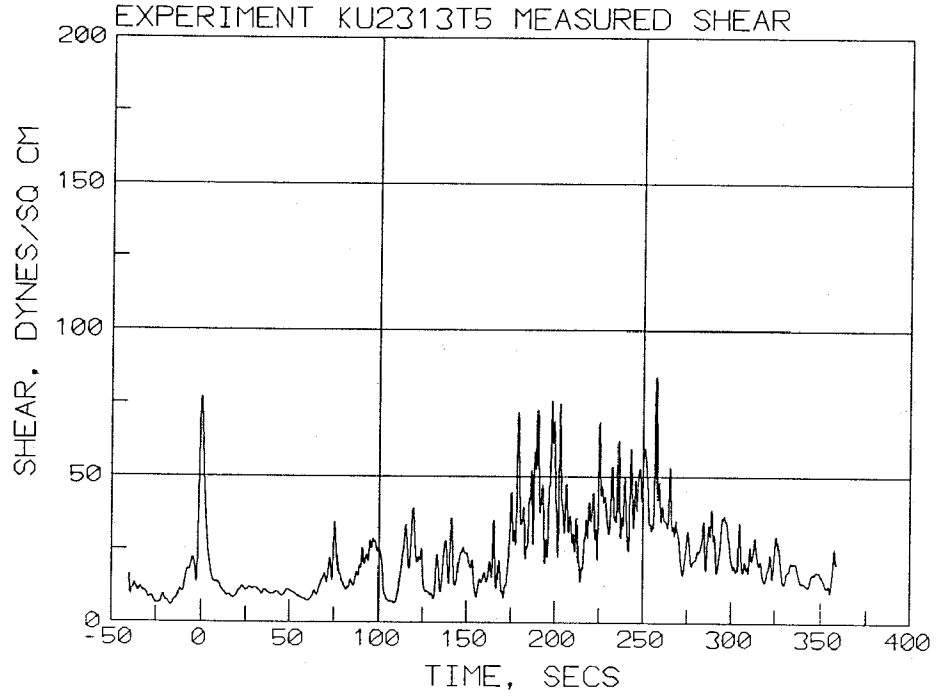
EXPERIMENT KU2313T5 MEASURED SHEAR
SHEAR, DYNES/SQ CM
200
150
100
50
0
-50
0
50
100
150
200
250
300
350
400
TIME, SECS

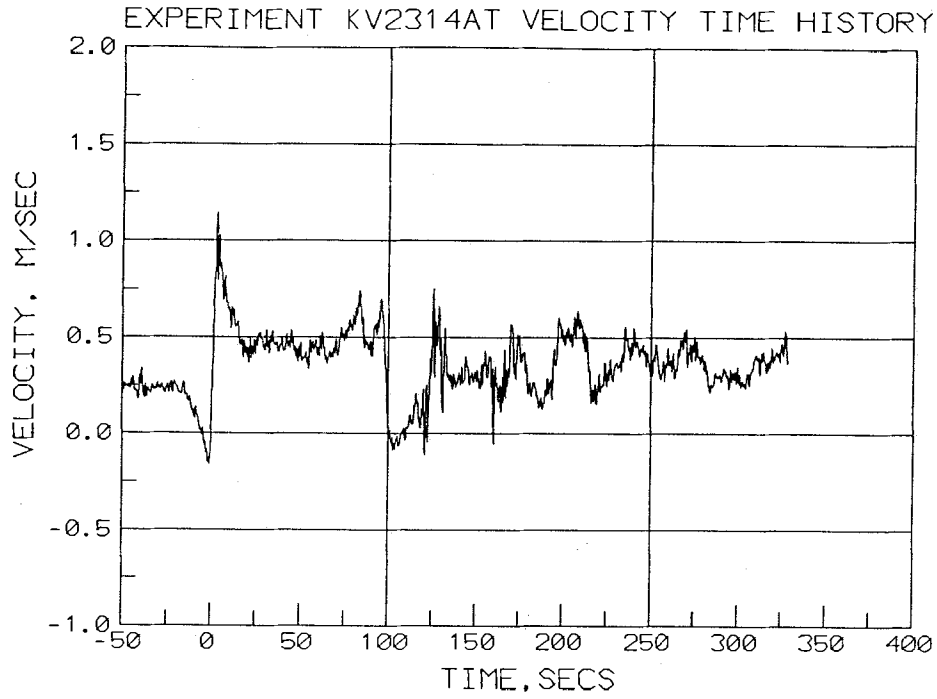
EXPERIMENT KV2314AT VELOCITY TIME HISTORY
VELOCITY, M/SEC
2.0
1.5
1.0
0.5
0.0
-0.5
-1.0
-50
0
50
100
150
200
250
300
350
400
TIME, SECS

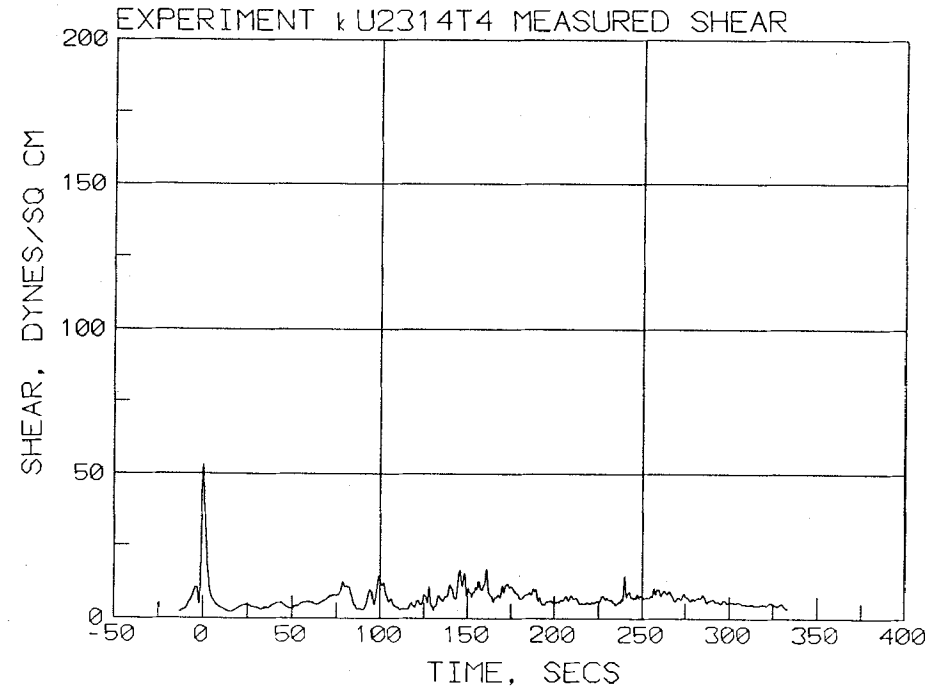
EXPERIMENT kU2314T4 MEASURED SHEAR
SHEAR, DYNES/SQ CM
200
150
100
50
0
-50
0
50
100
150
200
250
300
350
400
TIME, SECS

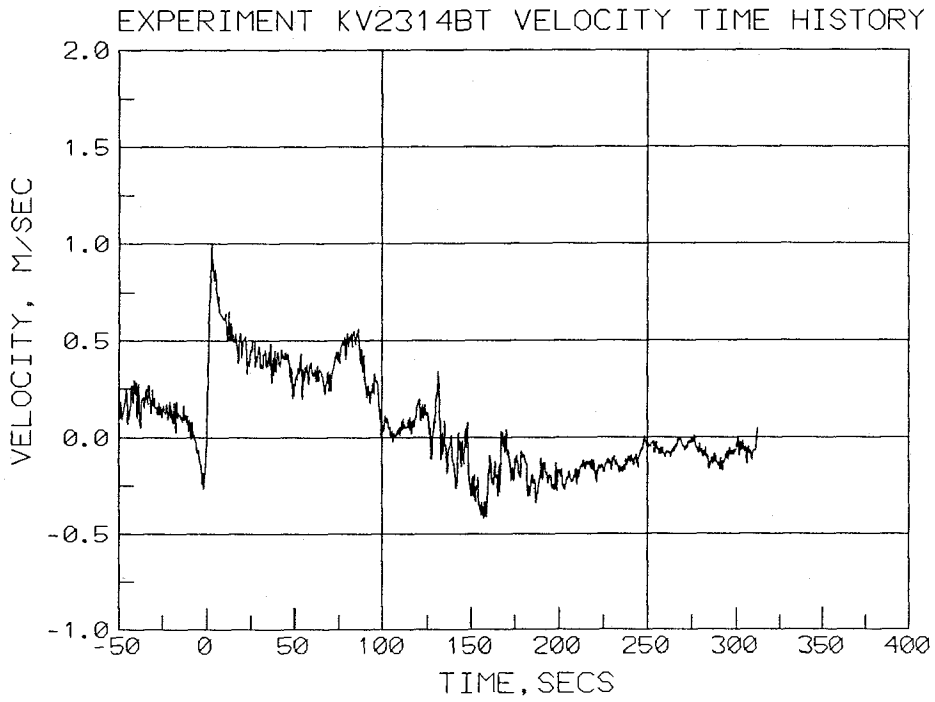
EXPERIMENT KV2314BT VELOCITY TIME HISTORY
VELOCITY, M/SEC
2.0
1.5
1.0
0.5
0.0
-0.5
-1.0
-50
0
50
100
150
200
250
300
350
400
TIME, SECS

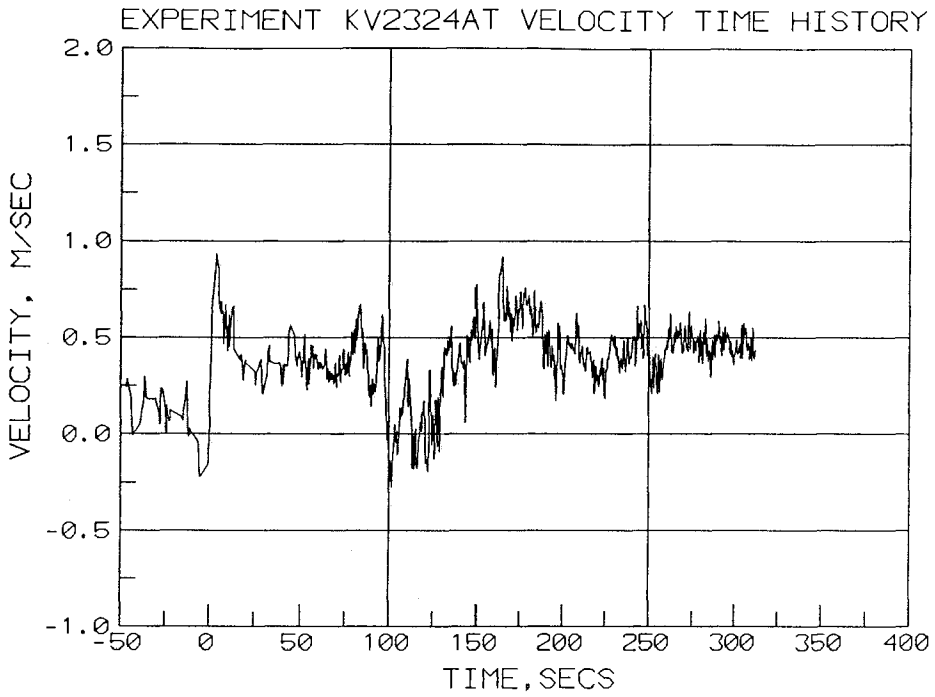
EXPERIMENT KV2324AT VELOCITY TIME HISTORY
VELOCITY, M/SEC
2.0
1.5
1.0
0.5
0.0
-0.5
-1.0
-50
0
50
100
150
200
250
300
350
400
TIME, SECS

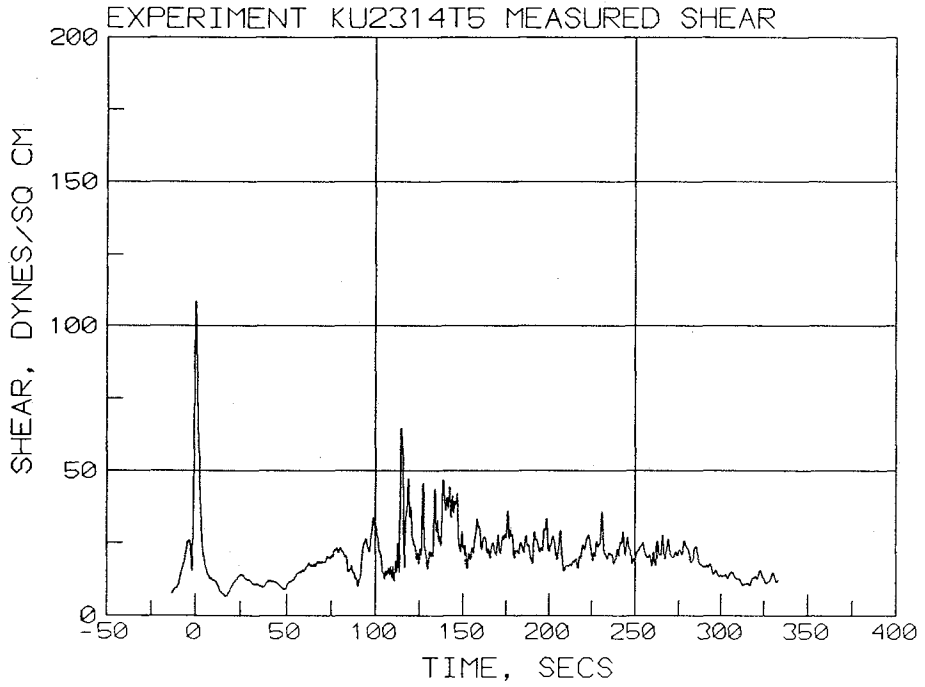
EXPERIMENT KU2314T5 MEASURED SHEAR
SHEAR, DYNES/SQ CM
200
150
100
50
0
-50
0
50
100
150
200
250
300
350
400
TIME, SECS

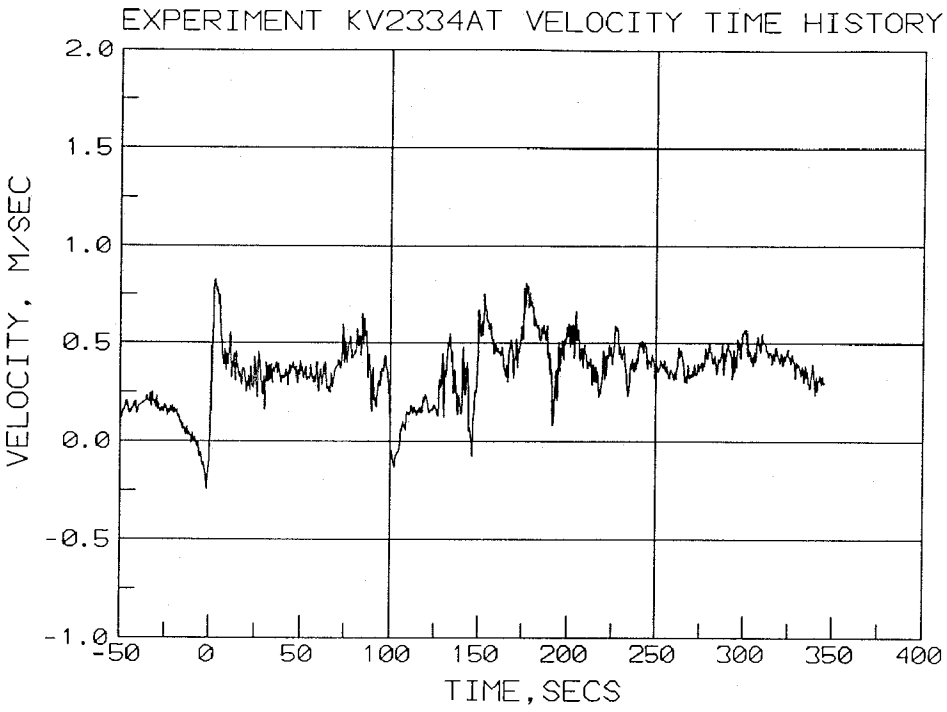
EXPERIMENT KV2334AT VELOCITY TIME HISTORY
VELOCITY, M/SEC
2.0
1.5
1.0
0.5
0.0
-0.5
-1.0
-50
0
50
100
150
200
250
300
350
400
TIME, SECS

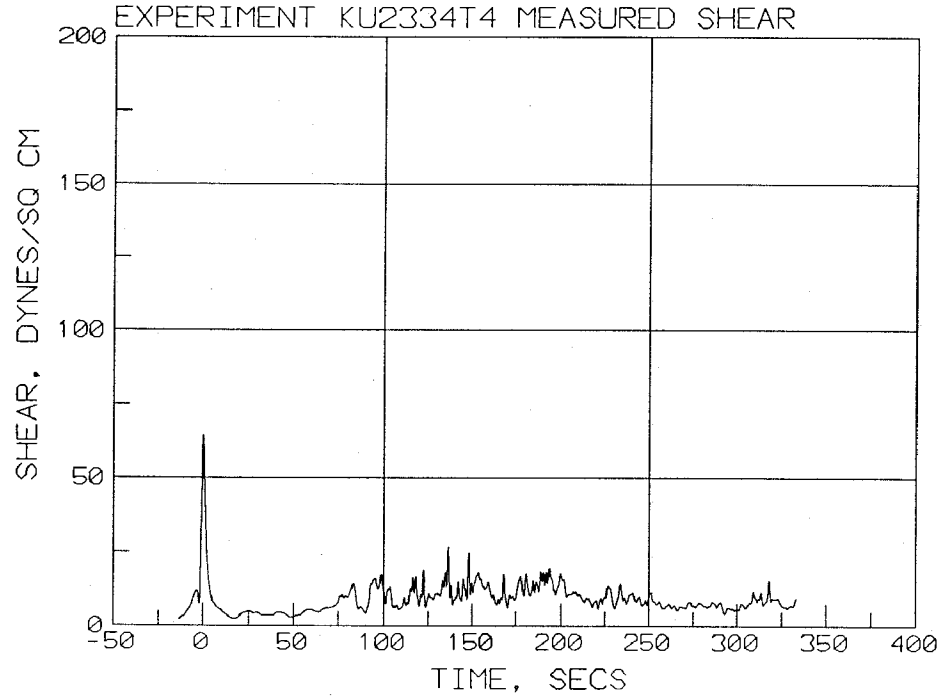
EXPERIMENT KU2334T4 MEASURED SHEAR
SHEAR, DYNES/SQ CM
200
150
100
50
0
-50
0
50
100
150
200
250
300
350
400
TIME, SECS

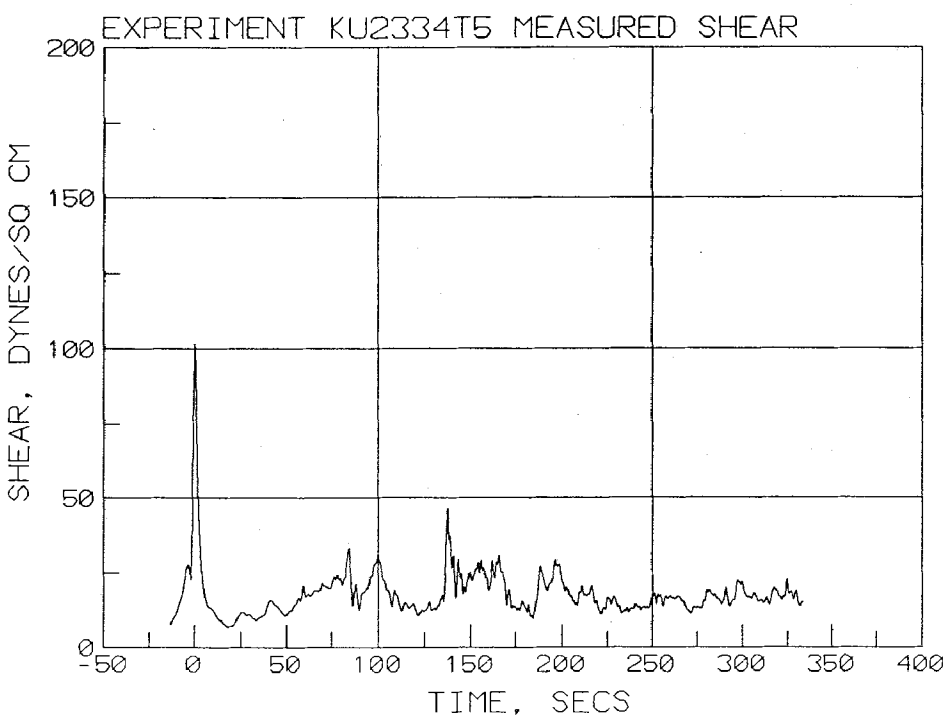
EXPERIMENT KU2334T5 MEASURED SHEAR
SHEAR, DYNES/SQ CM
200
150
100
50
0
-50
0
50
100
150
200
250
300
350
400
TIME, SECS

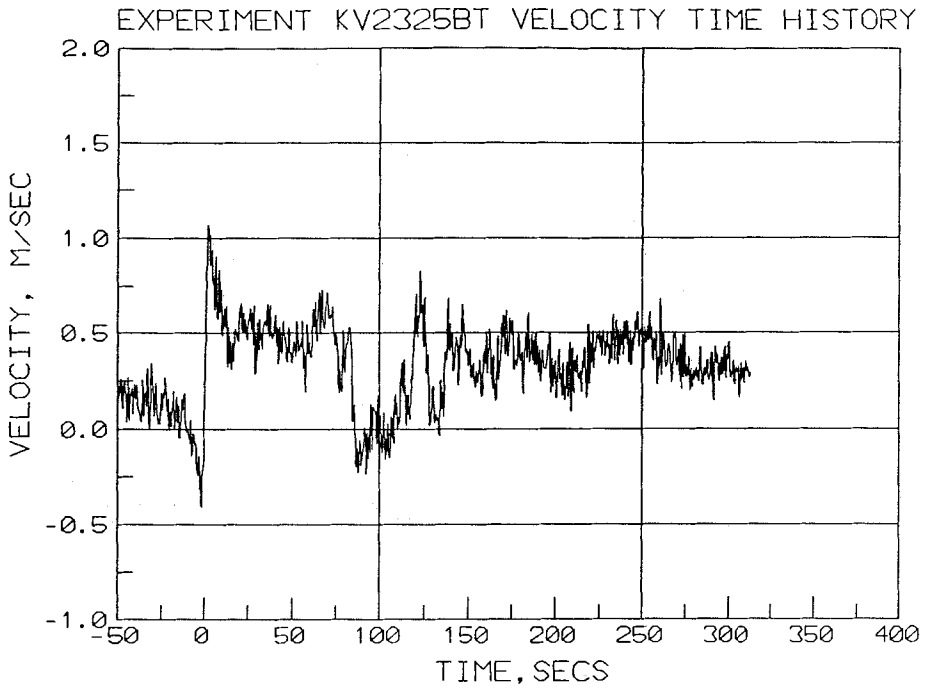
EXPERIMENT KV2325BT VELOCITY TIME HISTORY
VELOCITY, M/SEC
2.0
1.5
1.0
0.5
0.0
-0.5
-1.0
-50
0
50
100
150
200
250
300
350
400
TIME, SECS

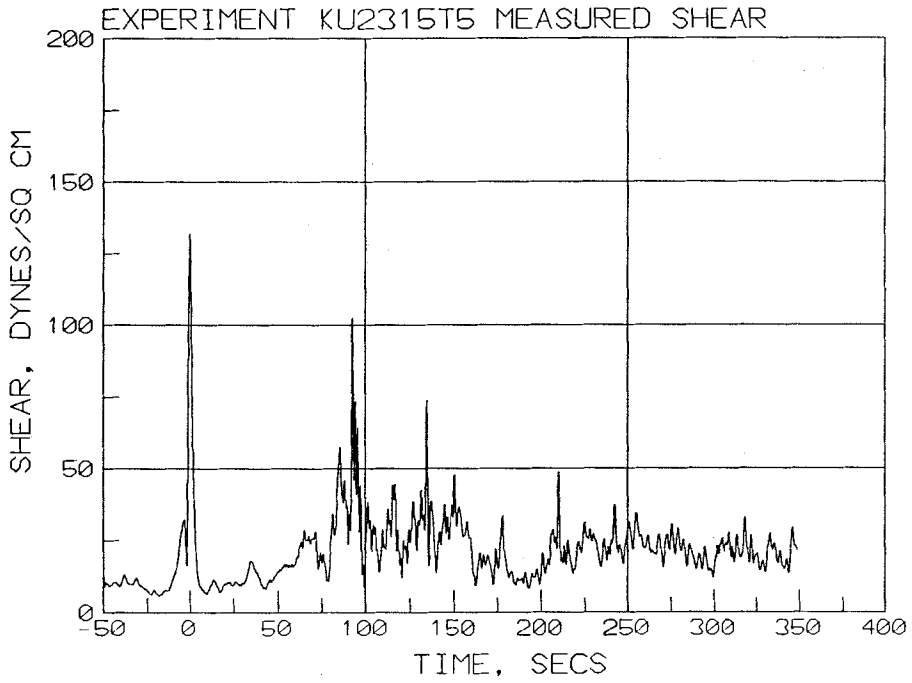
EXPERIMENT KU2315T5 MEASURED SHEAR
SHEAR, DYNES/SQ CM
200
150
100
50
0
-50
0
50
100
150
200
250
300
350
400
TIME, SECS

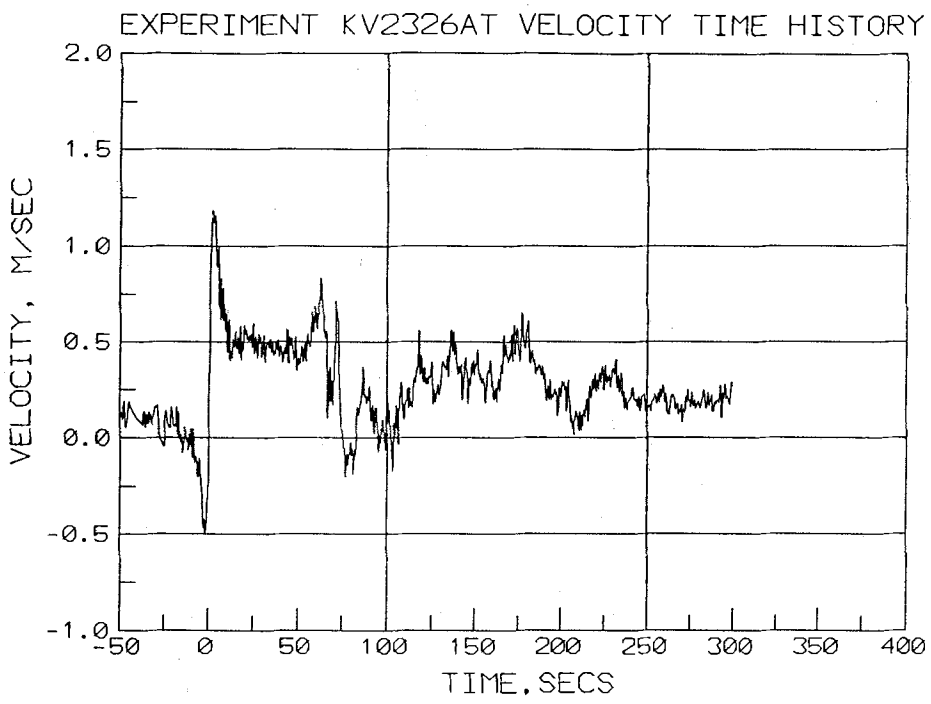
EXPERIMENT KV2326AT VELOCITY TIME HISTORY
VELOCITY, M/SEC
2.0
1.5
1.0
0.5
0.0
-0.5
-1.0
-50
0
50
100
150
200
250
300
350
400
TIME, SECS

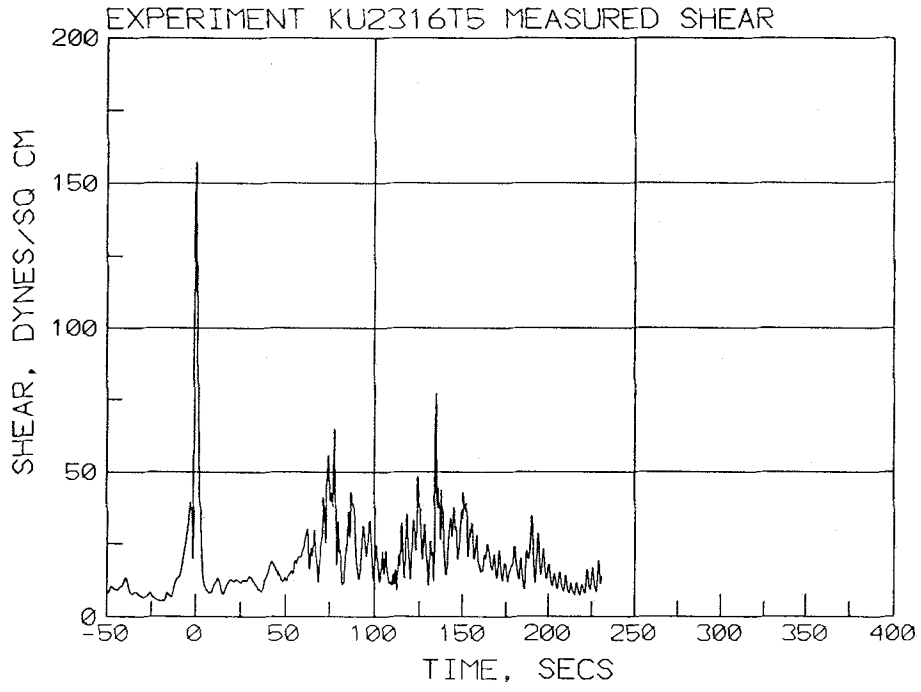
EXPERIMENT KU2316T5 MEASURED SHEAR
SHEAR, DYNES/SQ CM
200
150
100
50
0
-50
0
50
100
150
200
250
300
350
400
TIME, SECS

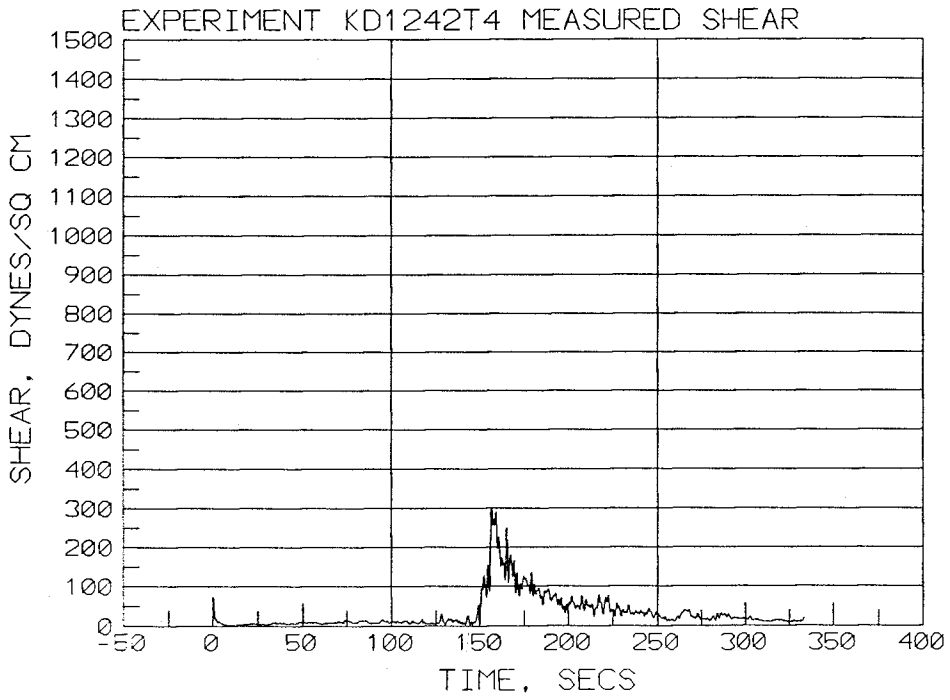
EXPERIMENT KD1242T4 MEASURED SHEAR
SHEAR, DYNES/SQ CM
1500
1400
1300
1200
1100
1000
900
800
700
600
500
400
300
200
100
0
-50
0
50
100
150
200
250
300
350
400
TIME, SECS

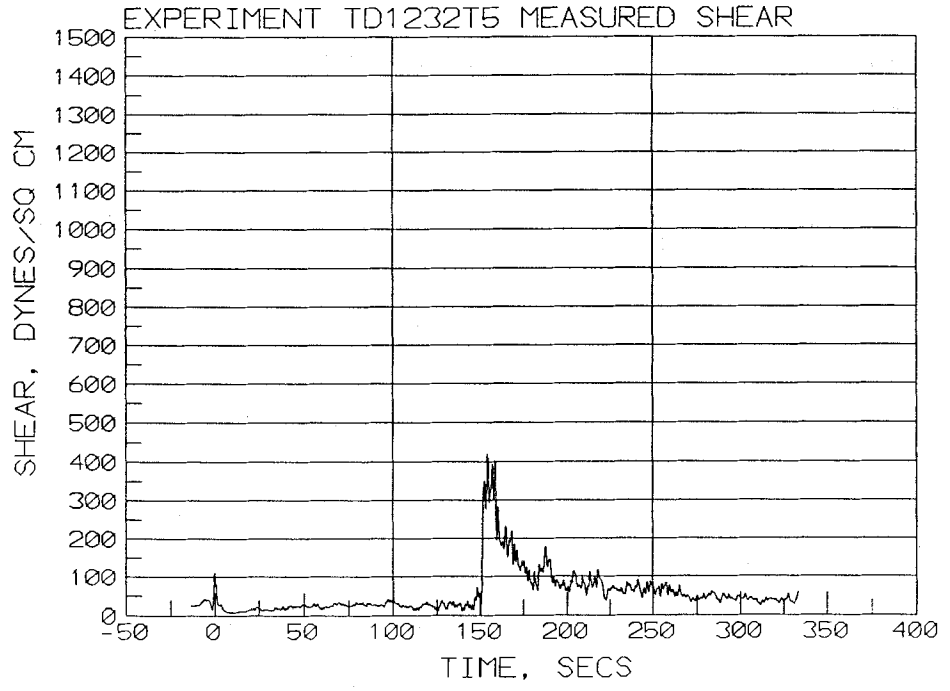
EXPERIMENT TD1232T5 MEASURED SHEAR
SHEAR, DYNES/SQ CM
1500
1400
1300
1200
1100
1000
900
800
700
600
500
400
300
200
100
0
-50
0
50
100
150
200
250
300
350
400
TIME, SECS

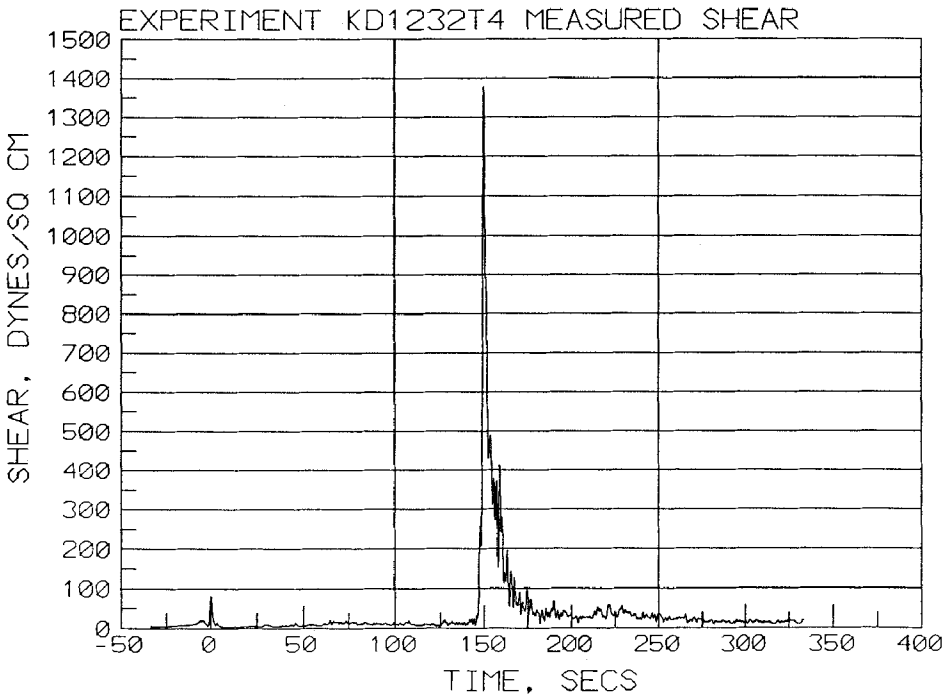
EXPERIMENT KD1232T4 MEASURED SHEAR
SHEAR, DYNES/SQ CM
1500
1400
1300
1200
1100
1000
900
800
700
600
500
400
300
200
100
0
-50
0
50
100
150
200
250
300
350
400
TIME, SECS

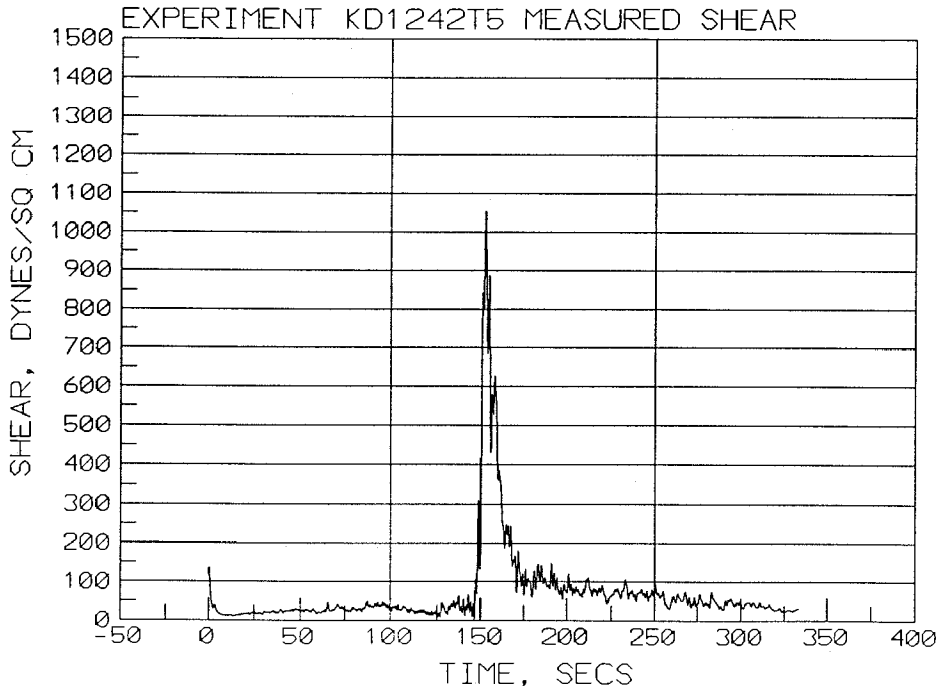
EXPERIMENT KD1242T5 MEASURED SHEAR
SHEAR, DYNES/SQ CM
1500
1400
1300
1200
1100
1000
900
800
700
600
500
400
300
200
100
0
-50
0
50
100
150
200
250
300
350
400
TIME, SECS

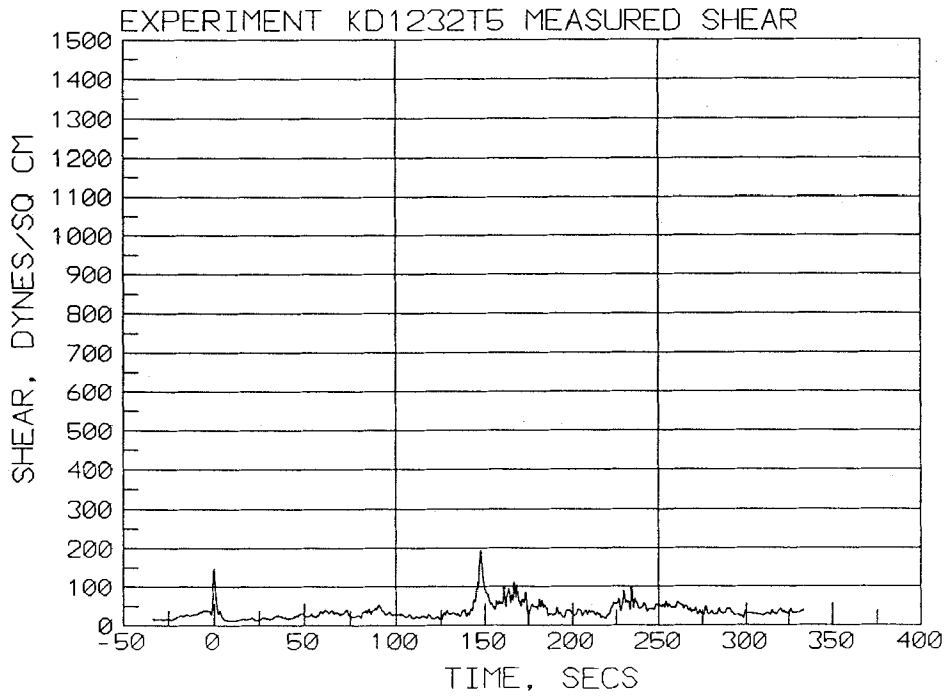
EXPERIMENT KD1232T5 MEASURED SHEAR
SHEAR, DYNES/SQ CM
1500
1400
1300
1200
1100
1000
900
800
700
600
500
400
300
200
100
0
-50
0
50
100
150
200
250
300
350
400
TIME, SECS

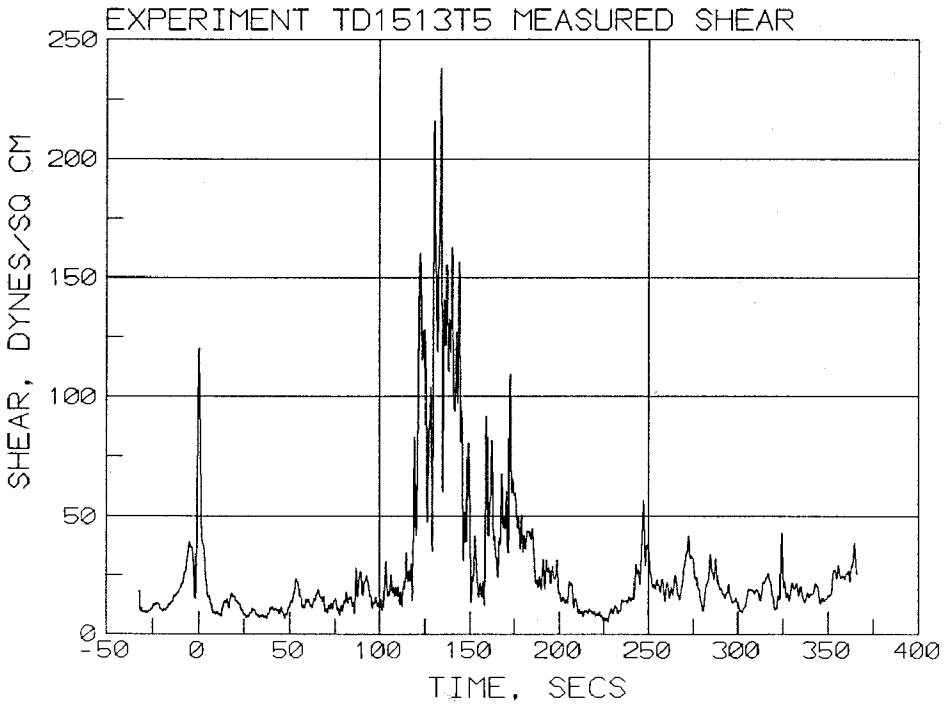
EXPERIMENT TD1513T5 MEASURED SHEAR
SHEAR, DYNES/SQ CM
250
200
150
100
50
0
-50
0
50
100
150
200
250
300
350
400
TIME, SECS

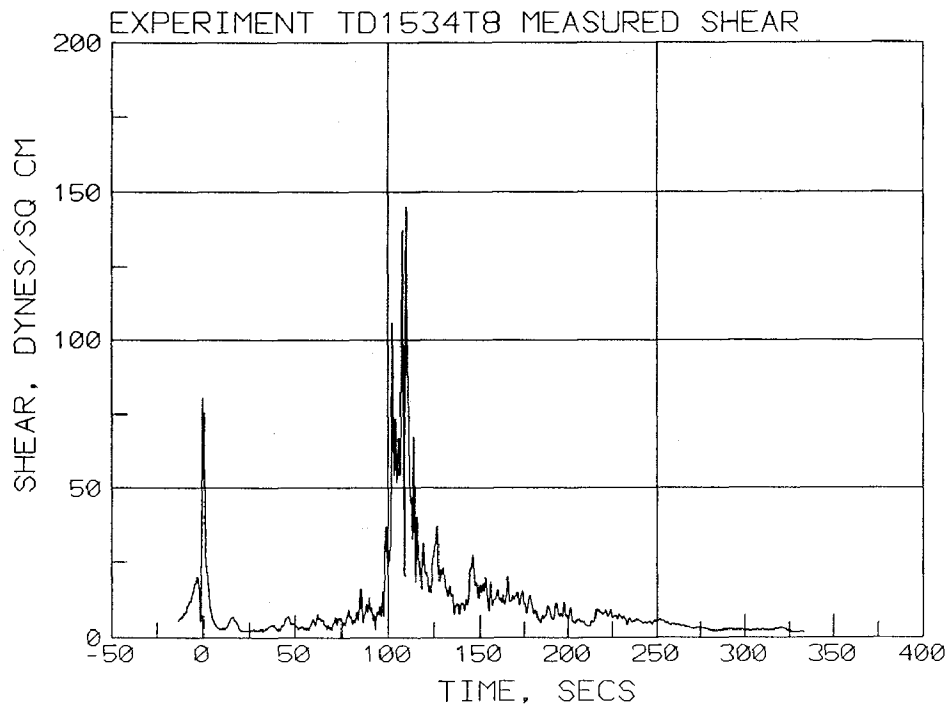
EXPERIMENT TD1534T8 MEASURED SHEAR
SHEAR, DYNES/SQ CM
200
150
100
50
0
-50
0
50
100
150
200
250
300
350
400
TIME, SECS

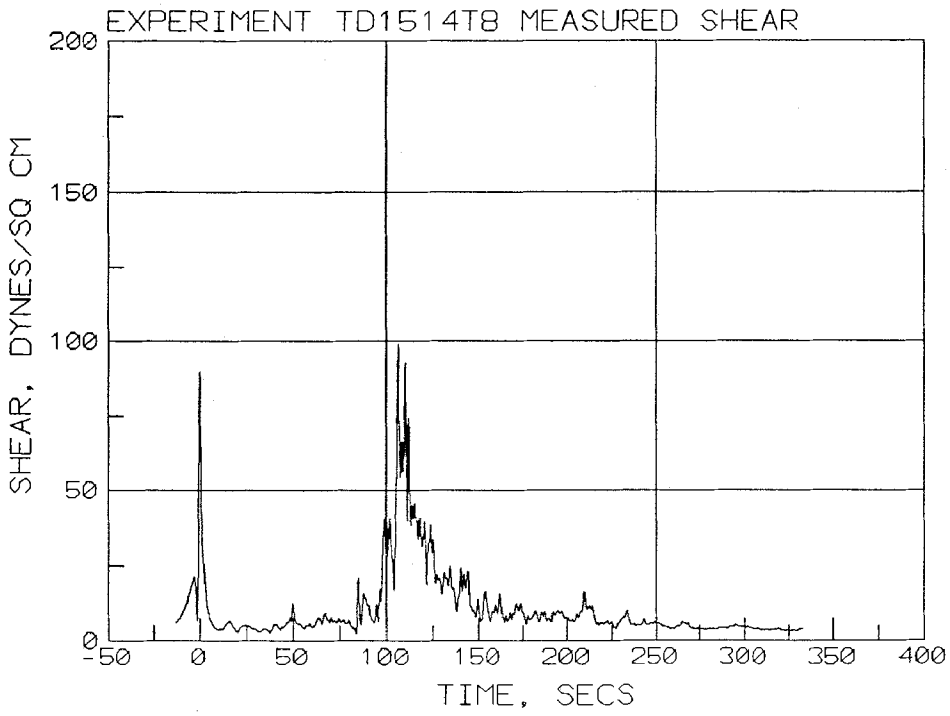
EXPERIMENT TD1514T8 MEASURED SHEAR
SHEAR, DYNES/SQ CM
200
150
100
50
0
-50
0
50
100
150
200
250
300
350
400
TIME, SECS

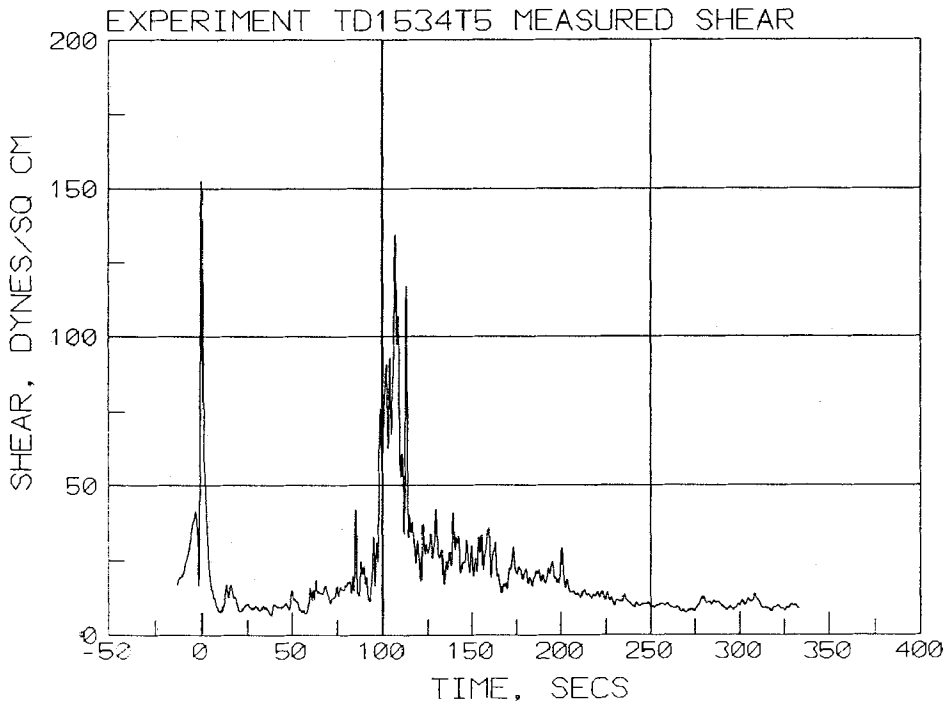
EXPERIMENT TD1534T5 MEASURED SHEAR
SHEAR, DYNES/SQ CM
200
150
100
50
0
-52
0
50
100
150
200
250
300
350
400
TIME, SECS

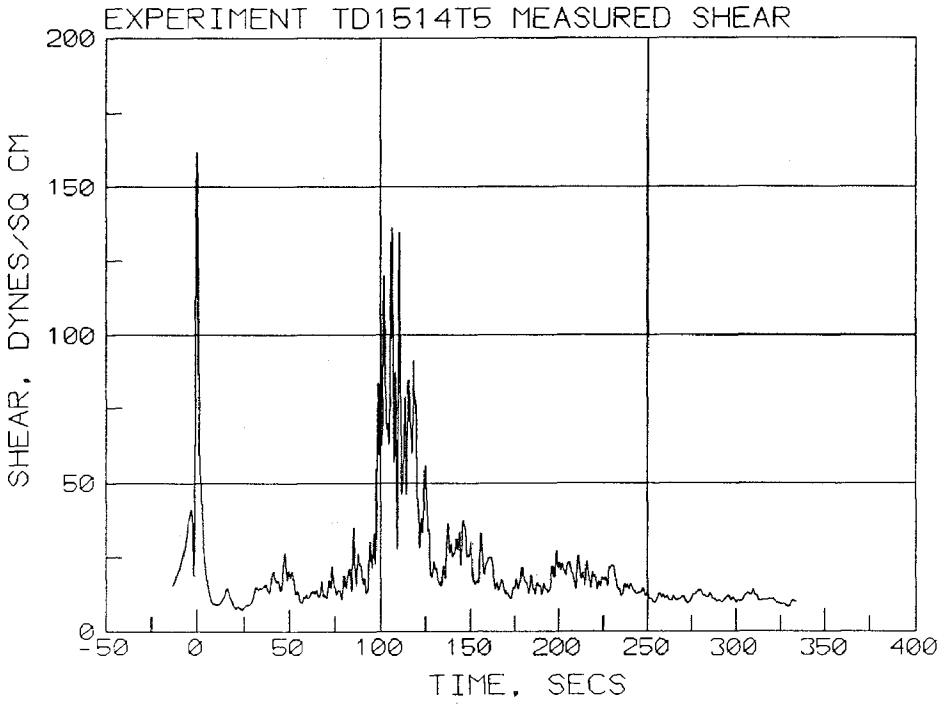
EXPERIMENT TD1514T5 MEASURED SHEAR
SHEAR, DYNES/SQ CM
200
150
100
50
0
-50
0
50
100
150
200
250
300
350
400
TIME, SECS

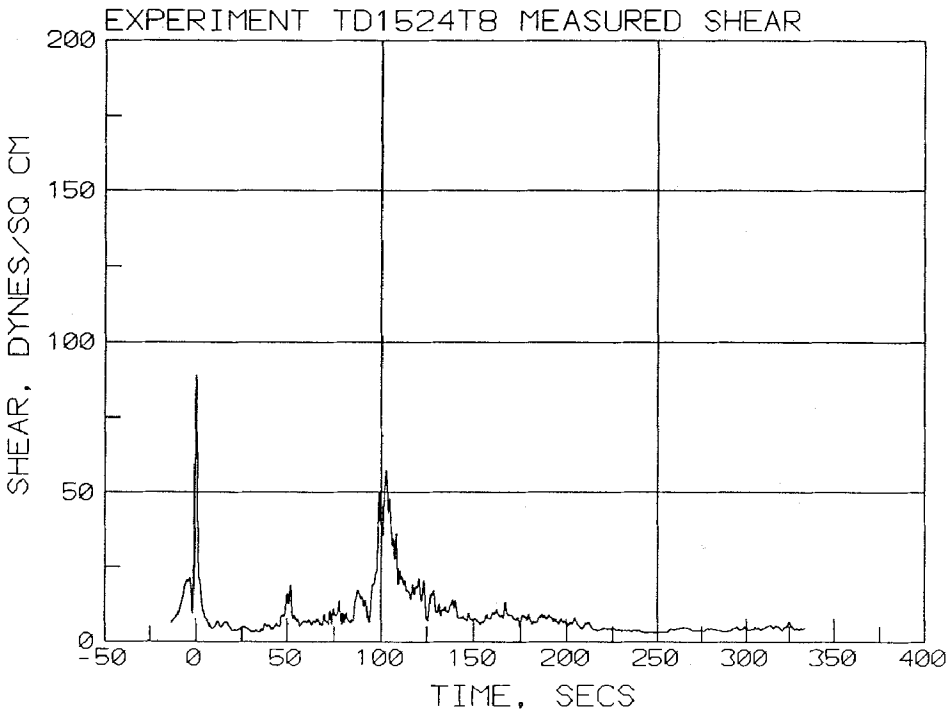
EXPERIMENT TD1524T8 MEASURED SHEAR
SHEAR, DYNES/SQ CM
200
150
100
50
0
-50
0
50
100
150
200
250
300
350
400
TIME, SECS

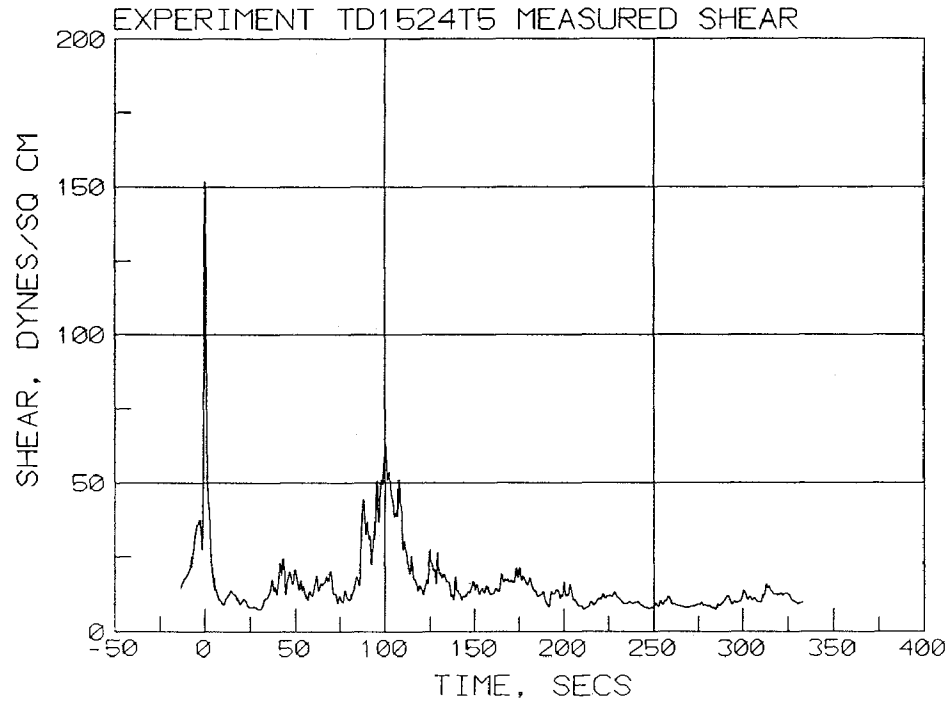
EXPERIMENT TD1524T5 MEASURED SHEAR
SHEAR, DYNES/SQ CM
200
150
100
50
0
-50
0
50
100
150
200
250
300
350
400
TIME, SECS

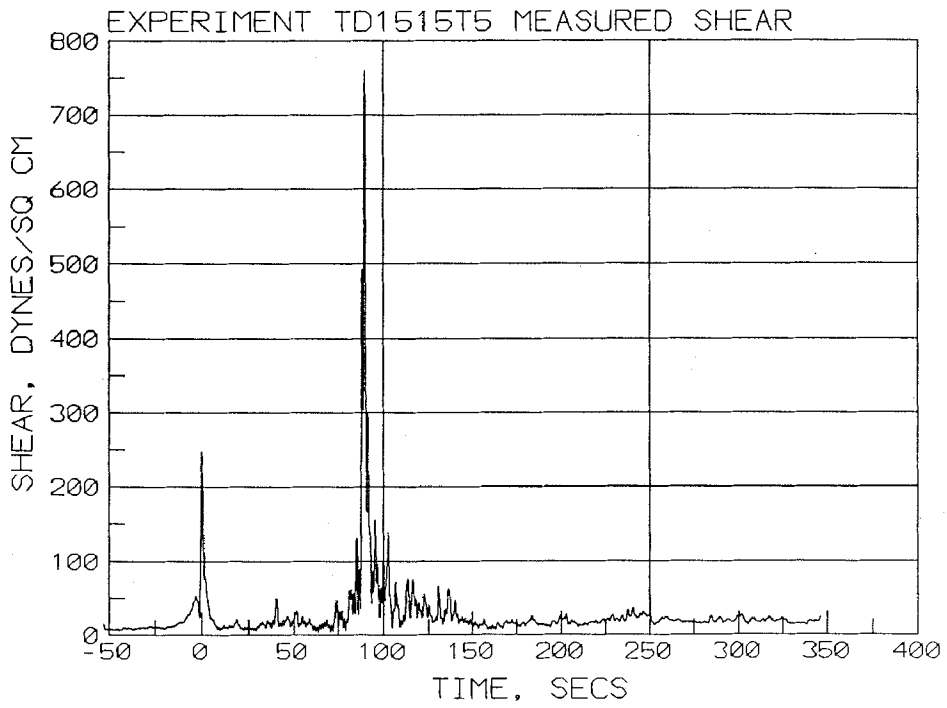
EXPERIMENT TD1515T5 MEASURED SHEAR
SHEAR, DYNES/SQ CM
800
700
600
500
400
300
200
100
0
-50
0
50
100
150
200
250
300
350
400
TIME, SECS

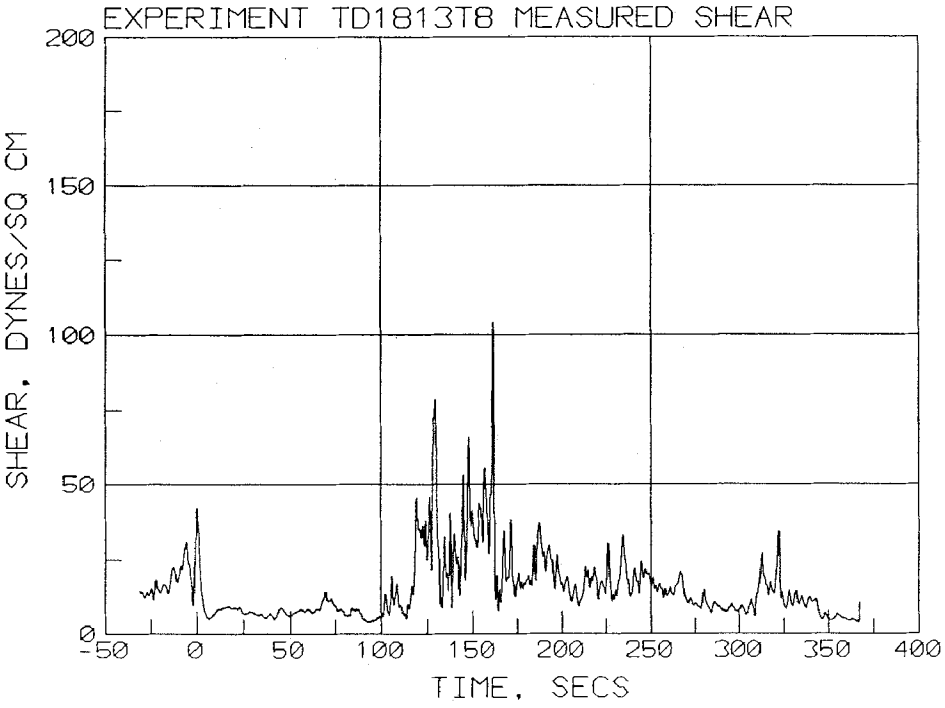
EXPERIMENT TD1813T8 MEASURED SHEAR
SHEAR, DYNES/SQ CM
200
150
100
50
0
-50
0
50
100
150
200
250
300
350
400
TIME, SECS

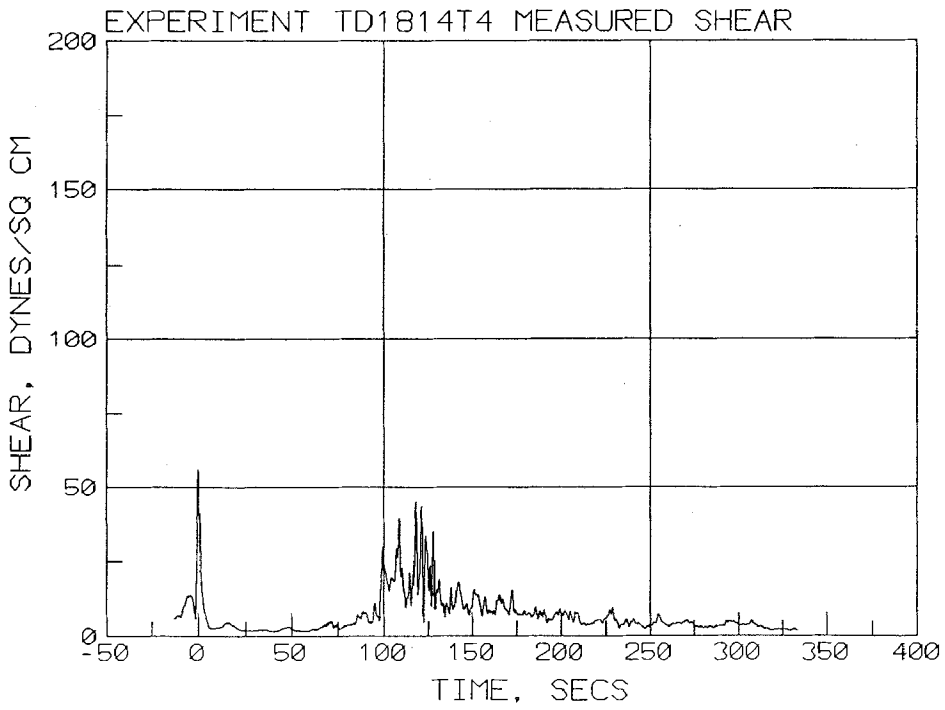
EXPERIMENT TD1814T4 MEASURED SHEAR
SHEAR, DYNES/SQ CM
200
150
100
50
0
-50
0
50
100
150
200
250
300
350
400
TIME, SECS

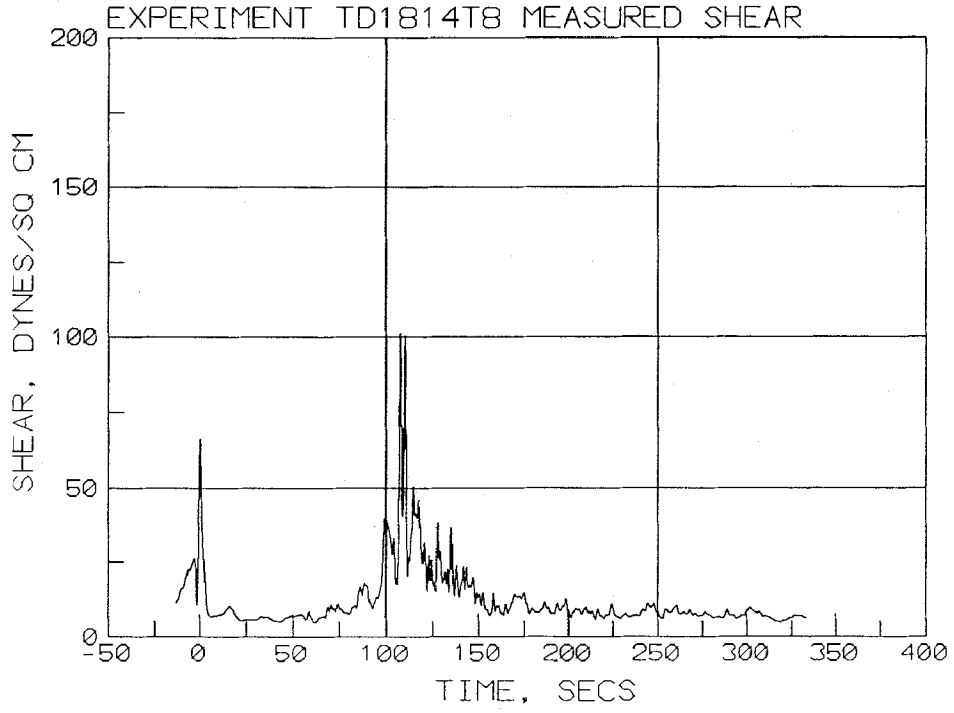
EXPERIMENT TD1814T8 MEASURED SHEAR
SHEAR, DYNES/SQ CM
200
150
100
50
0
-50
0
50
100
150
200
250
300
350
400
TIME, SECS

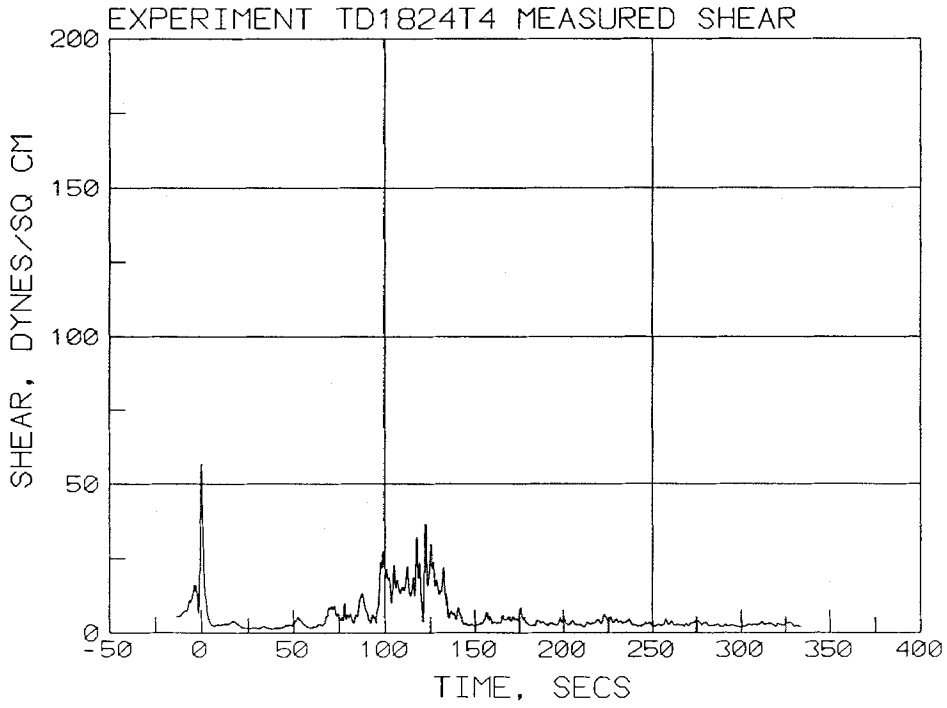
EXPERIMENT TD1824T4 MEASURED SHEAR
SHEAR, DYNES/SQ CM
200
150
100
50
0
-50
0
50
100
150
200
250
300
350
400
TIME, SECS

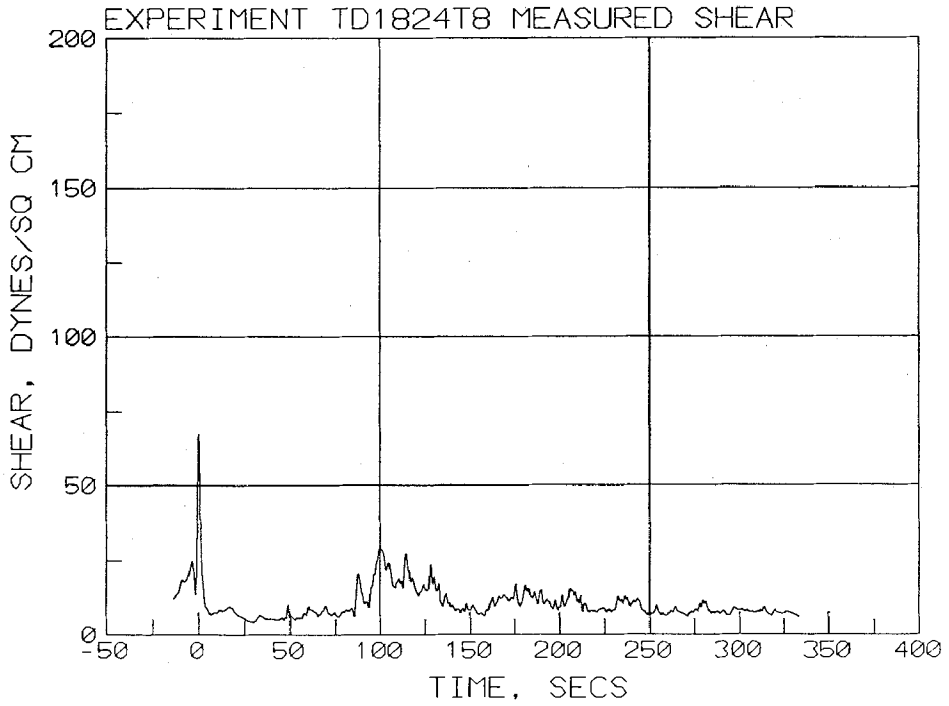
EXPERIMENT TD1824T8 MEASURED SHEAR
SHEAR, DYNES/SQ CM
200
150
100
50
0
-50
0
50
100
150
200
250
300
350
400
TIME, SECS

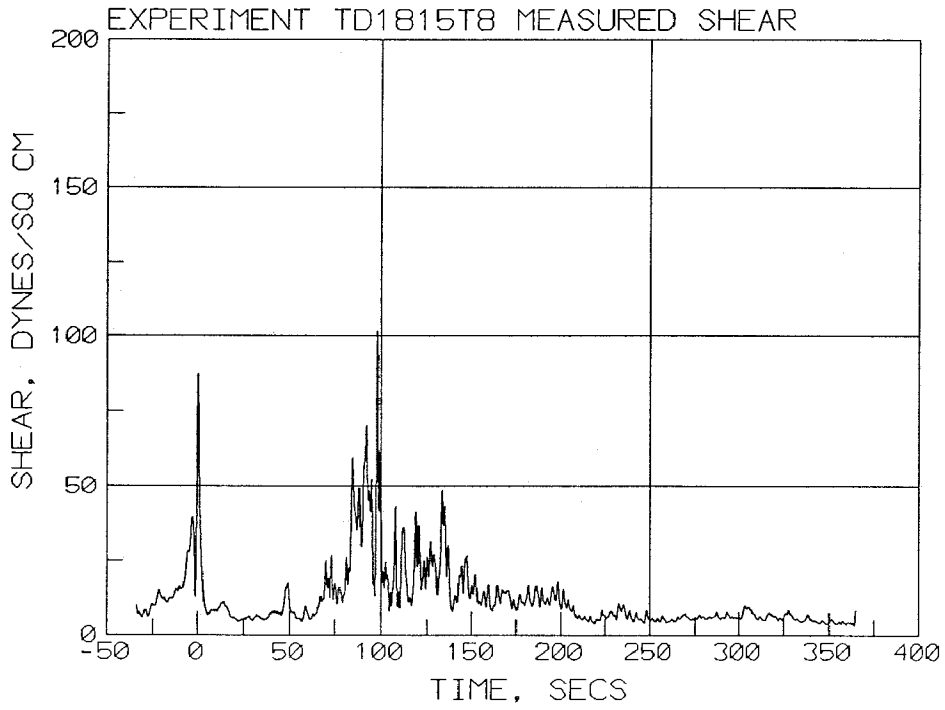
EXPERIMENT TD1815T8 MEASURED SHEAR
SHEAR, DYNES/SQ CM
200
150
100
50
0
-50
0
50
100
150
200
250
300
350
400
TIME, SECS

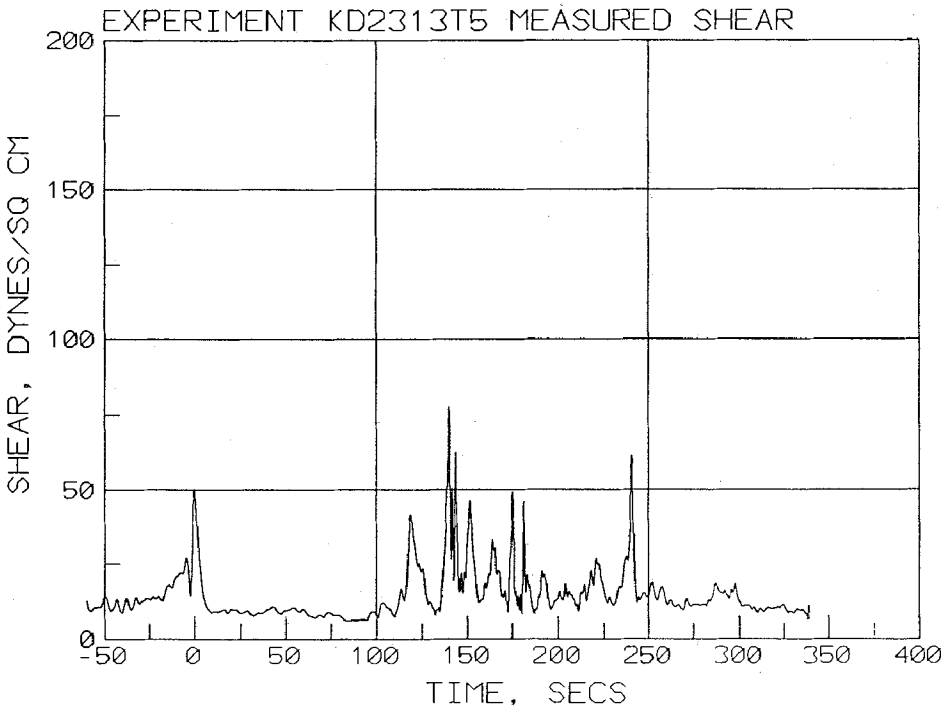
EXPERIMENT KD2313T5 MEASURED SHEAR
SHEAR, DYNES/SQ CM
200
150
100
50
0
-50
0
50
100
150
200
250
300
350
400
TIME, SECS

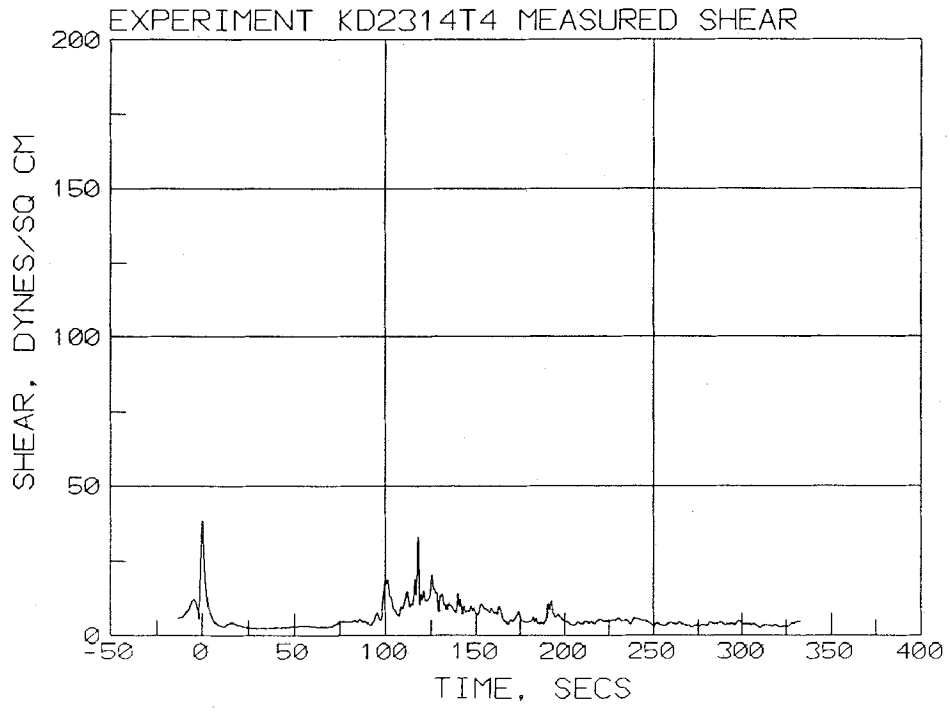
EXPERIMENT KD2314T4 MEASURED SHEAR
SHEAR, DYNES/SQ CM
200
150
100
50
0
-50
0
50
100
150
200
250
300
350
400
TIME, SECS

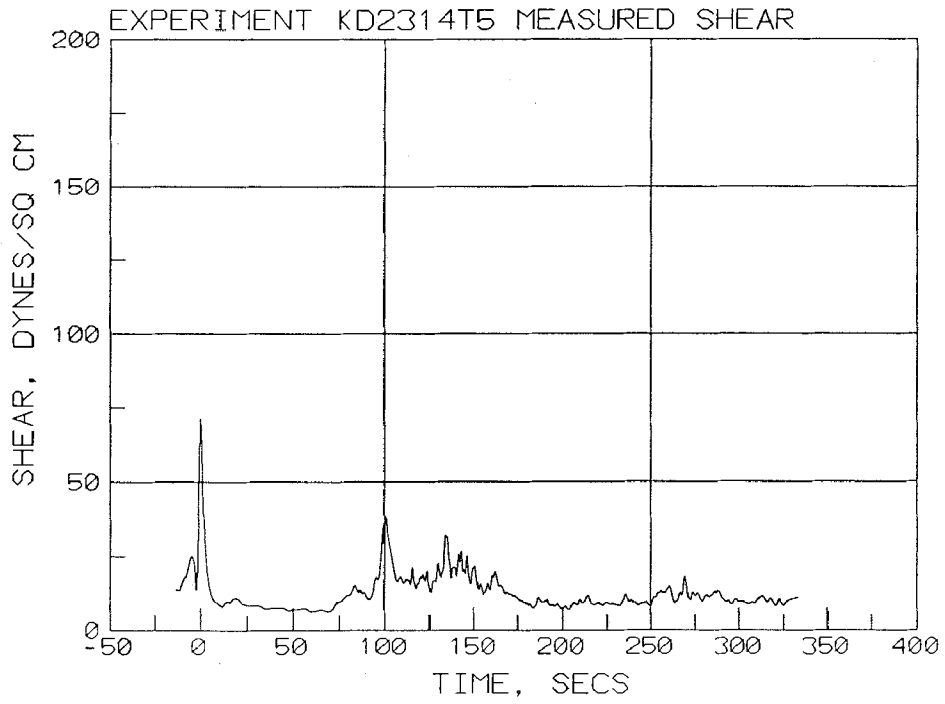
EXPERIMENT KD2314T5 MEASURED SHEAR
SHEAR, DYNES/SQ CM
200
150
100
50
0
-50
0
50
100
150
200
250
300
350
400
TIME, SECS

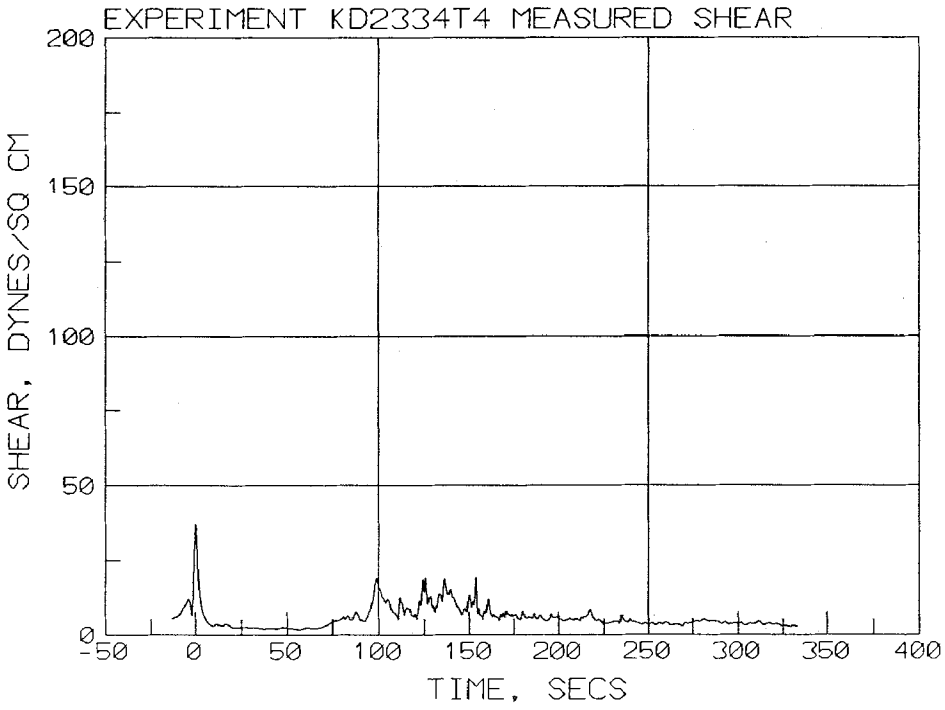
EXPERIMENT KD2334T4 MEASURED SHEAR
SHEAR, DYNES/SQ CM
200
150
100
50
0
-50
0
50
100
150
200
250
300
350
400
TIME, SECS

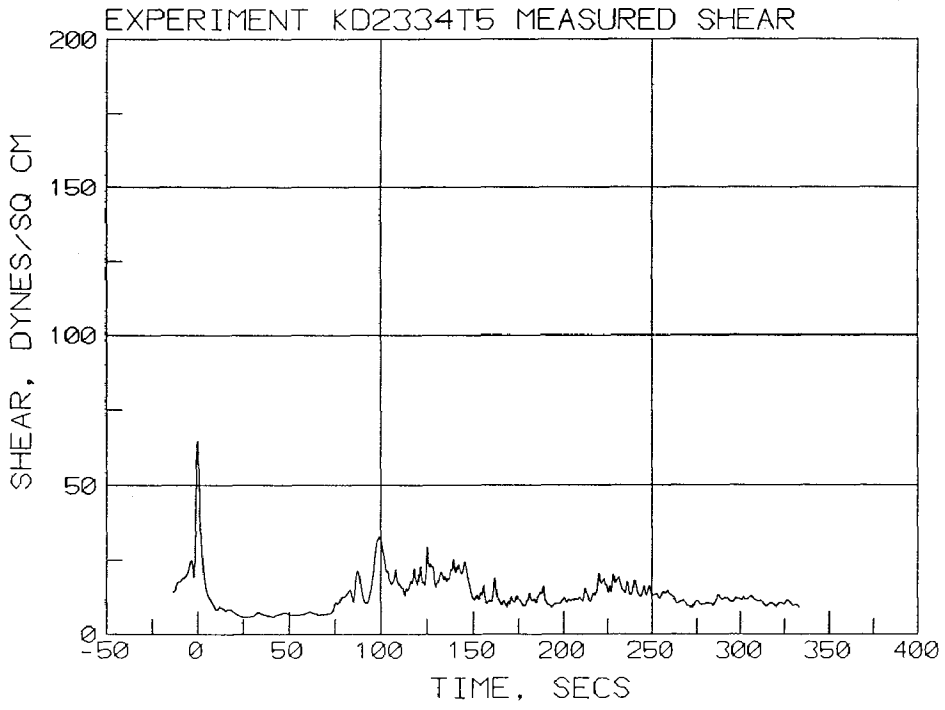
EXPERIMENT KD2334T5 MEASURED SHEAR
SHEAR, DYNES/SQ CM
200
150
100
50
0
-50
0
50
100
150
200
250
300
350
400
TIME, SECS

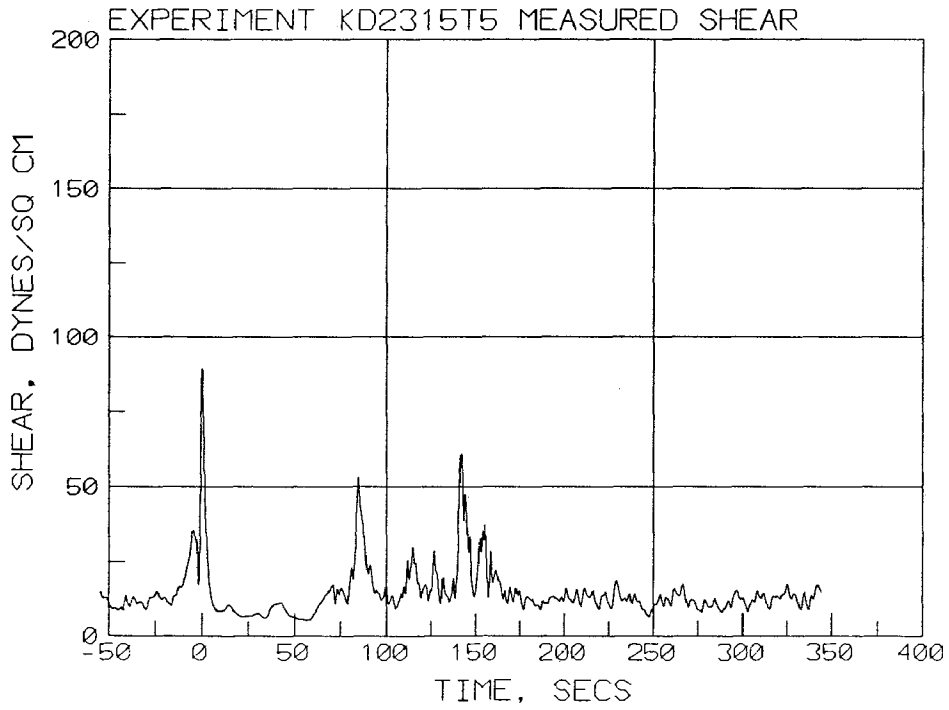
EXPERIMENT KD2315T5 MEASURED SHEAR
SHEAR, DYNES/SQ CM
200
150
100
50
0
-50
0
50
100
150
200
250
300
350
400
TIME, SECS

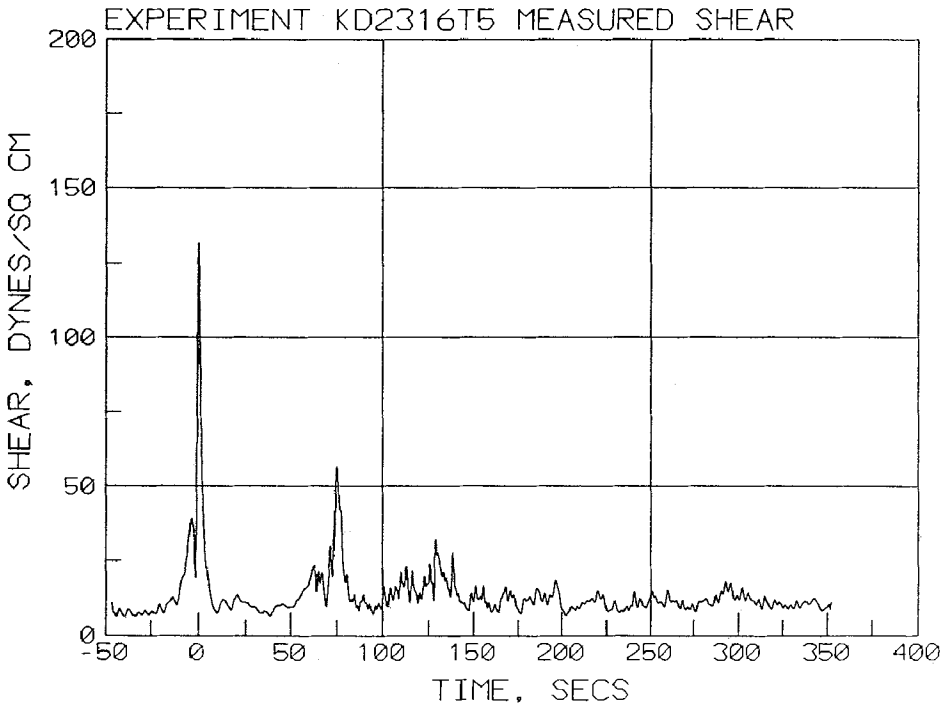
EXPERIMENT KD2316T5 MEASURED SHEAR
SHEAR, DYNES/SQ CM
200
150
100
50
0
-50
0
50
100
150
200
250
300
350
400
TIME, SECS

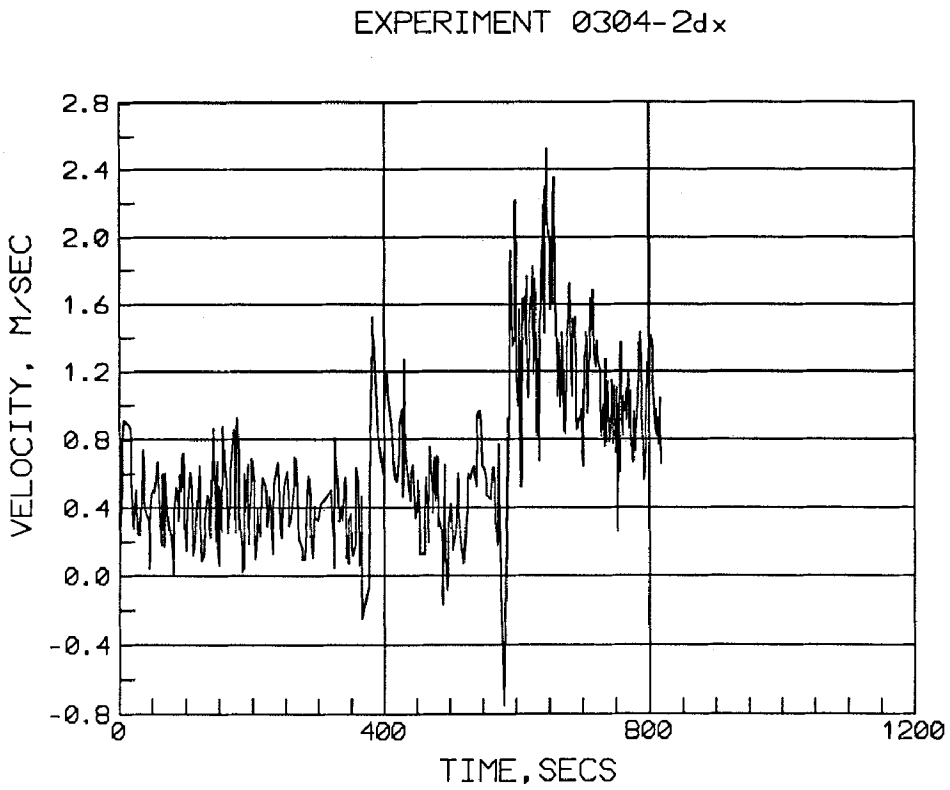
EXPERIMENT 0304-2dx
VELOCITY, M/SEC
2.8
2.4
2.0
1.6
1.2
0.8
0.4
0.0
-0.4
-0.8
0
400
800
1200
TIME, SECS

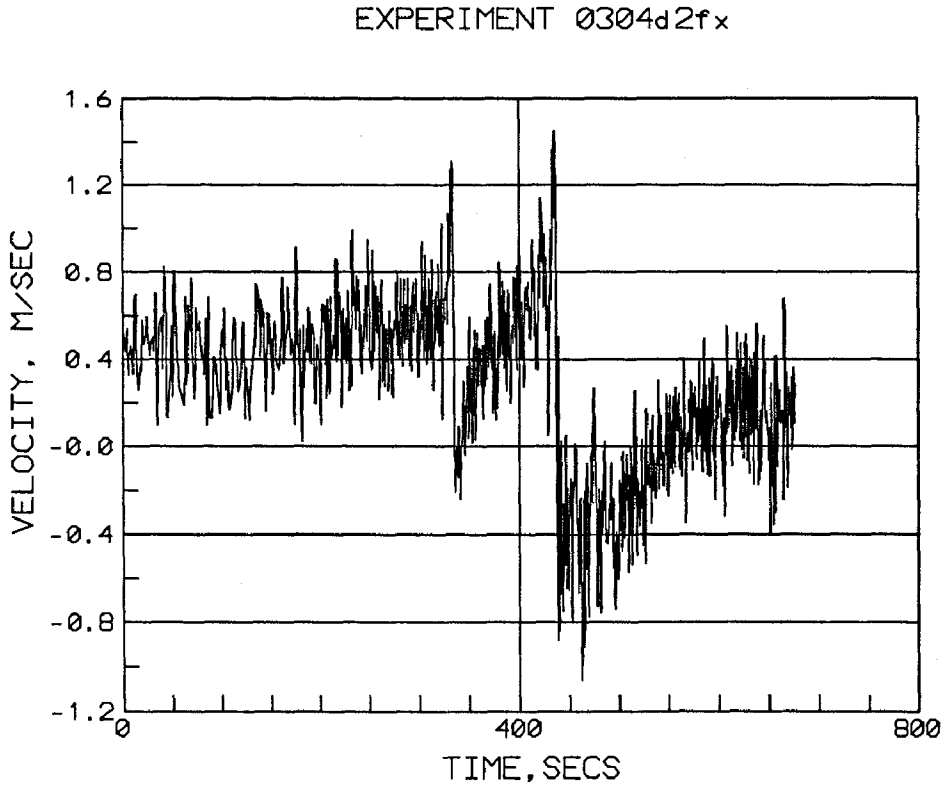
EXPERIMENT 0304d2fx
VELOCITY, M/SEC
1.6
1.2
0.8
0.4
-0.0
-0.4
-0.8
-1.2
0
400
800
TIME, SECS

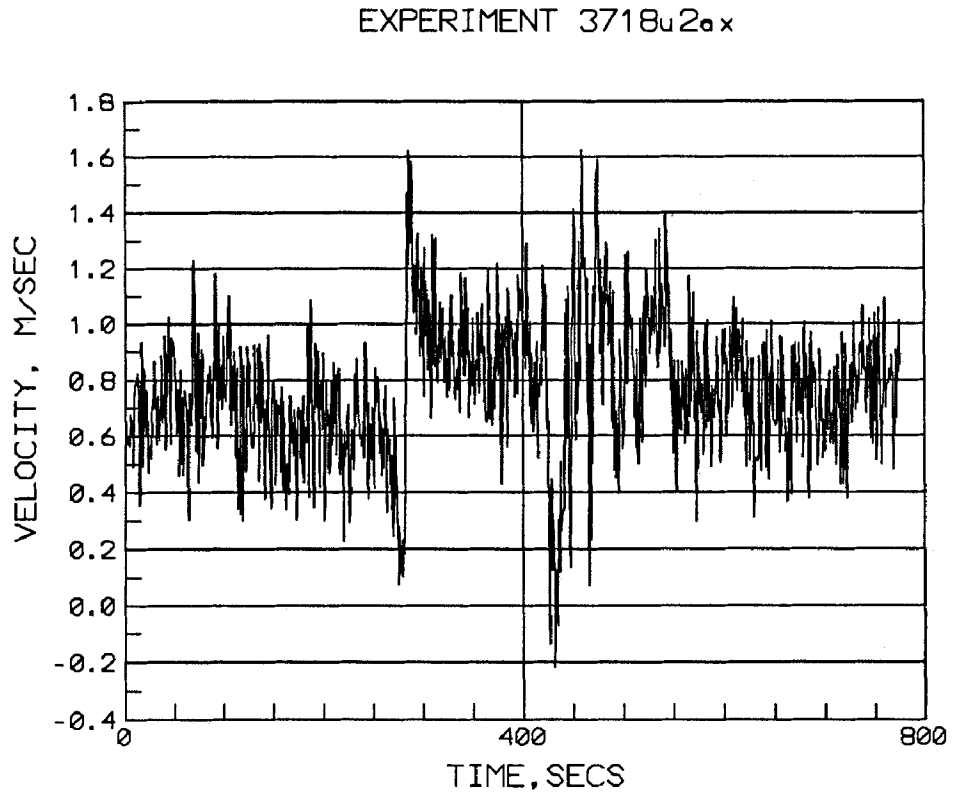
EXPERIMENT 3718u2ax
VELOCITY, M/SEC
1.8
1.6
1.4
1.2
1.0
0.8
0.6
0.4
0.2
0.0
-0.2
-0.4
0
400
800
TIME, SECS

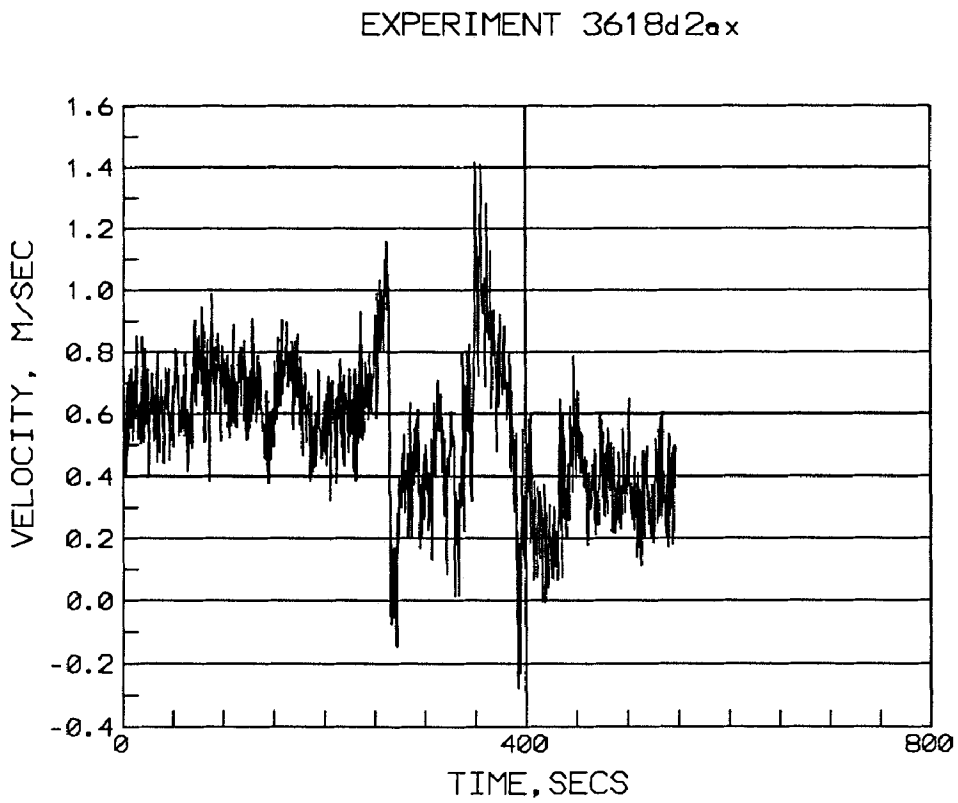
EXPERIMENT 3618d2ax
VELOCITY, M/SEC
1.6
1.4
1.2
1.0
0.8
0.6
0.4
0.2
0.0
-0.2
-0.4
0
400
800
TIME, SECS

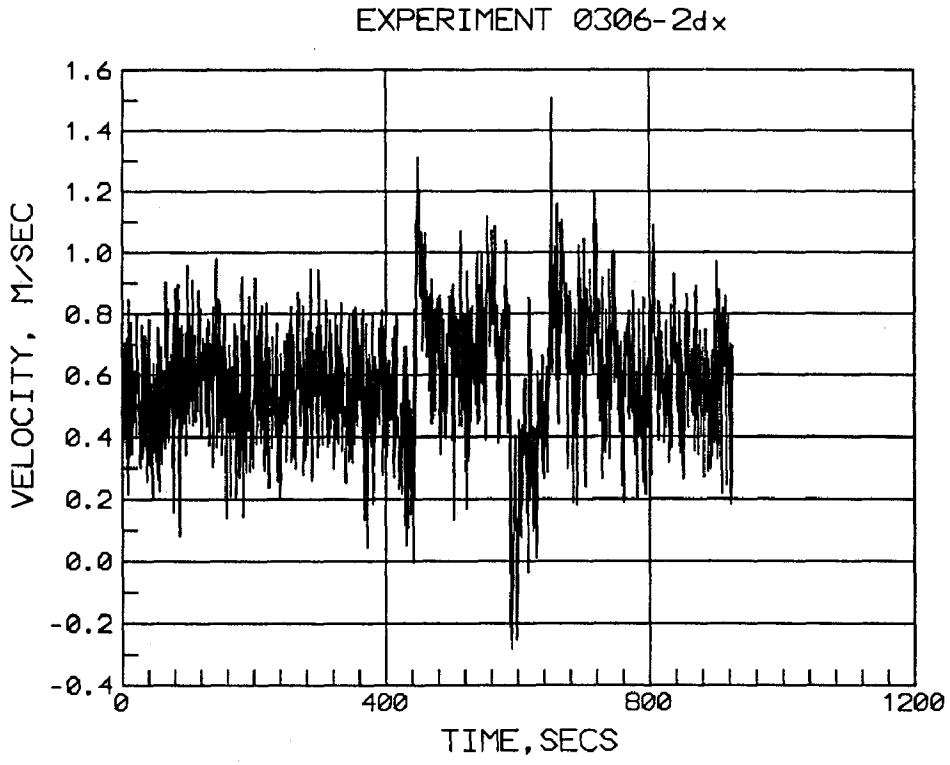
EXPERIMENT 0306-2dx
VELOCITY, M/SEC
1.6
1.4
1.2
1.0
0.8
0.6
0.4
0.2
0.0
-0.2
-0.4
0
400
800
1200
TIME, SECS

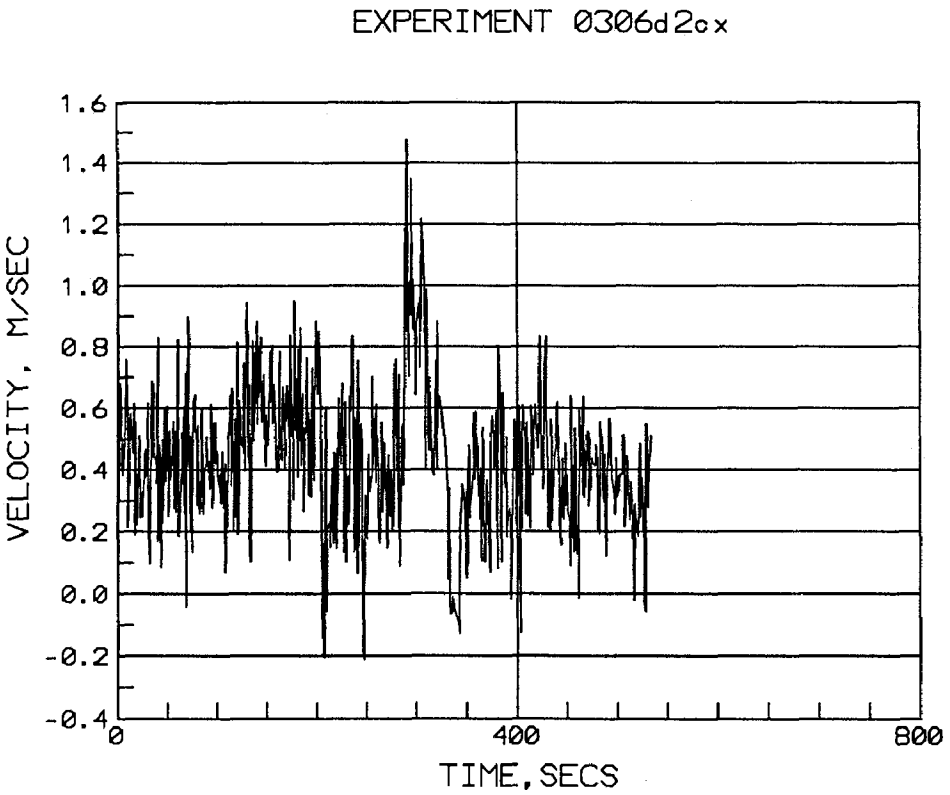
EXPERIMENT 0306d2cx
VELOCITY, M/SEC
1.6
1.4
1.2
1.0
0.8
0.6
0.4
0.2
0.0
-0.2
-0.4
0
400
800
TIME, SECS

Appendix B
PC Program “Prpvel.bas” for Distribution of Near-Bed Velocity Beneath Tow
and
Example Calculations for Open-Wheel and Kort Nozzle Tows

```
'   PROGRAM PRPVEL.BAS -FOR PROPELLOR JET VELOCITIES
    PRINT "based on lot of empiricism FOR PROPELLOR JET VELOCITIES"
    DIM VE(800, 10), XX(800), YY(50), zone(800)
'
    OPEN "\graf\TEMP.DAT" FOR OUTPUT AS #1
    INPUT "ENTER INPUT FILENAME ", INFI$
    OPEN INFI$ FOR INPUT AS #2
'
'   BEGIN INPUT
'
40  INPUT #2, G$ 'METRIC OR ENGLISH UNITS(M OR E)?
    IF G$ = "E" OR G$ = "M" OR G$ = "e" OR G$ = "m" THEN 70
    GOTO 40
70  INPUT #2, KO$ 'ENTER KORT(K) NOZZLE OR OPEN WHEEL(O)
    IF KO$ = "k" THEN KO$ = "K"
    IF KO$ = "o" THEN KO$ = "O"
    INPUT #2, DP 'PROPELLOR DIAMETER?
    INPUT #2, VG   ' ENTER vessel speed relative to ground
    INPUT #2, VA   ' enter ambient velocity
    INPUT #2, VDIRECT' ENTER VESSEL DIRECTION, -1 UP , 1, DOWN
    INPUT #2, VRET ' ENTER RETURN VELOCITY
    VRETURN = -1 * VDIRECT * VRET
    VG = VG * VDIRECT
    INPUT #2, B    ' ENTER TOTAL WIDTH OF BARGES
    INPUT #2, D    ' ENTER TOTAL DRAFT OF BARGES
    INPUT #2, LBARGES' ENTER TOTAL LENGHT OF BARGES
    INPUT #2, TBL  ' ENTER LENGTH OF TOWBOAT(52 M OR 170.6 FT)
    INPUT #2, PSPACE' DISTANCE BETWEEN PROPELLORS (19.7 FT OR 6 M)?
    INPUT #2, SETBACK' DISTANCE FROM PROP TO TOWBOAT STERN(16.4 FT OR 5 M)
    INPUT #2, THRUST' ENTER THRUST FROM BOTH PROPELLERS
'   THRUST IN LBS OR NEWTONS WHERE 1 LB = 4.448 NEWTONs
    THRUST = THRUST / 2 ' CONVERTS TO THRUST PER PROPELLER
'
'
    INPUT #2, dep' DEPTH OF FLOW AT POINT OF INTEREST?
'
'   SET HP = DEPTH MINUS 1/2 PROP DIAMETER
    HP = dep - DP / 2
'
'   VELOCITY PREDICTION AT 1.5 FT ABOVE CHANNEL BOTTOM TO AGREE WITH
'   MEASUREMENTS
    IF G$ = "E" THEN velloc = 1.5
    IF G$ = "M" THEN velloc = .46
```

```
    INPUT #2, VABOTT' AMBIENT VELOCITY 1.5-FT(0.46 M) ABOVE BOTTOM?
    BC = dep - D  ' BOTTOM CLEARANCE USED IN WAKE FLOW COMPUTATIONS
'   X IS MEASURED FROM BOW OF BARGES
'
    XBEGIN = 285    ' X BEGINNING POINT IF IN FEET
    XSPACE = 3.125  ' X SPACING IF IN FEET
    NUMX = 800
    ' X BEGIN AND SPACE IF IN METRIC
    IF G$ = "M" OR G$ = "m" THEN XBEGIN = -60
    IF G$ = "M" OR G$ = "m" THEN XSPACE = 1.905
'   Y IS MEASURED LATERALLY FROM CENTER OF TOWBOAT
'
    y = 0
    YSPACE = 9.85
    NUMY = 7
    IF G$ = "M" OR G$ = "m" THEN YSPACE = 3
'   ********************************************
'   MISCELLANEOUS INPUT
'   ********************************************
    RPS = rpm / 60
    grav = 32.16
    RHO = 1.94
    LUNIT$ = "FEET"
    VUNIT$ = "FEET/SEC"
    IF G$ = "M" THEN grav = 9.805
    IF G$ = "M" THEN LUNIT$ = "METERS"
    IF G$ = "M" THEN VUNIT$ = "METERS/SEC"
    IF G$ = "M" THEN RHO = 999.8
    IF KO$ = "K" THEN GOTO 150
'   THIS SECTION FOR SETTING OPEN WHEEL PARAMETERS
    D0 = .71 * DP
    E = .43
    CPARA = .12 * (DP / HP) ^ .66666
    CEXP = .66
    CDECAY = .34
    P1DECAY = .93
    P2DECAY = .24
    CFUNC = .5
    GOTO 190
150 ' THIS SECTION FOR SETTING KORT NOZZLE PARAMETERS
    D0 = DP
    E = .58
    CPARA = .04
```

```
    CEXP = .85
    CDECAY = .34
    P1DECAY = .93
    P2DECAY = .24
    CFUNC = .25
190 ' END OF KORT VERSUS OPEN
'
'
'   end input
'
    FOR JJ = 1 TO 10
    FOR KK = 1 TO 800
    VE(KK, JJ) = 0
    NEXT KK
    NEXT JJ
'
'
'   COMPUTE VELOCITY EXITING PROPELLER
'
'   ***********************************************
    V0 = 1.13 / D0 * (THRUST / RHO) ^ .5
    U2 = V0
    IF U2 = 0 THEN U2 = .00001
    PRINT "U2 = ", U2
'
'   BEGIN ITERATION LOOP FOR X AND Y
'
    FOR J = 1 TO NUMY
    X = XBEGIN  ' x = 0 at bow of barges
    FOR I = 1 TO NUMX
'
'   begin computations at BOW
'
    VBDMAX = (VA - VG) * .79 * (dep / D) ^ -1.21
    VBOWMAX = -.7 * VBDMAX
    VBOWX = 0
'   SKIP BOW IF -10D<X<15D OR OUTSIDE EDGE OF BARGES
    IF y > B / 2 THEN GOTO 200
    IF X < -10 * D THEN GOTO 200
    IF X >= 15 * D THEN GOTO 200
'
    VBOWX = X * VBOWMAX / (10 * D) + VBOWMAX
    IF X <= 0 THEN GOTO 200
```

```
    VBOWX = X * (VBDMAX - VBOWMAX) / (5 * D) + VBOWMAX
    IF X <= 5 * D THEN GOTO 200
    VBOWX = -X * VBDMAX / (10 * D) + 15 * VBDMAX / 10
200  ' end bow
'
'   SET LIMITS FOR RETURN VELOCITY
'
    VRET = VRETURN
    IF X < 15 * D THEN VRET = 0
    IF X > LBARGES THEN VRET = 0
'
'   compute wake velocity
'
    vwakamax = -1 * (VA - VG) * .78 * (D / dep) ^ 1.81
    VWAKEgx = 0
    IF X - LBARGES > TBL THEN GOTO 300
    coef = X - LBARGES
    IF coef < 0 THEN coef = 0
    IF y > B / 2 THEN coef = 0
    VWAKEgx = vwakamax * coef / TBL + VABOTT
    GOTO 400
300  temp1 = (1 + .0075 * (TBL / D) - .0075 * (X - LBARGES) / D)
    IF temp1 < 0 THEN temp1 = 0
    IF y > B / 2 THEN temp1 = 0
    VWAKEgx = vwakamax * temp1 + VABOTT
'
'    END WAKE VEL
'
400 'BEGIN PROPELLOR JET VELOCITY
'
    xprop = X - LBARGES - TBL + SETBACK  ' x relative to props
    vxrprop = 0
    XSTTOWB = X - LBARGES - TBL ' x relative to stern of towboat
    IF xprop < 0 THEN GOTO 700         ' GOES TO END OF PROPELLER
'
'   COMPUTE VELOCITY IN ZONE 1 WHICH IS TWO JETS ADDED TOGETHER
'
'
'   DECAY MAX JET VELOCITY USING SINGLE JET EQUATION
'
    XCALC = xprop
    IF xprop < 2.03 * DP THEN XCALC = 2.03 * DP
    VXMAX = U2 * 1.45 * (XCALC / DP) ^ -.524
```

```
    IF VXMAX > U2 THEN VXMAX = U2
'
'   COMPUTE LOCATION OF PARABOLIC JET OFF RUDDER
'
'   CJ IS THE LOCATION OF THE CENTER OF THE JET RELATIVE TO SHAFT
    CJTEMP = CPARA * grav * (xprop - SETBACK / 2) ^ 2 / U2 ^ 2 / .957
    cj = -(.2126 * (xprop - SETBACK / 2) - CJTEMP)
    zzb = HP + cj - velloc ' ZZB IS LOCATION OF CENTER OF JET RELATIVE TO VELLOC
    IF xprop < SETBACK / 2 THEN zzb = HP - velloc 'THIS IS BEFORE JET DEFLECTED
    IF xprop < SETBACK / 2 THEN GOTO 600         ' OFF OF THE RUDDER
    IF xprop / DP > 10 THEN GOTO 500 '    THIS DEFINES END OF ZONE 1
    IF zzb > dep - velloc THEN GOTO 645 ' transition between zone 1 & 2
600  YL = y + PSPACE / 2
    YR = y - PSPACE / 2
    RL = SQR(YL ^ 2 + (zzb) ^ 2)
    RR = SQR(YR ^ 2 + (zzb) ^ 2)
    CPZ1 = .18
    C1 = 1
    VXRL = VXMAX * EXP(-(RL) ^ 2 / (2 * (CPZ1 * C1) ^ 2 * (xprop) ^ 2))
    VXRR = VXMAX * EXP(-(RR) ^ 2 / (2 * (CPZ1 * C1) ^ 2 * (xprop) ^ 2))
    vxrprop = VXRR + VXRL
    VMAXTEST = E * (DP / HP) * U2
    IF vxrprop > VMAXTEST THEN vxrprop = VMAXTEST
    lastz1 = vxrprop
    zone(I) = 1
'
'
'
    GOTO 700  ' THIS SKIPS ZONE 2 CALC BECAUSE STILL IN ZONE 1
'
645  ' this is transition from zone 1 to 2
    vxrprop = lastz1
    GOTO 700
'   COMPUTE VELOCITY IN ZONE 2
'
500  RPROP2 = y
'
'   COMPUTE MAX PROP VEL IN ZONE 2
'
    VXMAX = U2 * CEXP * 2.7183 ^ (-.0178 * xprop / DP)
'
'   COMPUTE LATERAL DISTRIBUTION OF MAXIMUM WHICH IS AT SURFACE
'
```

```
    CPZ2 = .84 * (xprop / DP) ^ -.62
    vxrprop = VXMAX * EXP(-(RPROP2) ^ 2 / (2 * (CPZ2) ^ 2 * (xprop) ^ 2))
'
'   COMPUTE  DECAY FROM SURFACE TO BOTTOM
'
    K11 = CDECAY * (DP / HP) ^ P1DECAY * (xprop / DP) ^ P2DECAY
    IF K11 > .95 THEN K11 = .95
    vxrprop = vxrprop * K11
    zone(I) = 2
'
'   SUM OF VPROP, VWAKE, VSHIP, VAMBIENT
'
700  IF y > B / 2 THEN vxrprop = 0
    FUNC = 1 - CFUNC * ABS((VA - VG) / U2) * (HP / DP) ^ 1.5
    IF FUNC < 0 THEN FUNC = 0
    VE(I, J) = -1 * VDIRECT * vxrprop * FUNC + VWAKEgx + VBOWX + VRET
'
'
'
     XX(I) = X / ABS(VG)
'    IF J = 1 THEN PRINT #1, XX(I), VE(I, J)
    X = X + XSPACE
    NEXT I
    YY(J) = y
    y = y + YSPACE
    NEXT J
    CLOSE #2
'
'   END ITERATION LOOP ON X AND Y
'
'   ************************************************
    'OUTPUT
'   ************************************************
    PRINT "************************************************"
    PRINT "************************************************"
    PRINT
    PRINT "RESULTANT VELOCITIES BEHIND TOW"
    PRINT "DOWNSTREAM VELOCITIES ARE POSITIVE,UPSTREAM"
    PRINT "VELOCITIES ARE NEGATIVE. FOR SLACKWATER,"
    PRINT "POSITIVE VELOCITY IS OPPOSITE TO TOW DIRECTION"
    PRINT
    PRINT #1, "     Y=", " "
    FOR J = 1 TO NUMY
```

```
    PRINT #1, USING "#####.#"; YY(J);
    NEXT J
    PRINT #1,
    PRINT #1, " X="
    FOR I = 1 TO NUMX
    PRINT #1, USING "####.#"; XX(I);
    PRINT #1, "    ", zone(I);
    FOR J = 1 TO NUMY
    PRINT #1, USING "####.##"; VE(I, J);
    NEXT J
    PRINT #1, " "
    NEXT I
800  CLOSE #1
```

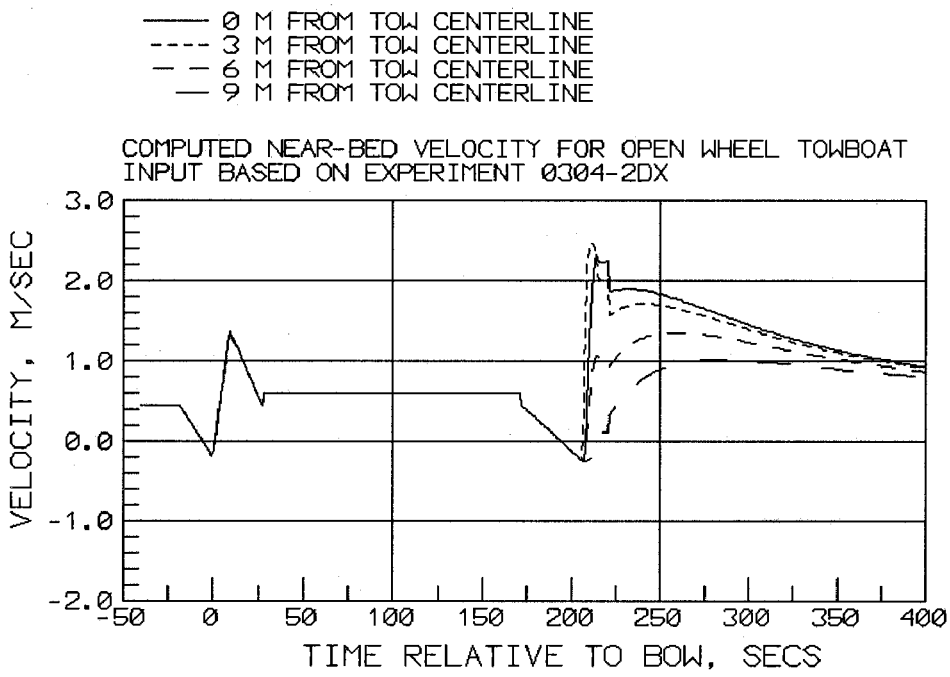
0 M FROM TOW CENTERLINE
3 M FROM TOW CENTERLINE
6 M FROM TOW CENTERLINE
9 M FROM TOW CENTERLINE
COMPUTED NEAR-BED VELOCITY FOR OPEN WHEEL TOWBOAT
INPUT BASED ON EXPERIMENT 0304-2DX
VELOCITY, M/SEC
3.0
2.0
1.0
0.0
-1.0
-2.0
-50
0
50
100
150
200
250
300
350
400
TIME RELATIVE TO BOW, SECS

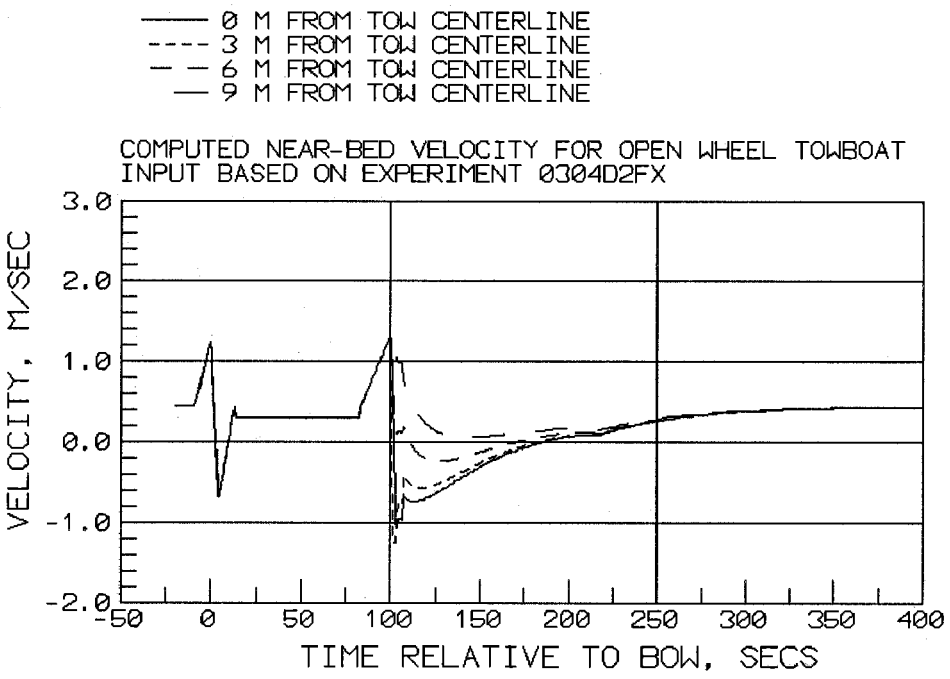
0 M FROM TOW CENTERLINE
3 M FROM TOW CENTERLINE
6 M FROM TOW CENTERLINE
9 M FROM TOW CENTERLINE
COMPUTED NEAR-BED VELOCITY FOR OPEN WHEEL TOWBOAT
INPUT BASED ON EXPERIMENT 0304D2FX
VELOCITY, M/SEC
3.0
2.0
1.0
0.0
-1.0
-2.0
-50
0
50
100
150
200
250
300
350
400
TIME RELATIVE TO BOW, SECS

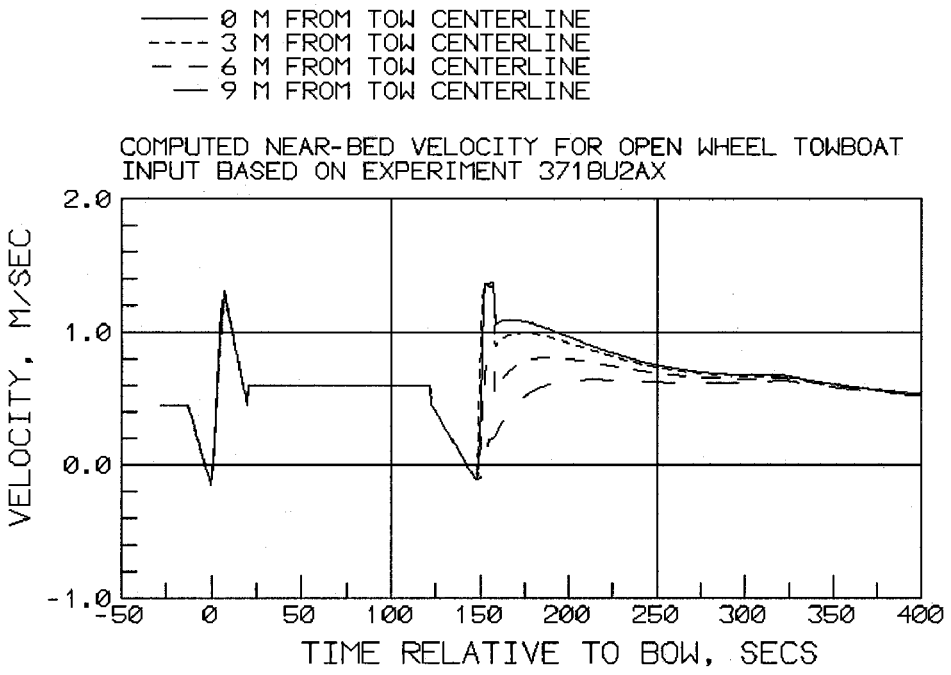
0 M FROM TOW CENTERLINE
3 M FROM TOW CENTERLINE
6 M FROM TOW CENTERLINE
9 M FROM TOW CENTERLINE
COMPUTED NEAR-BED VELOCITY FOR OPEN WHEEL TOWBOAT
INPUT BASED ON EXPERIMENT 371BU2AX
VELOCITY, M/SEC
2.0
1.0
0.0
-1.0
-50
0
50
100
150
200
250
300
350
400
TIME RELATIVE TO BOW, SECS

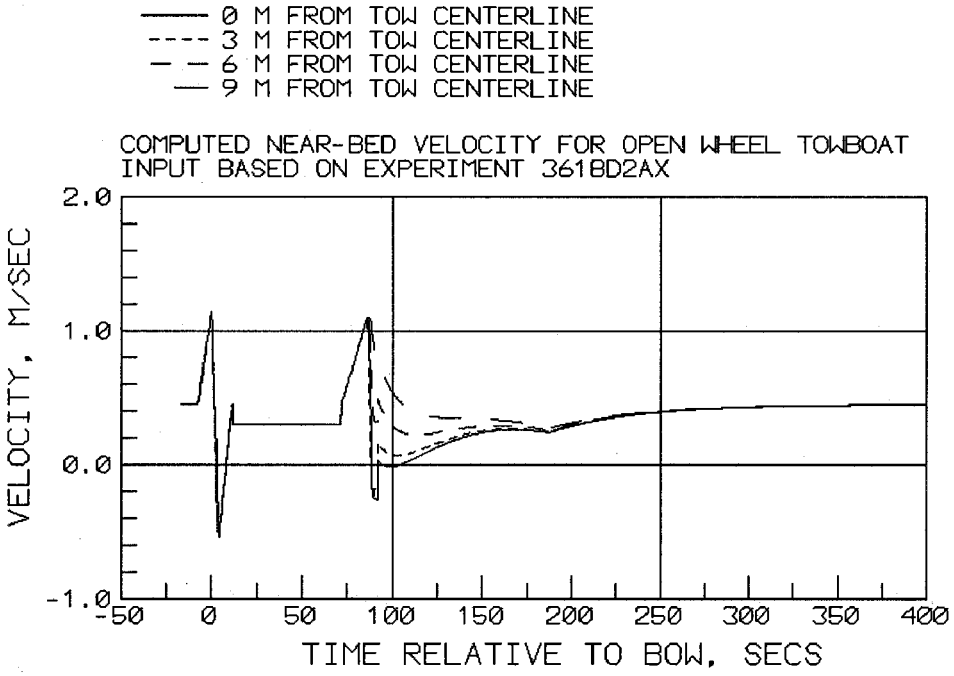
0 M FROM TOW CENTERLINE
3 M FROM TOW CENTERLINE
6 M FROM TOW CENTERLINE
9 M FROM TOW CENTERLINE
COMPUTED NEAR-BED VELOCITY FOR OPEN WHEEL TOWBOAT
INPUT BASED ON EXPERIMENT 361BD2AX
VELOCITY, M/SEC
2.0
1.0
0.0
-1.0
-50
0
50
100
150
200
250
300
350
400
TIME RELATIVE TO BOW, SECS

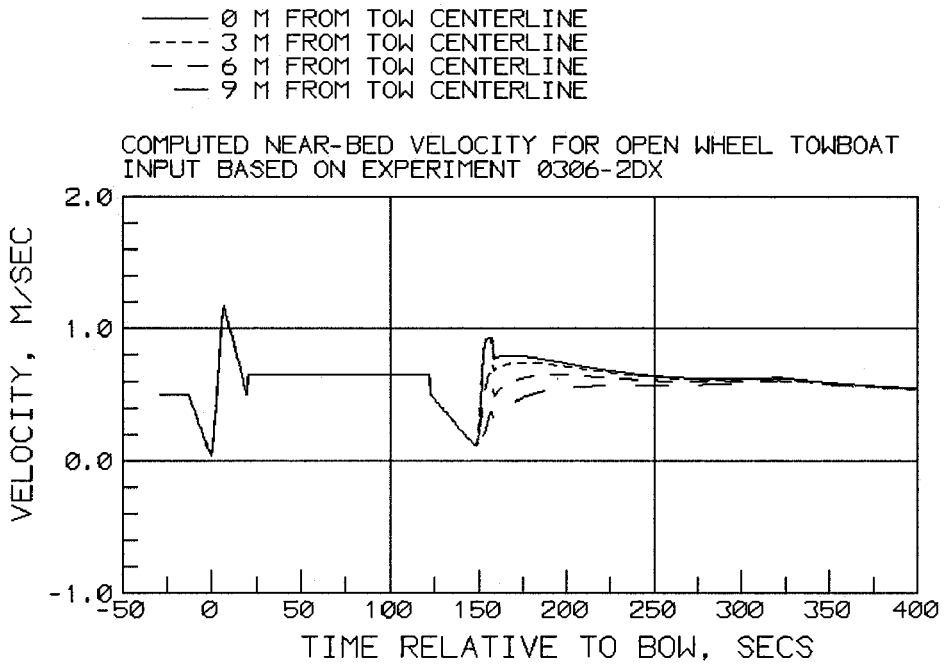
0 M FROM TOW CENTERLINE
3 M FROM TOW CENTERLINE
6 M FROM TOW CENTERLINE
9 M FROM TOW CENTERLINE
COMPUTED NEAR-BED VELOCITY FOR OPEN WHEEL TOWBOAT
INPUT BASED ON EXPERIMENT 0306-2DX
VELOCITY, M/SEC
2.0
1.0
0.0
-1.0
-50
0
50
100
150
200
250
300
350
400
TIME RELATIVE TO BOW, SECS

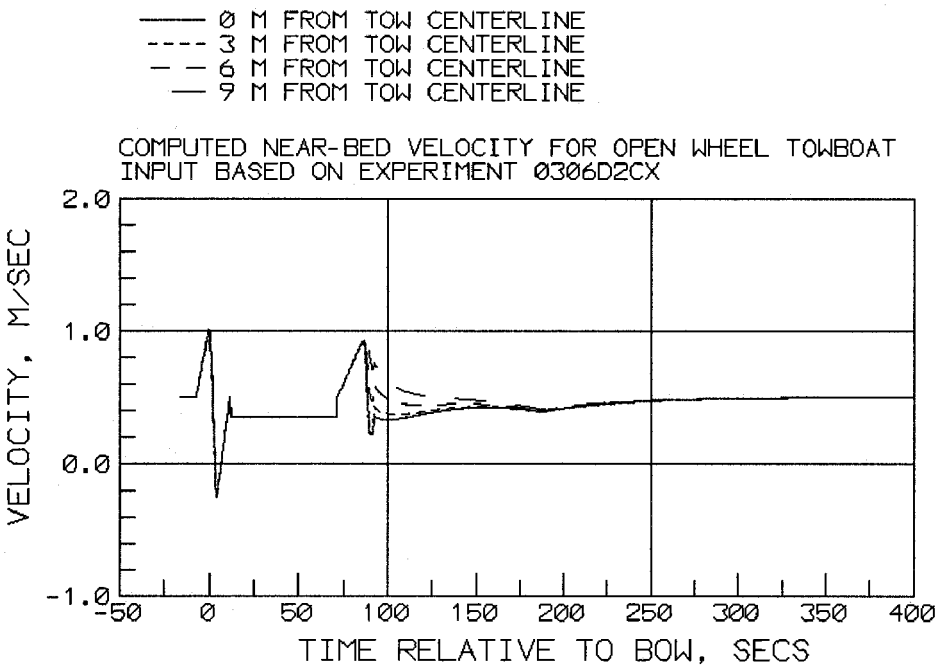
0 M FROM TOW CENTERLINE
3 M FROM TOW CENTERLINE
6 M FROM TOW CENTERLINE
9 M FROM TOW CENTERLINE
COMPUTED NEAR-BED VELOCITY FOR OPEN WHEEL TOWBOAT
INPUT BASED ON EXPERIMENT 0306D2CX
VELOCITY, M/SEC
2.0
1.0
0.0
-1.0
-50
0
50
100
150
200
250
300
350
400
TIME RELATIVE TO BOW, SECS

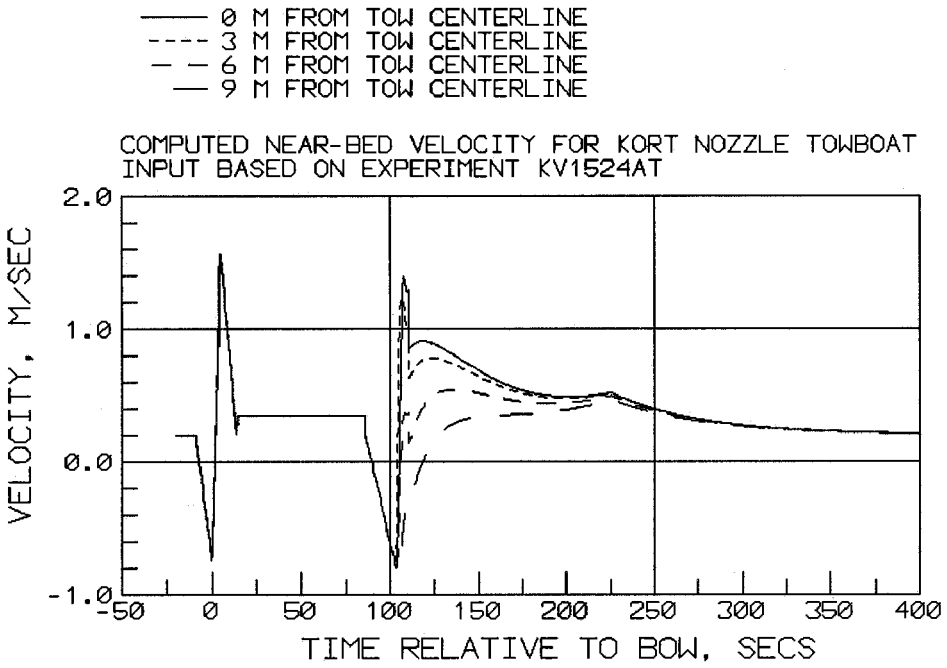
0 M FROM TOW CENTERLINE
3 M FROM TOW CENTERLINE
6 M FROM TOW CENTERLINE
9 M FROM TOW CENTERLINE
COMPUTED NEAR-BED VELOCITY FOR KORT NOZZLE TOWBOAT
INPUT BASED ON EXPERIMENT KV1524AT
VELOCITY, M/SEC
2.0
1.0
0.0
-1.0
-50
0
50
100
150
200
250
300
350
400
TIME RELATIVE TO BOW, SECS

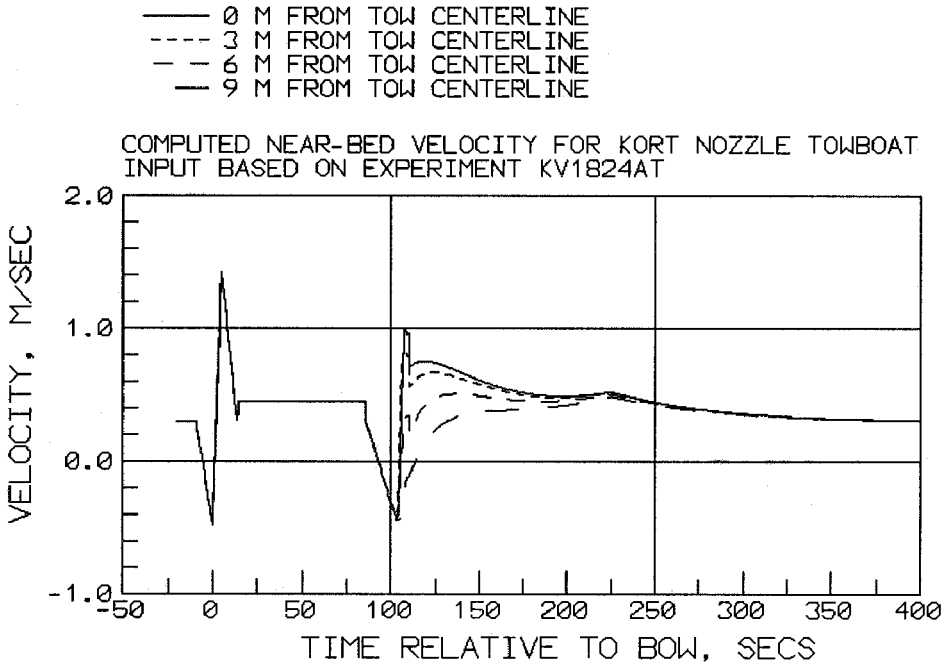
0 M FROM TOW CENTERLINE
3 M FROM TOW CENTERLINE
6 M FROM TOW CENTERLINE
9 M FROM TOW CENTERLINE
COMPUTED NEAR-BED VELOCITY FOR KORT NOZZLE TOWBOAT
INPUT BASED ON EXPERIMENT KV1824AT
VELOCITY, M/SEC
2.0
1.0
0.0
-1.0
-50
0
50
100
150
200
250
300
350
400
TIME RELATIVE TO BOW, SECS

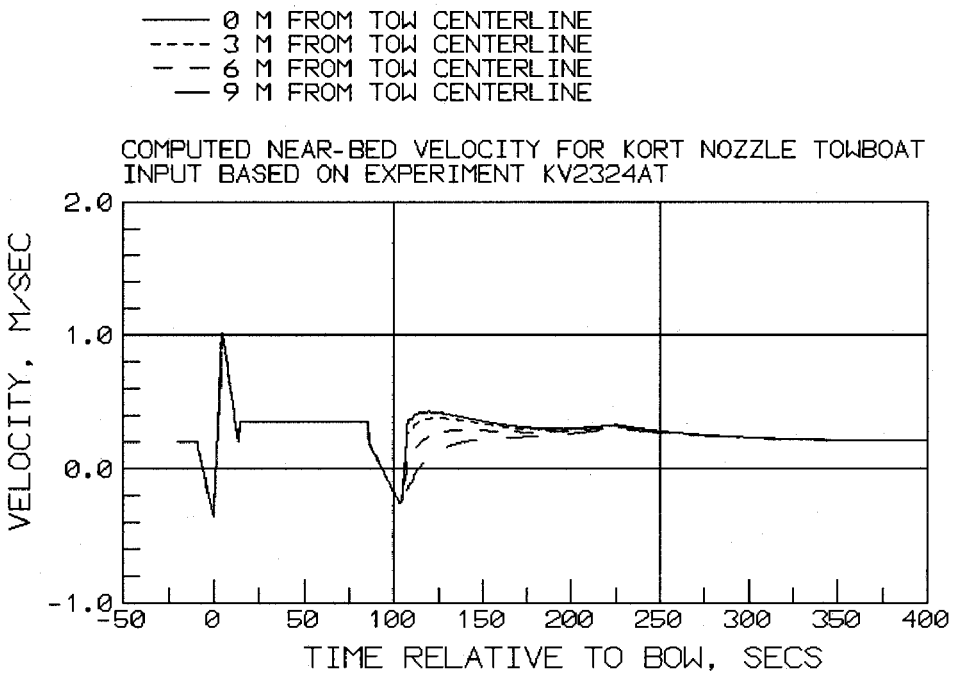
0 M FROM TOW CENTERLINE
3 M FROM TOW CENTERLINE
6 M FROM TOW CENTERLINE
9 M FROM TOW CENTERLINE
COMPUTED NEAR-BED VELOCITY FOR KORT NOZZLE TOWBOAT
INPUT BASED ON EXPERIMENT KV2324AT
VELOCITY, M/SEC
2.0
1.0
0.0
-1.0
-50
0
50
100
150
200
250
300
350
400
TIME RELATIVE TO BOW, SECS

Appendix C
PC Program “Prpshear.bas” for Bed Shear Stress Under Open-Wheel and Kort Nozzle Tows and Example Calculations

```
'   PROGRAM PRPSHEAR.BAS FOR DISTRIBUTION OF SHEAR AROUND VESSEL
    DIM TAU(7, 1500), taup(12, 5), taub(9, 2)
'
'   ARRAY FOR BOW DISTRIBUTION
'
    taub(1, 1) = 0
    taub(1, 2) = -1.17
    taub(2, 1) = .25
    taub(2, 2) = -.73
    taub(3, 1) = .5
    taub(3, 2) = -.51
    taub(4, 1) = .75
    taub(4, 2) = -.33
    taub(5, 1) = 1!
    taub(5, 2) = 0!
    taub(6, 1) = .75
    taub(6, 2) = .37
    taub(7, 1) = .5
    taub(7, 2) = .67
    taub(8, 1) = .25
    taub(8, 2) = 1.41
    taub(9, 1) = 0
    taub(9, 2) = 3.41
'
'   array for propeller
'
    taup(1, 1) = 0
    taup(1, 2) = -6
    taup(1, 3) = -25
    taup(1, 4) = -50
    taup(1, 5) = 0
    taup(2, 1) = .1
    taup(2, 2) = -3.3
    taup(2, 3) = -15
    taup(2, 4) = -30
    taup(2, 5) = 0
    taup(3, 1) = .25
    taup(3, 2) = -2.1
    taup(3, 3) = -6.4
    taup(3, 4) = -11
    taup(3, 5) = 0
    taup(4, 1) = .5
    taup(4, 2) = -1.4
    taup(4, 3) = -1.5
    taup(4, 4) = -2.7
    taup(4, 5) = 0
    taup(5, 1) = .75
    taup(5, 2) = -.54
    taup(5, 3) = -.6
    taup(5, 4) = -.7
    taup(5, 5) = 0
    taup(6, 1) = 1!
    taup(6, 2) = 0
    taup(6, 3) = 0
    taup(6, 4) = 0
    taup(6, 5) = 0
    taup(7, 1) = .75
    taup(7, 2) = .6
```

```
    taup(7, 3) = 1.3
    taup(7, 4) = 1.7
    taup(7, 5) = 0
    taup(8, 1) = .5
    taup(8, 2) = 2.2
    taup(8, 3) = 9.2
    taup(8, 4) = 15
    taup(8, 5) = 0
    taup(9, 1) = .25
    taup(9, 2) = 11
    taup(9, 3) = 37
    taup(9, 4) = 60
    taup(9, 5) = 0
    taup(10, 1) = .1
    taup(10, 2) = 23
    taup(10, 3) = 93
    taup(10, 4) = 125
    taup(10, 5) = 0
    taup(11, 1) = .05
    taup(11, 2) = 75
    taup(11, 3) = 153
    taup(11, 4) = 175
    taup(11, 5) = 0
    taup(12, 1) = 0
    taup(12, 2) = 230
    taup(12, 3) = 230
    taup(12, 4) = 230
    taup(12, 5) = 0
    PRINT
    PRINT
    PRINT "PROGRAM PRPSHEAR.BAS GIVES THE MAXIMUM BOTTOM VELOCITY "
    PRINT "FOR MOVING AND STATIONARY TOWS WITH "
    PRINT "A CENTRAL RUDDER.  SHEAR DISTRIBUTION IS COMPUTED BUT IS ONLY "
    PRINT "VALID FOR UNDERWAY VESSELS. "
    PRINT
'
'   BEGIN INPUT
'
    OPEN "\GRAF\temp.dat" FOR OUTPUT AS #3
    OPEN "PROPtest.dat" FOR INPUT AS #2
'
1   INPUT #2, G$  ' PROGRAM REQUIRES METRIC UNITS
    IF G$ = "M" OR G$ = "m" THEN GOTO 5
    GOTO 1000
5   INPUT #2, KO$ ' KORT(K) OR OPEN WHEEL (O)
    IF KO$ = "k" THEN KO$ = "K"
    IF KO$ = "o" THEN KO$ = "O"
    INPUT #2, DP 'PROPELLER DIAMETER
    INPUT #2, VG 'VESSEL SPEED RELATIVE TO GROUND
    INPUT #2, va 'AVG CHAN VEL
    INPUT #2, DIRECT ' -1 FOR UPBOUND, 1 FOR DOWNBOUND
    INPUT #2, VRET ' RETURN VELOCITY
    VRETURN = -1 * DIRECT * VRET
    VG = VG * DIRECT
    INPUT #2, BARBEAM ' TOTAL WIDTH OF BARGES
    INPUT #2, DRAFT ' TOTAL DRAFT OF BARGES
    INPUT #2, barlen ' TOTAL LENGTH OF BARGES
    INPUT #2, tbl ' TOWBOAT LENGTH
```

```
    INPUT #2, PSPACE ' DISTANCE BETWEEN PROPELLERS(6 M)
    INPUT #2, SETBACK ' DISTANCE FROM PROP TO TOWBOAT STERN(5 M)
    INPUT #2, THRUST ' THRUST FROM BOTH PROPELLERS (NEWTONS:1lb=4.448new)
    THRUST = THRUST / 2
10  INPUT #2, dep ' LOCAL DEPTH
    hp = dep - DP / 2
    INPUT #2, VABOTT' AMBIENT VEL AT BOTTOM
    INPUT #2, d50'average particle size in bed   '**********new
    bc = dep - DRAFT
15  YSPACE = 3
    XSPACE = .5
    XBEGIN = -20    ' beginning x
    Y = 0       ' beginning y
    numx = 1500
    NUMY = 7
    rho = 999.8 ' FOR THRUST IN NEWTONS
'
'   SET KORT OR OPEN PARAMETERS
'
    IF KO$ = "K" THEN GOTO 12
'
'   THIS SECTION FOR OPEN WHEEL
    D0 = .71 * DP
    E = .43
    CFUNC = .5
    GOTO 17
12  ' THIS SECTION FOR KORT
    D0 = DP
    E = .58
    CFUNC = .25
17  ' compute PEAK BOW SHEAR
    DOD = dep / DRAFT
    CBOWC = .0118
    CBOWP = -2.85
    IF DIRECT > 0 THEN GOTO 78
    CBOWC = .0148
78  CBOW = CBOWC * DOD ^ CBOWP' C BASED ON LEAVING 1/2 OUT OF EQUATION
    TAUBOWP = 10000 * CBOW * (va - VG) ^ 2
    VBOWP = (.69 * DOD ^ (-1.21) * (va - VG)) + VABOTT
'
'   END OF PEAK BOW COMPUTATIONS
'
'   COMPUTE VELOCITY EXITING PROPELLER
    U2 = 1.13 / D0 * (THRUST / rho) ^ .5
    PRINT "U2 = ", U2
'
'   COMPUTE WAKE VELOCITY AT PEAK PROP VELOCITY
'
    xprmax = hp / .1
    vwakamax = -1 * (va - VG) * (.78) * (DRAFT / dep) ^ (1.81)
    PRINT
    PRINT "MAXIMUM WAKE VELOCITY RELATIVE TO AMBIENT COND. = ", vwakamax
    PRINT "MAXIMUM WAKE VELOCITY PLUS AMBIENT BOT VEL = ", vwakamax + VABOTT
    VSHEAR = ABS(vwakamax + VABOTT)
    IF U2 = 0 GOTO 40
    F = (1 - CFUNC * (ABS(va - VG) / U2) * (hp / DP) ^ 1.5)
    GOTO 45
40  F = 0
```

```
45   IF F < 0 THEN F = 0
     PRINT "F = ", F
     vpropmax = E * (DP / hp) * U2 * F
'
'    compute wake vel at hp/.1 behind towboat
'
     vwake1 = (1 + .0075 * (tbl / DRAFT) - .0075 * (xprmax + tbl) / DRAFT)
     vwakegx = vwakamax * vwake1 + VABOTT
30   PRINT "WAKE VEL AT HP/X=.1 PLUS AMBIENT BOT VEL = ", vwakegx
'
'    compute max resultant vel
'
     Vres = -1 * DIRECT * vpropmax + vwakegx
     Velshear = ABS(vpropmax) + .5 * ABS(vwakegx)
     PRINT "MAXIMUM PROPELLER/WAKE/AMBIENT VEL AT HP/X = 0.1 ", Vres
     PRINT "Velshear =  ", Velshear
     CFPROP = .01 * DP / hp ' FOR PROP JET
     PROPSH = .5 * 10000 * CFPROP * Velshear ^ 2
     PRINT "MAXIMUM PROPELLER SHEAR = ", PROPSH;
     PRINT " DYNES/SQ CM "
'
'
'
'    start distribution- y measured from cl of tow, x measured
'    from bow of barges
'
'    SET ALL TAU TO ZERO
'
     FOR I = 1 TO NUMY ' num of y calc
     FOR J = 1 TO numx ' num of x calc
     TAU(I, J) = 0
     NEXT J
     NEXT I
'
'    START ITERATION ON X,Y
'
     FOR I = 1 TO NUMY
     x = XBEGIN
     FOR J = 1 TO numx
'
'    COMPUTE BOW SHEAR DISTRIBUTION
'
     XPEAKBOW = 10  ' DISTANCE FROM BOW TO PEAK BOW SHEAR
     IF Y > BARBEAM / 2 THEN GOTO 229
     XRATBOW = (x - XPEAKBOW) / dep
     IF XRATBOW <= -1.17 THEN GOTO 229
     IF XRATBOW > 3.41 THEN GOTO 229
     FOR JK = 1 TO 8
     IF XRATBOW > taub(JK + 1, 2) THEN GOTO 222
     TEMP1 = (taub(JK + 1, 1) - taub(JK, 1))
     TEMP2 = TEMP1 * (XRATBOW - taub(JK, 2)) / (taub(JK + 1, 2) - taub(JK, 2))
     TAUBRAT = taub(JK, 1) + TEMP2
     GOTO 228
222  NEXT JK
228  TAU(I, J) = TAUBRAT * TAUBOWP
229  ' CONTINUE
'
'    END BOW SHEAR
```

```
'
'   compute wake dist
'
    vwakegx = 0
    IF Y > BARBEAM / 2 THEN GOTO 100
    coef = x - barlen
    IF coef <= 0 THEN GOTO 100      '*****************mod
    xlim = 1
    cfc = .06 * (.4343 * LOG(12 * dep / (3 * d50))) ^ -2'*****************new
    cfr = (2.87 + 1.58 * .4343 * LOG(xlim / 3 / d50)) ^ (-2.5)  '********new
    IF x - barlen > tbl THEN GOTO 110
    deca = coef / tbl                           '*********mod
    vwakegx = vwakamax * deca + VABOTT                      '*********mod
    GOTO 120
110  deca = (1 + .0075 * (tbl / DRAFT) - .0075 * (x - barlen) / DRAFT)
    IF deca < 0 THEN deca = 0                           '*********mod
    vwakegx = vwakamax * deca + VABOTT
120  ctemp = .5 * 10 * cfc * rho                        '*********new
    TAU(I, J) = ctemp * (va + (cfr / cfc) ^ .5 * vwakamax * deca) ^ 2'**mod
'
100  ' END WAKE DIST
'
'   BEGIN PROP DIST*************************
'
    taurat = 0              '*****************************************new
    IF x < barlen THEN GOTO 700  '*****************************************new
'   COMPUTE LATERAL PEAK SHEAR
    YDP = Y / DP
    DPHP = DP / hp
    IF DPHP > 1.2 THEN DPHP = 1.2
    IF DPHP < .48 THEN DPHP = .48
    IF YDP > .547 THEN GOTO 200
'   LINEAR PORTION HERE
    SHRATY0 = 1.207 - .653 * DPHP      ' SHEAR RATIO AT Y = 0
    SHRATY = 1 - (.547 - YDP) / .547 * (1 - SHRATY0)
    peaksh = SHRATY * PROPSH
    GOTO 400
200  IF YDP > 1.095 THEN GOTO 300
'   SHEAR = PEAK SHEAR HERE
    peaksh = PROPSH
    GOTO 400
300  ' EXPONENTIAL SHEAR HERE
    C5 = .0221 * 2.7183 ^ (3.14 * DPHP)
    SHRATY = 2.7183 ^ (-C5 * ((Y - PSPACE / 2) / DP) ^ 2)
    peaksh = SHRATY * PROPSH
'
'   END FINDING LATERAL PEAK SHEAR
'
400  ' COMPUTE LONGITUDINAL SHEAR FROM PEAK LATERAL SHEAR
    XPEAK = barlen + tbl + hp / .2 - SETBACK
    XRAT = (x - XPEAK) / hp
    PS = peaksh ' PS DETERMINES WHICH INTERPOLATION COLUMN TO USE
    IF peaksh > 1000 THEN PS = 1000
    IF peaksh < 69 THEN PS = 69
    IF PS < 215 THEN GOTO 500
'   THIS PART IS FOR PS FROM 1000-215
    FOR jj = 1 TO 12
  taup(jj, 5) = taup(jj, 2) + (1000 - PS) / 785 * (taup(jj, 3) - taup(jj, 2))
```

```
    NEXT jj
    GOTO 600
500  ' THIS PART FOR PS <215 TO 69
    FOR kk = 1 TO 12
   taup(kk, 5) = taup(kk, 3) + (215 - PS) / 146 * (taup(kk, 4) - taup(kk, 3))
    NEXT kk
600  IF XRAT <= taup(1, 5) THEN GOTO 900
    IF XRAT >= 230 THEN GOTO 900
    FOR k = 1 TO 11
    IF XRAT > taup(k + 1, 5) THEN GOTO 650
    TEMP1 = (taup(k + 1, 1) - taup(k, 1))
    TEMP2 = TEMP1 * (XRAT - taup(k, 5)) / (taup(k + 1, 5) - taup(k, 5))
    taurat = taup(k, 1) + TEMP2
    GOTO 700
650  NEXT k
'
'    END LONGITUDINAL DISTRIBUTION
'
'    SET TAU TO MAX OF PROP OR WAKE SHEAR
'
700  IF taurat * peaksh > TAU(I, J) THEN TAU(I, J) = taurat * peaksh
900  '
    x = x + XSPACE
    NEXT J
150  '
    Y = Y + YSPACE
    NEXT I
'
'    END ITERATION ON X,Y
'
    PRINT #3, "     ";
    yprint = 0
    FOR I = 1 TO NUMY
    PRINT #3, USING "####.#"; yprint;
    yprint = yprint + YSPACE
    NEXT I
    PRINT #3, "    "
    PRINT #3, "   "
    XPRINT = XBEGIN / ABS(VG)
    FOR J = 1 TO numx
    PRINT #3, USING "####.#"; XPRINT;
    XPRINT = XPRINT + XSPACE / ABS(VG)
    FOR I = 1 TO NUMY
    PRINT #3, USING "#####."; TAU(I, J);
    NEXT I
    PRINT #3, " "
    NEXT J
1000 END
```

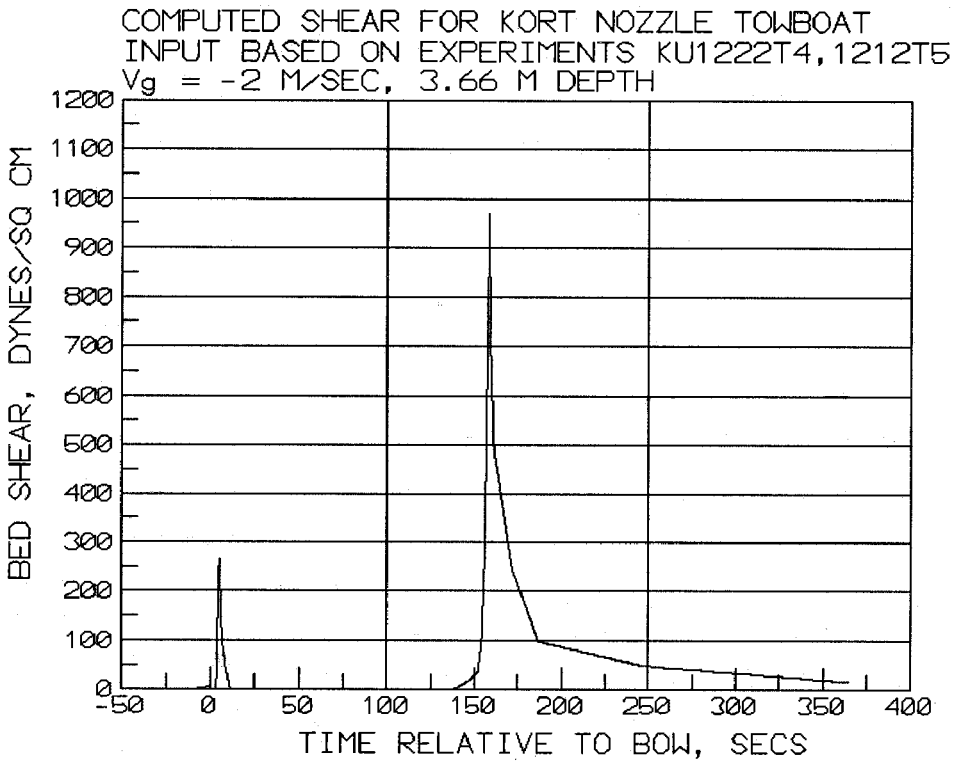
COMPUTED SHEAR FOR KORT NOZZLE TOWBOAT
INPUT BASED ON EXPERIMENTS KU1222T4,1212T5
Vg = -2 M/SEC, 3.66 M DEPTH
BED SHEAR, DYNES/SQ CM
1200
1100
1000
900
800
700
600
500
400
300
200
100
0
-50
0
50
100
150
200
250
300
350
400
TIME RELATIVE TO BOW, SECS

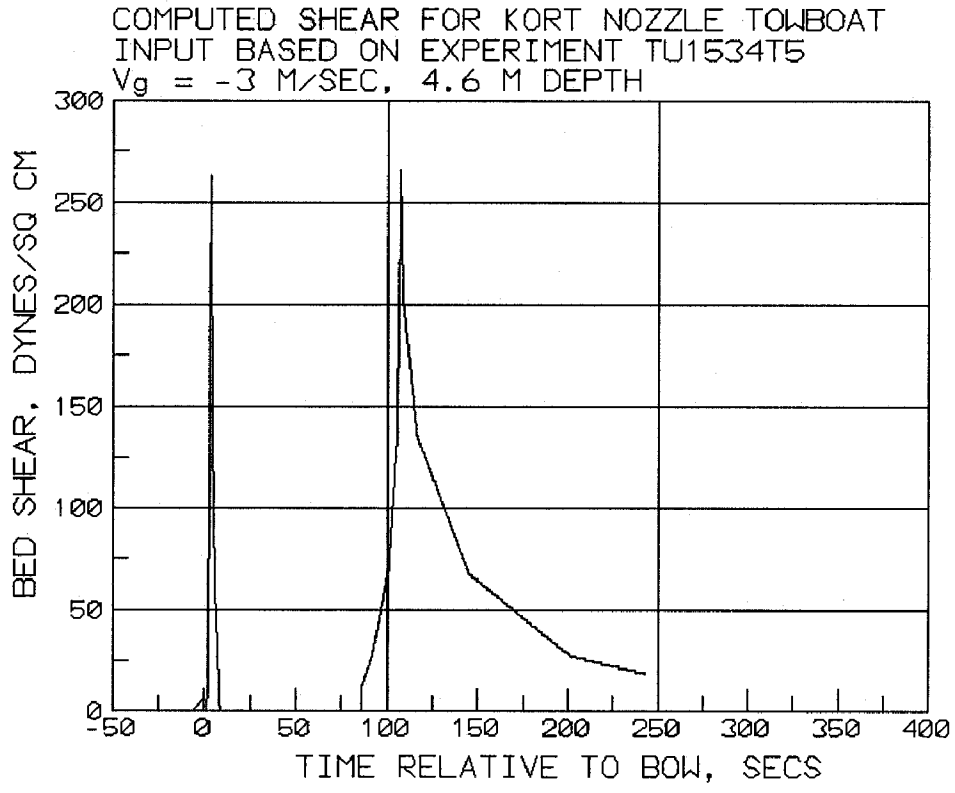
COMPUTED SHEAR FOR KORT NOZZLE TOWBOAT
INPUT BASED ON EXPERIMENT TU1534T5
Vg = -3 M/SEC, 4.6 M DEPTH
BED SHEAR, DYNES/SQ CM
300
250
200
150
100
50
0
-50
0
50
100
150
200
250
300
350
400
TIME RELATIVE TO BOW, SECS

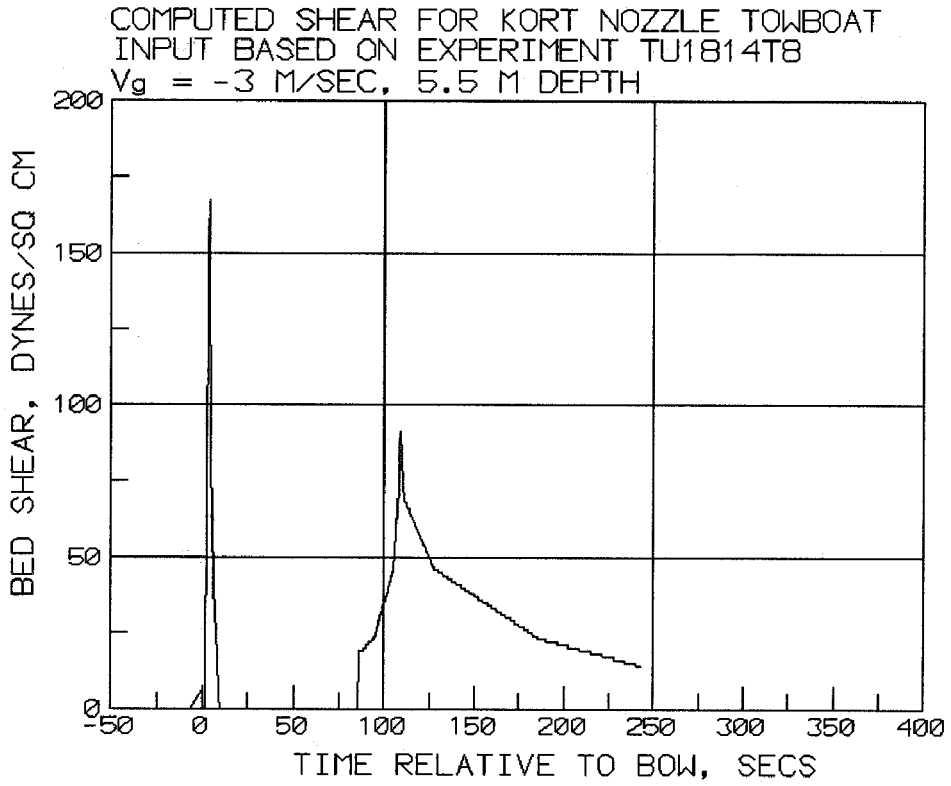
COMPUTED SHEAR FOR KORT NOZZLE TOWBOAT
INPUT BASED ON EXPERIMENT TU1814T8
Vg = -3 M/SEC, 5.5 M DEPTH
BED SHEAR, DYNES/SQ CM
200
150
100
50
0
-50
0
50
100
150
200
250
300
350
400
TIME RELATIVE TO BOW, SECS

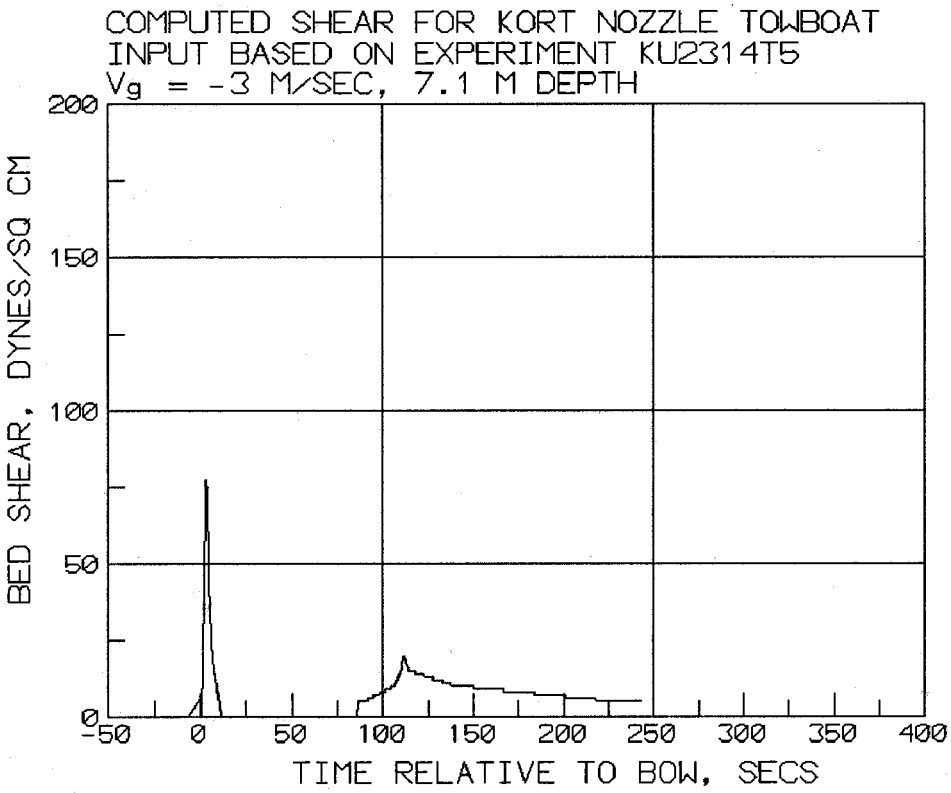
COMPUTED SHEAR FOR KORT NOZZLE TOWBOAT
INPUT BASED ON EXPERIMENT KU2314T5
Vg = -3 M/SEC, 7.1 M DEPTH
BED SHEAR, DYNES/SQ CM
200
150
100
50
0
-50
0
50
100
150
200
250
300
350
400
TIME RELATIVE TO BOW, SECS

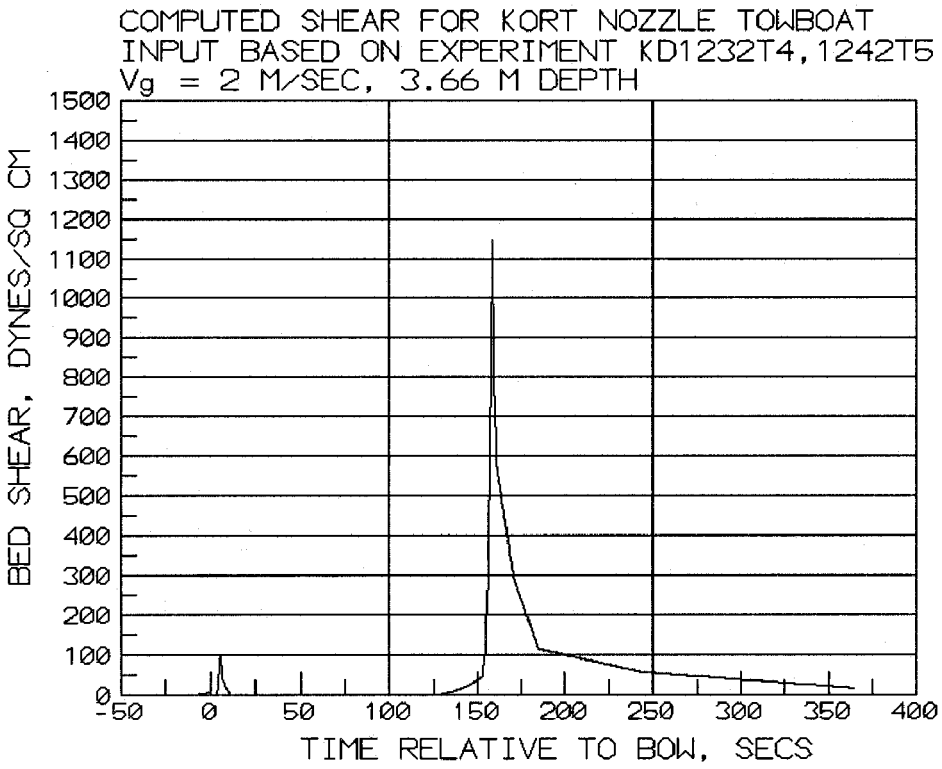
COMPUTED SHEAR FOR KORT NOZZLE TOWBOAT
INPUT BASED ON EXPERIMENT KD1232T4,1242T5
Vg = 2 M/SEC, 3.66 M DEPTH
BED SHEAR, DYNES/SQ CM
1500
1400
1300
1200
1100
1000
900
800
700
600
500
400
300
200
100
0
-50
0
50
100
150
200
250
300
350
400
TIME RELATIVE TO BOW, SECS

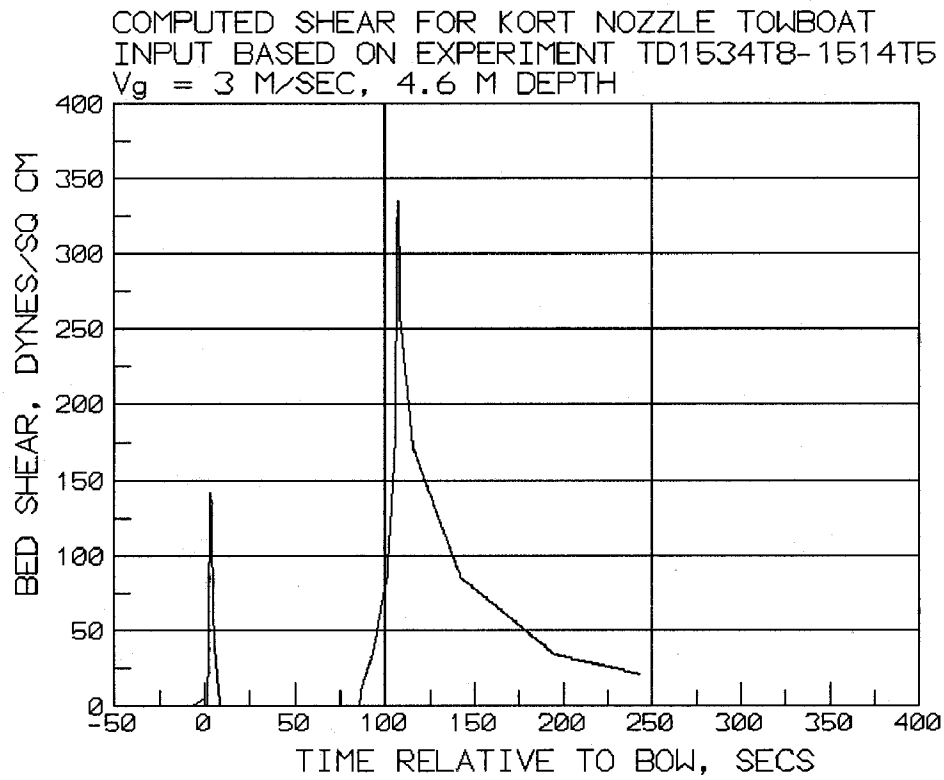
COMPUTED SHEAR FOR KORT NOZZLE TOWBOAT
INPUT BASED ON EXPERIMENT TD1534T8-1514T5
Vg = 3 M/SEC, 4.6 M DEPTH
BED SHEAR, DYNES/SQ CM
400
350
300
250
200
150
100
50
0
-50
0
50
100
150
200
250
300
350
400
TIME RELATIVE TO BOW, SECS

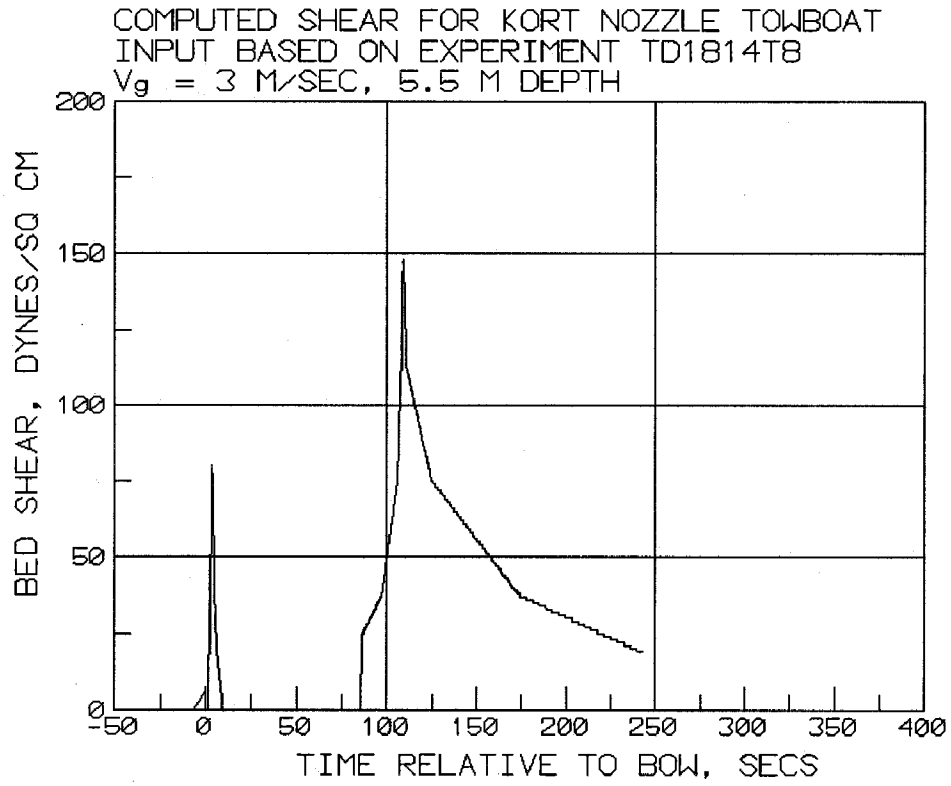
COMPUTED SHEAR FOR KORT NOZZLE TOWBOAT
INPUT BASED ON EXPERIMENT TD1814T8
Vg = 3 M/SEC, 5.5 M DEPTH
BED SHEAR, DYNES/SQ CM
200
150
100
50
0
-50
0
50
100
150
200
250
300
350
400
TIME RELATIVE TO BOW, SECS

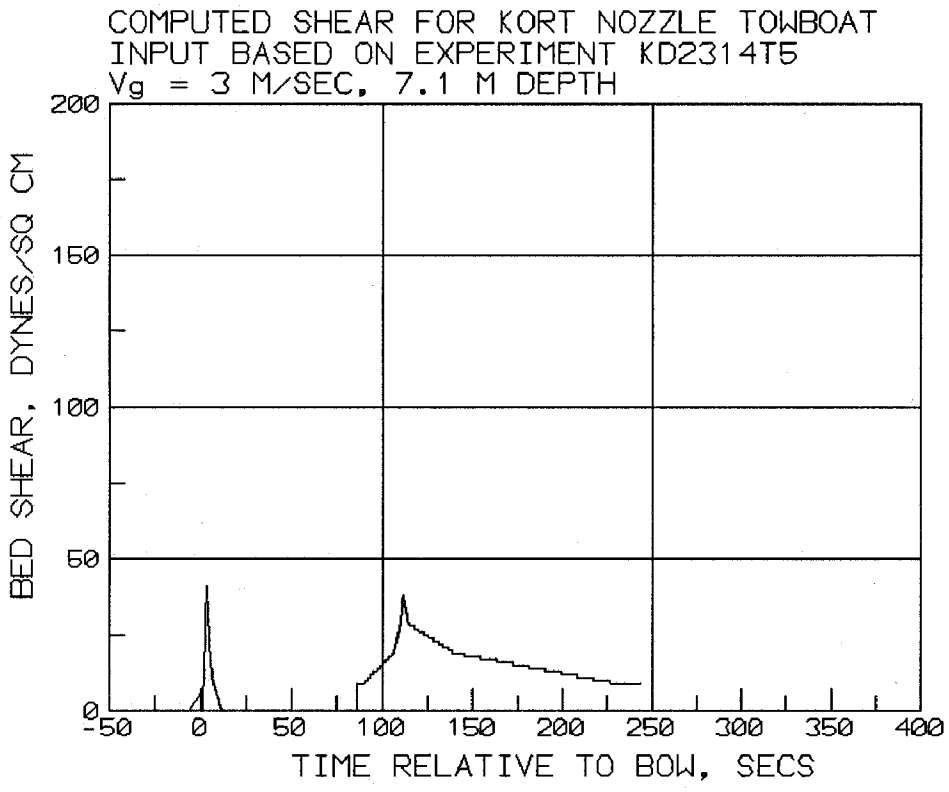
COMPUTED SHEAR FOR KORT NOZZLE TOWBOAT
INPUT BASED ON EXPERIMENT KD2314T5
Vg = 3 M/SEC, 7.1 M DEPTH
BED SHEAR, DYNES/SQ CM
200
150
100
50
0
-50
0
50
100
150
200
250
300
350
400
TIME RELATIVE TO BOW, SECS

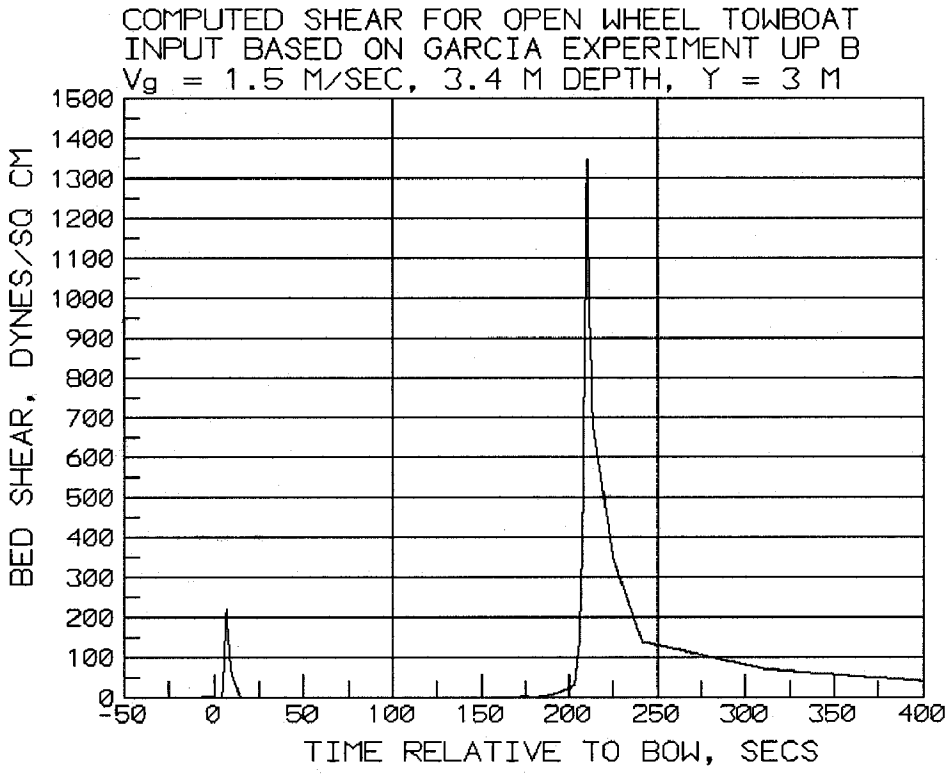
COMPUTED SHEAR FOR OPEN WHEEL TOWBOAT
INPUT BASED ON GARCIA EXPERIMENT UP B
Vg = 1.5 M/SEC, 3.4 M DEPTH, Y = 3 M
BED SHEAR, DYNES/SQ CM
1500
1400
1300
1200
1100
1000
900
800
700
600
500
400
300
200
100
0
-50
0
50
100
150
200
250
300
350
400
TIME RELATIVE TO BOW, SECS

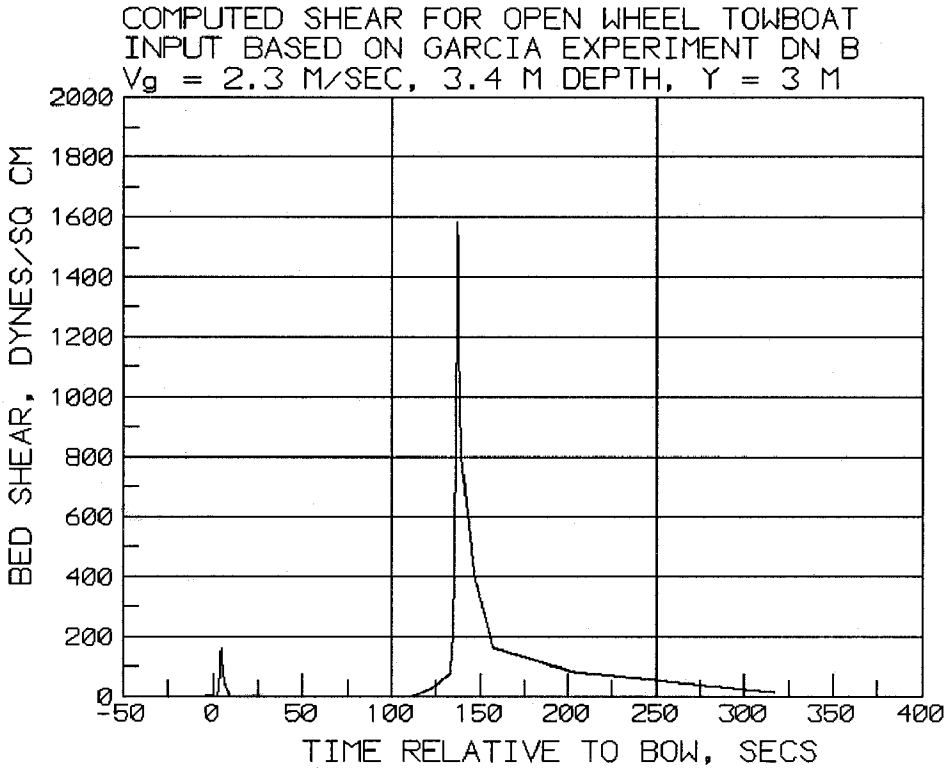
COMPUTED SHEAR FOR OPEN WHEEL TOWBOAT
INPUT BASED ON GARCIA EXPERIMENT DN B
Vg = 2.3 M/SEC, 3.4 M DEPTH, Y = 3 M
BED SHEAR, DYNES/SQ CM
2000
1800
1600
1400
1200
1000
800
600
400
200
0
-50
0
50
100
150
200
250
300
350
400
TIME RELATIVE TO BOW, SECS

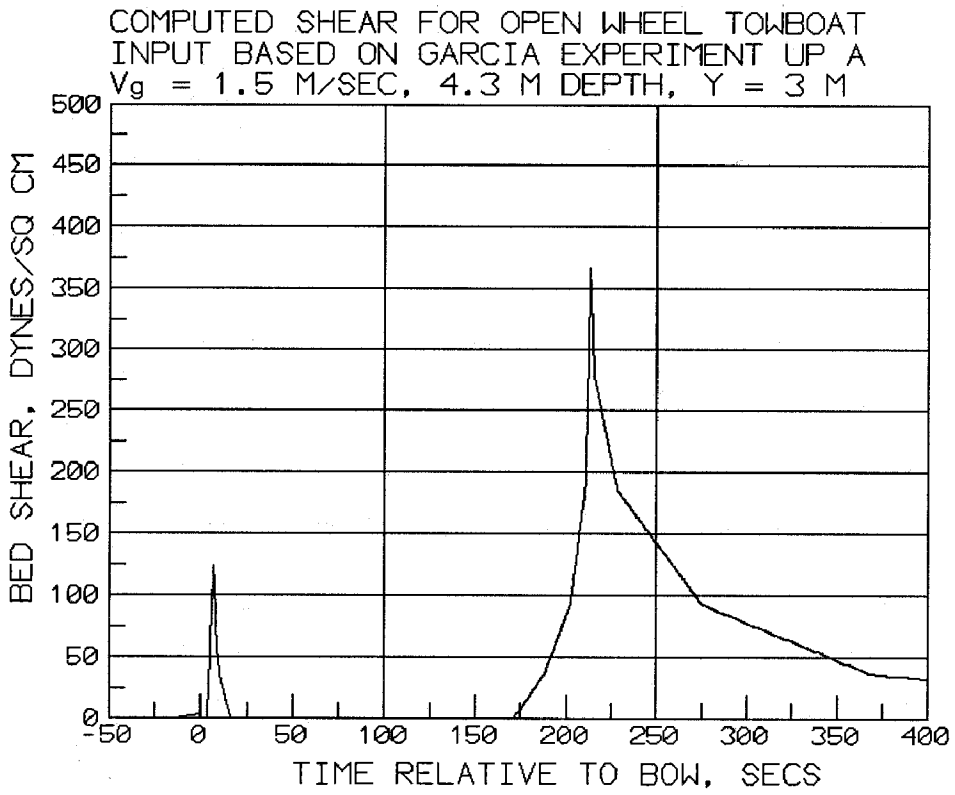
COMPUTED SHEAR FOR OPEN WHEEL TOWBOAT
INPUT BASED ON GARCIA EXPERIMENT UP A
Vg = 1.5 M/SEC, 4.3 M DEPTH, Y = 3 M
BED SHEAR, DYNES/SQ CM
500
450
400
350
300
250
200
150
100
50
0
-50
0
50
100
150
200
250
300
350
400
TIME RELATIVE TO BOW, SECS

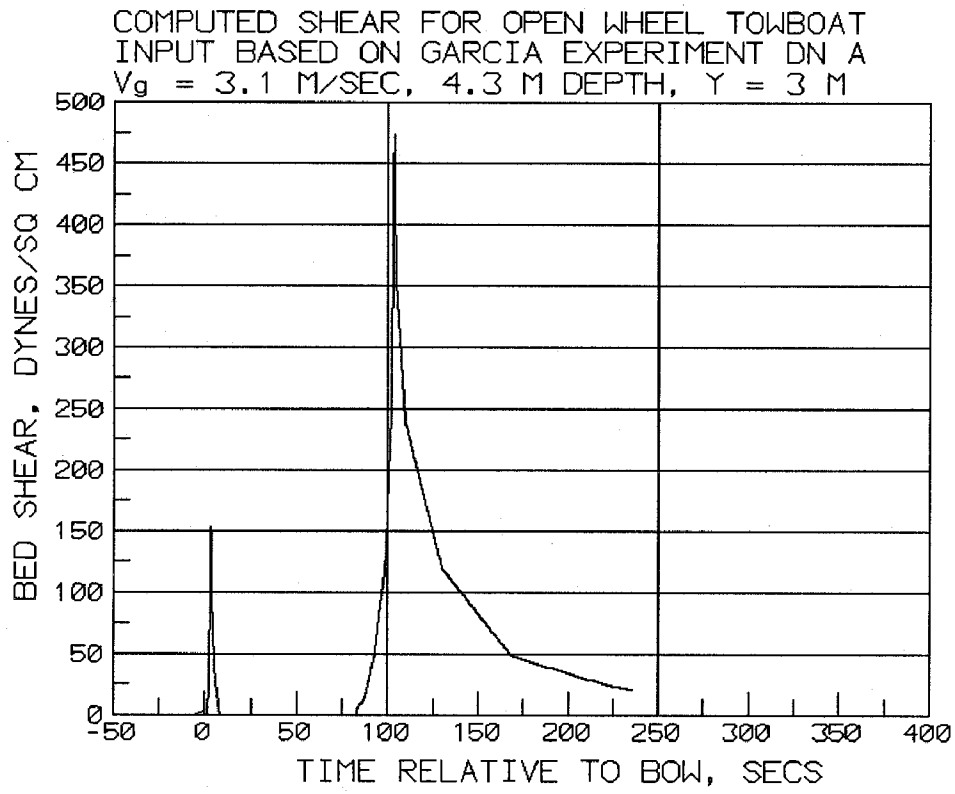
COMPUTED SHEAR FOR OPEN WHEEL TOWBOAT
INPUT BASED ON GARCIA EXPERIMENT DN A
Vg = 3.1 M/SEC, 4.3 M DEPTH, Y = 3 M
BED SHEAR, DYNES/SQ CM
500
450
400
350
300
250
200
150
100
50
0
-50
0
50
100
150
200
250
300
350
400
TIME RELATIVE TO BOW, SECS

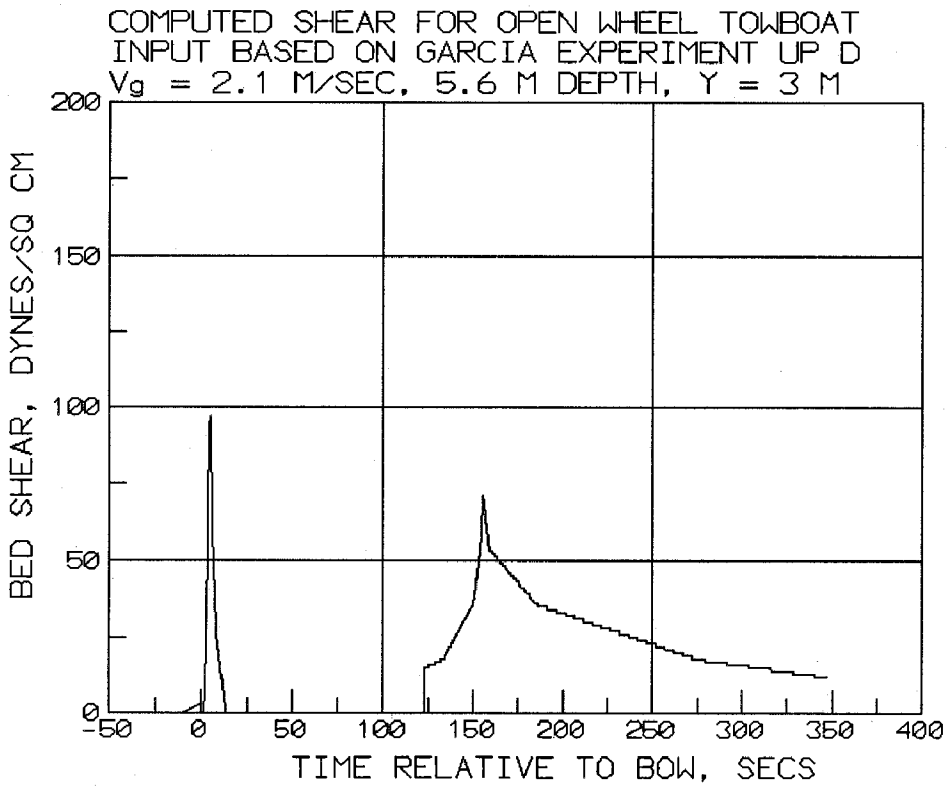
COMPUTED SHEAR FOR OPEN WHEEL TOWBOAT
INPUT BASED ON GARCIA EXPERIMENT UP D
Vg = 2.1 M/SEC, 5.6 M DEPTH, Y = 3 M
BED SHEAR, DYNES/SQ CM
200
150
100
50
0
-50
0
50
100
150
200
250
300
350
400
TIME RELATIVE TO BOW, SECS

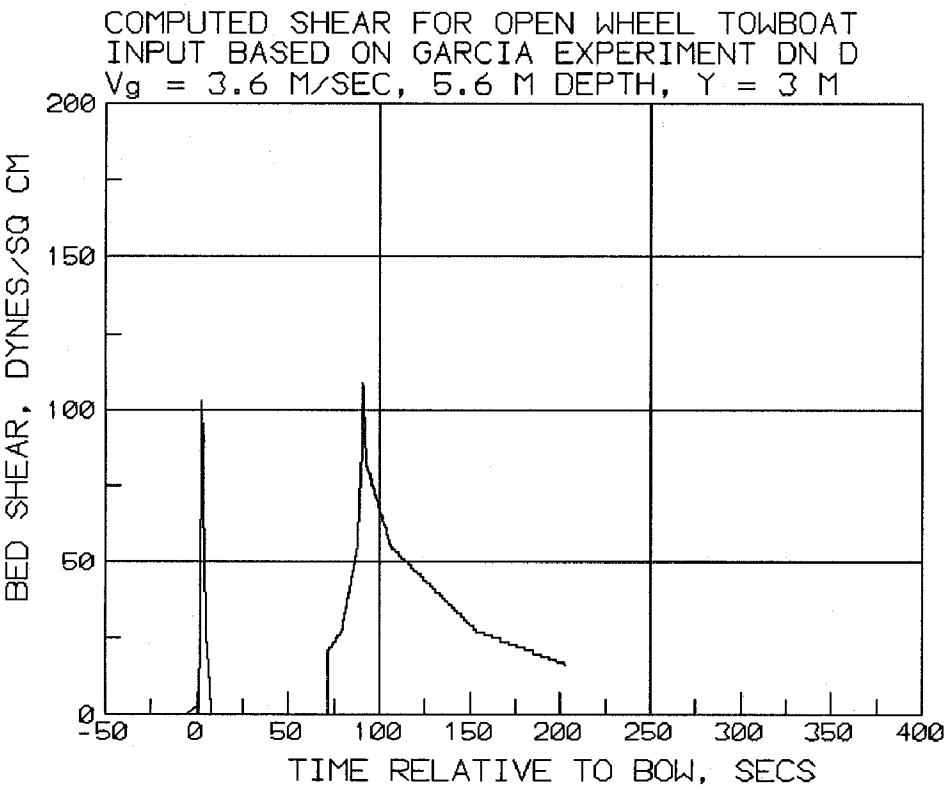
COMPUTED SHEAR FOR OPEN WHEEL TOWBOAT
INPUT BASED ON GARCIA EXPERIMENT DN D
Vg = 3.6 M/SEC, 5.6 M DEPTH, Y = 3 M
BED SHEAR, DYNES/SQ CM
200
150
100
50
0
-50
0
50
100
150
200
250
300
350
400
TIME RELATIVE TO BOW, SECS

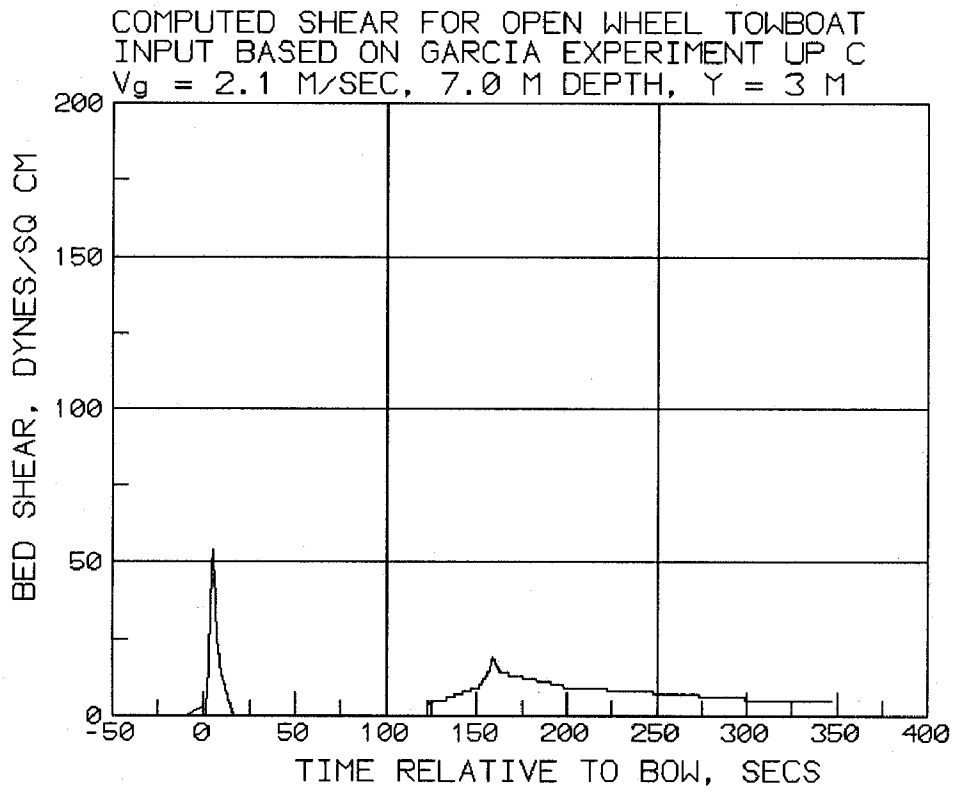
COMPUTED SHEAR FOR OPEN WHEEL TOWBOAT
INPUT BASED ON GARCIA EXPERIMENT UP C
Vg = 2.1 M/SEC, 7.0 M DEPTH, Y = 3 M
BED SHEAR, DYNES/SQ CM
200
150
100
50
0
-50
0
50
100
150
200
250
300
350
400
TIME RELATIVE TO BOW, SECS

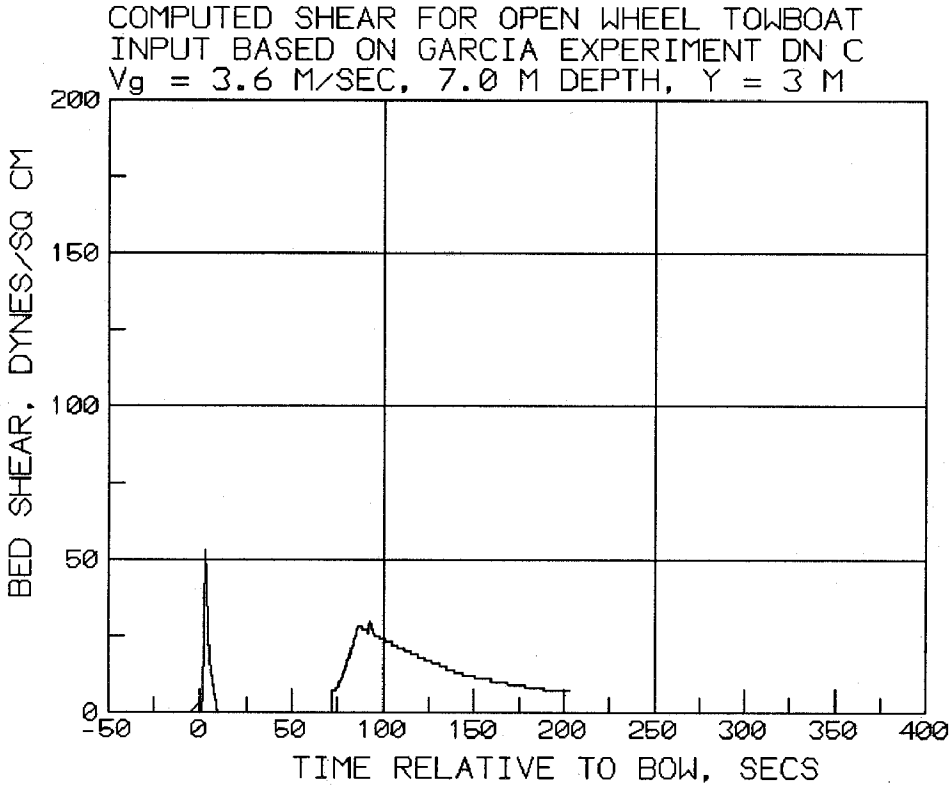
COMPUTED SHEAR FOR OPEN WHEEL TOWBOAT
INPUT BASED ON GARCIA EXPERIMENT DN C
Vg = 3.6 M/SEC, 7.0 M DEPTH, Y = 3 M
BED SHEAR, DYNES/SQ CM
200
150
100
50
0
-50
0
50
100
150
200
250
300
350
400
TIME RELATIVE TO BOW, SECS

Appendix D
Notation

Beam	Total width of barges
C	Coefficient in fully developed jet flow equation used in Zone 1
C_{bow}	Coefficient in defining $_{bow}$ (peak)
C_{fc}	Skin friction coefficient for rough surface, fully developed boundary layer
C_{fs}	Skin friction coefficient for smooth surface
C_{fr}	Skin friction coefficient for rough surface, developing boundary layer
C_s	Coefficient in equation to decay $_{peak}$ to $_{peak\ @\ Y}$
C_{z2}	Coefficient used for C in fully developed jet flow equation in Zone 2 to decay the surface velocity V(xp)max
Cfunc	Coefficient in propeller jet velocity equation = 0.5 for open wheels, 0.25 for Kort nozzles
CJ	Vertical distance from center of propeller to location of V(xp)max, Zone 1
C_{exp}	Coefficient in equation defining decay of V(xp)max in Zone 2
C_{para}	Coefficient in equation defining CJ, Zone 1
Depth	Local depth at center line of tow
Draft	Draft of barges
D_0	Contracted jet diameter = $0.71D_p$ for open wheel or D_p for Kort nozzle
D_p	Propeller diameter
D_{50}	Average bed particle size
E	Coefficient in propeller jet equation, depends on Kort or open-wheel propellers

EP_o	Effective push, equivalent to thrust, from both propellers, open-wheel
EP_k	Effective push, equivalent to thrust, from both propellers, Kort nozzle
g	Gravitational constant
h	Local water depth
H_p	Distance from channel bottom to center of propeller
HP	Total towboat power in horsepower in Toutant (1982) equations
K_s	Sand grain roughness
LBARGES	Total length of barges
n	Propeller speed in rev/sec
Pspace	Lateral distance between centers of propellers
r	Radial distance from location of V(xp)max to $V_{x,r}$
R_x	Reynold's number in developing boundary layer
SETBACK	Horizontal distance from stern of towboat to propellers
T	Time relative to passage of bow
Tp	Time to peak shear in propeller jet relative to passage of bow
Thrust	Thrust per propeller
TBL	Towboat length
U_c	Local depth averaged velocity
U_r	Return velocity
V_a	Ambient average channel velocity, all ambient velocities are always positive
$V_{a(bott)}$	Ambient average channel bottom velocity
$V_b$max	Maximum bottom velocity in propeller jet acting opposite to direction of tow travel, all tow velocities are positive downstream, negative upstream
V_{bd}	Velocity change following V_{bow}, acting opposite to direction of tow travel
V_{bot}	Bottom velocity in Zone 2, based on V_{surf}
V_{bow}	Velocity change at bow acting in same direction as tow travels

V_g	Vessel speed relative to ground
$V_{prop,v}$	Propeller velocity relative to vessel
$V_{res,g}$	Resultant velocity relative to ground
$V_{res,v}$	Resultant velocity relative to vessel
$V_{shear\ calc}$	Velocity used to compute propeller jet global peak shear
V_{surf}	Surface velocity from Equation 21 using C_{z2} in Zone 2
V_w	Vessel speed relative to water, always positive = abs(V_a-V_g)
$V_{wake,a}$(max)	Maximum wake velocity relative to ambient conditions
$V_{wake,g}$	Wake velocity relative to ground
$V_{wake,g}$(x)	Wake velocity relative to ground as a function of x
$V_{wake,v}$	Wake velocity relative to vessel
$V_{x,r}$	Velocity acting along axis of tow at r from location of V(xp)max and xp from propeller
V(xp)max	Maximum propeller jet velocity as a function of xp, for a single propeller in Zone 1 or both propellers in Zone 2
V_2	Velocity increase caused by propeller
x	Distance along tow axis measured from bow
xbl	Distance from beginning of boundary layer development
xp	Distance along tow axis measured from propeller
Y	Lateral distance from tow center line
	Water density
	Bed shear stress from return current
$_{bow}$ (peak)	Peak bed shear stress at bow of barges
$_{peak}$	Global peak bed shear stress
$_{peak\ @\ Y}$	Peak shear bed stress at Y

REPORT DOCUMENTATION PAGE

Form Approved
OMB No. 0704-0188

1. AGENCY USE ONLY *(Leave blank)*	2. REPORT DATE	3. REPORT TYPE AND DATES COVERED
	March 2000	Interim report

4. TITLE AND SUBTITLE
Physical Forces near Commercial Tows

5. FUNDING NUMBERS

6. AUTHOR(S)
Stephen T. Maynord

7. PERFORMING ORGANIZATION NAME(S) AND ADDRESS(ES)
U.S. Army Engineer Research and Development Center
Coastal and Hydraulics Laboratory
3909 Halls Ferry Road
Vicksburg, MS 39180-6199

8. PERFORMING ORGANIZATION REPORT NUMBER

9. SPONSORING/MONITORING AGENCY NAME(S) AND ADDRESS(ES)
See reverse.

10. SPONSORING/MONITORING AGENCY REPORT NUMBER
ENV Report 19

11. SUPPLEMENTARY NOTES

12a. DISTRIBUTION/AVAILABILITY STATEMENT
Approved for public release; distribution is unlimited.

12b. DISTRIBUTION CODE

13. ABSTRACT ***(Maximum 200 words)***

The Upper Mississippi River-Illinois Waterway System (UMR-IWWS) Navigation Study evaluates the justification of additional lockage capacity at sites on the UMR-IWWS while maintaining the social and environmental qualities of the river system. The system navigation study is implemented by the Initial Project Management Plan (IPMP) outlined in the "Upper Mississippi River-Illinois Waterway System Navigation Study," (U.S. Army Corps of Engineers (USACE) 1994). The IPMP outlines Engineering, Economic, Environmental, and Public Involvement Plans.

Physical forces in the region near and beneath commercial tows occur because of the propeller jet and the displacement of water by the hull of the vessel. Physical forces are quantified in terms of the changes in pressure, velocity, and shear stress and are used to determine substrate scour, sediment resuspension, and effects on aquatic organisms.

This study of forces near and beneath commercial tows is conducted in a physical model. The reason for this is that field measurements beneath a vessel are difficult to obtain because some of the primary tows of interest are operating in shallow water with as little as a 0.6-m clearance beneath the tow. In addition, propeller jet bottom velocities can exceed 4 m/sec. Operation of velocity meters or other measuring devices in such an environment is quite difficult. The difficulty of obtaining field data means that verification data for the physical model is lacking. The approach used

(Continued)

14. SUBJECT TERMS

Barges	Pressure	Stress
Environmental effects	Propeller	Towboat
Navigation	Shear	Velocity

15. NUMBER OF PAGES
155

16. PRICE CODE

17. SECURITY CLASSIFICATION OF REPORT	18. SECURITY CLASSIFICATION OF THIS PAGE	19. SECURITY CLASSIFICATION OF ABSTRACT	20. LIMITATION OF ABSTRACT
UNCLASSIFIED	UNCLASSIFIED		

9. (Concluded).

U.S. Army Engineer District, Rock Island, Clock Tower Building, P.O. Box 2004, Rock Island, IL 61204-2004
U.S. Army Engineer District, St. Louis, 1222 Spruce Street, St. Louis, MO 63103-2833
U.S. Army Engineer District, St. Paul, Army Corps of Engineers Centre, 190 5th Street East, St. Paul, MN 55101-1638

13. (Concluded).

herein is to use a large physical model to minimize scale effects. Propeller jets, a main emphasis of this study, are operated at speeds where the thrust coefficients are independent of Reynold's number, suggesting similarity with the prototype.

The results presented herein for the physical forces near commercial tows focus on the design tow using the UMR-IWWS. The design tow is a three-wide by five-long barge tow, loaded to about 2.74 m and pushed by a twin-screw towboat with open-wheel for Kort nozzle propellers, typically about 2.74 m in diameter. These data are from experiments in a 1:25-scale model channel, barges, and towboat that has operating propellers, rudders, and open-wheel or Kort nozzle propellers.

The following parameters were measured in the model:

a. Channel bottom pressure under moving tow.
b. Near-bed velocity and bed shear stress changes under the barges of a moving tow.
c. Near-bed velocity and bed shear stress changes in the stern region from the propeller jet for a stationary tow and from the combined effects of the propeller jet and the wake flow for a moving tow.

Analytical/empirical methods were developed to describe near-bed velocity and shear stress as a function of tow parameters.